Sulfonate Functionalisation of Transition Metal Complexes:

A Versatile Tool Towards Catalyst Recovery

Functionalisatie van Overgangsmetaalcomplexen met Sulfonaatgroepen: een Veelzijdige Strategie voor Hergebruik van Katalysatoren

(met een samenvatting in het Nederlands)

La Fonction Sulfonate: une Stratégie Polyvalente pour le Recyclage de Catalyseurs Basés sur des Métaux de Transition

(avec un résumé en français)

Proefschrift

ter verkrijging van de graad van doctor aan de Universiteit Utrecht
op gezag van de rector magnificus, prof. dr. G.J. van der Zwaan,
ingevolge het besluit van het college voor promoties in het openbaar te verdedigen
op dinsdag 19 april 2011 des ochtends te 10.30 uur

door

Morgane Aline Nadia Virboul

geboren op 18 november 1977 te Rennes, Frankrijk

Promotor: Prof. dr. R. J. M. Klein Gebbink

The work described in this Ph. D. thesis was financially supported by the Council for the Chemical Sciences of The Netherlands Organization for Scientific Research (NWO-CW) through a VIDI scholarship.

Virboul, Morgane Aline Nadia

Title: Sulfonate Functionalisation of Transition Metal Complexes: A Versatile Tool Towards Catalyst Recovery

Utrecht, Utrecht University, Faculty of Science
Ph. D. thesis Utrecht University – with ref. – with summary in Dutch and French
ISBN: 978-90-393-5517-6

The work described in this thesis was carried out at the Organic Chemistry & Catalysis group, Faculty of Science, Utrecht University

TABLE OF CONTENTS

PREFACE

The development of sustainable approaches to industrial processes is an important aspect of contemporary research in the field of homogeneous catalysis. Inherently, the separation, recuperation, and reuse of homogeneous catalysts have always been an issue. Now more than ever, the reuse of catalysts has become a major concern both from an economic and environmental point of view, and consequently the development of recyclable homogeneous catalysts is a very active field of research. Several conceptual strategies for catalyst recycling have been formulated over the years and several, including strategies for the immobilisation of catalysts on soluble macroscopic supports or for supported aqueous phase catalysis, have met many of the requirements for catalyst recovery and reuse. In particular, the immobilisation of enantioselective homogeneous catalysts on dendritic supports has proven to be a valuable approach to overcome the difficulties in recycling homogeneous catalysts. *Chapter One* of this thesis provides an overview of the different strategies that were investigated over the years to develop enantioselective dendritic catalysts. Besides the excellent activities and selectivities that these dendritic catalysts can achieve, their ease of recovery by means of nanofiltration or precipitation has greatly contributed to their success in synthetic chemistry. Further efforts should, however, be pursued towards the design of dendritic catalysts that continue to show reaction rates comparable to freshly made ones upon their consecutive reuse.

The aim of the work described in this thesis was to develop a methodology for the functionalisation of transition metal complexes with alkyl sulfonate groups. The interest in this moiety is manifold, yet our goal was to utilise this functional group as a handle for catalyst immobilisation and, accordingly, catalyst recovery.

As strong σ-donors and poor π-acceptors, *N*-Heterocyclic Carbene (NHC) ligands have become a very attractive family of ligands in homogeneous catalysis, bringing robustness and high reactivity to the catalyst. The design and synthesis of alkyl-sulfonate

functionalised NHC ligands have been investigated in *Chapter Two*. The electronic and structural properties of these sulfonato-NHC ligands was evaluated through the spectroscopic characterisation of their (NHC)-Rh(I) and (NHC)-Ir(I) complexes.

The affinity of ammonium groups for sulfonate moieties was the foundation to investigate the non-covalent immobilisation of NHC transition metal complexes on octa-cationic dendrimers. *Chapter Three* presents a convenient method for the preparation of metallodendrimers using a one pot procedure, including concomitant transmetallation and immobilisation reactions on NHC-metal complexes. The so-formed gold and rhodium metallodendrimers were used as catalyst in the hydration of alkynes and the hydrosilylation of ketones, respectively. A study of the gold metallodendrimer by means of DOSY NMR did shed further light on the dynamic exchanges during the catalytic reactions and the resulting structural modification of the catalyst. The rhodium metallodendrimer proved to be active in the hydrosilylation of ketones, albeit that an overall lower activity per rhodium centre was observed in comparison to its mononuclear counterpart.

A similar strategy was employed in *Chapter Four* for the synthesis of multimetallic dendrimers consisting of a hexammonium Dendriphos ligand and sulfonate-functionalised transition metal complex building blocks, and assembled via ionic interactions. The resulting homo- or hetero-multimetallic dendrimers comprise up to 13 metal fragments, whose structure was fully corroborated by means of NMR and ESI-MS analysis.

Chapter Five describes the synthesis of arene ruthenium(II) dimers functionalised with an alkyl sulfonate group, which were used in the synthesis of transition metal complexes with inverted solubility profiles. Specifically, the deprotection of the starting sulfonate esters conferred a very high hydrophilicity to the transition metal complexes, which enabled "immobilisation" of the complexes in water. A chiral diamine ligand was coordinated to the ruthenium metal centre and the resulting chiral complex was tested in the asymmetric hydrogen transfer of prochiral ketones in aqueous solvent. The catalyst showed an excellent reactivity and enantioselectivity for this reaction and could be easily recycled several times without loss of stereoselectivity.

Finally, the *Addendum* describes preliminary investigations on the use of a sulfonated (NHC)-Ag(I) complex described in this thesis as an antimicrobial agent. (NHC)-Ag(I)

complexes are commonly used as carbene transfer agent for the synthesis of other (NHC) transition metal complexes as is described in *Chapter Two* and *Chapter Three*. However, due to their electronic properties, these complexes have recently also been proposed to be used as antimicrobial agents, since silver is known for centuries to have bactericidal activity. The alkyl-sulfonate functionalised biscarbene silver complex was found to be active against various strains of bacteria.

CHAPTER ONE

Enantioselective Catalytic Dendrimers

ABSTRACT

The development of chiral transition metal complexes for asymmetric catalysis has seen the concomitant emergence of strategies for their recovery and recyclability in order to render these catalysts economically interesting for industrial applications. In particular, the synthesis of enantioselective metallodendrimers is an interesting approach that combines the advantages of both homogeneous and heterogeneous catalysis without violating the highly active and stereoselective properties of the parent catalyst. In this chapter, a comprehensive overview of the state of the art in enantioselective catalytic dendrimers is given with an emphasis on the catalytic and recyclability properties of these macromolecules.

1.1 Introduction

Because of its applications in organic synthesis, bulk and fine chemicals production, homogeneous catalysis is a very active area of research. In this area, efforts in ligand design and fine-tuning are being pursued to develop catalysts with improved catalytic performance, stability and selectivity. This phenomenon is even more marked in asymmetric catalysis where the use of efficient enantioselective catalysts is still increasing. Unfortunately, these optimised enantioselective catalysts are often expensive due to their sophisticated ligand and precious metal components. It is for this reason that the recovery and/or reuse of enantioselective catalysts are required in many cases to make them industrially attractive.

In order to overcome the difficulties of recovering homogeneous catalysts, several methods have been developed, among which aqueous and fluorous biphasic catalysis, the use of ionic liquids and supercritical carbon dioxide as reaction medium, and catalyst immobilisation on insoluble and soluble supports like dendrimers.[1-4] Dendrimers are large macromolecules with well-defined spherical or globular architectures that offer the advantages of being recoverable by precipitation, nanofiltration or ultrafiltration. In addition, dendrimers display enhanced solubility profiles as compared to other polymeric supporting materials. Figure 1 provides a schematic representation of the two main types of metal complex attachment to dendrimers. Core-functionalised metallodendrimers (right) have a metal complex encapsulated at the centre of the dendrimer. Conversely, peripherally substituted systems (left) incorporate multiple metal species on the outer dendritic surface.

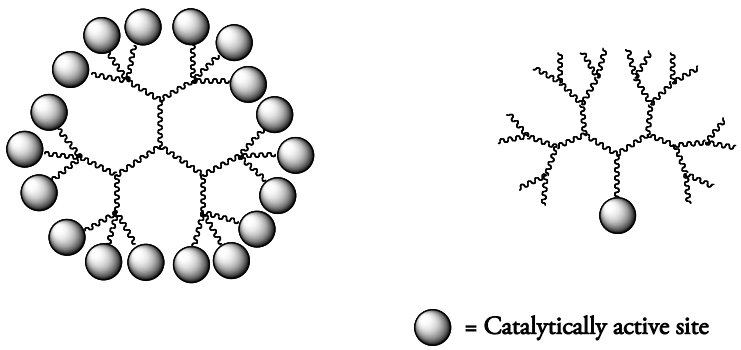

Figure 1. Attachment of catalysts at the periphery or at the core of the dendrimer.

Anchoring a catalyst on a dendritic support is expected to leave the catalytic properties of the homogeneous catalysts unaltered and to potentially improve the activity by modulating the catalyst microenvironment. In this context, the type of dendrimer used for immobilisation plays an important role as it can by its intrinsic nature or its molecular geometry have an impact on the activity of the catalyst.

In this introduction chapter, we present an overview of the work on enantioselective homogeneous catalysts immobilised on dendrimers, where we compile all the typical examples from the literature.[5-7] The overview is organised in distinctive sections based on the position of the metal center, either inside the dendrimer or on its surface. Next, the examples are classified according to the type of ligand that is used, where a difference is made between P-based, N-based, and O-based ligand, as well as between monodentate and bidentate ligands. All examples are discussed in terms of catalytic activity, enantioselectivity, and the comparison between non-immobilised and dendrimer-immobilised catalyst performance. Finally, the possibility to recover and reuse the dendrimer catalysts is discussed in terms of activity and stereoselectivity.

1.2 Dendrimer functionalisation at the core

1.2.1 Phosphorus-based ligands functionalisation

1.2.1.1 Bisphosphine ligands

In 1994 Brunner and co-workers were the first to report the synthesis of a chiral core-functionalised dendrimer.[8] Brunner proposed that the structure of such expanded phosphines (Figure 2) would allow chirality to be induced to the catalyst's pocket thanks to the space filling nature of the molecule and named these new molecules dendrizymes, as this concept is based on the resemblance to enzymatic systems.[9] The activity of the phosphines was tested in the rhodium-catalysed asymmetric hydrogenation of (α)-N-acetamidocinammic acid (see equation in Figure 2). The substrate was efficiently reduced but no significant enantiomeric excess was observed. The use of these ligands in the hydrosilylation of acetophenone and the cyclopropanation of styrene with ethyl diazoacetate did not show chiral induction either. Even though the chirality inducing effect of the 'dendrizymes' was disappointing, these studies represent the onset of many future studies in the field of enantioselective dendrimer catalysis.

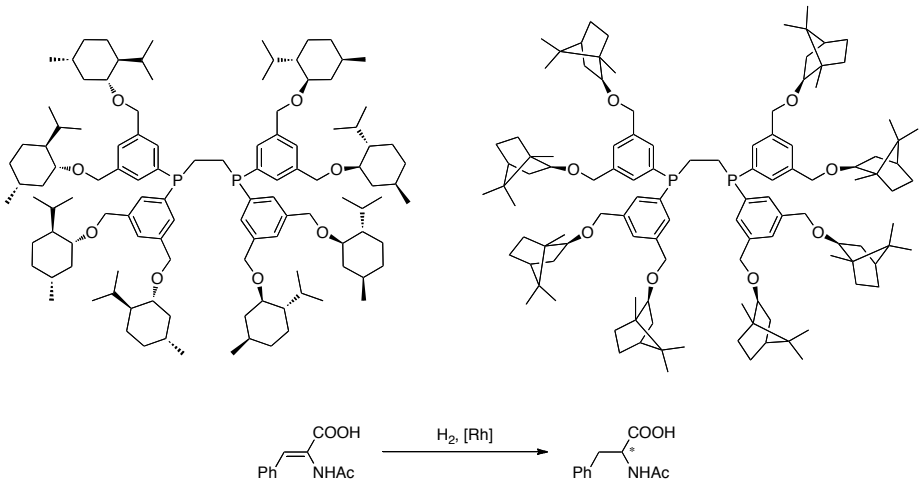

Figure 2. Brunner's example of dendritic phosphines.

In a communication by Fan and Chan *et al.*,[10] the authors report the synthesis of (*R*)-BINAP ligand derivatives decorated with polyether dendrons (so-called Fréchet dendrons) of different generations. The different generations of Fréchet dendrons are thought to increase the steric bulk around the metal center with increasing dendritic generation. The ligands **1-3** were used in the ruthenium catalysed asymmetric hydrogenation of 2-[*p*-(2-methylpropyl)phenyl]acrylic acid (Figure 3) and showed complete conversion after 24 h with good enantioselectivities. Remarkably the enantiomeric excess increased while going from the first to the second generation (ligand **1** to **2**, 91.8 to 92.6 % ee) but with a slightly lower enantioselectivity when the third generation was used (ligand **3**, 91.6 % ee). The rate of the reaction increased as well with the size of the wedges, indicative of a positive dendritic effect. The catalysts were recycled by precipitation and reused without showing any decrease in activity or selectivity.

In a later report the same authors presented the synthesis of similar BINAP-ligands **4-7** bearing an alkyl chain at the periphery to provide specific solubility properties to the catalyst.[11] The ligands were used in the ruthenium-catalysed asymmetric hydrogenation of 2-phenylacrylic acid in an ethanol/hexane mixture that enabled an easy recovery of the catalyst by phase separation upon addition of water. The different catalytic systems displayed full substrate conversions after 4 h and good product enantioselectivities (84-91 % ee). However, upon recycling the catalyst with ligand **5** showed a decreased reactivity already after the first run.

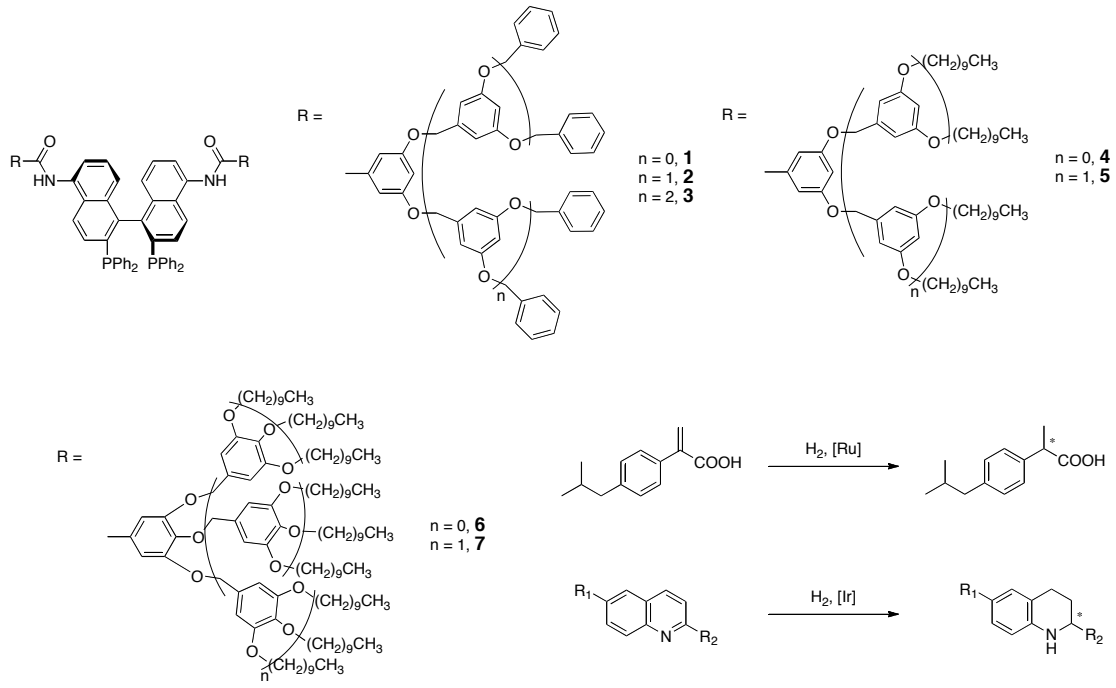

Figure 3. Dendritic BINAP ligands **1-7** developed by Fan's group.

Ligands **1-3** were used in the asymmetric hydrogenation of quinoline derivatives catalysed by an iridium catalyst in a recent paper by Fan *et al.*[12] Full conversion and good enantiomeric excesses (85-90 % ee) were obtained after 1.5 h. The rate of the reaction increased with the dendrimer generation, reaching a TOF for the most hindered ligand **3** never achieved before for this reaction (1580 h^{-1}). This strong dendritic effect could not be explained by the authors, however they suggest that a shielding effect of the dendritic structure around the metal center might contribute to the rate enhancement.

In 2006, Fan *et al.* reported the synthesis of axially chiral dendritic bisphosphines derived from the bridged biphenyl phosphine ligand BIPHEP (Figure 4).[13] The ligands **8-10** were tested in the ruthenium-catalysed hydrogenation of β-ketoesters, in order to check the influence of the dendrimer generation on the catalyst activity. It was found that the size of the dendrimer had a major impact on the enantioselectivity, with the enantiomeric excess decreasing with dendrimer generation. At the same time the catalytic activity did not seem to suffer from the increased steric bulk. The authors could correlate this "dendritic effect" with the dihedral angle of the ligands, as it is known that a larger dihedral angle tends to give reduced enantioselectivity.

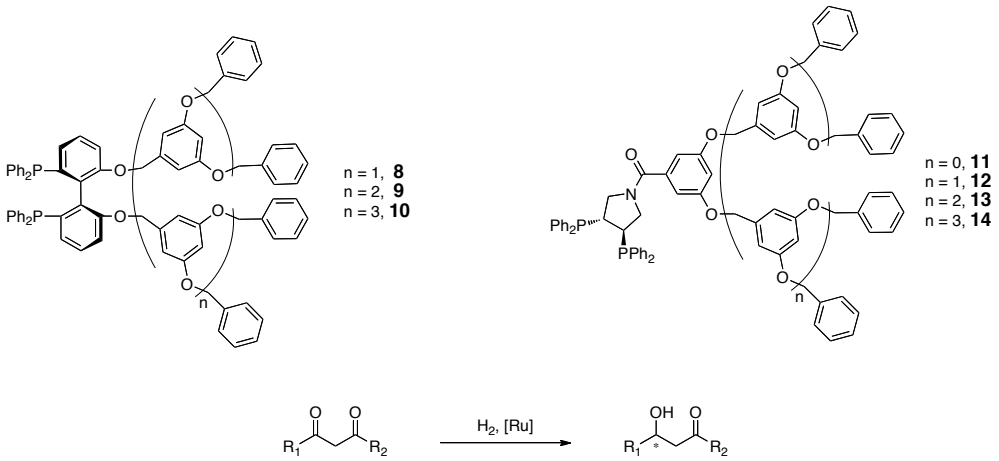

Figure 4. Other chiral bisphosphines dendritic ligands.

Fan and Chan also reported the synthesis of pyrphos ligands **11-14** modified at the focal point with dendritic Fréchet wedges (Figure 4).[14] The activity of the different generations of these chiral bisphosphine ligands was investigated in the rhodium catalysed asymmetric hydrogenation of α-acetamidocinnamic acid (reaction shown in Figure 2). When the reaction was performed in methanol/toluene, a clear decrease in reactivity was observed upon increasing the dendrimer generation (from 91 to 79 % conversion), however without loss of enantioselectivity (96.9 % ee). This effect was particularly flagrant when ligand **14** was used (only 20 % conversion was observed), suggesting a possible encapsulation of the active site and thus a more difficult diffusion of the substrate to the active site. To further assess this hypothesis, a series of dendrimers was synthesised with a more congested catalytic center, which displayed an even more decreased reactivity as well as a decreased enantioselectivity (from 96.9 to 94.6 % ee). The recyclability of ligand **13** showed a rapid decrease of reactivity without loss of enantioselectivity. In an extension of this work, Yi and coworkers reported the synthesis of dendritic ligands similar to **11-14,** decorated with alkyl chains at the periphery.[15] The recovery of these compounds was greatly improved compared to ligand **13** and the activity started to decrease only after the fourth cycle.

1.2.1.2 Monophosphine ligand

In 2008, Seco *et al.* published a report on the synthesis of P-stereogenic dendritic phosphines and their catalytic application in the palladium catalysed asymmetric hydrovinylation of styrene (Figure 5).[16] The authors were expecting an influence of the

specific catalytic environment on the activity and stereoselectivity of the catalyst depending on the dendrimer generation. The steric congestion around the metal center induced by the carbosilane dendrons is indeed believed to enhance the chiral induction by restricting the access to the metal centre. The steric bulk around the metal centre was first evidenced by the formation of an allyl palladium complex displaying diastereotopic protons in ^{1}H NMR, indicative of a high steric hindrance. The catalytic results reflect that increasing the dendrimer generation has a negative influence on the stereoselectivity, the best ee values being obtained with the least hindered ligand **15** (83 %), ligand **16** yielding up to 82 % ee, and only 73 % ee for **17**. The TOF steadily decreased while increasing the steric bulk around the metal centre, suggesting a negative dendritic effect on the activity of the catalyst.

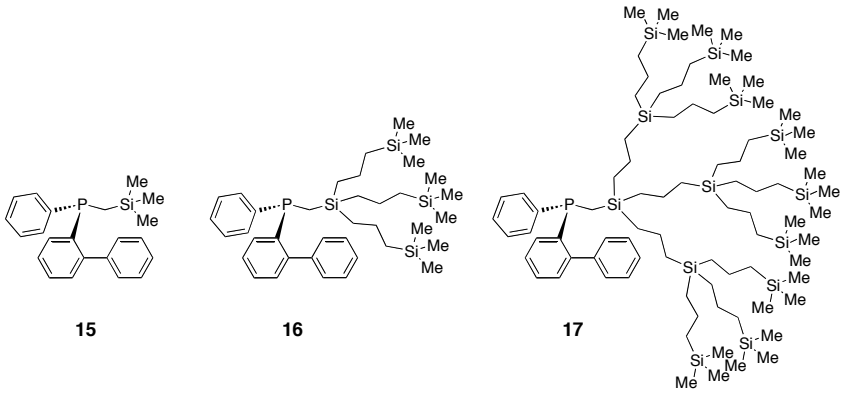

Figure 5. Chiral mono-phosphines **15**-**17** developed by Seco.

In a report by Klein Gebbink and coworkers, a new approach was investigated for the synthesis of chiral dendritic phosphine ligands.[17] In this case the chirality was induced by the presence of chiral Δ-Trisphat anions acting as counter ions for the six permanent positive charges present in the structure of the phosphine ligand (Figure 6). The influence of the steric bulk of ligand **18** on the activity and regioselectivity in the rhodium-catalysed hydroformylation of styrene was investigated with different dendrimer generations, evidencing a decrease of activity and regioselectivity in comparison to PPh_3 (*b:l* ratio is 10 *vs.* 21 for PPh_3). The stereoselectivity of **18** was also studied in the hydrogenation of dimethyl itaconate. In both reactions no significant enantiomeric excess was observed. The authors suggested that the chiral auxiliaries are located too far away from the metal center and that long-range effects are not occurring even when tight ion pairing is favoured in CH_2Cl_2 solution.

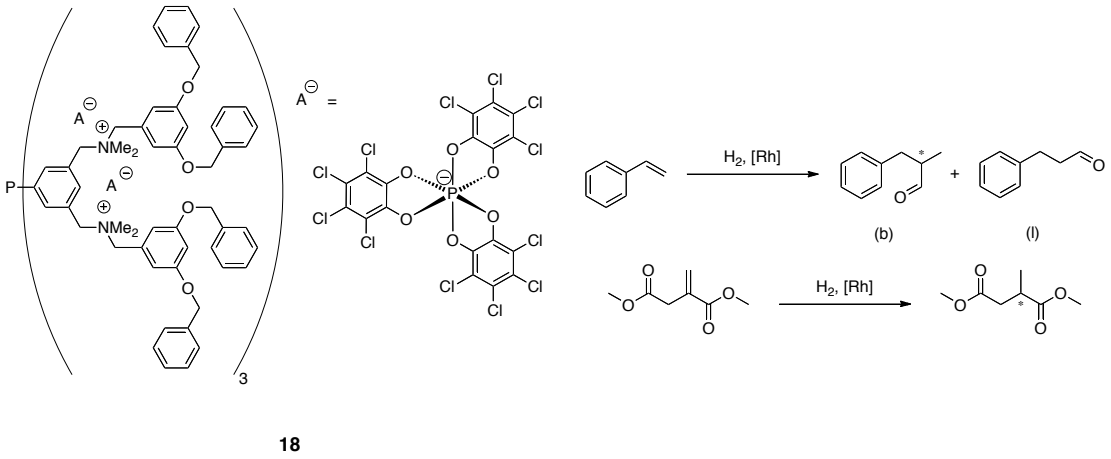

18

Figure 6. Chiral *Dendriphos* ligand **18** developed by Klein Gebbink.

1.2.1.3 Phosphite and phosphoramidite based ligand

In 2008, Fan *et al.* reported on the synthesis of chiral monophosphite ligands **19**-**24** assembled by means of complementary hydrogen bonding between a dendritic Hamilton receptor and a barbituric acid derivative functionalised with a monophosphite moiety (Figure 7).[18]

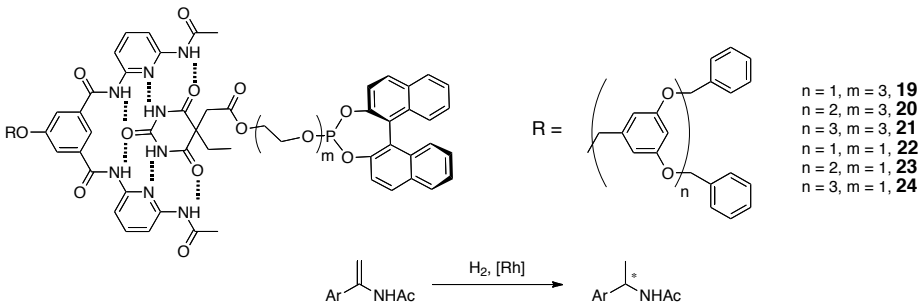

Figure 7. Fan's chiral dendritic phosphite ligand.

These dendritic ligands were employed in the rhodium-catalysed asymmetric hydrogenation of α-phenylenamide and α-dehydroamino acid esters (see reaction in Figure 2). Interestingly, the enantioselectivity in these reactions improved with dendrimers of higher generation (from **19** (80 % ee) to 20 (82 % ee) and from **20** to **21** (86 % ee)). On the other hand, ligands **22**-**24** bearing a shorter linkage displayed a reduced reactivity and enantioselectivity (88 % conversion and 64 % ee) compared to ligands **19**-**21** and the free ligand (100 % yield-93 % ee) in the hydrogenation of α-phenylenamide. It is thought that this negative dendritic effect is induced by the

increased steric bulk. The catalyst formed with ligand **21** was efficiently recycled and did not show deactivation even after five times.

Since the discovery that chiral monodentate ligand based on a BINOL backbone can be as efficient as the reknown bidentate BINAP ligands, a lot of efforts have been pursued in order to fine tune the selectivity and activity of this type of ligands, in particular in the development of chiral phosphoramidite ligands.

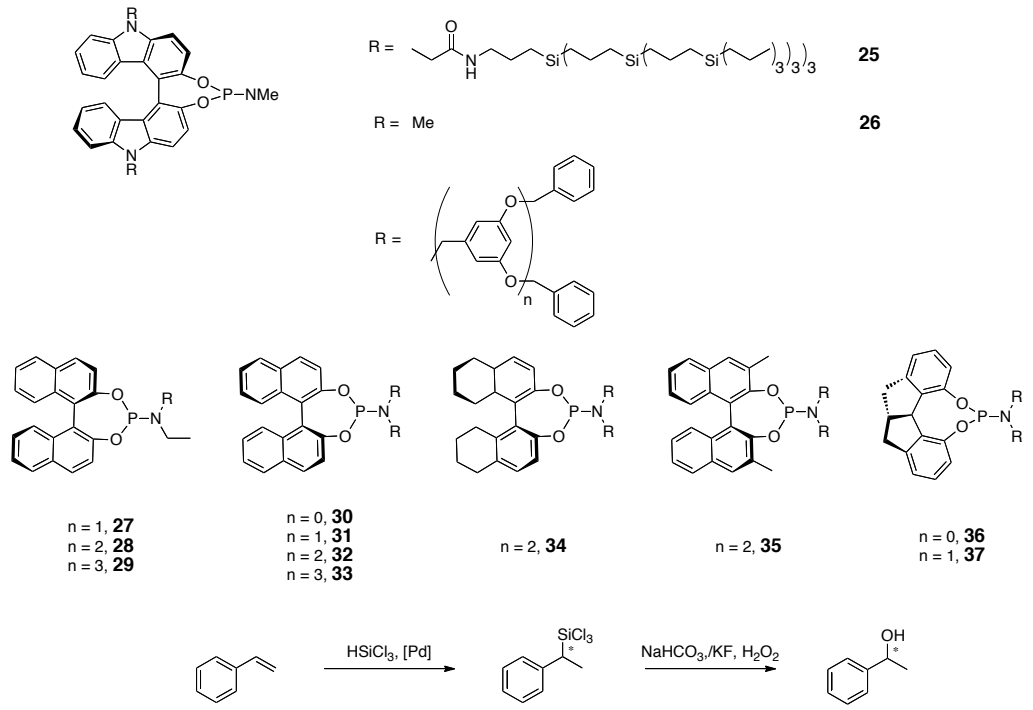

Figure 8. Dendritic phosphoramidite ligands developed by Reek and Fan.

Ligands **25-26**, developed by Reek *et al.*,[19] were the first examples of chiral dendritic phosphoramidites ligands synthesised starting from the BICOL backbone (BICOL = bicarbazolediol, carbazole equivalent of BINOL), which can be readily functionalised with carbosilanes dendritic wedges. These two ligands were tested in the rhodium-catalysed hydrogenation of methyl 2-acetamido cinnamate (see reaction in Figure 2) and compared with the very active and enantioselective MonoPhos ligand.[20] Ligand **25** showed a comparable reactivity to MonoPhos and the non-dendritic ligand **26**, indicating that the steric bulk has no negative effect on the reactivity of the catalysts. Likewise, the enantioselectivity in the reaction was not affected by the attachment of the ligand to the dendritic carbosilane scaffold (ee: **25**, 95 %; **26**, 93 %; MonoPhos, 95 %). Shortly after the report by Reek, Fan *et al.* published several reports on the synthesis of

chiral dendritic phosphoramidites ligands (compounds **27**-**37**, Figure 8) and their use in the rhodium catalysed asymmetric hydrogenation of pro-chiral alkenes (methyl 2-acetamido cinnamate, enamides and dimethyl itaconate, see reactions in Figure 2, 7 and 6 respectively) and palladium-catalysed hydrosilylation of styrene (Figure 8).[21-23] The approach developed involves a functionalisation of the phosphoramidites with Fréchet wedges on the nitrogen atoms, despite the established fact that the substituents on the nitrogen play an important role in the enantioselectivity. In the hydrogenation of methyl 2-acetamido cinnamate, ligands **27**-**29** exhibited a good reactivity and an even higher enantioselectivity than with the MonoPhos ligand (97.5 % vs. 95 % ee). On the other hand, a prolonged reaction time and higher H_2 pressure than with MonoPhos or **25** were required for **27**-**29**. Hydrogenation of α-dehydroamino acid esters and dimethyl itaconate gave satisfying results with similar or better enantioselectivities than MonoPhos (ee: 97.0-97.7 % vs. 93.6 %), with no evidence of the influence of the dendritic wedges on the activity of the catalyst. The modification of the chiral backbone in ligands **30**-**37** had no significant influence on the enantioselectivity in the hydrogenation of methyl 2-acetamido cinnamate with a rhodium catalyst. The authors could demonstrate though that a higher generation of dendrimer improved the stereoselectivity of the catalyst with other α-dehydroamino acid esters and enamides. Recycling experiments with ligand **32** showed a good recyclability of the catalyst by precipitation without loss of reactivity up to the fifth run. Ligands **30**, **32**, **35** and 3,3' substituted derivatives were also tested in the hydrosilylation of styrene.[23] Ligand **30** exhibited a moderate reactivity and enantioselectivity (20 % conversion, 11 % ee), while the introduction of steric bulk by substitution on the 3,3' position, as in **35**, increased the reactivity (>95 % conversion, 43 % ee), in particular with bulkier subsitutents like phenyl, naphtyl or phenanthryl.

1.2.2 Nitrogen based ligand functionalisation

1.2.2.1 Chiral diamines

After the discovery by Noyori *et al.* of the outstanding properties of (*S*, *S*)-*N*-(*p*-tolylsulfonyl)-1,2-diphenylethylenediamine, (*S*, *S*)-TsDPEN, as ligand in the ruthenium catalysed asymmetric transfer hydrogenation (ATH),[24] efforts have been pursued towards the synthesis of recyclable dendritic analogues for application in asymmetric catalysis. In 2001, Deng and coworkers reported on the synthesis and application of

chiral dendritic ligands **38**-**41**, which were synthesised by a three steps procedure involving the condensation of Fréchet type dendrons with amine functionalised (*S*, *S*)-TsDPEN (Figure 9).[25] The activity of these different ligand generations was tested in the asymmetric transfer hydrogenation of acetophenone with [RuCl(*p*-cymene)]$_2$ as the metal precursor. No significant influence of the dendrimer generation on the activity and the stereoselectivity of the catalyst was observed compared to those of the monomeric ligand (i.e. 97 % conversion in 20 h with 97.2 % ee vs. 99 % conversion in 20 h and 97.2 % ee). The catalysts formed with ligands **40** and **41** were recovered at the end of the reaction by precipitation and reused up to six times showing a decreasing reactivity, however without loss of enantioselectivity up to the fifth run for **40** and to the sixth run for **41**. In an extension of this work, the same group reported on the synthesis of similar ligand structures and their use in ATH with prochiral ketones, imines and activated alkenes.[26] A good activity and enantioselectivity was exhibited by these dendritic ligands, again very similar to the monomeric ligand.

The Deng group published two further consecutive reports on the development of dendritic ligands for catalytic ATH applications.[27, 28] Ligands **42**-**48** were synthesised by introduction of the dendritic functionality on the phenyl rings of the 1,2 ethylene diamine as opposed to the amino-functionalised vicinal diamines ligands **38**-**41**.[25, 26] The ligands were used in the ATH of the benchmark substrate acetophenone as well as of more challenging substrates like imines and alkenes. The authors noticed a slight influence of the dendrimer generation on the activity of the catalyst in the ATH of acetophenone when the reaction was performed in the presence of [RuCl(*p*-cymene)]$_2$. Ligand **44** showed a first drop in activity, which enhanced upon further increase of the steric bulk, i.e. the dendritic generation, however without loss of enantioselectivity (96.1 %).[28] The same observation was made when the reaction was performed with (*S*)-BINAP-RuCl$_2$, along with a loss of stereoselectivity though (82 % ee).[27] The authors attribute this loss of reactivity to the structure of the ligands, which changes from an extended to a more globular conformation as the steric bulk induced by the dendritic wedge generation increases. In both reports recyclability studies of the catalysts by precipitation gave satisfactory results and the catalysts could be recycled without loss of stereoselectivity up to five times (up to 94 % ee), however with a decrease in activity that can be ascribed to metal leaching as determined by ICP analysis.[28]

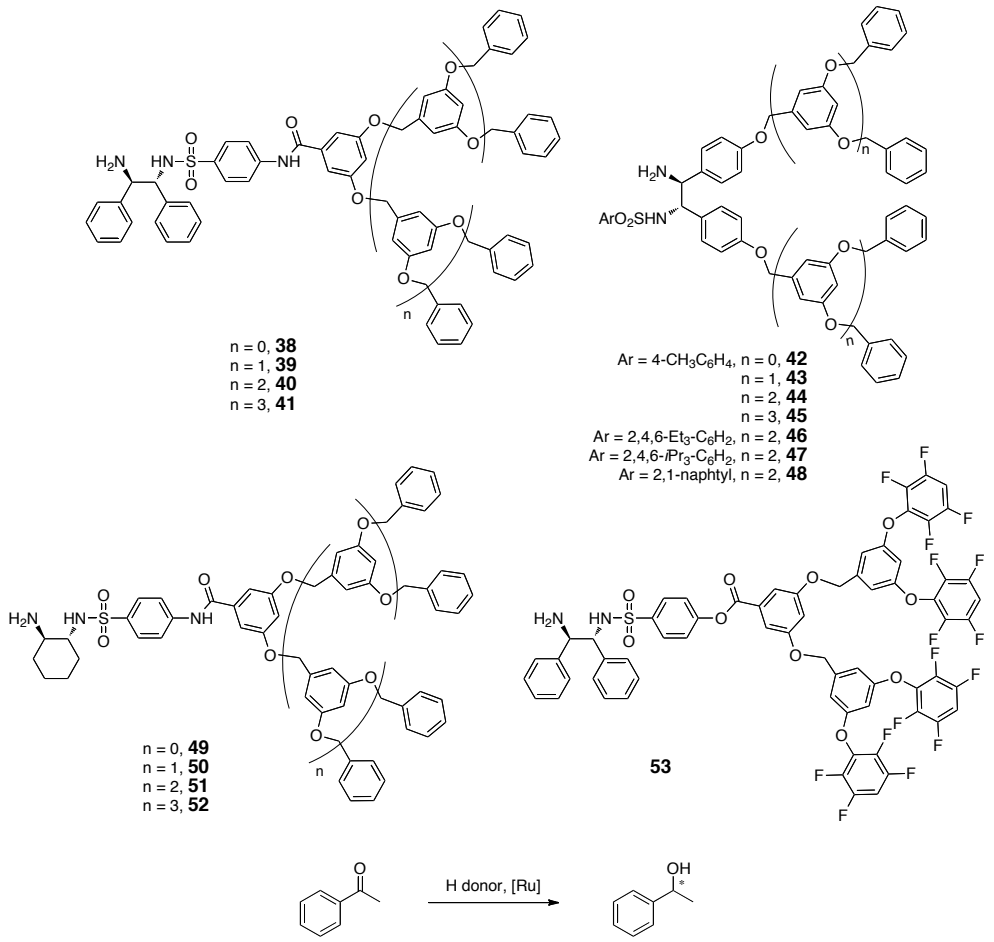

Figure 9. Chiral dendritic diamine ligands.

In their search for chiral catalysts with enhanced recyclability, the group of Deng also developed dendritic ligands **49**-**52** comprising a chiral 1,2-diaminocyclohexane core, which were synthesised in a similar fashion as ligands **38**-**41**.[29] The ligands were tested in the ruthenium and rhodium catalysed ATH of prochiral ketones and showed a decreased reactivity under various reaction conditions when the steric ligand **52** was used. No influence of the dendritic generation was observed; the ligands **49**-**51** performing equally well as the monomeric ligand both in terms of activity and enantioselectivity, with conversions superior to 99 % and ee values ranging from 85-96 % depending on the conditions used for the reaction. The ligands also performed well when the reaction was performed in water with either a ruthenium or rhodium metal precursor. The enantioselectivity using the rhodium metal precursor was higher under these conditions than with ruthenium (96% ee vs. 88% ee). The recyclability of ligand **50** by precipitation from water with hexane showed remarkable results as the catalyst could be reused up to six times in the rhodium catalysed ATH without loss of

stereoselectivity, while only a slight decrease in reactivity was observed. Interestingly, the authors mention that the recyclability of **50** in organic solvents compared to that of **40** or **41** is very limited; the authors noted that the reactivity dropped drastically after the second use with a conversion of 46 % (the first use gave a conversion of 99 %) and only 7 % after the third use.

In 2010, Wang and coworkers reported on the synthesis of a fluorinated TsDPEN derived ligand (**53**) and its application in the ruthenium-catalysed ATH of prochiral ketones in an aqueous medium.[30] Ligand **53**, which was synthesised in a six-step procedure with an overall yield of 65 %, exhibited a good catalytic activity and enantioselectivity (93%) in water. The presence of tetrabutylammonium iodide further improved the enantioselectivity of the reaction to 97 % ee. By a precipitation method, the catalyst could be recovered at the end of the reaction and reused up to an unprecedented 26 times without loss of activity and stereoselectivity. The authors suggested that this exceptional stability of the catalyst (no metal leaching was observed by ICP analysis) can be ascribed to the introduction of fluorine atoms on the ligand, thus conferring robustness to the ligand and to the catalyst.

1.2.2.2 Proline-based ligands

Proline-based ligands represent another important type of easily accessible chiral ligands have been well studied for their application in asymmetric catalysis. Their derivatisation with dendritic wedges has been investigated by several groups, in particular by Zhao and coworkers. In 2005, they reported on the synthesis of ligands **54**-**57** and their application in the enantioselective addition of organozinc reagents to aldehydes (Figure 10).[31] This topic had been already studied by Bolm *et al.* in 1996 using a chiral pyridyl alcohol ligand decorated with Fréchet dendrons.[32] However, no other effect of the dendrimer on the activity of the catalyst was demonstrated and a slight decrease of stereoselectivity of the dendritic ligands compare to the monomeric pyridyl alcohol was found. With the proline-based ligands, very good activities and stereoselectivities were obtained for the reaction of *p*-chlorobenzaldehyde with Et_2Zn in the presence of 20 mol% ligand. Ligands **54**-**56** gave better ee values than the monomeric species (98 % ee vs. 94 % ee), except for the highest generation dendrimer **57** that exhibited a slightly reduced enantioselectivity (91 % ee). Ligand **56** was recovered by precipitation at the end of the reaction and was recycled at least five times without a decrease in activity and

stereoselectivity. Substituted benzaldehydes were efficiently transformed into the corresponding diaryl alcohol with the use of the dendritic proline liagnds. Aliphatic aldehydes, on the other hand, were converted with lower selectivity and lower efficiency (77 % conversion and 65 % ee).

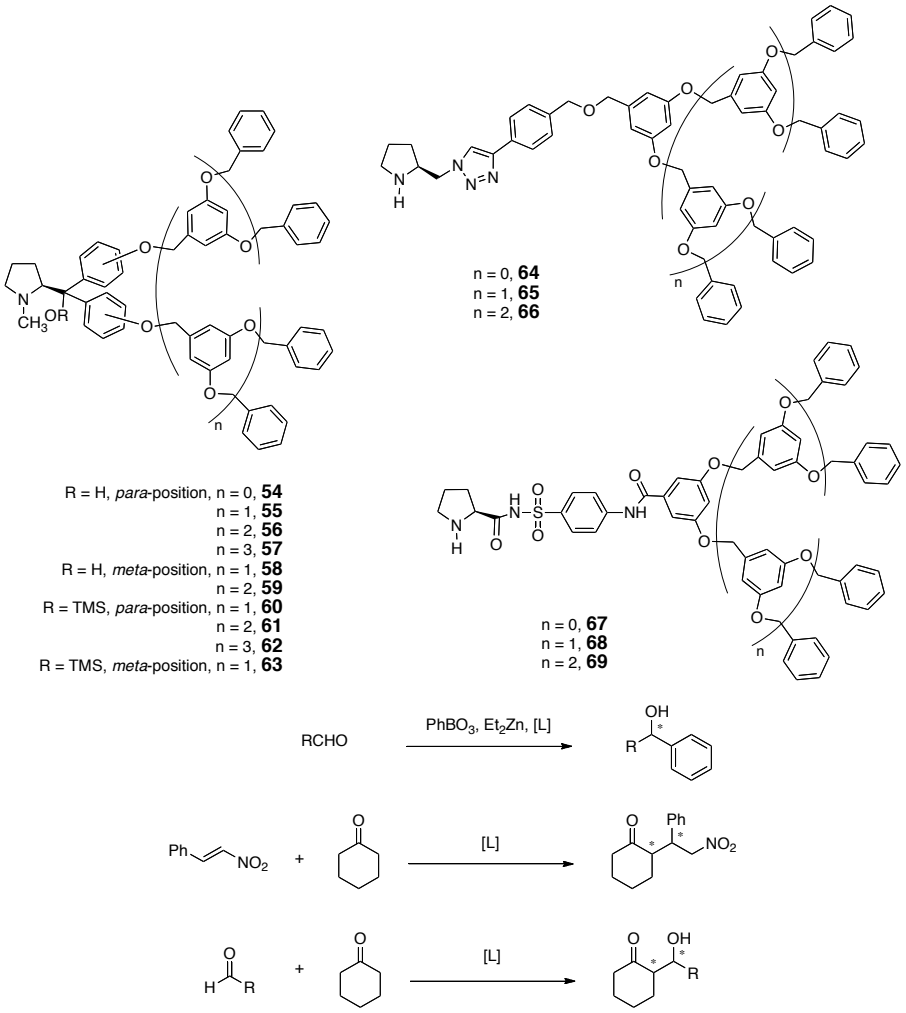

Figure 10. Chiral proline-derived dendritic ligands **54-69**.

The use of ligands **54-57** and **58-59** as asymmetric organocatalysts was further investigated in the enantioselective reduction of ketones,[33] the enantioselective epoxidation of enones[34], and the asymmetric reduction of indolones and tetrolones.[35] The modified counterparts **60-63** were used in the organocatalytic asymmetric Michael addition of aldehydes to nitrostyrenes[36] and in a tandem cyclopropanation/Wittig reaction of α, β-unsaturated aldehydes with arsonium ylides.[37] These ligands showed a great versatility in their application and in all cases exhibited good activities and stereoselectivities (78-99 % ee). Recovery and reuse of these ligands by means of

precipitation was possible without loss of activity up to five consecutive runs. The synthesis of pyrrolidine-derived ligands **64**-**66** decorated with Fréchet dendrons via click chemistry was reported by Gao and coworkers.[38] These organocatalysts were tested in the Michael addition of ketones to nitroolefins and exhibited a good activity (up to 99 % conversion) and stereoselectivity (up to 95 % ee) as well as a good recyclability with a little loss of reactivity after six runs (80 % conversion and 90 % ee).

In 2006, Zhao *et al.* reported the synthesis of proline-derived ligands **67**-**69** functionalised with dendritic wedges and their application as organocatalysts in the asymmetric direct aldol reaction in water (Figure 10).[39] The authors hypothesised that these chiral amphiphilic ligands would assemble in water with the hydrophobic reagents, keeping the reaction site away from water and thus enabling a high asymmetric induction. The aldol reaction proceeded as expected, yielding the product in good yields with high stereo- and enantioselectivity, especially with ligand **68** (*anti/syn* 99:1, 99 % ee). This same ligand was used in a recycling test and could be recycled by precipitation up to four times without a decrease in activity and stereoselectivity.

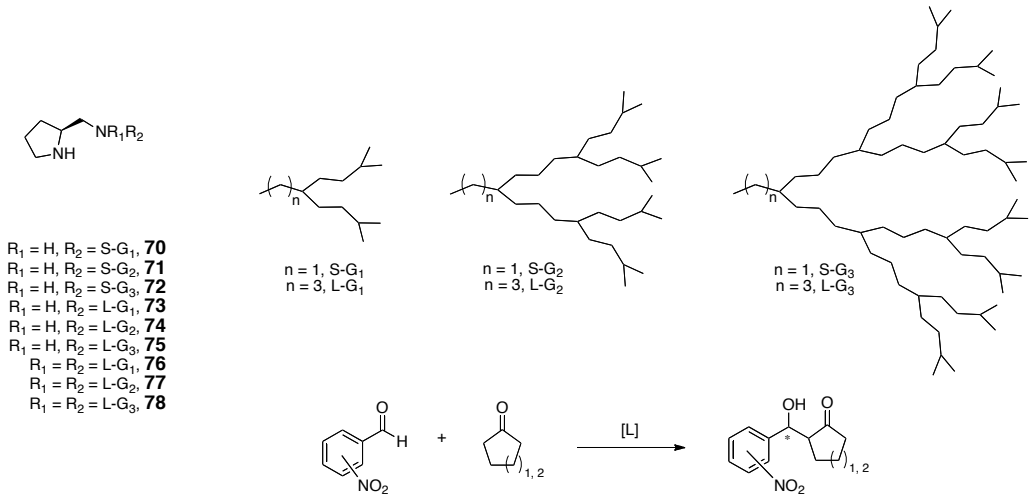

Figure 11. Amphiphilic dendritic organocatalysts.

In a similar approach, Chow *et al.* synthesised three series of proline-derived chiral dendritic organocatalysts for the application in aqueous asymmetric catalysis (Figure 11).[40] The functionalisation of the proline with hydrophobic hydrocarbon dendrons was expected to induce the formation of emulsions in water and to enhance the reactivity and selectivity during the catalytic reaction. The authors found that the properties of these compounds are indeed mainly due to their ability to form emulsions in water and that

compounds **71**, **74**, and **77** are best suited to catalyse asymmetric aldol reactions and nitro-Michael additions, for which they exhibited a good reactivity (78-87 % conversion), diastereoselectivity (*syn*/*anti* > 90:10) and enantioseectivity (80-84 % ee). The authors also showed that the catalysts could be recovered by solvent partitioning with heptane/methanol in which little decrease in reactivity and selectivity was found until the fifth run.

1.2.2.3 Oxazoline based ligands

In 2002, Moberg and coworkers investigated the functionalisation of oxazolines with dendritic wedges.[41] Pyridinooxazolines and bisoxazolines were functionalised with achiral and chiral polyester dendrons to yield the ligands **79**-**89**, which were used in a palladium catalysed allylic alkylation (Figure 12). Ligands **84**-**89** showed a enantioselectivity similar to the parent ligand (76-80 % vs. 79 % ee) and no specific influence of the dendritic wedges on the reaction was observed. On the other hand, ligands **79**-**83** showed a better enantioselectivity than their monomeric counterpart (94 % vs. 79 % ee). The catalytic activity of the bulkier ligand **80** was quite low; i.e. only 10 % of product was obtained after prolonged reaction time. Furthermore, the introduction of a chiral dendron on the oxazoline core moiety (ligands **81**-**82** and **87**-**88**) had no beneficial influence on the enantioselectivity (79 % ee, as for the parent ligand).

Fan *et al.* reported on the synthesis of the chiral bisoxalines ligands **90**-**92** functionalised with different generations of polyether dendrons (Figure 12).[42] In combination with $Cu(OTf)_2$, these ligands were used as Lewis acid catalysts in the enantioselective aldol reaction of benzaldehyde with a silyl enol ether in aqueous solvent. ligands **90**-**92** exhibited a good reactivity (75 % conversion) but moderate stereoselectivity (*syn*/*anti* = 2.1/1 and 60 % ee). A slight increase in product enantioselectivity was observed for higher dendritic generation. The catalysts were recovered at the end of the reaction by precipitation, however the recycled catalyst gave lower yields 40 %) and ee values (30 % ee) compared to the freshly prepared catalysts.
The same approach was pursued by Du and coworkers by the functionalisation of a slightly different bisoxazoline core with Fréchet dendrons (not shown).[43] These ligands were applied in the asymmetric alkylation of indoles with nitroalkenes and showed an activity similar to the monomeric ligand (93-99 % vs. 96 % conversion). The dendritic generation had no significant influence on the enantioselectivity but a slightly decreased

reactivity was observed when the steric bulk was increased (93 % conversion for the bulkier dendritic ligand vs. 99 % for the less hindered dendritic ligand).

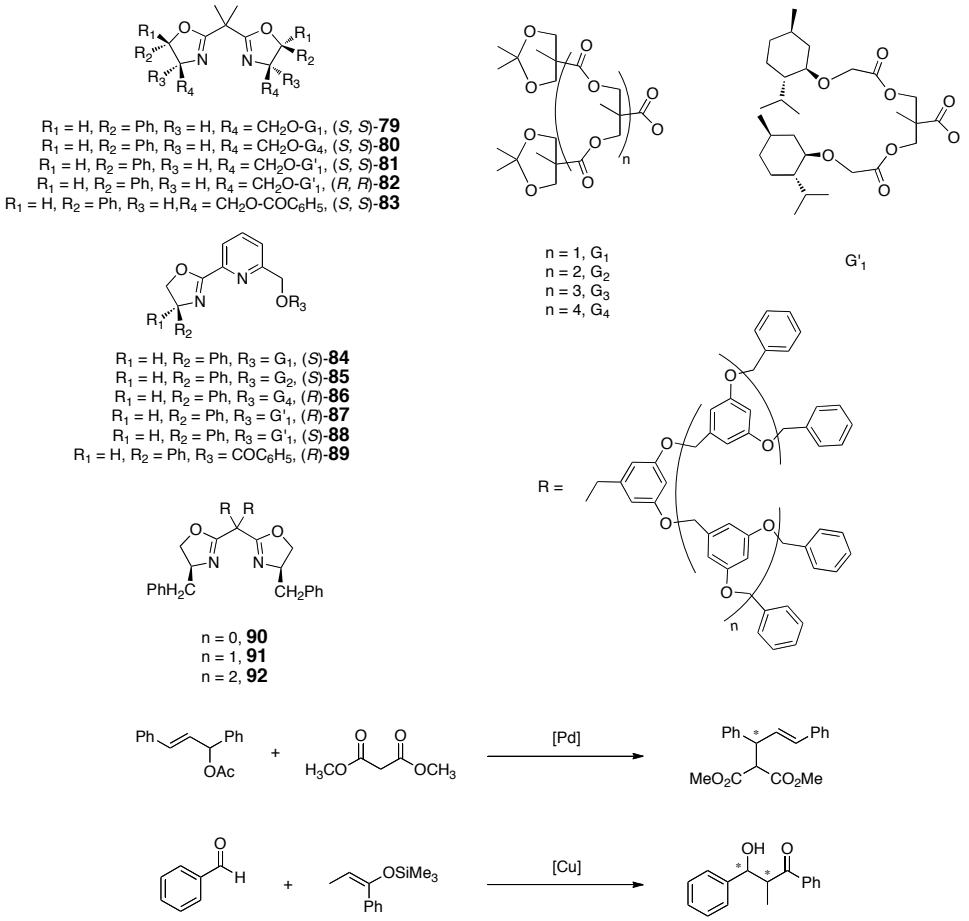

Figure 12. Oxazoline-based dendritic ligands.

1.2.3 Oxygen-based ligands

1.2.3.1 TADDOL-derived ligands

In two consecutive reports from 1999, Seebach *et al.* presented the synthesis of core-functionalised TADDOL dendrimers. [44, 45] The TADDOL center was decorated by four Fréchet dendrons in **93**-**97** and by four chiral polyether dendrons in **98** and **99** (Figure 13). These dendrimers were used as ligands in the synthesis of titanium taddolates, which in turn were employed as catalysts in the asymmetric addition of Et_2Zn to benzaldehydes (see reaction in Figure 10). Compounds **93**-**99** all showed a good stereoselectivity (89-97 % ee) for this reaction, which was found to be comparable to the performance of the monomeric TADDOL ligand (98 % ee). Much like in several of the previous examples, the enantioselectivity dropped slightly upon increase of the dendrimer generation. This

observation was also true for the activity of the catalyst, for which a marked decrease between the activity of **96** and **97** was observed (94 % vs. 47 % conversion, respectively). No influence of the chiral dendrons **98-99** on the stereoselectivity was demonstrated.

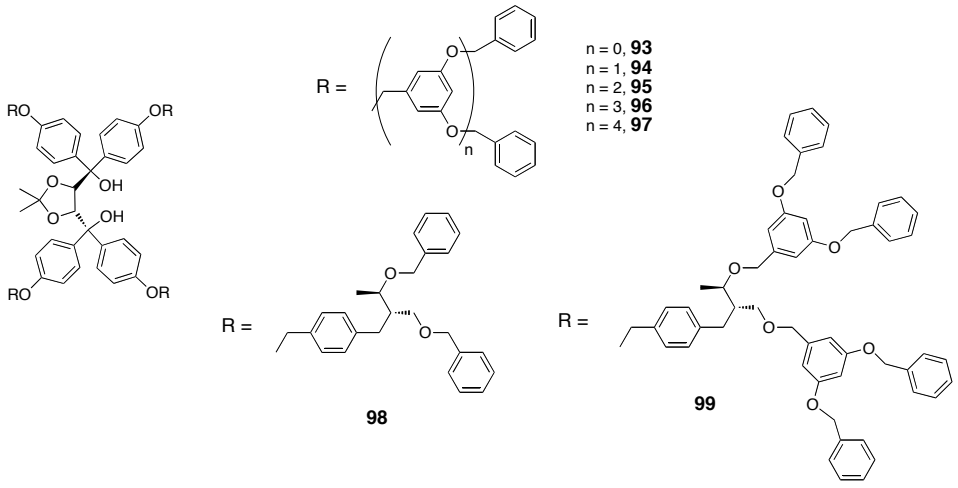

Figure 13. Seebach's TADDOL derived dendrimers.

1.2.3.2 BINOL-derived ligands

In 1998, Yamago and coworkers reported the synthesis of BINOL derivatives decorated with dendritic polyether dendrons (Figure 14).[46] Ligands **100-102** were used in the titanium-catalysed allylation of aldehydes using allyl stannane and showed a poor activity (18-36 % conversion) for this reaction, albeit with good enantioselectivities (88-92 % ee) similar to what was reported for BINOL (89 % ee). This preliminary work on BINOL derivatives paved the way for other groups to further investigate the influence of dendritic wedges on the activity of BINOL-based catalysts.[47, 48] Ligands **100-110** were tested in the titanium catalysed asymmetric addition of diethyl zinc to benzaldehyde (see reaction in Figure 10). All dendritic catalysts were found to be very active for this reaction (>99 % conversion) giving 77 to 87 % ee. Variations in dendron branching point (R_1/R_4 position vs. R_2/R_3 position) or dendrimer size had limited to no influence on the overall catalytic performances in these cases.

Ding et al. described the synthesis of the NOBIN-derived ligands **111-116** bearing Fréchet dendrons (Figure 14).[49] The authors employed these dendritic ligands in titanium-mediated enantioselective Hetero-Diels-Alder reaction (HDA) on Danishefsky's diene with aldehydes. The reactions proceeded with high efficiency and good enantioselectivity (94-97 % ee), though the best results were obtained with ligands

carrying Fréchet wedges that are branched on the meta-position (ligands **114-116**). For ligands **111-113**, the enantioselectivity was influenced by the increasing dendrimer generation, with the enantioselectivity ranging from 92 % for **111** to 75 % ee for **113**. The authors also showed that catalyst **115** could be recycled by precipitation and reused in up to three catalytic runs with a slightly decreasing reactivity (99 to 90 % conversion for the first to the third run).

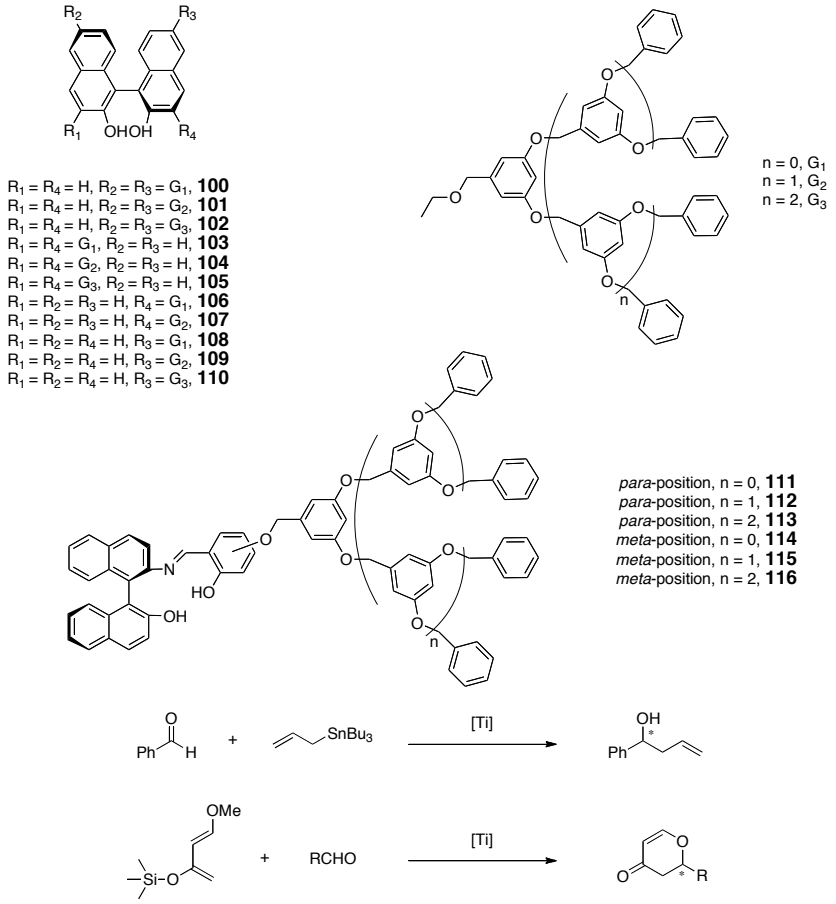

Figure 14. BINOL and NOBIN-derivatived dendritic ligands.

1.2.4 Other functionalisation

The groups of Van Koten and Majera described the synthesis of cinchonidine-derived ammonium salts and their application as phase transfer catalyst (Figure 15).[50] The different ligands **117-123** were used as phase transfer catalyst in the biphasic alkylation of *N*-(diphenylmethylene)glycine isopropyl ester with benzyl bromide. A study on the effect of the different generations of dendrimers on the catalytic activity showed no correlation between the dendrimer size and the enantioselectivity. Overall reaction

rates were found to range between 44-76 % ee without an apparent trend. The recyclability of compounds **119** and **121** were tested by performing the reaction in a membrane dialysis tube, which was used as a "tea bag" in which the reaction could take place and which could be easily transferred to a next reaction batch. Both compounds performed in a similar manner as the fresh catalyst for the first two rounds, while **119** showed a dramatic decrease in the third round for with ee values going from 60 to 40 % ee over a prolonged reaction time.

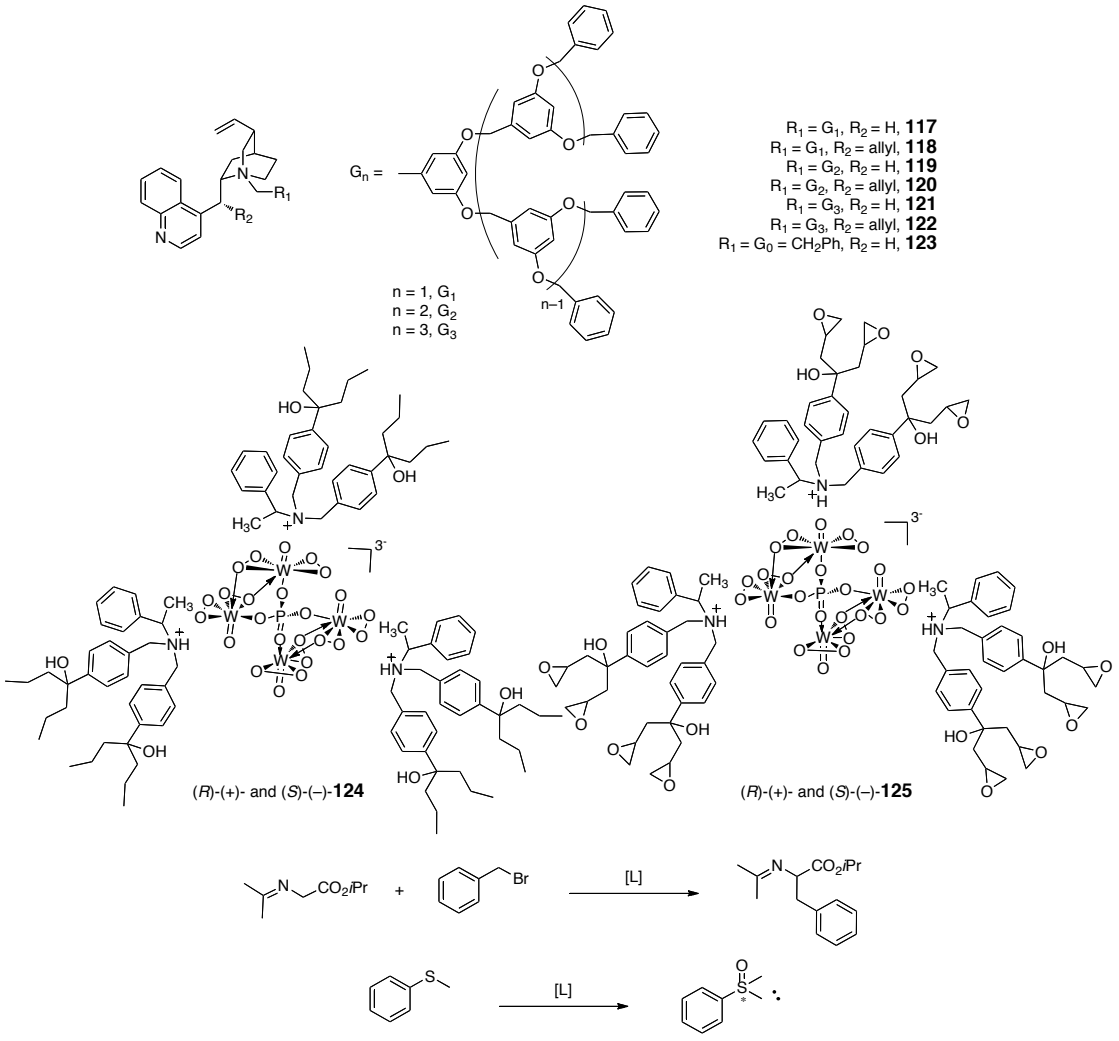

Figure 15. Dendritic cinchonidines and dendritic POM-salts.

Recently, Nlate and coworkers reported on the synthesis of enantiopure polyoxometalates (POM) and their use as catalyst in the asymmetric sulfide oxidation (Figure 15).[51] Their original approach created chiral dendritic POMs through the interaction of three enantiopure ammonium ions with the achiral trianionic POM. The activity of compounds (*R*)-(+)-**125** and (S)-(+)-**125** was tested in the oxidation of

thioanisole with H_2O_2, which resulted in the full oxidation to the corresponding sulfoxide with 14 % ee. The POM-catalysts could be recovered by precicpitation with ether and were reuse up to three times without any noticeable deactivation. Despite the low enantioselectivity of these catalysts, this work showed an unprecedented example of chirality transfer from an organic dendritic counterion to the activity of a non-chiral catalyst.

1.3 Dendrimer functionalisation at the periphery

1.3.1 Phosphorus-based ligands

1.3.1.1 Diphosphines ligands

In a number of papers, Togni and coworkers reported the immobilisation of the chiral ferrocenyl-based diphosphine ligand Josiphos on the periphery of dendrimers (Figure 16).[52] This study represents one of the earlier studies on enantioselective catalysis used peripherally functionalized dendrimers. Up to eight Josiphos ligands were immobilised on different core molecules via linkers that ensured sufficient flexibility of the bisphosphine moieties. These dendritic 'multi-ligands' were tested in the rhodium-catalysed asymmetric hydrogenation of dimethyl itaconate (reaction shown in Figure 6). The parent Josiphos ligand is known to catalyse this reaction with good activity and enantioselectivity. The performances of compounds **126-129** were very similar to the monomeric Josiphos (98.7-98.0 vs. 99 % ee, respectively); the slight decrease in enantioselectivity was correlated to the increasing size of the dendrimer. The recyclability of these catalysts was not investigated, although the authors demonstrated that a commercially available nano-filtration membrane was able to retain the dendrimers.

Next, the same group reported the synthesis of dendrimers **130-131** with different core molecules that could bear up to 16 Josiphos moieties.[53, 54] These dendrimers were also tested in the rhodium catalysed asymmetric hydrogenation of dimethyl itaconate and showed a very similar performance as ligands **126-129** (the product was obtained with 98 % ee), with no significant influence of the dendrimer generation on the performance of the catalyst. When the same dendrimers were used in the palladium-catalysed substitution of allylic acetate with dimethyl malonate (85-92 % yield, 85-91 % ee) or

the rhodium-catalysed hydroboration of styrene (63-97 % yield, 60-68 % ee), no remarkable effect of the nature or generation of the dendrimer could be observed.

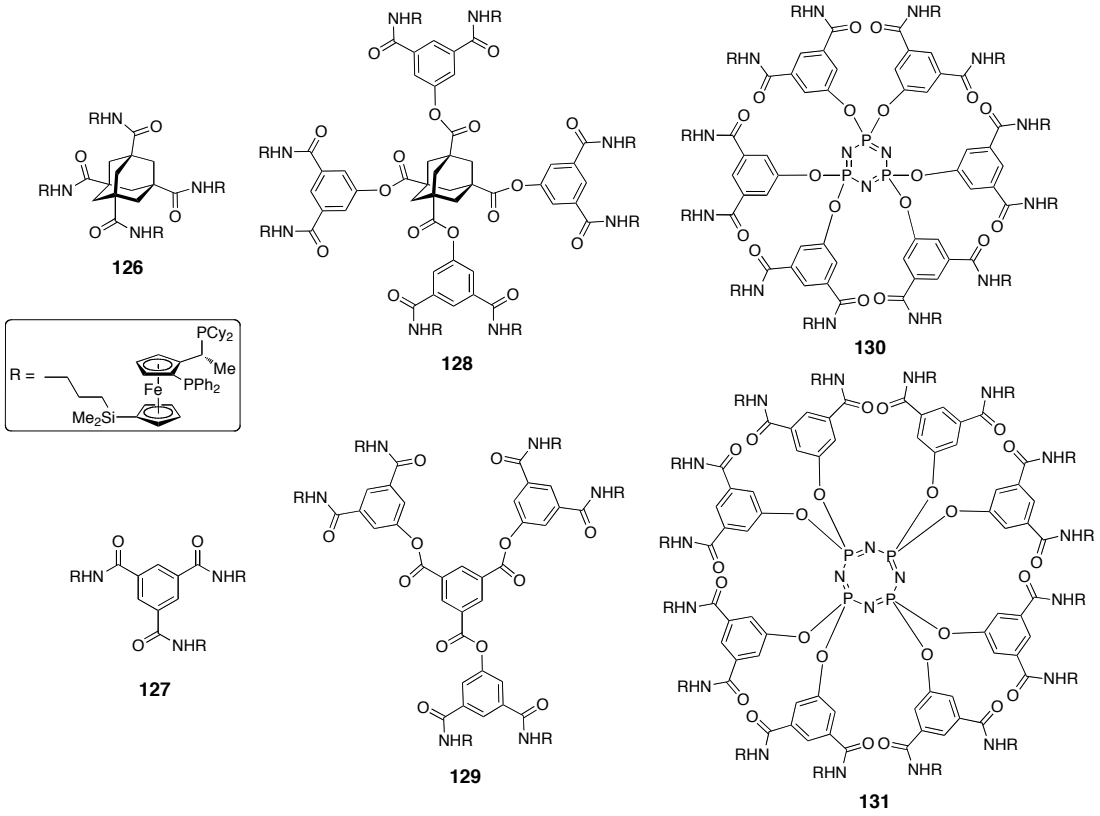

Figure 16. Josiphos dendrimers.

In a report from 2002, Gade *et al.* reported the synthesis of dendrimers bearing chiral diphosphine ligands on their peripheries (Figure 17).[55] Pyrphos-derived ligands were linked to the outer shell of different generations of poly(propyleneimine) (PPI) dendrimers to form dendrimers **132-136** with up to 32 immobilised ligands. The different dendrimers were employed in the rhodium-catalysed asymmetric hydrogenation of Z-methyl-α-acetomidocinammate and dimethyl itaconate (reaction shown in Figure 2 and 6, respectively) for which a clear relationship between the activity and the dendrimer size could be established. The stereoselectivity as well as the activity of the catalysts indeed showed a decrease with increasing dendrimer generation that was explained by the authors as the result of a potentially reduced accessibility of all metal centres. In an extension of this work, Gade *et al.* reported the synthesis of pyrphos ligands immobilised on the periphery of poly(amidoamine) dendrimers (PAMAM) (ligands **137-141**) and their use in the palladium-catalysed allylic amination of 1,3-diphenyl-1-acetoxypropene

with morpholine.[56] The performance of these dendritic catalysts was compared to the monomeric pyrphos ligand and showed a dramatic improvement in the stereoselectivity, with up to 69 % ee for the most selective catalyst vs. 9 % ee for the parent pyrphos. It was shown that the increasing stereoselectivity of the catalysts correlated with the higher dendrimer generation. Interestingly, this positive dendritic effect was also observed when PPI dendrimers **132-136** were used for this reaction, albeit that a lower extent was reached with **136** than with the higher generation **141** (40 vs. 69 % ee).

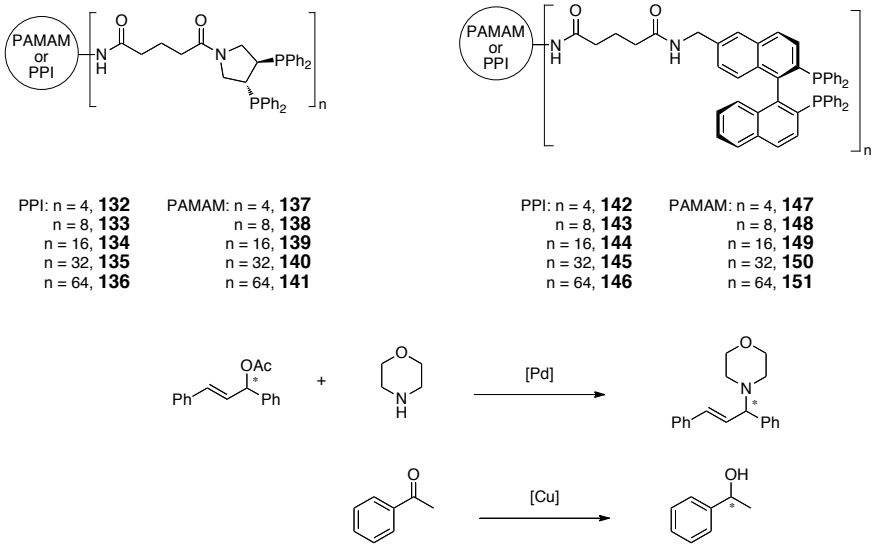

Figure 17. PPI and PAMAM dendrimer immobilised pyrphos (left) and BINAP (right) ligands.

Despite their widespread application in homogeneous asymmetric catalysis, the first example of BINAP ligands immobilised at the periphery of a dendrimer was reported in 2008 by Gade *et al.*[57] The authors immobilised BINAP derivatives on PPI and PAMAM dendrimers of different generations in order to study the influence of the dendritic support on the catalytic performances of the compounds (Figure 17). The latter was studied in the copper-catalysed hydrosilylation of acetophenone, where it was found that the compounds **142-151** performed similarly as the non-immobilised ligand with a slightly better enantioselectivity (90 % ee for BINAP and 93-94 % ee for ligands **142-151**). No evidence for an influence of the type of support or the dendrimer generation was observed for this reaction, indicating that the conversion is controlled by the first coordination sphere around copper and that there is no mutual interaction between individual BINAP moieties that imparts the enantioselectivity.

1.3.1.2 Monophosphines

In a similar approach to the one developed by Togni,[53] Majoral and coworkers reported the synthesis of chiral ferrocenyl P, S ligands immobilised on dendrimers and their use as ligands in asymmetric catalysis (Figure 18).[58] The dendrimers **151-154** were used in the palladium-catalysed allylic substitution reaction with dimethyl malonate (see reaction in Figure 12), where they showed high activities (87-95 % yield) and enantioselectivities (81-93 % ee), similar to the parent catalyst (96 % yield and 93 % ee) and independent of the dendrimer generation. A preliminary study on the recyclability of the dendrimer **154** by means of precipitation revealed a decrease in activity and stereoselectivity.

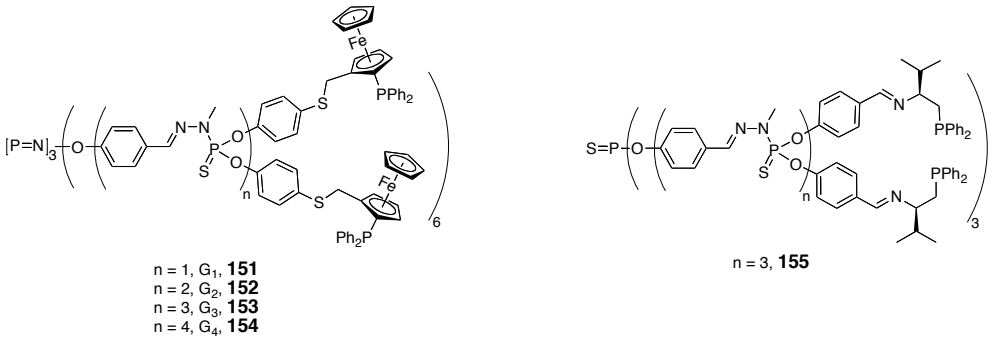

Figure 18. Chiral monophosphine dendrimers.

In 2005, the same group synthesised a new dendrimer functionalised with a P, N-iminophosphine ligand and investigated its use in the palladium catalysed allylic substitution, for which this ligand had previously been applied in a successful manner.[59] Dendrimer **155** showed a good activity and selectivity (87-97 % yield and 84-95 % ee, depending on the reaction conditions), however the recycled catalyst showed a slight decrease in reactivity and enantioselectivity upon reuse.

In 2006, Rossell and coworkers reported the immobilisation of chiral P-stereogenic monophosphine ligands at the periphery of different generations of carbosilane dendrimers (Figure 19).[60] The reaction of compounds **156-161** with $[Pd(\mu\text{-}Cl)(\eta^3\text{-}2\text{-}MeC_3H_4)]_2$ afforded the corresponding palladodendrimers which were employed as catalysts in the hydrovinylation of styrene. The catalysts were found to have a good activity (54-95 % conversion) and good enantioselectivity (up to 79 % ee), which did not seem to depend on the structure of the dendrimer. The nature of the halide

scavenger, and in particular its corresponding counter ion was found to have a large influence on the performances of the catalysts, in particular the use of NaBARF instead of AgBF4 increased the chemoselectivity and enantioselectivity. The same reaction was also performed in supercritical carbon dioxide and the catalytic results were very similar to those obtained in organic solvents.[61]

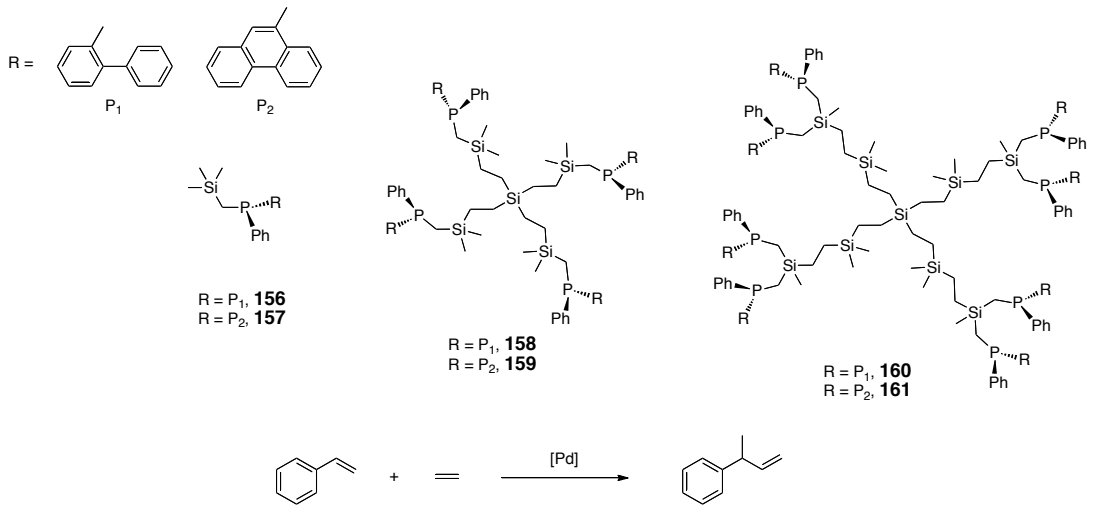

Figure 19. P-stereogenic ligands immobilised on carbosilane dendrimers.

Compounds **156-161** were also applied in the rhodium-catalysed asymmetric hydrogenation of dimethyl itaconate and their activity was found to decrease when increasing the dendrimer generation from **158** to **160** from 94.4 % to 68.6 % conversion, respectively. Furthermore, the catalysts failed to induce any chirality. The ruthenium-catalysed ATH of acetophenone was also tested with the immobilised phosphines. For this reaction, a positive effect of the dendrimer generation on the catalytic activity was observed, albeit without any enantioselectivity.[62, 63]

1.3.2 Nitrogen-based ligands

1.3.2.1 Proline-derived ligand

Kokotos *et al.* reported in 2005 on the immobilisation of trans-4-hydroxyproline on the periphery of different generations of PPI dendrimers (Figure 20).[64] The catalytic performance of dendrimers **162-166** was evaluated in the asymmetric aldol reaction of 4-nitrobenzaldehyde and acetone and compared to the activity of non-immobilised L-proline. The activity of the second generation dendrimer **163** was found to be the most

efficient with a yield and ee value comparable to the parent compound (63 % yield and 69 % ee vs. 61 % yield and 65 % ee). The authors found that with this catalyst the reaction ran faster than with proline itself, however with an actual catalyst loading of 52 mol% of proline (compared to 20 mol% for the free proline). A negative dendritic effect was observed when the higher dendrimers generations **164**-**166** were used, with both the activity and the enantioselectivity decreasing.

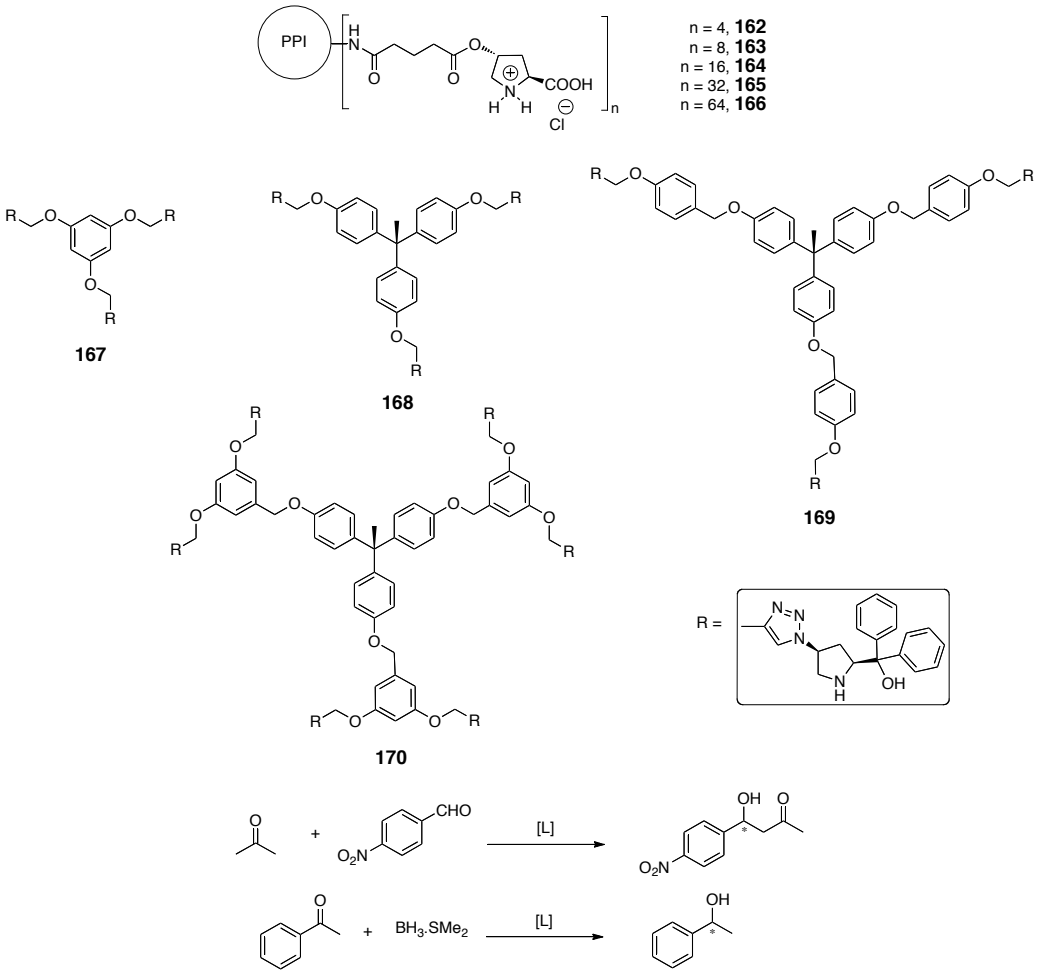

Figure 20. Dendrimer-immobilised proline derivatives.

Diphenylprolinol ligands were used by Liang *et al.* to decorate the periphery of different types of dendrimers with varying core moeities through triazole linkers (Figure 20).[65] Dendrimers **167**-**170** were used as catalysts in the enantioselective borane reduction of ketones where they proved to be excellent catalysts. Dendrimer **170** even showed a higher reactivity than the parent, monomeric diphenylprolinol catalyst

(95 % ee vs. 89 % ee). This hexa-prolinol dendrimer could be recycled by precipitation up to four times without appreciable loss of reactivity or enantioselectivity.

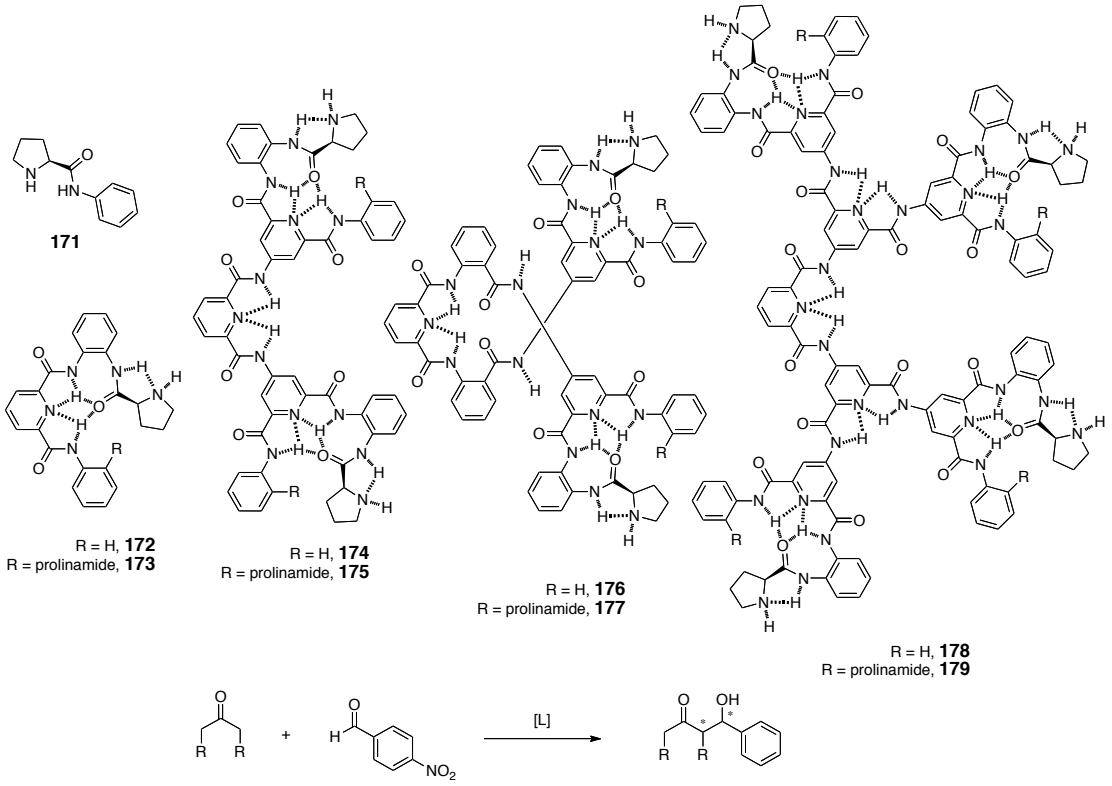

Figure 21. Parquette's proline derived dendrimers.

Parquette *et al.* prepared folded dendritic organocatalysts by attaching proline derivatives to pyridine-2,6-dicarboxyamide branching units and used dendrimers **172-179** in the asymmetric aldol reaction of 4-nitrobenzaldehyde with acyclic and cyclic ketones (Figure 21).[66] A significant increase in selectivity was observed when cyclic or substituted ketones were employed in these reactions (ee: 36-59 % to 63-92 %). Interestingly, the stereoselectivity turned out to be independent of the prolinamide density at the dendrimer periphery, i.e. no significant difference in ee was opbserved between compounds bearing all prolinamides or alternately (compounds with R = H or prolinamide).

1.3.2.2 Amino alcohol derivatives

Another early example in this field comes from Soai and coworkers, who reported the immobilisation of chiral ephedrine ligands on the periphery of different dendritic supports. The so-formed dendrimers were applied in the enantioselective catalytic

addition of dialkylzincs to aldehydes (Figure 22).[67, 68] After some investigations on the addition of dialkylzincs to *N*-diphenylphosphinylimines, the authors concluded on a negative interaction of the PAMAM support and restricted their study to the catalytic activity of dendrimers **182**-**185** with an inert backbone. These catalysts all exhibited a good activity for this reaction with excellent enantioselectivities (32-70 % yield and 77-86 % ee).

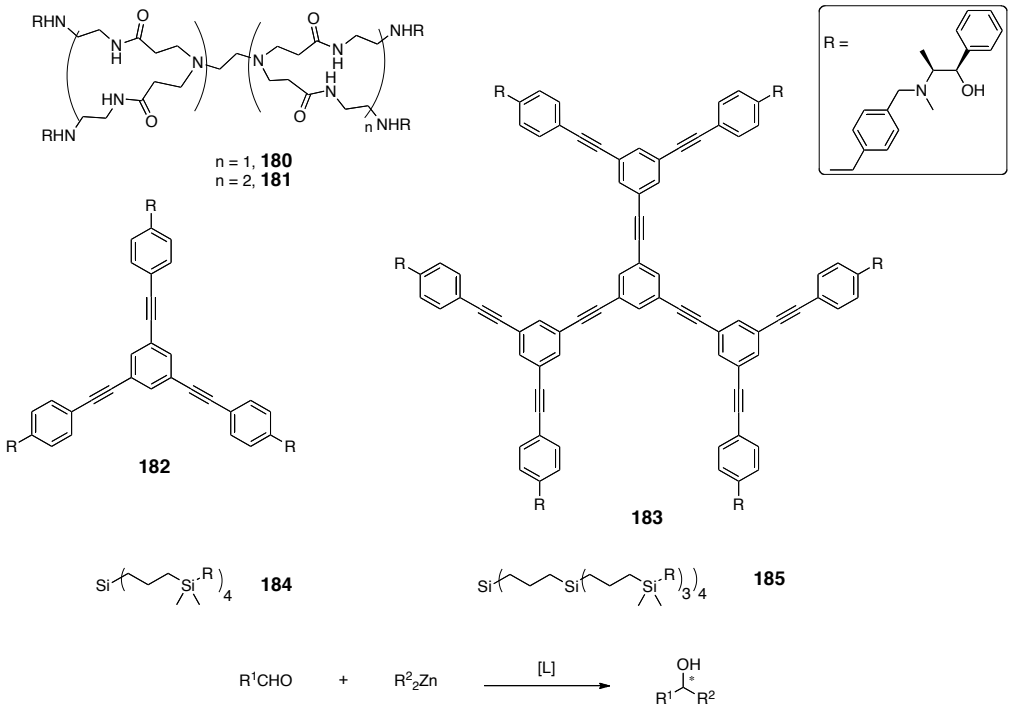

Figure 22. Ephedrine-derived ligand immobilised on different dendritic supports.

Later, Eilbracht and coworkers developed a new synthetic protocol for the preparation of polyamino alcohol dendrimers (not shown).[69] These polyamine-based dendrimers were employed in the ruthenium catalysed ATH reaction of acetophenone. The authors observed in general good to excellent conversions (71-86 %) and moderate to good ee's (22-69 % ee). Upon increase of the dendrimer generation, a negative dendritic effect on the enantioselectivity of the catalysts was observed.

1.3.2.3 Oxazoline derivatives

Recently, Gade et al. immobilised bis and tris(oxazoline)ligands on carbosilane dendrimers and investigated their efficiency as ligand in the copper(II) catalysed α-hydrazination of a β-keto ester as well as in the Henry reaction of 2-nitrobenzaldehyde

with nitromethane (Figure 23).[70] In the first reaction, the performances of ligands **186-194** proved to be excellent with good activities and enantioselectivities (90-99 % ee) obtained with a minimal catalyst loading of 1 mol%.

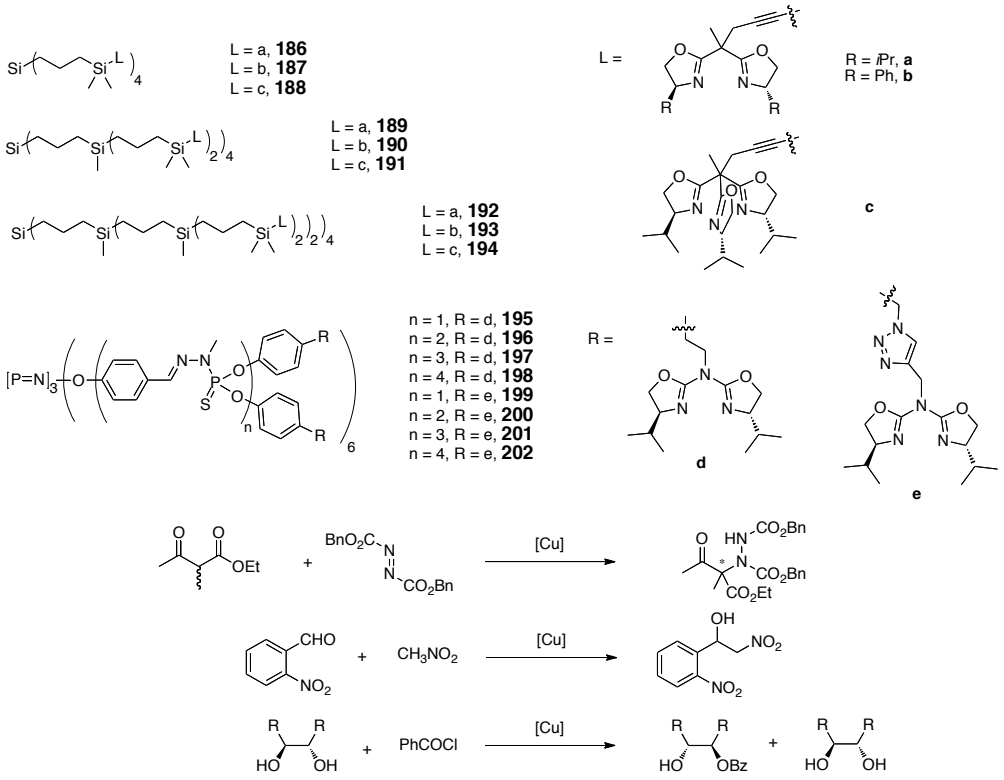

Figure 23. Dendrimer-immobilised bis and tris(oxazoline) ligands.

The activity of ligands **188**, **191** and **194** of the tris(oxazoline) series (type c) displayed a decreased reactivity in the Henry reaction compared to the bis(oxazoline) series (type b, Figure 22), albeit that the enantioseelctivitiy was higher for the tris(oxazolines) (81-84 % ee vs. 52-53 % ee). The latter series exhibited an improved reactivity and enantioselectivity compared to the parent compound, however without correlation with the dendrimer generation. In order to investigate the recyclability of dendrimers **190** and **191**, the catalysts were placed in a "tea-bag", a membrane bag made of dialysis tubing, and this "tea-bag" was placed in a fresh batch of substrates after a certain reaction time. The catalyst activity slightly decreased as well as the enantioselectivity; still displaying 77 % ee after the seventh run for **190** (compared to 82 % ee in the first run), but only 14 % ee for **191** (69 % ee in the first run).

The group of Majoral reported on the synthesis azabis(oxazoline) ligands immobilised on phosphorus-based dendrimers via click chemistry (Figure 23).[71] The

performance of ligands **199-202** was evaluated in the copper-catalysed asymmetric benzoylation of diols and compared with the performance of ligands **195-198**, in order to determine the influence of the backbone on the catalysis, in particular the influence of the triazole ring, which is known to coordinate to copper. The catalytic results indicated a moderate yield (34-41 %) but a good selectivity (73-80 % ee) for **195-198** and did not show any interference of the backbone on the catalytic activity, which suggested a strong affinity of the azabis(oxazoline) ligand for copper. Ligands **199-202** appeared to be less reactive (28-31 % yield) than **195-198,** however with similar enantioselectivities except for the higher generation dendrimer **202** (33 % ee). The recyclability of these catalysts by means of precipitation was also investigated with **200** and did not show any deterioration of the catalytic performances after three successive runs.

1.3.2.4 Other types of ligand

In a report from 2000, Jacobsen *et al.* reported the immobilisation of [Co^{III}(salen)] complexes on the periphery of PAMAM dendrimers (Figure 24).[72] By doing so, the authors were expecting the proximity of the metal centres, induced by the geometry of the dendrimer, to have a positive effect on the reactivity, as it was shown earlier that the mechanism of the asymmetric ring opening (ARO) of epoxides involves a cooperative bimetallic catalysis (i.e. a second order kinetic dependence on [Co^{III}(salen)]). Dendrimers **203-205** were then employed in the hydrolytic kinetic resolution (HKR) of terminal epoxides and showed a dramatic improvement of the reactivity relative to the monomer: at a catalyst loading of 0.025 mol% no conversion was detected for the monomer whereas with 0.027 mol% of **204** 98 % ee was obtained with 50 % conversion. A further increase of the dendrimer generation, and accordingly the number of [Co^{III}(salen)] units per dendrimer, resulted in a decrease in activity/selectivity (relative rate going from 24 to 11 and ee from 42.8 to 39.8 %). According to the authors, this positive dendritic effect may be attributed to higher order productive cooperative interactions between the [Co^{III}(salen)] units, that apparently were most optimal in **204**.

In a continuation of their work on the influence of the dendritic backbone on the ruthenium-catalysed ATH reaction of pro-chiral ketones with chiral diamine ligands (see Figure 9), Deng and coworkers reported the synthesis of dendrimers functionalised at the periphery with TsDPEN-derived ligands (Figure 24).[73] The performance of dendrimers **206-208** was investigated in the ATH of acetophenone and showed good activities

(97 % conversion) and enantioselectivities (97.6 % ee), which were comparable to the monomeric TsDPEN catalyst (>99 % conversion and 97.7 % ee). The scope of the reaction was extended to other ketones and imines and showed in general good activities and enantioselectivities.

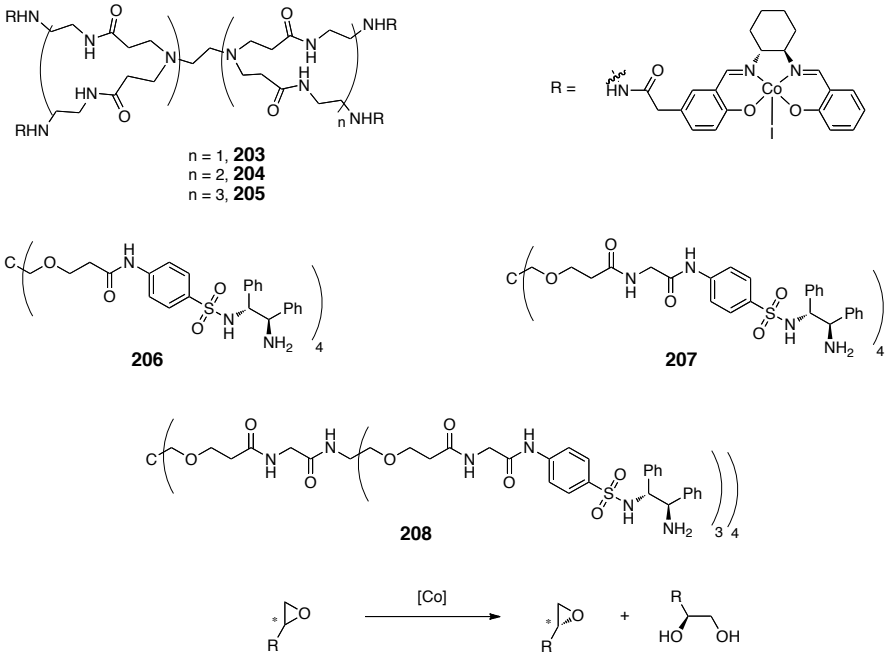

Figure 24. Other types of peripherally immobilised ligands.

1.3.3 Oxygen-based ligands

In 2002, Sasai and coworkers synthesised polyether dendrimers **209**-**210** functionalised with BINOL ligands at their periphery and the corresponding hetero bimetallic catalysts, synthesised by coordination of the BINOL ligands with the complex AlLibis(binaphtoxide) containing aluminium and lithium metals (Figure 25).[74] These dendrimers were used as catalysts in the Michael addition of dibenzylmalonate to 2-cyclohexanone and exhibited a moderate activity (57-63 % yield) but excellent enantioselectivity (91-94 % ee). No evidence of the influence of the dendrimer size could be observed and the catalyst could be reused without showing a diminished activity.

In a report by Ma *et al.*, the synthesis of BINOL ligands **211**-**212** immobilised on Fréchet type dendrimers is presented.[74] Their use as catalysts in the asymmetric addition of diethyl zinc to benzaldehyde (reaction shown in Figure 22) was evaluated and revealed a good activity (94-96 % yield) and enantioselectivity (87.1-89.2 % ee) with all the catalysts in the presence of Ti(O*i*Pr)$_4$, similar to the reactivity of the non-immobilised

BINOL ligand. Interestingly, without addition of $Ti(OiPr)_4$ the dendrimers showed a good activity (75-78 %) and moderate enantioselectivity (40 % ee), though significantly higher than the BINOL ligand (17 % yield and 5.2 % ee). The dendritic catalyst was precipitated at the end of the reaction and reused in two extra catalytic runs without loss of reactivity.

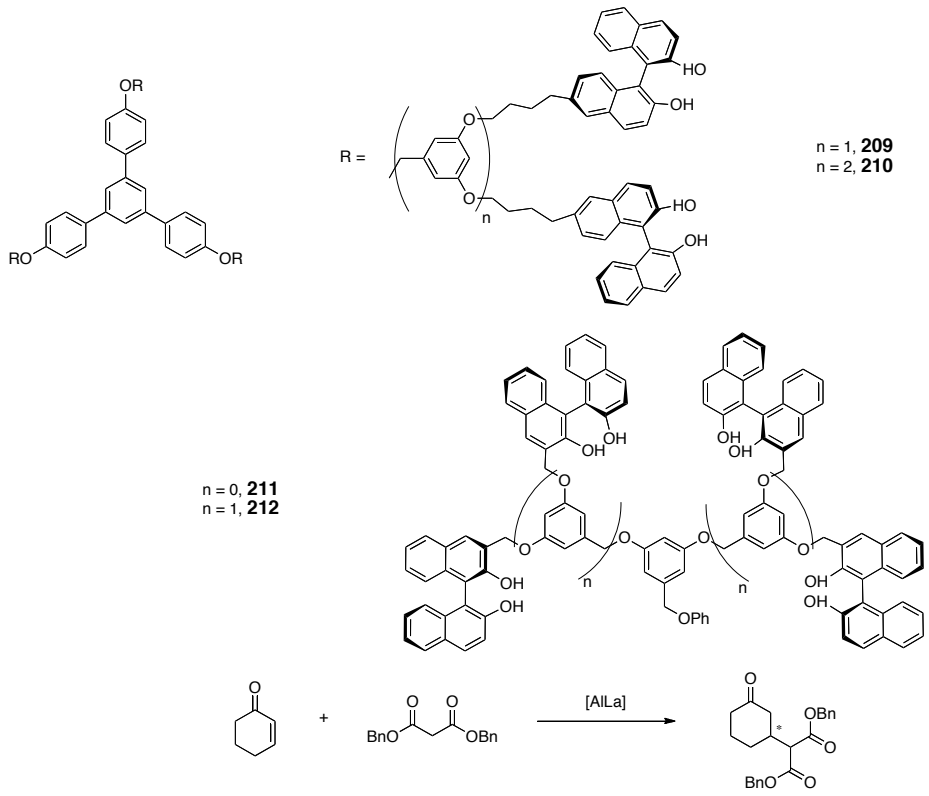

Figure 25. Immobilised BINOL ligands.

1.4 Concluding remarks

After about fifteen years of active research, the field of catalytic metallodendrimers has seen many advances, particularly in enantioselective catalysis. In its early days, the idea of using a chiral dendrimer that would be able to induce chirality to a non-chiral reaction site over a long distance range was a tempting concept. Investigations on this concept were never successful so far and lead to a general consensus that enantioselectivity can only be induced if chirality is present in the close vicinity of the metal centre.

The success of the dendrimer immobilisation approach was validated by the induction of enantiomeric product excesses observed in both types of catalyst attachments, either when the catalyst is shielded by the core of a dendrimer or dendron or when it is more exposed on the surface on a dendrimer. These investigations have also shown that the dendrimer backbone itself can be responsible for an enhancement of the catalytic activity or enantioselectivity through steric congestion induced by increasing dendrimer generation. This dendritic effect is in most cases limited to a size range above which catalytic sites are hardly accessible or where the ever closer proximity of metallic centres interferes with their activity, even though this interference can be constructive in some rare cases. The recyclability of the catalyst via different methods, i.e. precipitation or filtration, gave interesting results, nevertheless little care is taken to really "measure" the activity of the recovered catalyst by for example determining the kinetic profiles upon reuse of the dendritic catalyst, which would be indicative of a truly unaltered catalyst performance.

These findings are now of crucial importance to make progression towards 'the Holy Grail' of homogeneous catalysis: the synthesis of highly (enantio)selective catalysts that are recoverable and reusable without alteration of their performance. In order to reach this goal it is expected that ligand and dendrimer design have to go hand in hand with kinetic studies and advanced separation technology.

1.5 References

[1] Q. H. Fan, Y. M. Li, A. S. C. Chan, *Chem. Rev.* **2002**, *102*, 3385-3465.

[2] J. M. Fraile, J. I. Garcia, J. A. Mayoral, *Chem. Rev.* **2009**, *109*, 360-417.

[3] J. M. Fraile, J. I. Garcia, C. I. Herrerias, J. A. Mayoral, E. Pires, *Chem. Soc. Rev.* **2009**, *38*, 695-706.

[4] A. F. Trindade, P. M. P. Gois, C. A. M. Afonso, *Chem. Rev.* **2009**, *109*, 418-514.

[5] Y. Ribourdouille, G. D. Engel, L. H. Gade, *C. R. Chimie* **2003**, *6*, 1087-1096.

[6] J. K. Kassube, L. H. Gade, *Top. Organomet. Chem.* **2006**, *20*, 60-91.

[7] A. M. Caminade, P. Servin, R. Laurent, J. P. Majoral, *Chem. Soc. Rev.* **2008**, *37*, 56-67.

[8] H. Brunner, J. Furst, *Tetrahedron* **1994**, *50*, 4303-4310.

[9] H. Brunner, *J. Organomet. Chem.* **1995**, *500*, 39-46.

[10] Q. H. Fan, Y. M. Chen, X. M. Chen, D. Z. Jiang, F. Xi, A. S. C. Chan, *Chem. Commun.* **2000**, 789-790.

[11] G. J. Deng, Q. H. Fan, X. M. Chen, D. S. Liu, A. S. C. Chan, *Chem. Commun.* **2002**, 1570-1571.

[12] Z. J. Wang, G. J. Deng, Y. Li, Y. M. He, W. J. Tang, Q. H. Fan, *Org. Lett.* **2007**, *9*, 1243-1246.

[13] G. J. Deng, G. R. Li, L. Y. Zhu, H. F. Zhou, Y. M. He, Q. H. Fan, Z. G. Shuai, *J. Mol. Catal. A: Chem.* **2006**, *244*, 118-123.

[14] B. Yi, Q. H. Fan, G. J. Deng, Y. M. Li, L. Q. Qiu, A. S. C. Chan, *Org. Lett.* **2004**, *6*, 1361-1364.

[15] B. Yi, H. P. He, Q. H. Fan, *J. Mol. Catal. A: Chem.* **2010**, *315*, 82-85.

[16] L. I. Rodriguez, O. Rossell, M. Seco, G. Muller, *Organometallics* **2008**, *27*, 1328-1333.

[17] D. J. M. Snelders, K. Kunna, C. Muller, D. Vogt, G. van Koten, R. J. M. Klein Gebbink, *Tetrahedron: Asymmetry* **2010**, *21*, 1411-1420.

[18] Y. Li, Y. M. He, Z. W. Li, F. Zhang, Q. H. Fan, *Org. Biomol. Chem.* **2009**, *7*, 1890-1895.

[19] P. N. M. Botman, A. Amore, R. van Heerbeek, J. W. Back, H. Hiemstra, J. N. H. Reek, J. H. van Maarseveen, *Tetrahedron Lett.* **2004**, *45*, 5999-6002.

[20] M. van den Berg, A. J. Minnaard, E. P. Schudde, J. van Esch, A. H. M. de Vries, J. G. de Vries, B. L. Feringa, *J. Am. Chem. Soc.* **2000**, *122*, 11539-11540.

[21] W. J. Tang, Y. Y. Huang, Y. M. He, Q. H. Fan, *Tetrahedron: Asymmetry* **2006**, *17*, 536-543.

[22] F. Zhang, Y. Li, Z. W. Li, Y. M. He, S. F. Zhu, Q. H. Fan, Q. L. Zhou, *Chem. Commun.* **2008**, 6048-6050.

[23] F. Zhang, Q. H. Fan, *Org. Biomol. Chem.* **2009**, *7*, 4470-4474.

[24] R. Noyori, S. Hashiguchi, *Acc. Chem. Res.* **1997**, *30*, 97-102.

[25] Y. C. Chen, T. F. Wu, J. G. Deng, H. Liu, Y. Z. Jiang, M. C. K. Choib, A. S. C. Chan, *Chem. Commun.* **2001**, 1488-1489.

[26] Y. C. Chen, T. F. Wu, L. Jiang, J. G. Deng, H. Liu, J. Zhu, Y. Z. Jiang, *J. Org. Chem.* **2005**, *70*, 1006-1010.

[27] W. G. Liu, X. Cui, L. F. Cun, J. Wu, J. Zhu, J. G. Deng, Q. H. Fan, *Synlett* **2005**, 1591-1595.

[28] W. G. Liu, X. Cui, L. F. Cun, J. Zhu, J. Deng, *Tetrahedron: Asymmetry* **2005**, *16*, 2525-2530.

[29] L. Jiang, T. F. Wu, Y. C. Chen, J. Zhu, J. G. Deng, *Org. Biomol. Chem.* **2006**, *4*, 3319-3324.

[30] W. W. Wang, Q. R. Wang, *Chem. Commun.* **2010**, *46*, 4616-4618.

[31] X. Y. Liu, X. Y. Wu, Z. Chai, Y. Y. Wu, G. Zhao, S. Z. Zhu, *J. Org. Chem.* **2005**, *70*, 7432-7435.

[32] C. Bolm, N. Derrien, A. Seger, *Synlett* **1996**, 387-388.

[33] G. Y. Wang, X. Y. Liu, G. Zhao, *Synlett* **2006**, 1150-1154.

[34] X. Y. Liu, Y. W. Li, G. Y. Wang, Z. Chai, Y. Y. Wu, G. Zhao, *Tetrahedron: Asymmetry* **2006**, *17*, 750-755.

[35] G. Y. Wang, C. W. Zheng, G. Zhao, *Tetrahedron: Asymmetry* **2006**, *17*, 2074-2081.

[36] Y. W. Li, X. Y. Liu, G. Zhao, *Tetrahedron: Asymmetry* **2006**, *17*, 2034-2039.

[37] Y. H. Zhao, C. W. Zheng, G. Zhao, W. G. Cao, *Tetrahedron: Asymmetry* **2008**, *19*, 701-708.

[38] G. H. Lv, R. H. Jin, W. P. Mai, L. X. Gao, *Tetrahedron: Asymmetry* **2008**, *19*, 2568-2572.

[39] Y. Y. Wu, Y. Z. Zhang, M. L. Yu, G. Zhao, S. W. Wang, *Org. Lett.* **2006**, *8*, 4417-4420.

[40] C. M. Lo, H. F. Chow, *J. Org. Chem.* **2009**, *74*, 5181-5191.

[41] M. Malkoch, K. Hallman, S. Lutsenko, A. Hult, E. Malmstrom, C. Moberg, *J. Org. Chem.* **2002**, *67*, 8197-8202.

[42] B. Y. Yang, X. M. Chen, G. J. Deng, Y. L. Zhang, Q. H. Fan, *Tetrahedron Lett.* **2003**, *44*, 3535-3538.

[43] H. Liu, D. M. Du, *Eur. J. Org. Chem.* **2010**, 2121-2131.

[44] P. B. Rheiner, H. Sellner, D. Seebach, *Helv. Chim. Acta* **1997**, *80*, 2027-2032.

[45] P. B. Rheiner, D. Seebach, *Chem. Eur. J.* **1999**, *5*, 3221-3236.

[46] S. Yamago, M. Furukawa, A. Azuma, J. Yoshida, *Tetrahedron Lett.* **1998**, *39*, 3783-3786.

[47] Q. H. Fan, G. H. Liu, X. M. Chen, G. J. Deng, A. S. C. Chan, *Tetrahedron: Asymmetry* **2001**, *12*, 1559-1565.

[48] G. H. Liu, W. J. Tang, Q. H. Fan, *Tetrahedron* **2003**, *59*, 8603-8611.

[49] B. M. Ji, Y. Yuan, K. L. Ding, A. B. Meng, *Chem. Eur. J.* **2003**, *9*, 5989-5996.

[50] G. Guillena, R. Kreiter, R. van de Coevering, R. J. M. Klein Gebbink, G. van Koten, P. Mazon, R. Chinchilla, C. Najera, *Tetrahedron: Asymmetry* **2003**, *14*, 3705-3712.

[51] C. Jahier, M. Cantuel, N. D. McClenaghan, T. Buffeteau, D. Cavagnat, F. Agbossou, M. Carraro, M. Bonchio, S. Nlate, *Chem. Eur. J.* **2009**, *15*, 8703-8708.

[52] C. Kollner, B. Pugin, A. Togni, *J. Am. Chem. Soc.* **1998**, *120*, 10274-10275.

[53] R. Schneider, C. Kollner, I. Weber, A. Togni, *Chem. Commun.* **1999**, 2415-2416.

[54] C. Kollner, A. Togni, *Can J Chem* **2001**, *79*, 1762-1774.

[55] G. D. Engel, L. H. Gade, *Chem. Eur. J.* **2002**, *8*, 4319-4329.

[56] Y. Ribourdouille, G. D. Engel, M. Richard-Plouet, L. H. Gade, *Chem. Commun.* **2003**, 1228-1229.

[57] J. K. Kassube, H. Wadepohl, L. H. Gade, *Adv. Synth. Catal.* **2008**, *350*, 1155-1162.

[58] L. Routaboul, S. Vincendeau, C. O. Turrin, A. M. Caminade, J. P. Majoral, J. C. Daran, E. Manoury, *J. Organomet. Chem.* **2007**, *692*, 1064-1073.

[59] R. Laurent, A. M. Caminade, J. P. Majoral, *Tetrahedron Lett.* **2005**, *46*, 6503-6506.

[60] L. I. Rodriguez, O. Rossell, M. Seco, A. Grabulosa, G. Muller, M. Rocamora, *Organometallics* **2006**, *25*, 1368-1376.

[61] L. I. Rodriguez, O. Rossell, M. Seco, A. Orejon, A. M. Masdeu-Bulto, *J. Organomet. Chem.* **2008**, *693*, 1857-1860.

[62] L. I. Rodriguez, O. Rossell, M. Seco, G. Muller, *J. Organomet. Chem.* **2007**, *692*, 851-858.

[63] L. I. Rodriguez, O. Rossell, M. Seco, G. Muller, *J. Organomet. Chem.* **2009**, *694*, 1938-1942.

[64] E. Bellis, G. Kokotos, *J. Mol. Catal. A: Chem.* **2005**, *241*, 166-174.

[65] Y. N. Niu, Z. Y. Yan, G. Q. Li, H. L. Wei, G. L. Gao, L. Y. Wu, Y. M. Liang, *Tetrahedron: Asymmetry* **2008**, *19*, 912-920.

[66] K. Mitsui, S. A. Hyatt, D. A. Turner, C. M. Hadad, J. R. Parquette, *Chem. Commun.* **2009**, 3261-3263.

[67] I. Sato, T. Shibata, K. Ohtake, R. Kodaka, Y. Hirokawa, N. Shirai, K. Soai, *Tetrahedron Lett.* **2000**, *41*, 3123-3126.

[68] K. Soai, I. Sato, *C. R. Chimie* **2003**, *6*, 1097-1104.

[69] M. A. Subhani, K. S. Muller, P. Eilbracht, *Adv. Synth. Catal.* **2009**, *351*, 2113-2123.

[70] M. Gaab, S. Bellemin-Laponnaz, L. H. Gade, *Chem. Eur. J.* **2009**, *15*, 5450-5462.

[71] A. Gissibl, C. Padie, M. Hager, F. Jaroschik, R. Rasappan, E. Cuevas-Yanez, C. O. Turrin, A. M. Caminade, J. P. Majoral, O. Reiser, *Org. Lett.* **2007**, *9*, 2895-2898.

[72] R. Breinbauer, E. N. Jacobsen, *Angew. Chem. Int. Ed.* **2000**, *39*, 3604-3607.

[73] Y. C. Chen, T. F. Wu, J. G. Deng, H. Liu, X. Cui, J. Zhu, Y. Z. Jiang, M. C. K. Choi, A. S. C. Chan, *J. Org. Chem.* **2002**, *67*, 5301-5306.

[74] T. Arai, T. Sekiguti, Y. Iizuka, S. Takizawa, S. Sakamoto, K. Yamaguchi, H. Sasai, *Tetrahedron: Asymmetry* **2002**, *13*, 2083-2087.

CHAPTER TWO

Synthesis of Alkylsulfonate-functionalised NHC ligands: Characterisation and Coordination with Rh(I) and Ir(I) metal Centers

ABSTRACT

The synthesis of two butyl-sulfonate-functionalised imidazolium salts has been achieved and these compounds were used to prepare a series of transition metal complexes coordinated with sulfonate-functionalised N-Heterocyclic Carbene (NHC) ligands. The differences between the two NHC ligands were evidenced through the spectroscopic characterisation of metal complexes of the type [(NHC)MCl(cod)] (M = Rh, Ir), demonstrating the influence of the structural geometry of the ligand on the properties exhibited by the transition metal complexes.

2.1 Introduction

N-Heterocyclic carbene (NHCs) ligands have received more and more attention this last decade in particular because they have proven to be very versatile ligands in showing wide applicability in homogeneous catalysis.[1] These compounds are known to form very strong coordination bonds with a transition metal centre due to their excellent feature in terms of σ-donation, even surpassing the most electron donating of their concurrent phosphines.[2] The direct consequence of this property of NHC ligands is a strong coordination to the metallic centre, minimising the risks of metal-ligand bond rupture, which has to be minimal for enhanced catalyst activity. The success story of NHC ligands also originates from their ease of functionalisation. Their electronic and steric properties can indeed be fine-tuned to target a precise application of the metal complex. The electronic properties of the ligand have a direct influence -through the metal centre- on the elementary steps of the catalytic cycle. Following these findings, the need for NHC ligands with fine-tuned electronic properties and functionalities targeted to specific catalytic applications has naturally arisen. Rational design of ligands for specific catalytic applications is very important in the field of homogeneous catalysis as well as the need for specific functionalisations. In view of these new challenges, we designed and synthesised new types of sulfonate-functionalised NHC carbene ligands (see Figure 1).

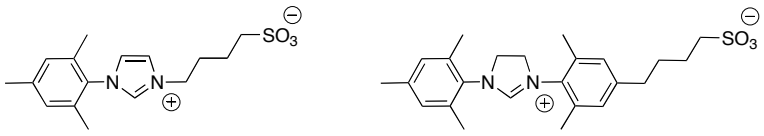

1 2

Figure 1. Mono-functionalised NHC carbene ligand precursors.

Elaboration of processes enabling the recovery of the homogeneous catalysts by means of biphasic systems or simply greener processes allowing the reaction to be performed in water are of great interest for industry, both from an environmental and an economic point of view.[3] Since the first industrial application of water-mediated homogeneous catalysis,[4] the use of sulfonate-modified phosphine ligands that render a catalyst water soluble has tremendously increased. Beyond the hydrophilicity brought by a sulfonate group, the functionalisation of a ligand by an ionic tag has several advantages

that can be employed notably in homogeneous catalyst immobilisation in ionic liquids, on dendrimers, on ion-exchange resins, and other insoluble supports.[5] Despite their potential applications, little has been done in the functionalisation of NHCs with sulfonate tags, nevertheless with promising results.[6-9] In 2006, Shaughnessy *et al.* reported on the synthesis of the first example of an alkylsulfonate-functionalised NHC ligand and their corresponding water-soluble silver and palladium complexes, although they did not apply them catalytically.[6] Shortly after this first report, Plenio described the synthesis and the successful application of sulfonated NHC ligands in palladium catalysed Suzuki cross-coupling reactions in water.[7] In the same year, Hoveyda published the synthesis of a sulfonated NHC ligand and its corresponding silver complex used as catalyst precursor in the copper catalysed asymmetric conjugate addition of organozinc species, however without making a clear usage of this functionality.[8] Very recently, the group of Nozaki reported on the synthesis of sulfonated NHC ligands and their corresponding palladium complexes, which interestingly coordinate to the palladium centre in a bidentate fashion.[9]

Here, we describe the synthesis of new sulfonate-functionalised NHC ligands with both a saturated and an unsaturated backbone and different substitution patterns and investigate their electronic properties as well as their coordination chemistry with Rh(I) and Ir(I) metal centres.

2.2 Results

Synthesis and characterisation of sulfonate-functionalised ligand precursors

There are several possible routes to synthesise NHC carbene ligand precursors, also called imidazolium salts.[10] The most common ones are the quaternisation of the second nitrogen atom of an imidazole precursor with a suitable electrophile or the synthesis of the imidazole heterocycle by a condensation reaction. Tuning of the imidazolium salts by introduction of a specific substitution pattern can increase the difficulty of the synthesis of the NHC carbene precursor. There is indeed no simple and efficient method to synthesise *N, N* unsymmetrical diaryl NHC ligands, although such ligands can be highly interesting from a catalytic point of view.

Following the quaternisation strategy, the synthesis of functionalised alkyl sulfonate imidazolium compound **1** is efficiently achieved by reacting 1,4-butane sultone and *N*-mesityl imidazole in toluene (Scheme 1).[11] This reaction led to the quantitative formation of an unsymmetrical imidazolium salt with a butyl sulfonate chain directly connected to the heterocycle.

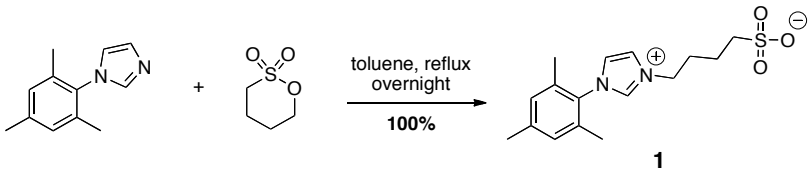

Scheme 1. Synthesis of sulfonate-functionalised imidazolium **1**.

The imidazolium ligand precursor 1 crystallised from a saturated dichloromethane solution, enabling an X-ray crystal structure determination. The molecular structure of **1**, as shown in Figure 2, shows that the planes of the heterocycle and the mesityl ring are close to orthogonality as indicated by the torsion angle C9-C4-N1-C2 = -99.5(2)°. The torsion angle between the imidazolium and the alkyl sulfonate chain is C14-C13-N2-C1 = -120.9(2)°, indicative of a *gauche* conformation.

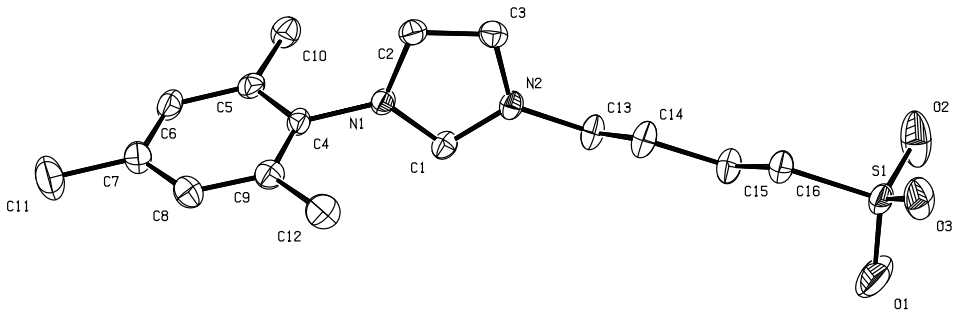

Figure 2. Displacement ellipsoid plot (50% probability level) of the asymmetric unit of **1** at 150(2) K. H atoms are omitted for clarity.

The molecular structure of the NHC ligand precursor **1** was compared to similar imidazolium salts, **I1** reported by Shaughnessy *et al.*[6] and **I2** reported by Nozaki *et al.*,[9] which have a shorter appended alkyl sulfonato chain:

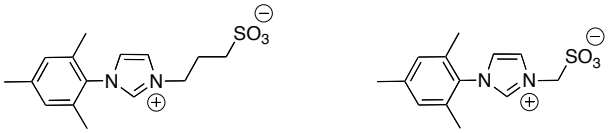

I1 **I2**

Figure 3. Reported mono-alkysulfonate imidazolium salts.

Table 1. Selected bond distances (Å) and angles (deg) in the crystal structures of compounds **1**, **I1**, and **I2**.

	1[a]	**I1**[b]	**I2**[c]
	Bond Length		
N1-C1	1.332(3)	1.341(2)	1.342(8)
N2-C1	1.322(3)	1.330(2)	1.334(7)
C2-C3	1.344(3)	1.349(2)	1.354(8)
	Bond Angles		
N1-C1-N2	107.84(17)	108.1(1)	107.9(3)

Crystal structure determined at [a] 150(2) K, [b] 173(2) K, [c] 103(3) K.

Variation of the bond lengths of the heterocycle can be induced by an increased or decreased aromatic character of the five-membered ring. This aromatic character can be influenced by the electronic effects of the *N* substituents of the heterocycle. In the examples presented in Table 1, the geometries of the heterocycles of the different imidazolium salts are equal within standard uncertainties, independent of the chain lengths.

Our interest then focused on the synthesis of *N*,*N*'-diaryl substituted imidazolidinium salts, which are thought to possess a higher catalytic reactivity due to their specific hindrance and basicity.[12] The increased sigma donation of this type of ligands has a direct influence on the properties of the transition metal complex, e.g. its robustness, its higher catalytic activity.[13, 14] In order to address the question of the steric influence of the NHC compounds on metal coordination, we were interested in the synthesis of an *N*,*N*'-diaryl substituted imidazolium salt. For this type of compounds, direct functionalisation of an already prepared imidazole is not an option due to the poor

nucleophilic nature of *N*-aryl imidazoles towards hindered aryl halides. This type of imidazolinium salt is however readily accessible by a condensation reaction with a suitable bisamine (Scheme 2).[15]

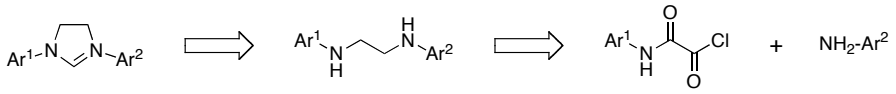

Scheme 2. Retrosynthetic preparation of N,N'-diaryl substituted imidazolidinium salts.

The unsymmetric saturated NHC ligand precursor **2** was synthesised through a multi step procedure starting from the methylisobutylsulfonate **3** (Scheme 3).[16] This sulfonic ester was subjected to a lithiation with *n*-BuLi in THF at -78 °C and the resulting lithiated species was reacted *in situ* with allyl bromide allowing the formation of compound **4** by nucleophilic substitution in 62 % isolated yield.[17] Hydroboration of **4** with 9-BBN and subsequent Suzuki coupling with 2,6-dimethyl-4-bromoaniline using $Pd(PPh_3)_4$ as catalyst in combination with NaOH afforded the functionalised aniline **5** in 86 % yield. The functionalised aniline **5** was reacted with 2-(mesitylamino)-2-oxoacetyl chloride[15] in the presence of NEt_3 to obtain the bisamide **6** in 68 % yield. Subsequent reduction of **6** using BH_3.THF led to the formation of the bis-amine **7** with 69 % yield.

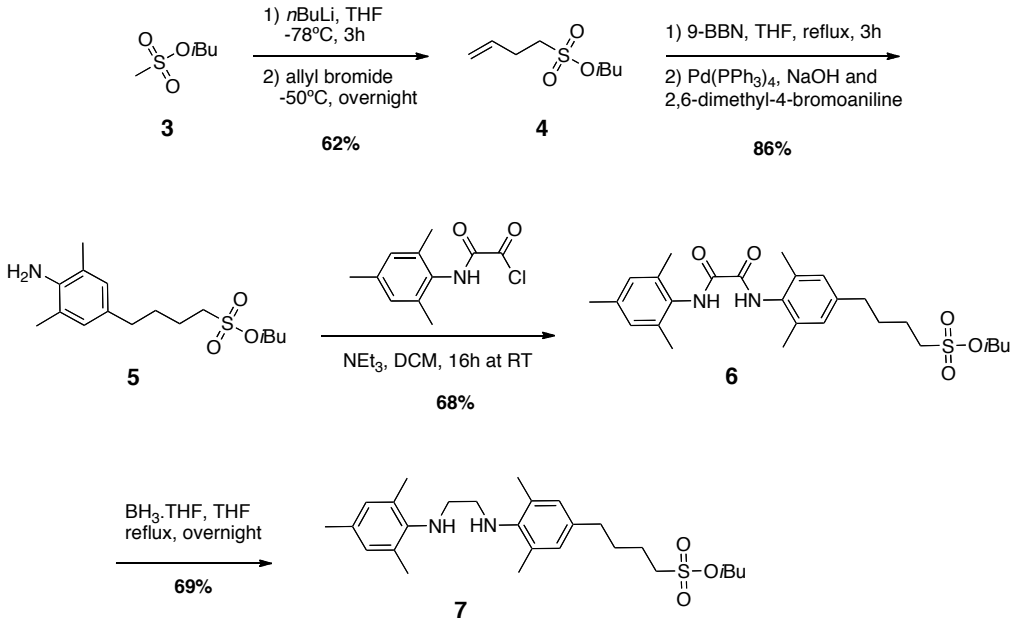

Scheme 3. Synthesis of the functionalised bisamine **7**.

Compound **2** was then synthesised either directly from **7** in triethyl orthoformate at reflux temperature for 1 h to give the expected product in 42 % yield or in a separate two steps procedure involving first the formation of the heterocycle in triethyl orthoformate to yield the sulfonate-protected compound **8** in 85 % yield and finally the deprotection of the sulfonic ester in presence of NaI to yield the imidazolinium salt **2** with 87 % yield (Scheme 4). Despite the more time consuming process, the two steps procedure happened to be more effective with an overall yield of 66 % than the direct synthesis from the compound **6**.

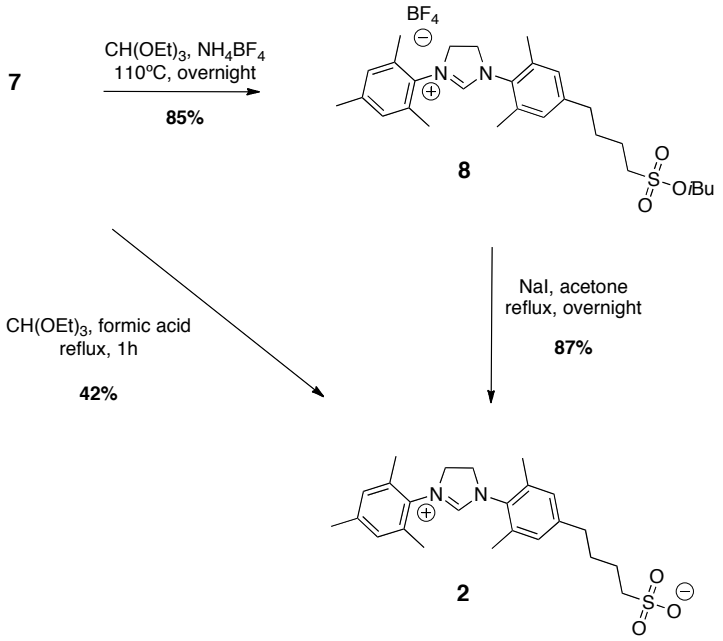

Scheme 4. Synthesis of the preligand **8**.

Synthesis of NHC Rh(I) and Ir(I) complexes

To evaluate the potential of sulfonate-functionalised NHCs as ligands for transition metal complexes, a series of Rh(I) and Ir(I) complexes were synthesised. The synthesis of transition metal complexes bearing NHCs ligands most commonly proceeds via two different routes: either the *in situ* deprotonation of the preligand with a strong non-nucleophilic base followed by coordination with a suitable metal precursor or the *in situ* formation of a [(NHC)-Ag] complex followed by transmetallation in the presence of an adequate transition metal precursor.[18] In order to avoid any side reactions that could occur in the presence of a strong base, the synthesis of the Rh(I) and Ir(I) complexes was attempted using the transmetallation approach as this technique involves milder conditions.

The imidazolium salt **1** was reacted with Ag_2O to form *in situ* a silver complex that subsequently acted as a carbene transfer agent in the presence of a suitable metal precursor, either $[RhCl(cod)]_2$ or $[IrCl(cod)]_2$ (Scheme 5). In order to ensure the electron neutrality of the transition metal complex -by providing a counter ion for the sulfonate moiety- and to avoid any chloride abstraction from the metal precursor, an ancillary organic salt, PPh_4Cl, was added to the reaction mixture (see Chapter Three). This strategy efficiently yielded the NHC-Rh(I) complex **9** and the NHC-Ir(I) complex **10** (see scheme 7) in 92 % and 30 % respectively. Alternatively, the NHC-Ag(I) intermediate may be isolated and used as a transmetallating agent (see Chapter Three).

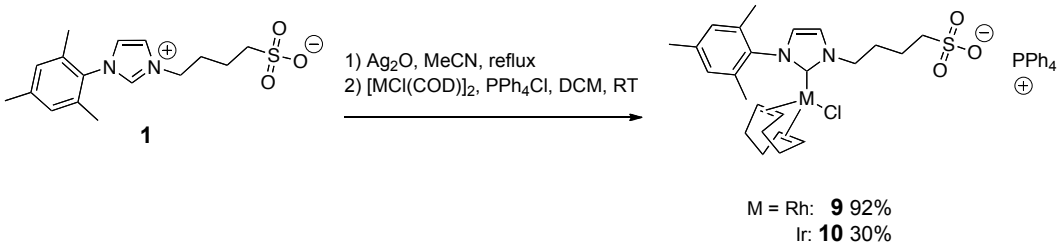

Scheme 5. Synthesis of Rh(I) and Ir(I) complexes **9** and **10**.

The imidazolinium ligand precursor **2** was reacted with Ag_2O to form a [(NHC)-Ag] complex followed by addition of the metal precursors. This strategy previously described did not lead to the formation of the desired NHC-Rh(I) complex or in a quantity so limited that it could only be detected by ESI-MS. Analysis of the reaction mixture by ^1H NMR did not give satisfying results, suggesting the presence of several species in the crude mixture. $^{13}C\{^1H\}$ NMR displayed two clear doublets at 207.7 ppm and 205.9 ppm with coupling constants $^1J(^{107}Ag\text{-}^{13}C)$ = 167.4 Hz and $^1J(^{109}Ag\text{-}^{13}C)$ = 192.9 Hz (Figure 3). The coupling constants nicely reflect the gyromagnetic ratio for the Ag nuclei and this typical pattern is clearly indicative of a carbene-Ag bond, thus of the presence of an NHC-Ag complex in the crude reaction mixture.

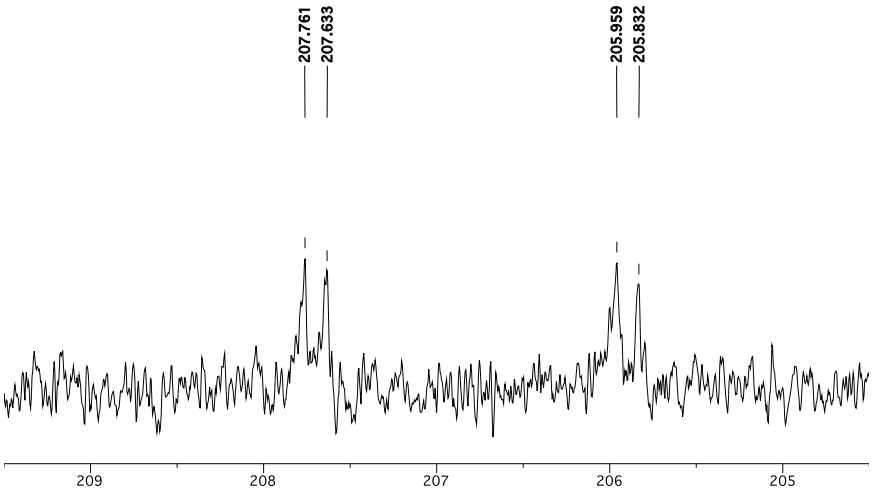

Figure 3. $^{13}C\{^{1}H\}$ NMR spectrum of the [(NHC)Ag] complex.

Solvent evaporation of the reaction mixture led to the formation of single crystals suitable for X-ray analysis. X-ray crystal structure elucidation unexpectedly showed that $[RhCl_2(cod)][PPh_4]$ had formed during the reaction (see Figure 4).

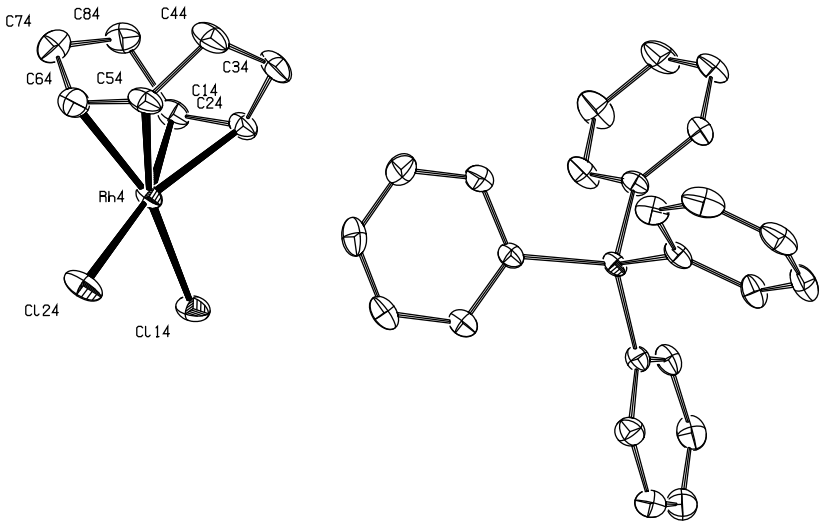

Figure 4. Displacement ellipsoid plot (50% probability level) of one of two independent molecules of the asymmetric unit of $[RhCl_2(cod)][PPh_4]$ at 150(2) K. Hydrogen atoms and CH_2Cl_2 solvent molecules are omitted for clarity. Selected bond length (Å): Rh4–Cl14 2.3881(7), Rh4–Cl24 2.3767(7), Rh4–C14 2.116(3), Rh4–C24 2.101(3), Rh4–C54 2.115(3), Rh4–C64 2.097(3).

The only connectivity between the anion and the cation in the molecular structure of $[RhCl_2(cod)][PPh_4]$ resides in the presence of weak hydrogen bonds.

The difficulties encountered to metallate preligand **2** by transmetallation prompted us to investigate another route, i.e. the *in situ* formation of the free carbene in the presence of a strong non-nucleophilic base and subsequent coordination with an appropriate metal precursor. This strategy was applied to the imidazolium salt **2**, using KO*t*Bu as the base, $[IrCl(cod)]_2$ or $[RhCl(cod)]_2$ as the metal precursor and again the ancillary organic salt PPh_4Cl (Scheme 6). After purification with silica gel column chromatography, the complexes **11** and **12** were obtained as yellow and orange solids in 56 % and 40 % yield, respectively.

Scheme 6. Synthesis of NHC-Rh(I) and NHC-Ir(I) complexes.

Characterisation

The high resolution ESI-MS spectra of compounds **9**-**12** were measured in negative ion mode, showing in all cases the presence of a typical anion peak corresponding to the metal complex of the form $[M - PPh_4]^-$:

Table 1. ESI-MS data for compounds **9**-**12**.

Compound	Formula	m/z calculated	m/z found
9	$C_{24}H_{33}ClN_2O_3RhS$	567.0955	567.0978
10	$C_{24}H_{33}ClN_2O_3IrS$	657.1530	657.1489
11	$C_{32}H_{43}ClN_2O_3RhS$	673.1738	673.1741
12	$C_{32}H_{43}ClN_2O_3IrS$	763.2312	763.2321

The ^1H NMR spectra of complexes **9** and **10** displayed splitted signals for the carbene ligand, especially for the aromatic protons of the mesityl group, indicating a hindered rotation around the metal-carbon bond ($M\text{-}C_{carb}$).[19] Variable temperature NMR study

conducted in $CDCl_3$ did not show any coalescence of the peaks up to 60 °C (higher temperature could not be reached because of the poor solubility of compounds **9** and **10** in high boiling point solvents). Interestingly, no such splitting was observed for compounds **11** and **12**. $^{13}C\{^1H]$ NMR spectra of the compounds **11** and **12** displayed a clear downfield shift of the carbenic carbon compared to compounds **9** and **10** (see Table 2). The $^1J_{C\text{-}Rh}$ coupling constant is also higher upon coordination with saturated ligand **2** as compared to ligand **1**. The $^{13}C\{^1H]$ NMR chemical shifts presented in Table 2 are consistent with data reported of similar compounds, for which an upfield shift is observed upon replacement of a lighter by a heavier metal. Saturation of the heterocycle of the imidazole induces a downfield shift of the carbene carbon for a similarly substituted ligand coordinated to the same metal centre.[20]

Table 2. $^{13}C\{^1H\}$ NMR chemical shift of C^2 for compounds **9-12**.[a]

Entry	δ (in ppm)	$^1J_{C\text{-}Rh}$ (in Hz)
9	181.2	51.2
10	179.1	
11	212.4	46.9
12	207.1	

[a] The NMR spectra were recorded in CD_2Cl_2 at 25 °C.

Synthesis and characterisation of [(NHC)MCl(CO)$_2$] (M = Rh, Ir) and IR spectroscopy

Formation of metal carbonyl complexes is a very convenient method to investigate the electronic properties of ligands. The basicity of the ligand has a direct influence on the carbonyl ligand, which can be estimated through spectroscopic methods, i.e. IR spectroscopy. Carbonyl complexes of the type [(NHC)MCl(CO)$_2$] can be easily synthesised from the [(NHC)MCl(cod)] complexes by bubbling CO through a solution of the metal complex in dichloromethane at room temperature, inducing a displacement of the bidentate cyclooctadiene ligand for two carbonyl ligands. The metal complexes **9-12** were quantitatively transformed into their carbonyl counter parts following this strategy (Scheme 7).

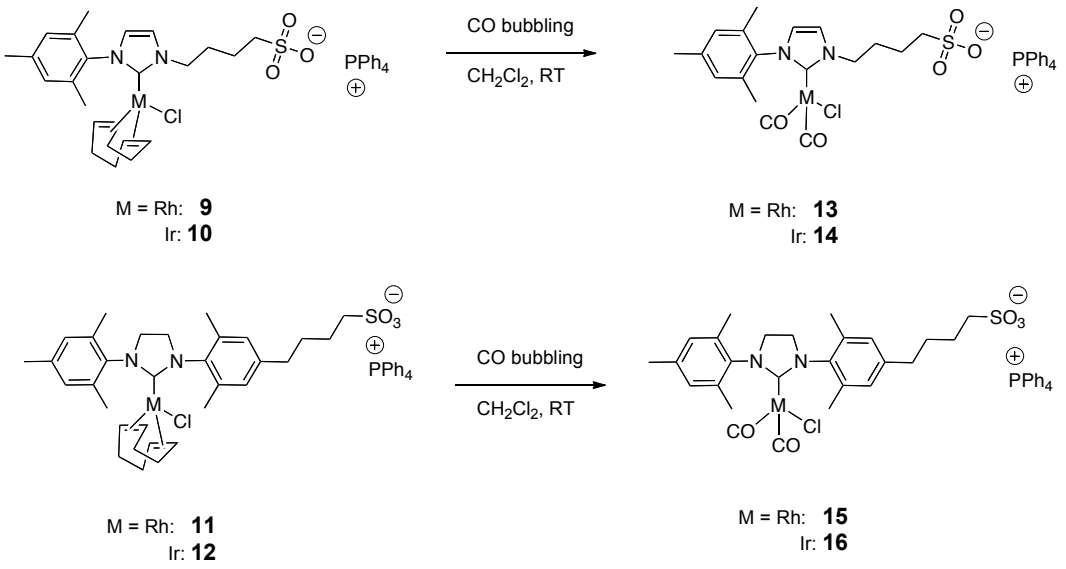

Scheme 7. Synthesis of bis-carbonyl NHC complexes **13-16**.

ESI-MS spectroscopy analysis of the compounds **13-16** in negative ion mode confirmed the successful formation of the carbonyl compounds, as evidenced by the presence of a characteristic anion peak for each complex (Table 3).

Table 3. Negative ion mode HR-MS of compounds **13-16**.

Compound	Formula[a]	m/z calculated	m/z found
13	$C_{18}H_{21}ClN_2O_5RhS$	514.9915	514.9938
14	$C_{18}H_{21}ClN_2O_5IrS$	605.0489	605.0508
15	$C_{26}H_{31}ClN_2O_5RhS$	621.0697	621.0699
16	$C_{26}H_{31}ClN_2O_5IrS$	711.1271	711.1255

[a] Refers to the anions of general formula $[M - PPh_4]^-$. The calculated and measured m/z values correspond to the monoisotopic masses.

The ^1H NMR spectra of compounds **13** and **14** did not show any splitting of the signals corresponding to the carbene ligand. Upon coordination of the carbonyl ligands, the steric hindrance observed for compounds **9** and **10** has totally disappeared. Attempts to measure $^{13}C\{^1H]$ NMR of the compounds **13-16** were unsuccessful. This is attributed to the fact that these compounds decompose in solution and therefore the longer measurement time required by the $^{13}C\{^1H]$ NMR spectroscopy is not compatible with the poor stability of these complexes.

The CO stretch vibration frequencies of compounds **13-16** were recorded in dichloromethane and the spectra displayed in all cases two characteristic bands of similar intensities. This feature is indicative of the *cis* geometry of the two carbonyl ligands for the square planar complexes. Table 4 reports the values obtained for **13** and **15** as well as data from literature for analogous Rh(I) complexes measured in dichloromethane (careful attention needs to be taken while compiling literature data, very often the values presented do not mention the conditions of the measurement). Similarly, Table 5 presents the CO stretch vibrations of compounds **14** and **16** along with values from the literature for similar compounds.

Table 4. CO stretch vibration of *cis*-[(**L**)RhCl(CO)$_2$].

Entry	L	ν**CO** (cm^{-1})	ν**CO$_{Av}$** (cm^{-1})
1	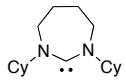	1976, 2062	2019[21]
2	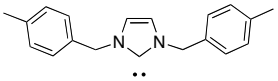	1995, 2076	2035.5[19]
3	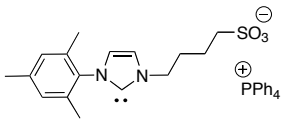	1998, 2078	2038
4	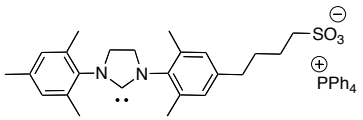	1996, 2081	2038.5
5	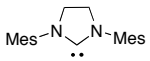	1996, 2081	2038.5[22]
6	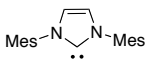	1997, 2081	2039[22]
7		2004, 2087	2045.5[23]
8		2005, 2090	2047.5[23]

The average carbonyl stretching frequency of **15** and **13** are identical with a wavenumber of 2038 cm^{-1} which is very similar to the one reported for the common SIMes ligand (entry 6).

Table 5. CO stretch vibration of *cis*-[(**L**)IrCl$(CO)_2$].

Entry	L	νCO (cm^{-1})	$νCO_{Av}$ (cm^{-1})
1	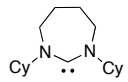	1973, 2058	2016[24]
2	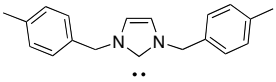	1976, 2063	2020[19]
3	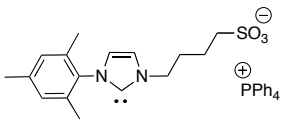	1981, 2065	2023
4	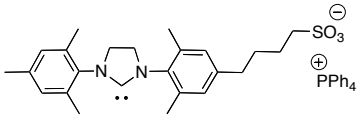	1980, 2066	2023
5	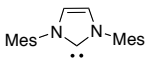	1979.8, 2066.4	2023.1[25]
6	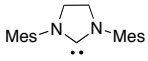	1981.2, 2068	2024.6[25]
7	PCy_3	1984, 2072	2028[19]
8	PPh_3[a]	2002, 2085	2043.5[19]

[a] Measured in $CHCl_3$.

The average frequencies for **14** and **16** exhibit the same value at 2023 cm^{-1} which is comparable to the IMes ligand (entry 5).

2.3 Discussion

This report presents the synthesis of new alkylsulfonate-functionalised NHC ligands with structural variations of the heterocycle and the *N* substituents. Starting from the

imidazolium preligands, several Rh and Ir complexes were prepared that contain these "amphiphilic" ligands. The spectroscopic characterisation of these complexes has focused on the electronic nature of the new NHC-ligands and the possible relationship between these properties and those of the metal complexes.

The unsaturated ligand precursor **1** was characterised in the solid state and the structural features of its crystal structure were compared with those of homologous structures. The data presented in Table 1 show that the chain length of the alkyl sulfonate moiety has no remarkable influence on the bond length of the heterocycles of the different imidazolium salts. Even though we could presume that the sulfonate group can have a negative inductive effect on the heterocycle when the alkyl sulfonate chain is short enough inducing a decreased aromatic character of the five-membered ring of the imidazolium salts, no clear influence of the chain length on the aromatic character could be evidenced. This suggests that the alkyl sulfonate group has no real electronic influence on the imidazolium salts and we can extrapolate that the NHC carbene ligand will probably not be influenced by the sulfonate moiety either.

The coordination chemistry of ligands **1** and **2** differs drastically as could be expected in view of their very different structures. Where **1** can be introduced via transmetallation using its Ag-analogue, Rh(I) and Ir(I) complexes of **2** could not be obtained by transmetallation in this manner. Instead of a clean transmetallation, several species were observed in the reaction mixture by NMR. At the end of this reaction the [(NHC)Ag] complex that formed *in situ*, whose presence was elucidated by ^{1}H and $^{13}C\{^{1}H\}$ NMR, remained completely unaltered and a triphenylphosphonium dichlororhodate complex, $[RhCl_2(cod)][PPh_4]$, was formed. The presence of this complex was evidenced by X-ray analysis of single crystals obtained from the reaction mixture.

$$[(NHC)Ag] + ½\ [RhCl(cod)]_2 + PPh_4Cl \rightarrow [RhCl_2(cod)][PPh_4] + [(NHC)Ag]$$

The triphenylphosphonium dichlororhodate complex, which has already been reported with other counter cation,[26] is thought of not being as reactive as $[RhCl(cod)]_2$ towards transmetallation, probably because of its high electron richness. Furthermore, the coupling constants observed in $^{13}C\{^{1}H\}$ NMR for the [(NHC)Ag] complex are indicative

of relatively strong metal-carbon bonds, which translates into none or only slow exchange of the carbene moiety between silver atoms (at least on an NMR time scale).[20]

The $^{13}C\{^{1}H]$ NMR obtained for complexes **9-12** are displayed in Table 2 and show a downfield shift between **9/11** and **10/12** that can be clearly ascribed to the electronic variation between the two types of ligands. It is known that a comparison of identical substituted imidazol- and imidazolin-2-ylidenes reveals that saturation of the imidazole ring produces a downfield shift of the C^2 carbon.[20] Compounds **1** and **2** do not possess the same *N* substitution but the saturation of compound **2** can by itself explain the higher downfield shift observed. Nevertheless no conclusions can be drawn considering the σ-donating ability of the ligand based on these chemical shifts, the shifts being influenced by the Lewis acidity of the metal and this Lewis acidity being influenced by the donating ability of the ligand.[27] The coupling constants between two nuclei being directly related to the electron density present in the σ orbital of the metal-carbon bond,[28] we can reasonably assume that the lower ^{1}J(Rh-C) value observed for **11** reflects a higher σ-donor strength for **8** compared to **1**.

The differences observed between the two NHC alkyl sulfonate ligand precursors **1** and **2** prompted us to investigate further their intrinsic features and especially their electronic properties. Since the pioneering work of Tolman on the evaluation of electronic properties of phosphine ligands,[29] the use of metal carbonyl complexes has proven to be a very valuable method to assess the basicity of donating ligands, e.g. NHC ligands. The infrared carbonyl stretching frequencies of [(NHC)RhCl$(CO)_2$] and [(NHC)IrCl$(CO)_2$] complexes are well known methods to establish the electronic properties of *N*-heterocyclic carbene ligands and are nowadays preferred over the (toxic) [Ni$(CO)_3$L] system. The stretching vibration frequencies of the two carbonyl ligands are directly correlated to the amount of π-back donation and its magnitude is induced by the electron density on the metal centre, which depends mainly on the σ-donating ability of the NHC ligand.[30] σ-Donor ligands can therefore be compared to each other on the basis of the wavenumber of the CO stretching vibration band: the presence of a stronger σ-donor result in a lower wavenumber for the carbon monoxide bands. The Rh(I) complexes **13** and **15** were successfully synthesised and IR spectra of these complexes give identical results with an average frequency of $\nu(CO)_{av}$ = 2038 cm^{-1}. In this case the

IR analysis is therefore not indicative of the possible electronic differences between the ligand precursors **1** and **2**.

Ir(I) complexes **14** and **16** were successfully synthesised and compared with similar structures as well as with complexes bearing a phosphine ligand instead of an NHC ligand (see Table 4). Again the CO stretching vibration frequencies of **14** and **16** are identical and very similar to those obtained with the common IMes and SIMes ligands (entries 5 and 6 in Table 4). The basicity of the NHC ligands **1** and **2** is significantly higher than electron rich PCy_3 (entry 7), and this difference is even increased when compared to PPh_3 (entry 8).

As can be seen from this study, variations of the IR frequencies among the different NHC complexes are not very significant and render an unambiguous understanding of electronic properties difficult.[28] It is conceivable that other stereoelectronic effects influence the carbonyl ligands to such an extent that the IR frequencies may reflect steric effects of the ligand and not only electronic parameters.[31]

2.4 Conclusion

A new series of alkyl sulfonate-functionalised NHC ligands was successfully synthesised, displaying different saturation and substitution of the heterocycle. The consequence of these structural differences was investigated. The coordination chemistry of the zwitterionic ligand precursors was studied with Ir and Rh metal centre, showing fundamental differences in their behaviour. These differences were further studied through their carbonyl stretching frequencies, which were measured in order to give an insight in their donating abilities. Despite their obvious structural differences and chemical behavior, IR spectroscopy does not seem to be an appropriate method to estimate these differences. The catalytic activity of the new sulfonate-functionalised NHC metal complexes could bring new insights on the specificity of the ligands and through their reactivity enlighten the intrinsic properties of the sulfonate-functionalised carbene.

2.5 Experimental section

General information: All reactions (unless otherwise mentioned) were performed under a N_2 atmosphere using standard Schlenk techniques. Toluene, Et_2O and THF were dried by passage through purification columns and CH_2Cl_2 was dried over CaH_2. The solvents were degassed prior to use. All reagents were purchased from Aldrich or Acros and were used as received. $[IrCl(cod)]_2$,[32] $[RhCl(cod)]_2$,[33] mesitylimidazole,[34] oxo-(2, 4, 6-trimethylphenylamino)-acetylchloride[15] and 2, 6-dimethyl-4-bromoaniline[35] were synthesised according to literature procedures. ^1H and $^{13}C\{^1H\}$ NMR spectroscopic measurements were conducted on a Varian Inova 300 or a Varian Oxford AS400 spectrometer at 25 °C and chemical shifts (δ) are given in ppm referenced to the residual solvent peak. Coupling constants are given in Hertz (Hz). Time-of-flight electrospray ionisation mass spectra (ESI-MS) were measured by the Biomolecular Mass Spectrometry and Proteomics Group, Utrecht University, on a Micromass LC-T mass spectrometer (Waters, Manchester, UK), operating in negative ion mode. Samples were introduced at concentrations of 20-50 µM. The nanospray needle potential was typically set to 1300 V and the cone voltage to 20-60 V. The source block temperature was set to 80 °C. The Elemental Analyses were performed by Dornis and Kolbe, Mikroanalytische Laboratorium, Mülheim a/d Ruhr, Germany. Infrared spectra were recorded on a Perkin Elmer system 2000 FTIR instrument (res 4 cm^{-1}, 10 scans per spectrum, DTGS detector) using a fixed KBr 0,1 mm cell.

1-Mesityl-3-(4-sulfonatobutyl)imidazolium (1): Mesitylimidazole (2.044 g, 11 mmol) was added to a solution of 1,4-butane sultone (2.35 mL, 22 mmol) in dry toluene (40 mL). After 48 h of stirring at reflux temperature, a white suspension was obtained. The solids were filtered off and washed successively with toluene (10 mL) and acetone (15 mL) and dried in vacuum yielding **1** as a white solid (3.54 g, 100 %).
^1H NMR (300 MHz, DMSO-d_6): δ = 9.46 (s, 1H; NC*H*N), 8.11 (s, 1H; NCH_{IMes}), 7.94 (s, 1H; CHN_{IMes}), 7.14 (s, 2H; Ar*H* Mes), 4.32 (m, 2H; NC$H_2(CH_2)_3SO_3$), 2.48 (m, 2H; $N(CH_2)_3CH_2SO_3$), 2.33 (s, 3H; CH_3 Mes), 2.02 (s, 6H; CH_3 Mes), 2.02-1.96 (m, 2H; $NCH_2CH_2(CH_2)_2SO_3$), 1.60-1.54 (m, 2H; $N(CH_2)_2CH_2CH_2SO_3$). **$^{13}C\{^1H\}$ NMR (75 MHz, DMSO-d_6):** δ = 140.1, 137.4, 134.3, 131.1, 129.2, 123.9, 123.2, 50.3, 48.9, 28.4, 21.6, 20.6, 16.9. **Elemental Analysis:** Calculated for $C_{16}H_{22}N_2O_3S$: C, 59.60; H, 6.88; N, 8.69; O, 14.89; S, 9.95 Found: C, 59.53; H, 6.80; N, 8.56; O, 15.06; S, 9.91.

Isobutylmethanesulfonate (3): In a Schlenk flask were introduced isobutanol (4.87 g, 65.7 mmol), triethylamine (6.98 g, 69 mmol) and dry toluene (50 mL). The flask was then

cooled with an ice bath and mesylchloride (7.53 g, 65.7 mmol) was added dropwise. After addition, $HCl.NEt_3$ was filtered off and the solids were washed with toluene. The filtrate was washed with 1M HCl (20 mL) and with demineralised water (2 x 20 mL), dried over $MgSO_4$, filtered, concentrated *in vacuo* and vacuum distilled to give a colorless liquid (57.1 mmol, 87 %).

^{1}H NMR (300MHz, $CDCl_3$): δ = 3.97 (d, 2H, $^3J_{HH}$ 6.8 Hz; CH_2 *i*Bu), 2.98 (s, 3H; CH_3SO_3), 2.01 (m, 1H; C*H* *i*Bu), 0.97 (d, 6H, $^3J_{HH}$ 6.8 Hz; (CH_3)$_2$ *i*Bu). **^{13}C{^{1}H} NMR (75 MHz, $CDCl_3$):** δ = 75.9, 37.2, 28.3, 18.7. **Elemental Analysis:** Calculated for $C_5H_{12}O_3S$: C, 39.45; H, 7.95 Found: C, 39.52; H, 8.56.

Isobutyl but-3-ene-1-sulfonate (4): In a Schlenk flask was introduced a solution of isobutylmethanesulfonate **3** (1.19 g, 7.79 mmol) in THF (8.5 mL). The reaction mixture was cooled to –78 °C and *n*BuLi 1.6 M in hexane (3.48 mL, 5.56 mmol) was added dropwise. After 1 h of stirring at this temperature, the resulting solution was added via canula to a solution of allylbromide (0.605 g, 5 mmol) in THF (13 mL) and NMP (5 mL) previously cooled to –50 °C. The reaction mixture was stirred for overnight at –50 °C. The mixture was quenched with water (10 mL) and extracted with diethyl ether (3 x 20 mL). The crude product was concentrated *in vacuo* and purified by silica gel column chromatography using hexane/ether (8:2, v/v) as the eluent, yielding a colorless liquid (0.601 g, 62 %).

^{1}H NMR (400 MHz, $CDCl_3$): δ = 5.85-5.75 (m, 1H), 5.15-5.08 (m, 2H), 3.97 (d, 2H, $^3J_{HH}$ 6.8 Hz; CH_2 *i*Bu), 3.15 (t, 2H), 2.61-2.55 (q, 2H), 2.06-1.96 (m, 1H; C*H* *i*Bu), 0.97 (d, 6H, $^3J_{HH}$ 6.8 Hz; (CH_3)$_2$ *i*Bu). **^{13}C{^{1}H} NMR (100 MHz, $CDCl_3$):** δ = 133.8, 117.5, 75.6, 49.6, 28.4, 27.8, 18.7. **Elemental Analysis:** Calculated for $C_8H_{16}O_3S$: C, 49.97; H, 8.39; O, 24.96; S, 16.68 Found: C, 49.76; H, 8.34; O, 24.84; S, 16.78.

Isobutyl 4-(4-amino-3,5-dimethylphenyl)butane-1-sulfonate (5): In a Schlenk flask was introduced **4** (1.23 g, 6.37 mmol) followed by the addition of THF (30 mL). 9-BBN (0.933 g, 7.64 mmol) was added by small portion and the reaction mixture was refluxed for 3 h. After cooling to room temperature and degassing, the resulting mixture was transferred to a second Schlenk flask, preliminary filled with 2,6-dimethyl-4-bromoaniline (1.062 g, 5.31 mmol) and $Pd(PPh_3)_4$ (0.307 g, 0.265 mmol). NaOH 3M in degassed water (6.33 mL, 19.0 mmol) was subsequently added and the mixture was allowed to stir at 85 °C for 20 h. After removal of the volatiles, the residue was extracted with DCM (3 x 20 mL) and washed with NaOH 1M (2 x 15 mL). The organic layer was dried over $MgSO_4$ and concentrated *in vacuo*. The crude compound was purified by silica gel column chromatography using hexane/EtOAc (2:1, v/v) as the eluent to yield a yellowish oil (1.431 g, 86 %).

^{1}H NMR (300 MHz, $CDCl_3$): δ = 6.75 (s, 2H; Ar*H*), 3.95 (d, 2H, $^3J_{HH}$ 6.6 Hz; C*H*$_2$ *i*Bu), 3.09 (t, 2H, $^3J_{HH}$ = 7.5 Hz; C*H*$_2$S), 2.51 (t, 2H, $^3J_{HH}$ = 7.5 Hz; ArC*H*$_2$), 2.16 (s, 6H; ArC*H*$_3$) 2.05-1.96 (m, 1H; C*H* *i*Bu), 1.88-1.83 (m, 2H; C*H*$_2$CH$_2$S), 1.73-1.68 (m, 2H; ArCH$_2$C*H*$_2$), 0.97 (d, 6H, $^3J_{HH}$ 6.6 Hz; (C*H*$_3$)$_2$ *i*Bu). **^{13}C{^{1}H} NMR (100 MHz, $CDCl_3$):** δ = 141.1, 130.8, 128.4, 122.1, 75.6, 50.4, 34.6, 30.5, 28.5, 23.3, 18.9, 17.9. **Elemental Analysis:** Calculated for $C_{16}H_{27}NO_3S$: C, 61.31; H, 8.68; N, 4.47; O, 15.31; S, 10.23 Found: C, 61.20; H, 8.74; N, 4.41; O, 15.31, S, 10.40.

Isobutyl 4-(4-(2-(mesitylamino)-2-oxoacetamido)-3,5-dimethylphenyl)butane-1-sulfonate (6): A solution of the aniline **5** (3.00 g, 9.57 mmol) in dichloromethane (9 mL) and triethylamine (1.30 mL, 9.30 mmol) was added dropwise at 0 °C to oxo-(2, 4, 6-trimethylphenylamino)acetylchloride dissolved in 25 mL of dichloromethane (2.02 g, 8.94 mmol). The mixture was stirred for 15 min at this temperature and allowed to warm up to room temperature. After overnight stirring at ambient temperature, the reaction mixture was quenched with water, the organic phase was washed with water (3 x 25 mL) and finally dried over $MgSO_4$. The organic phase was concentrated *in vacuo* and the crude product recrystallised from cold Et_2O, yielding an off-white powder (3.31 g, 75 %).

^{1}H NMR (400 MHz, $CDCl_3$): δ = 8.90 (s, 1H; N*H*), 8.87 (s, 1H; N*H*), 6.92 (s, 2H; Ar*H*), 6.91 (s, 2H; Ar*H*), 3.97 (d, 2H, $^3J_{HH}$ = 6.8 Hz; C*H*$_2$ *i*Bu), 3.11 (t, 2H; $^3J_{HH}$ = 7.6 Hz; C*H*$_2$), 2.60 (t, 2H; $^3J_{HH}$ = 7.6 Hz; C*H*$_2$), 2.30 (s, 3H; C*H*$_3$ Mes), 2.22 (s, 6H, C*H*$_3$ Mes), 2.21 (s, 6H; C*H*$_3$ Mes), 2.07-1.97 (m, 1H; C*H* *i*Bu), 1.95-1.87 (m, 2H; C*H*$_2$), 1.80-1.73 (m, 2H; C*H*$_2$), 0.98 (d, 6H, $^3J_{HH}$ = 6.8 Hz; (C*H*$_3$)$_2$ *i*Bu). **^{13}C{^{1}H} NMR (100 MHz, $CDCl_3$):** δ = 158.4, 158.3, 141.0, 137.8, 135.1, 134.8, 130.4, 129.7, 129.2, 128.5, 75.4, 50.2, 34.9, 29.9, 28.4, 23.3, 21.1, 18.8, 18.6, 18.5. **Elemental Analysis:** Calculated for $C_{27}H_{38}N_2O_5S$: C, 64.51; H, 7,62; N, 5.57 Found: C, 64.45; H, 7.56; N, 5.51.

isobutyl 4-(4-((2-(mesitylamino)ethyl)amino)-3,5-dimethylphenyl)butane-1-sulfonate (7): A 1M solution of BH_3.THF in THF (6 mL, 6 mmol) was added to the solid oxamide **6** (0.471 g, 0.937 mmol) dissolved in 15 mL of THF and refluxed overnight. The resulting mixture was carefully quenched with water (5 mL) and the THF was evaporated. The water layer was extracted with diethyl ether (3 x 15 mL). The ether layer was dried with $MgSO_4$ and concentrated *in vacuo.* The product was purified with silica gel column chromatography using hexane/EtOAc (2:1, v/v) as eluent, yielding the pure compound as a colorless oil (0.304 g, 68 %).

^{1}H NMR (400 MHz, $CDCl_3$): δ = 6.84 (s, 2H; Ar*H*), 6.80 (s, 2H; Ar*H*), 3.96 (d, 2H, $^3J_{HH}$ = 6.4 Hz; CH_2 *i*Bu), 3.24 (m, 4H; NCH_2CH_2N), 3.10 (t, 2H, $^3J_{HH}$ = 7.8 Hz; $(CH_2)_3CH_2SO_3$), 2.53 (t, 2H, $^3J_{HH}$ = 7.4 Hz; $CH_2(CH_2)_3SO_3$), 2.31 (s, 6H; CH_3 Mes), 2.30 (s, 6H; CH_3 Mes), 2.24 (s, 3H; CH_3 Mes), 2.05-1.96 (m, 1H; C*H* *i*Bu), 1.93-1.85 (m, 2H; $(CH_2)_2CH_2CH_2SO_3$), 1.77-1.69 (m, 2H; $CH_2CH_2(CH_2)_2SO_3$), 0.98 (d, 6H, $^3J_{HH}$ = 6.8 Hz; $(CH_3)_2$ *i*Bu). **^{13}C{^{1}H} NMR (100 MHz, $CDCl_3$):** δ = 144.0, 143.1, 134.9, 131.8, 129.9, 129.8, 129.6, 128.9, 75.4, 50.3, 49.2, 49.1, 34.6, 30.1, 28.4, 23.2, 20.7, 18.8, 18.7, 18.5. **Elemental Analysis:** Calculated for $C_{27}H_{42}N_2O_3S$: C, 68.31; H, 8.92; N, 5.89 Found: C, 68.43; H, 8.87; N, 5.89.

(8): The bisamine **7** (2.00 g, 4.21 mmol) and NH_4BF_4 (0.442 g, 4.22 mmol) were dissolved in triethyl orthoformate (42 mL) and heated at 110 ºC. After 5 h of stirring, the mixture was cooled to room temperature and the triethyl orthoformate was decanted. The crude solid was dissolved in acetone and the product precipitated upon addition of EtO_2. The solids were filtered and the filtrate concentrated *in vacuo* to give a brown solid. The combined solids were precipitated several times to yield the pure imidazolinium salt as a white solid (2.04 g, 85 %).
^{1}H NMR (400 MHz, $CDCl_3$): δ = 7.96 (s, 1H; NC*H*N), 6.98 (s, 2H; Ar*H*), 6.99 (s, 2H; Ar*H*), 4.53 (s, 4H; NCH_2CH_2N), 3.97 (d, 2H, $^3J_{HH}$ = 6.4 Hz; CH_2 *i*Bu), 3.10 (t, 2H, $^3J_{HH}$ = 7.6 Hz; $(CH_2)_3CH_2SO_3$), 2.62 (t, 2H, $^3J_{HH}$ = 7.6 Hz; $CH_2(CH_2)_3SO_3$), 2.38 (s, 6H; CH_3 Mes), 2.36 (s, 6H; CH_3 Mes), 2.31 (s, 3H; CH_3 Mes), 2.06-1.99 (m, 1H; C*H* *i*Bu), 1.91-1.80 (m, 2H; $(CH_2)_2CH_2CH_2SO_3$), 1.80-1.73 (m, 2H; $CH_2CH_2(CH_2)_2SO_3$), 0.98 (d, 6H, $^3J_{HH}$ = 6.8 Hz; $(CH_3)_2$ *i*Bu). **^{13}C{^{1}H} NMR (100 MHz, CD_3OD):** δ = 161.0, 144.6, 140.8, 135.7, 135.4, 131.3, 131.2, 130.8, 130.7, 129.8, 129.3, 75.8, 51.3, 49.1, 34.4, 29.3, 28.4, 23.0, 19.9, 17.8, 16.6, 16.5. **Elemental Analysis:** Calculated for $C_{28}H_{41}BF_4N_2O_3S$: C, 58.74; H, 7.22; N, 4.89; Found: C, 58.75; H, 7.37; N, 4.81.

(2): The imidazolinium salt **8** (0.100 g, 0.175 mmol) and NaI (0.052 g, 0.347 mmol) were dissolved in 5 mL of acetone and refluxed for overnight. The off-white precipitate was collected by filtration and washed with acetone. The product was dissolved in MeOH and precipitated two times with EtO_2, yielding a white precipitate (0.065 g, 87 %).
This compound was also synthesised directly from the hydrochloride salt of **7** (0.180 g, 0.329 mmol) suspended in triethylorthoformate (3 mL, 18 mmol) and one drop of formic acid and the resulting mixture was heated at reflux temperature for 1h. After cooling to room temperature, hexane was added and the solution was stirred for 1h. The solids were collected by filtration, washed with hexane (3 x 10 mL) and dried under vacuum. The product was obtained as a white solid (0.06 g, 42 %).

^{1}H NMR (400 MHz, MeOH-d$_4$): δ = 8.88 (s, 1H, NC*H*N), 7.13 (s, 2H; Ar*H*), 7.10 (s, 2H; Ar*H*), 4.51 (s, 4H, NCH_2CH_2N), 2.77 (t, 2H, $^3J_{HH}$ = 7.2 Hz; $(CH_2)_3CH_2SO_3$), 2.64 (t, 2H, $^3J_{HH}$ = 6.9 Hz; $CH_2(CH_2)_3SO_3$), 2.41 (s, 3H; CH_3 Mes), 2.40 (s, 3H; CH_3 Mes), 2.33 (s, 3H; CH_3 Mes), 1.76-1.73 (m, 4H; $CH_2CH_2CH_2CH_2SO_3$). **^{13}C{^{1}H} NMR (100 MHz, MeOH-d$_4$):** δ = 162.3, 146.4, 142.0, 136.7, 136.6, 132.3, 132.0, 131.0, 130.6, 52.5, 52.4, 36.0, 31.2, 25.5, 21.1, 17.8, 17.7. **Elemental Analysis:** Calculated for $C_{24}H_{32}N_2O_3S$: C, 67.26; H, 7.53; N, 6.54; Found: C, 66.76; H, 7.52; N, 6.08.

(9): Compound **1** (0.336 g, 1.04 mmol) was dissolved in 20 mL of acetonitrile in the presence of Ag_2O (0.108 g, 0.466 mmol) and the mixture was refluxed overnight. The crude mixture was passed through a plug of celite and the resulting solution concentrated *in vacuo*. The product was dissolved in dichloromethane (10 mL) followed by addition of $[RhCl(cod)]_2$ (0.229 g, 0.466 mmol) and PPh_4Cl (0.120 g, 0.932 mmol). A white precipitate formed immediately and the reaction mixture was stirred at room temperature for one extra hour. After this time the reaction mixture was filtered over Celite and the solvent evaporated in vacuum. The resulting crude product was purified by column chromatography using a gradient of DCM/acetone from (1:1, v/v) to DCM/acetone/MeOH (32:64:4, v/v/v). The pure compound was obtained as a bright yellow solid (0.803 g, 95 %).

^{1}H NMR (400 MHz, CD_2Cl_2): δ = 7.90 (m, 4H; Ar*H* PPh_4), 7.75 (m, 8H; Ar*H* PPh_4), 7.61 (m, 8H; Ar*H* PPh_4), 7.11 (d, 1H, $^3J_{HH}$ = 1.6 Hz; NCH_{IMes}), 7.02 (s, 1H; Ar*H* Mes), 6.89 (s, 1H; Ar*H* Mes), 6.71 (d, 1H, $^3J_{HH}$ = 1.6 Hz; CHN_{IMes}), 5.15-5.08 (m, 1H; C*H* cod), 4.75-4.70 (m, 1H; C*H* cod), 4.58-4.53 (m, 1H; C*H* cod), 4.26-4.18 (m, 1H; C*H* cod), 3.39 (m, 1H; NC*H*H$(CH_2)_3SO_3$), 2.96 (m, 1H; NCH*H*$(CH_2)_3SO_3$), 2.77-2.70 (m, 2H; N$(CH_2)_3CH_2SO_3$), 2.32 (s, 3H, CH_3 Mes), 2.31 (s, 3H, CH_3 Mes), 2.39-2.27 (m, 2H; CH_2 cod), 2.24-2.17 (m, 2H; CH_2 cod), 2.15-2.05 (m, 2H; CH_2 cod), 1.95-1.85 (m, 2H; $NCH_2CH_2(CH_2)_2SO_3$), 1.78 (s, 3H; CH_3 Mes), 1.70-1.56 (m, 2H; CH_2 cod) 1.53-1.39 (m, 2H; $N(CH_2)_2CH_2CH_2SO_3$). **^{13}C{^{1}H} NMR (100 MHz, CD_2Cl_2):** δ = 181.4 (d, $^1J_{Rh\text{-}C}$ = 51.2 Hz; N*C*N), 138.5, 136.7, 136.4, 135.8 (d, $^4J_{P\text{-}C}$ = 3 Hz; PPh_4), 134.8, 134.5 (d, $^3J_{P\text{-}C}$ = 10.2 Hz; PPh_4), 130.7 (d, $^2J_{P\text{-}C}$ = 12.9 Hz; PPh_4), 129.2, 128.2, 122.9, 121.2. 117.6 (d, $^1J_{P\text{-}C}$ = 89 Hz; PPh_4), 96.4 (d, $^1J_{Rh\text{-}C}$ = 7.3 Hz), 95.8 (d, $^1J_{Rh\text{-}C}$ = 7 Hz), 68.4 (d, $^1J_{Rh\text{-}C}$ = 14.1 Hz), 67.6 (d, $^1J_{Rh\text{-}C}$ = 14.4 Hz), 51.5, 51.3, 33.8, 31.7, 30.3, 28.9, 28.2, 23.1, 20.8, 19.4, 17.6. **HRMS (ES^-):** calculated for $C_{24}H_{33}ClN_2O_3RhS$: 567.0955 found: 567.0978 $[M\text{-}PPh_4]^-$.

(10): The compound was synthesised following the same procedure as described for **9**, with 0.412 g (1.28 mmol) of **1**, 0.066 g (0.284 mmol) of Ag_2O, 0.191 g (0.284 mmol) of

[IrCl(cod)]$_2$ and 0.214 g (0.571 mmol) of PPh_4Cl yielding **10** as an orange solid (0.170 g, 30 %).

^{1}H NMR (400 MHz, CD_2Cl_2): δ = 7.93 (m, 4H; Ar*H* PPh_4), 7.77 (m, 8H; Ar*H* PPh_4), 7.63 (m, 8H; Ar*H* PPh_4), 7.21 (d, 1H, $^3J_{HH}$ = 2 Hz; NC*H*$_{IMes}$), 6.98 (s, 1H; Ar*H* Mes), 6.91 (s, 1H; Ar*H* Mes), 6.74 (d, 1H, $^3J_{HH}$ = 2 Hz; C*H*N$_{IMes}$), 4.93-4.86 (m, 1H; C*H* cod), 4.33-4.28 (m, 1H; C*H* cod), 4.21-4.11 (m, 2H; C*H* cod), 3.08-3.05 (m, 1H; NC*H*H$(CH_2)_3SO_3$), 2.79-2.70 (m, 3H; NCH*H*$(CH_2)_3SO_3$ overlapping with N$(CH_2)_3$C*H*$_2SO_3$), 2.33 (s, 3H, C*H*$_3$ Mes), 2.24 (s, 3H, C*H*$_3$ Mes), 2.36-2.26 (m, 2H; C*H*$_2$ cod), 2.18-2.09 (m, 2H; C*H*$_2$ cod), 2.07-1.95 (m, 2H; C*H*$_2$ cod), 1.92-1.82 (m, 2H; NCH$_2$C*H*$_2$$(CH_2)_2SO_3$), 1.89 (s, 3H; C*H*$_3$ Mes), 1.76-1.66 (m, 2H; C*H*$_2$ cod), 1.49-1.41 (m, 2H; N$(CH_2)_2SO_3$C*H*$_2$$CH_2SO_3$), 1.39-1.30 (m, 2H; N$(CH_2)_2SO_3$C*H*$_2$$CH_2SO_3$).

^{13}C{^{1}H} NMR (100 MHz, CD_2Cl_2): δ = 179.6 (N*C*N), 141.3, 138.8, 136.9, 136.1 (d, $^4J_{P\text{-}C}$ = 3 Hz; PPh_4), 134.9, 134.8 (d, $^3J_{P\text{-}C}$ = 10.3 Hz; PPh_4), 131.0 (d, $^2J_{P\text{-}C}$ = 12.8 Hz; PPh_4), 129.4, 128.4, 123.0, 121.5, 117.8 (d, $^1J_{P\text{-}C}$ = 89.1 Hz; PPh_4), 82.6 (CH cod), 82.0 (CH cod), 52.2 (CH cod), 51.5 (CH cod), 51.3, 50.7, 49.8, 34.5, 33.0, 32.3, 30.5, 29.7, 29.5, 29.2, 23.3, 21.6, 21.2, 21.1, 19.5, 18.0, 17.6.

HRMS (ES$^-$): calculated for $C_{24}H_{33}ClIrN_2O_3S$: m/z = 657.1530 found: 657.1489 [M-PPh_4]$^-$.

(11): 53 µL of a solution of KO*t*Bu in THF (1.6 M, 0.085 mmol) was added to a suspension of **8** (36 mg, 0.085 mmol) in THF (3 mL). After 1 h of stirring at room temperature the solution became clear, [RhCl(cod)]$_2$ (19 mg, 0.038 mmol) was added and the mixture was further stirred for overnight. PPh_4Cl (31 mg, 0.083 mmol) was subsequently added and left to react for 2 h. The reaction mixture was concentrated *in vacuo*, the crude product purified by column chromatography using a gradient of DCM/acetone from (1:1, v/v) to DCM/acetone/MeOH (32:64:4, v/v/v), yielding the pure product as a bright yellow solid (47 mg, 56 %).

^{1}H NMR (400 MHz, CD_2Cl_2): δ = (m, 4H; Ar*H* PPh_4), (m, 8H; Ar*H* PPh_4), (m, 8H; Ar*H* PPh_4), (s, 2H; Ar*H* Mes), (s, 2H; Ar*H* Mes), (s, 3H, C*H*$_3$ Mes), (m, 2H; NCH$_2$C*H*$_2$$(CH_2)_2SO_3$), (m, 2H; N$(CH_2)_2$C*H*$_2$$CH_2SO_3$), (m, 2H; C*H*$_2$ cod), (m, 1H; NC*H*$_2$$(CH_2)_3SO_3$), (m, 2H; N$(CH_2)_3$C*H*$_2SO_3$), (m, 1H; C*H* cod). **^{13}C{^{1}H} NMR (100 MHz, CD_2Cl_2):** δ = 212.7 (d, $^1J_{Rh\text{-}C}$ = 46.9 Hz; N*C*N), 143.1, 138.6, 138.4, 138.0, 137.1, 136.9, 136.1 (d, $^4J_{P\text{-}C}$ = 3 Hz; PPh_4), 135.9, 135.7, 134.8 (d, $^3J_{P\text{-}C}$ = 10.3 Hz; PPh_4), 131.0 (d, $^2J_{P\text{-}C}$ = 12.8 Hz; PPh_4), 129.8, 129.2, 128.9, 128.3, 117.9 (d, $^1J_{P\text{-}C}$ = 89.2 Hz; PPh_4), 97.1 (d, $^1J_{Rh\text{-}C}$ = 6.9 Hz), 96.8 (d, $^1J_{Rh\text{-}C}$ = 7.0 Hz), 68.4 (d, $^1J_{Rh\text{-}C}$ = 14.3 Hz), 68.1 (d, $^1J_{Rh\text{-}C}$ = 14.3 Hz), 52.3, 51.8, 35.8, 33.0, 32.9, 31.6, 28.5, 28.4, 25.9, 21.1,

20.0, 18.6, 18.5, 15.5. **HRMS (ES⁻):** calculated for $C_{32}H_{43}ClN_2O_3RhS$: m/z = 673.1738 found: 673.1741 $[M\text{-}PPh_4]^-$.

(12): Compound **12** was synthesised following the same procedure as for **11** using 58 µL of KOtBu (1.6 M, 0.092 mmol), 36 mg (0.084 mmol) of **8**, 26 mg (0.039 mmol) of $[IrCl(cod)]_2$ and 29 mg (0.077 mmol) of PPh_4Cl, yielding **12** as an orange solid (26 mg, 40 %).

^{1}H NMR (400 MHz, CD_2Cl_2): δ = 7.95-7.91 (m, 4H; Ar*H* PPh_4), 7.79-7.74 (m, 8H; Ar*H* PPh_4), 7.66-7.60 (m, 8H; Ar*H* PPh_4), 6.97 (s, 2H; Ar*H* Mes), 6.95 (s, 2H; Ar*H* Mes), 3.95-3.83 (m, 4H+2H; NC*H*$_2$C*H*$_2$N overlap with C*H* cod), 3.15-3.06 (m, 2H; C*H* cod), 2.73-2.69 (m, 2H; $N(CH_2)_3CH_2SO_3$), 2.60-2.56 (m, 1H; $NCH_2(CH_2)_3SO_3$), 2.50 (s, 6H, C*H*$_3$ Mes), 2.35 (s, 3H, C*H*$_3$ Mes), 2.34 (s, 3H, C*H*$_3$ Mes), 2.31 (s, 3H, C*H*$_3$ Mes), 1.85-1.77 (m, 2H; $NCH_2CH_2(CH_2)_2SO_3$), 1.72-1.66 (m, 4H; C*H*$_2$ cod), 1.65-1.58 (m, 2H; $N(CH_2)_2CH_2CH_2SO_3$), 1.57-1.50 (m, 4H; C*H*$_2$ cod). **^{13}C{^{1}H} NMR (100 MHz, CD_2Cl_2):** δ = 207.3 (N*C*N), 143.1, 138.3, 138.0, 136.9, 136.8, 136.1 (d, $^4J_{P\text{-}C}$ = 2.8 Hz; PPh_4), 135.9, 135.7, 134.8 (d, $^3J_{P\text{-}C}$ = 10.3 Hz; PPh_4), 131.0 (d, $^2J_{P\text{-}C}$ = 12.8 Hz; PPh_4), 129.7, 129.2, 128.8, 128.3, 117.9 (d, $^1J_{P\text{-}C}$ = 89.1 Hz; PPh_4), 83.4, 83.2, 52.4, 51.9, 35.8, 33.8, 33.6, 31.5, 30.1, 29.0, 28.8, 25.7, 21.1, 20.0, 19.9, 18.7. **HRMS (ES⁻):** calculated for $C_{32}H_{43}ClN_2O_3IrS$: m/z = 763.2312 found: 763.2321 $[M\text{-}PPh_4]^-$.

- **General procedure for the synthesis of the $(NHC)M(CO)_2Cl$ complexes**

[(NHC)M(cod)Cl] (20 mg) was dissolved in dichloromethane (2 mL). CO (100% CO Linde Gas) was then bubbled through the solution for 30 min. The reactions were in all cases quantitative as was determined by IR spectroscopy. The stability of the compounds in dichloromethane did not allow for $^{13}C\{^1H\}$ NMR analysis, the measurement time being too long and leading to decomposition of the products. Nevertheless the products were analysed by ^{1}H NMR spectroscopy and HRMS.

(13): Compound **9** is dissolved in dichloromethane and CO bubbled through the solution. **^{1}H NMR (400 MHz, CD_2Cl_2):** δ = = 7.95-7.91 (m, 4H; Ar*H* PPh_4), 7.79-7.75 (m, 8H; Ar*H* PPh_4), 7.66-7.61 (m, 8H; Ar*H* PPh_4), 7.35 (d, 1H, $^3J_{HH}$ = 2 Hz; C*H*N_{IMes}), 6.99 (s, 2H; Ar*H* Mes), 6.92 (d, 1H, $^3J_{HH}$ = 2 Hz; C*H*N_{IMes}), 4.41 (t, 2H, $^3J_{HH}$ = 7.2 Hz; $N(CH_2)_3CH_2SO_3$), 2.73 (t, 2H, $^3J_{HH}$ = 7.2 Hz; $NCH_2(CH_2)_3SO_3$), 2.35 (s, 3H; C*H*$_3$ Mes), 2.15-2.06 (m, 2H; $NCH_2CH_2(CH_2)_2SO_3$), 2.06 (s, 6H; C*H*$_3$ Mes), 1.88-1.80 (m, 2H;

$N(CH_2)_2CH_2CH_2SO_3$). **HRMS (ES⁻):** calculated for $C_{18}H_{21}ClN_2O_5RhS$: m/z = 514.9915 found: 514.9938 $[M\text{-}PPh_4]^-$.

(14): Compound **10** is dissolved in dichloromethane and CO bubbled through the solution. **^{1}H NMR (400 MHz, CD_2Cl_2): δ =** 7.95-7.91 (m, 4H; Ar*H* PPh_4), 7.79-7.74 (m, 8H; Ar*H* PPh_4), 7.65-7.60 (m, 8H; Ar*H* PPh_4), 7.41 (d, 1H, $^3J_{HH}$ = 2 Hz; C*H*N_{IMes}), 6.98 (s, 2H; Ar*H* Mes), 6.91 (d, 1H, $^3J_{HH}$ = 2 Hz; C*H*N_{IMes}), 4.40 (m, 2H; $N(CH_2)_3CH_2SO_3$), 2.74 (t, 2H, $^3J_{HH}$ = 7.2 Hz; $NCH_2(CH_2)_3SO_3$), 2.35 (s, 3H; C*H*$_3$ Mes), 2.15-2.08 (m, 2H; $NCH_2CH_2(CH_2)_2SO_3$), 2.06 (s, 6H; C*H*$_3$ Mes), 1.88-1.80 (m, 2H; $N(CH_2)_2CH_2CH_2SO_3$). **HRMS (ES⁻):** calculated for $C_{18}H_{21}ClN_2O_5IrS$: m/z = 605.0489 found: 605.0508 $[M\text{-}PPh_4]^-$.

(15): Compound **11** is dissolved in dichloromethane and CO bubbled through the solution. **^{1}H NMR (400 MHz, CD_2Cl_2): δ =** 7.94-7.89 (m, 4H; Ar*H* PPh_4), 7.78-7.73 (m, 8H; Ar*H* PPh_4), 7.65-7.59 (m, 8H; Ar*H* PPh_4), 6.96 (bs, 4H; Ar*H* Mes), 3.95 (bs, 4H, NCH_2CH_2N), 2.84-2.75 (m, 2H; $N(CH_2)_3CH_2SO_3$), 2.60-2.55 (t, 2H, $^3J_{HH}$ = 7.2 Hz; $NCH_2(CH_2)_3SO_3$), 2.39 (s, 6H, C*H*$_3$ Mes), 2.38 (s, 6H, C*H*$_3$ Mes), 2.31 (s, 3H, C*H*$_3$ Mes), 1.86-1.77 (m, 2H; $NCH_2CH_2(CH_2)_2SO_3$), 1.74-1.65 (m, 2H; $N(CH_2)_2CH_2CH_2SO_3$). **HRMS (ES⁻):** calculated for $C_{26}H_{31}ClN_2O_5RhS$: m/z = 621.0697 found: 621.0699 $[M\text{-}PPh_4]^-$.

(16): Compound **12** is dissolved in dichloromethane and CO bubbled through the solution. **^{1}H NMR (400 MHz, CD_2Cl_2): δ =** 7.94-7.90 (m, 4H; Ar*H* PPh_4), 7.78-7.73 (m, 8H; Ar*H* PPh_4), 7.64-7.59 (m, 8H; Ar*H* PPh_4), 6.95 (bs, 4H; Ar*H* Mes), 3.96 (bs, 4H, NCH_2CH_2N), 2.88-2.78 (m, 2H; $N(CH_2)_3CH_2SO_3$), 2.57 (t, 2H, $^3J_{HH}$ = 7.6 Hz; $NCH_2(CH_2)_3SO_3$), 1.88-1.78 (m, 2H; $NCH_2CH_2(CH_2)_2SO_3$), 1.73-1.65 (m, 2H; $N(CH_2)_2CH_2CH_2SO_3$), 2.39 (s, 6H, C*H*$_3$ Mes), 2.38 (s, 6H, C*H*$_3$ Mes), 2.31 (s, 3H, C*H*$_3$ Mes). **HRMS (ES⁻):** calculated for $C_{26}H_{31}ClN_2O_5IrS$: m/z = 711.1271 found: 711.1255 $[M\text{-}PPh_4]^-$.

- **X-ray crystal structure determination:**

(1): $C_{16}H_{22}N_2O_3S$, Fw = 322.42, colourless block, 0.23 x 0.19 x 0.18 mm^3, orthorhombic, Pbca (no. 61), a = 15.5195(5), b = 9.4608(3), c = 22.2366(9) Å, V = 3264.9(2) Å^3, Z = 8, D_x = 1.312 g/cm^3, μ = 0.21 mm^{-1}. 21618 Reflections were measured on a Nonius Kappa CCD diffractometer with rotating anode (graphite monochromator, λ = 0.71073 Å) up to a

resolution of $(\sin\theta/\lambda)_{max}$ = 0.62 Å^{-1} at a temperature of 150(2) K. Intensity integration was performed with EvalCCD.[36] The SADABS[37] program was used for absorption correction and scaling based on multiple measured reflections (0.96-0.97 correction range). 3211 Reflections were unique (R_{int} = 0.041), of which 2383 were observed [I>2σ(I)]. The structure was solved with automated Patterson methods using the program DIRDIF2008.[38] The structure was refined with SHELXL-97[39] against F^2 of all reflections. Non hydrogen atoms were refined with anisotropic displacement parameters. Hydrogen atoms were located in difference Fourier maps and refined with a riding model. 202 Parameters were refined with no restraints. R1/wR2 [I > 2σ(I)]: 0.0432 / 0.0958. R1/wR2 [all refl.]: 0.0687 / 0.1089. S = 1.041. Residual electron density between -0.34 and 0.46 e/Å^3. Geometry calculations and checking for higher symmetry was performed with the PLATON program.[40]

[$RhCl_2$(cod)][PPh_4]: $[C_{24}H_{20}P][C_8H_{12}Cl_2Rh] \cdot 1.5CH_2Cl_2$, Fw = 748.74, yellow block, 0.36 x 0.33 x 0.21 mm^3, monoclinic, $P2_1/c$ (no. 14), a = 18.7746(17), b = 18.090(2), c = 19.4039(13) Å, β = 93.059(8)°, V = 6580.8(11) Å^3, Z = 8, D_x = 1.511 g/cm^3, μ = 1.00 mm^{-1}. 203596 Reflections were measured on a Nonius Kappa CCD diffractometer with rotating anode (graphite monochromator, λ = 0.71073 Å) up to a resolution of $(\sin\theta/\lambda)_{max}$ = 0.65 Å^{-1} at a temperature of 150(2) K. Intensity integration was performed with EvalCCD.[36] The SADABS[37] program was used for absorption correction and scaling based on multiple measured reflections (0.69-0.75 correction range). 15098 Reflections were unique (R_{int} = 0.041), of which 12218 were observed [I>2σ(I)]. The structure was solved with Direct Methods using the program SHELXS-97[39]. The structure was refined with SHELXL-97[39] against F^2 of all reflections. Non hydrogen atoms were refined with anisotropic displacement parameters. Hydrogen atoms were located in difference Fourier maps. Hydrogen atoms of the *cod* double bonds were refined freely with isotropic displacement parameters; all other hydrogen atoms were refined with a riding model. 762 Parameters were refined with no restraints. R1/wR2 [I > 2σ(I)]: 0.0386 / 0.0977. R1/wR2 [all refl.]: 0.0534 / 0.1082. S = 1.060. Residual electron density between -0.84 and 2.20 e/Å^3 (maximum peak in the solvent region). Geometry calculations and checking for higher symmetry was performed with the PLATON program.[40]

2.6 References

[1] S. P. Nolan, *N-Heterocyclic Carbenes in Synthesis*, Wiley-VCH, Weinheim, **2006**.

[2] L. Cavallo, A. Correa, C. Costabile, H. Jacobsen, *J. Organomet. Chem.* **2005**, *690*, 5407-5413.

[3] B. Cornils, Herrmann, W. A., *Aqueous-Phase Organometallic Catalysis*, Wiley-VCH, Weinheim, **2004**.

[4] B. Cornils, E. G. Kuntz, *J. Organomet. Chem.* **1995**, *502*, 177-186.

[5] K. H. Shaughnessy, *Chem. Rev.* **2009**, *109*, 643-710.

[6] L. R. Moore, S. M. Cooks, M. S. Anderson, H. J. Schanz, S. T. Griffin, R. D. Rogers, M. C. Kirk, K. H. Shaughnessy, *Organometallics* **2006**, *25*, 5151-5158.

[7] C. Fleckenstein, S. Roy, S. Leuthausser, H. Plenio, *Chem. Commun.* **2007**, 2870-2872.

[8] M. K. Brown, T. L. May, C. A. Baxter, A. H. Hoveyda, *Angew. Chem. Int. Ed.* **2007**, *46*, 1097-1100.

[9] Y. Nagai, T. Kochi, K. Nozaki, *Organometallics* **2009**, *28*, 6131-6134.

[10] Laure Benhamou, Edith Chardon, Guy Lavigne, Stéphane Bellemin-Laponnaz, V. César, *Chem. Rev.* **2011**, in press, DOI 10.1021/cr100328e

[11] M. A. N. Virboul, M. Lutz, M. A. Siegler, A. L. Spek, G. van Koten, R. J. M. Klein Gebbink, *Chem. Eur. J.* **2009**, *15*, 9981-9986.

[12] M. Scholl, S. Ding, C. W. Lee, R. H. Grubbs, *Org. Lett.* **1999**, *1*, 953-956.

[13] J. Huang, G. Grasa, S. P. Nolan, *Org. Lett.* **1999**, *1*, 1307-1309.

[14] M. Scholl, S. Ding, C. W. Lee, R. H. Grubbs, *Org. Lett.* **1999**, *1*, 953-956.

[15] G. P. Xu, S. R. Gilbertson, *Org. Lett.* **2005**, *7*, 4605-4608.

[16] M. Q. Xie, T. S. Widlanski, *Tetrahedron Lett.* **1996**, *37*, 4443-4446.

[17] M. A. Hempenius, F. F. Brito, G. J. Vancso, *Macromolecules* **2003**, *36*, 6683-6688.

[18] E. Peris, *Top. Organomet. Chem.* **2007**, *21*, 83 - 116.

[19] A. R. Chianese, X. W. Li, M. C. Janzen, J. W. Faller, R. H. Crabtree, *Organometallics* **2003**, *22*, 1663-1667.

[20] D. Tapu, D. A. Dixon, C. Roe, *Chem. Rev.* **2009**, *109*, 3385-3407.

[21] M. Mayr, K. Wurst, K. H. Ongania, M. R. Buchmeiser, *Chem. Eur. J.* **2004**, *10*, 2622-2622.

[22] S. Wolf, H. Plenio, *J. Organomet. Chem.* **2009**, *694*, 1487-1492.

[23] M. J. Doyle, M. F. Lappert, P. L. Pye, P. Terreros, *J. Chem. Soc., Dalton Trans.* **1984**, 2355-2364.

[24] M. Iglesias, D. J. Beetstra, A. Stasch, P. N. Horton, M. B. Hursthouse, S. J. Coles, K. J. Cavell, A. Dervisi, I. A. Fallis, *Organometallics* **2007**, *26*, 4800-4809.

[25] R. A. Kelly, H. Clavier, S. Giudice, N. M. Scott, E. D. Stevens, J. Bordner, I. Samardjiev, C. D. Hoff, L. Cavallo, S. P. Nolan, *Organometallics* **2008**, *27*, 202-210.

[26] M. V. Jimenez, J. J. Perez-Torrente, M. I. Bartolome, V. Gierz, F. J. Lahoz, L. A. Oro, *Organometallics* **2008**, *27*, 224-234.

[27] H. V. Huynh, Y. Han, R. Jothibasu, J. A. Yang, *Organometallics* **2009**, *28*, 5395-5404.

[28] S. Fantasia, J. L. Petersen, H. Jacobsen, L. Cavallo, S. P. Nolan, *Organometallics* **2007**, *26*, 5880-5889.

[29] C. A. Tolman, *Chem. Rev.* **1977**, *77*, 313-348.

[30] K. Denk, P. Sirsch, W. A. Herrmann, *J. Organomet. Chem.* **2002**, *649*, 219-224.

[31] O. Schuster, L. R. Yang, H. G. Raubenheimer, M. Albrecht, *Chem. Rev.* **2009**, *109*, 3445-3478.

[32] J. L. Herde, J. C. Lambert, C. V. Senoff, *Inorg. Synth.* **1974**, *15*, 18-20.

[33] G. Giordano, R. H. Crabtree, *Inorg. Synth.* **1990**, *1990*, 88-90.

[34] J. Liu, J. Chen, J. Zhao, Y. Zhao, L. Li, H. Zhang, *Synthesis* **2003**, *17*, 2661-2666.

[35] M. M. Heravi, N. Abdolhosseini, H. A. Oskooie, *Tetrahedron Lett.* **2005**, *46*, 8959-8963.

[36] A. J. M. Duisenberg, L. M. J. Kroon-Batenburg, A. M. M. Schreurs, *J. Appl. Crystallogr.* **2003**, *36*, 220-229.

[37] G. M. Sheldrick, *SADABS: Area-Detector Absorption Correction, v2.10*, University of Göttingen, Göttingen (Germany), **1999**.

[38] P. T. Beurskens, G. Beurskens, R. d. Gelder, S. Garcia-Granda, R. O. Gould, J. M. M. Smits, *The DIRDIF2008 program system*, Crystallography Laboratory, University of Nijmegen, Nijmegen (The Netherlands), **2008**.

[39] G. M. Sheldrick, *Acta Cryst.* **2008**, *A64*, 112-122.

[40] A. L. Spek, *J. Appl. Crystallogr.* **2003**, *36*, 7-13.

CHAPTER THREE

One Pot Synthesis and Immobilisation of Sulfonate-Tethered *N*-Heterocyclic Carbene Complexes on Polycationic Dendrimers

ABSTRACT

The synthesis of new sulfonate functionalised NHC carbene complexes of gold and rhodium is presented through transmetallation from a bis-carbene silver complex. This strategy was successfully apply to synthesise gold and rhodium metallodendritic assemblies in a one pot process involving concomitant transmetallation and immobilisation reactions. The newly formed metal transition complexes and assemblies were applied in different catalysed organic transformations.

Parts of this chapter have been published in: M. A. N. Virboul, M. Lutz, M. A. Siegler, A. L. Spek, G. van Koten, R. J. M. K. Gebbink, *Chem. Eur. J.* **2009**, *15*, 9981.

3.1 Introduction

Since their first isolation by Arduengo in 1991, *N*-Heterocyclic carbenes (NHCs) have been widely used as versatile ligands in organometallic chemistry and homogeneous catalysis.[1-5] Due to their strong σ-donor characteristics, these compounds are known to form robust transition metal complexes. As a consequence, the use of NHCs as ligands allows for the synthesis of highly functionalised organometallic complexes that combine catalytic properties of the metal centre with a variety of other functional group properties.[6, 7] The stability of NHC complexes has attracted our interest from the viewpoint of catalyst immobilisation, where loss of functional metal sites from the construct by metal leaching should be minimal.

We and others have earlier proven the utility of carbosilane[8-14] and polycationic dendrimers as supports for transition metal complexes immobilisation via covalent and non-covalent attachment, respectively. In particular the use of polycationic dendrimers allows for the easy (reversible) loading of dendrimers with larger numbers of functional molecules and renders the synthesis of catalytically active and recoverable dendritic assemblies feasible.[15-22] Following these investigations we have turned our attention to the synthesis of functionalised NHC complexes that are suitable for the preparation of non-covalently immobilised homogeneous catalysts.

Gold catalysis has received tremendous interest this last decade since the general consensus was made that gold is not an inert metal but that it has great potential in catalysis. The (re-)discovery that gold can be an efficient catalyst in more and more organic transformations has sharpened the interest for organometallic chemist to develop new gold entities able to perform reactions in a sustainable manner.[23-26] The introduction of NHC ligands to prepare Au(I) complexes has a major impact on the field.[27, 28] (NHC)Au(I) complexes have been studied in different organic transformations, among which the hydration of alkynes.[29]

Here, we report on the development of an *in situ* transmetallation-immobilisation strategy for the construction of non-covalent NHC-metallodendrimers starting from a common polycationic dendrimer in combination with an anion-tethered NHC ligand and different metal precursors. The catalytic application of the metallodendritic assemblies are also investigated.

3.2 Results and discussion

Synthesis and characterisation of (NHC)-Au(I) and (NHC)-Rh(I) complexes

The zwitterionic imidazolium **1** was synthesised in a single step procedure by nucleophilic addition of mesityl imidazole to 1,4-butane sultone (Scheme 1) and was obtained in excellent yield (Scheme 1, see also Chapter Two).[30-33] Treatment of **1** with an excess of Ag_2O in acetonitrile at reflux temperature for 6 hours resulted in the formation of the corresponding bis-carbene silver complex **2**, which was isolated in 87% yield.

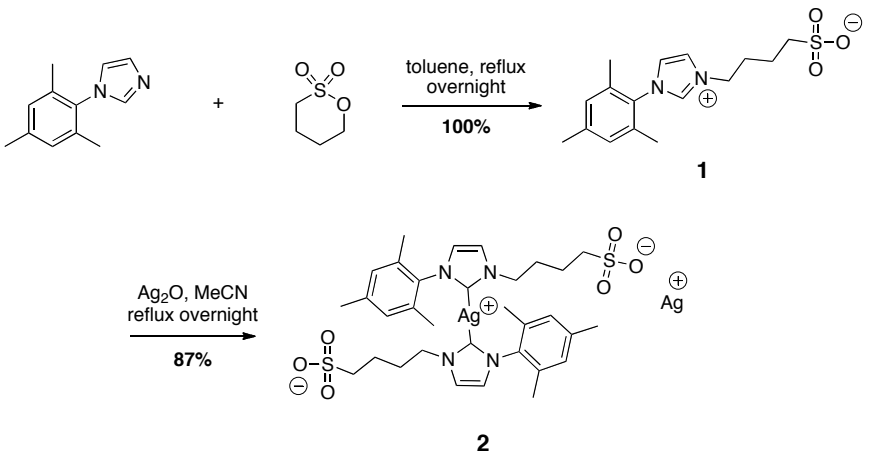

Scheme 1. Synthesis and metallation of functionalised ligand.

The ^1H NMR spectrum of **2** displayed clear upfield shifts of the signals corresponding to the protons of the imidazolium ring and lacked the signal corresponding to the C^2 proton. Characterisation of compound **2** by $^{13}C\{^1H\}$ NMR confirmed coordination of silver to the ligand by the presence of a typical signal at 180.2 ppm for the C^2 carbon. Single crystals of complex **2** suitable for X-ray diffraction analysis were grown by slow evaporation of a solution of **2** in dichloromethane/benzene. The molecular structure shows that **2** is a bis(imidazol-2-ylidene)-silver complex, in which a linear Ag bis-carbene fragment is present (C11-Ag1-C12=178.55(14)°) (Figure 1). The silver-carbon bond distances (range 2.073-2.083 Å, the individual s.u.'s are 0.004 Å) in this moiety are consistent with those reported in literature, which are normally found in the range of 2.067-2.117 Å for bis-carbene silver complexes with non-coordinating anions.[34]

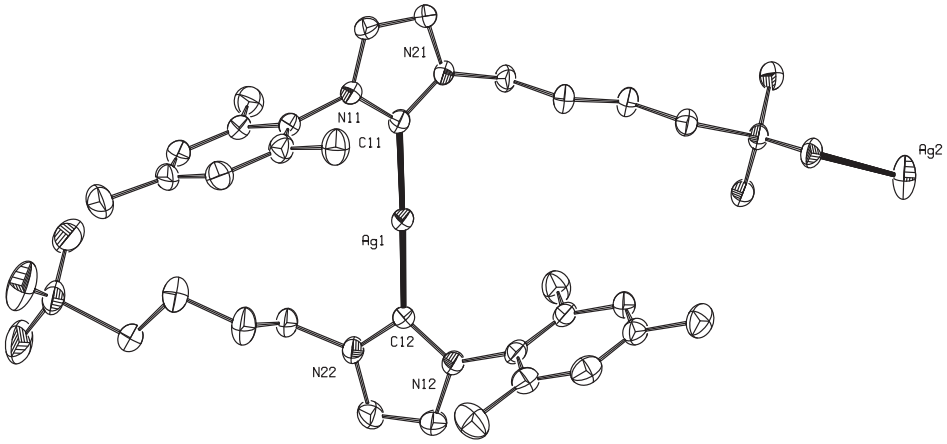

Figure 1. Displacement ellipsoid plot (50% probability level at 150(2) K) of a sulfonate-appended bis(imidazol-2-ylidene)silver complex, i. e. the monomeric unit of one independent polymeric chain of **2**. H-atoms and the non-coordinated water molecule are omitted for the sake of clarity. Selected bond length (Å) and angles (°) (second molecule in square brackets): Ag1-C11 2.078(4) [2.079(4)], Ag1-C12 2.073(4) [2.083(4)], C11-Ag1-C12 178.55(14) [176.48(14)], N11-C11-N21 104.0(3) [103.9(3)], N12-C12-N22 104.0(3) [103.9(3)].

The overall charge neutrality in crystals of **2** is complied with a second silver ion (Ag2). This counterion is bound to three sulfonate groups from three different Ag-bis carbene moieties via Ag-O bridges to form one-dimensional (hereafter 1-D) polymeric chains along the crystallographic c-axis. Non-coordinated water molecules are also part of the 1-D polymeric chains by forming hydrogen bonds between two sulfonate moieties (see Figure 2).

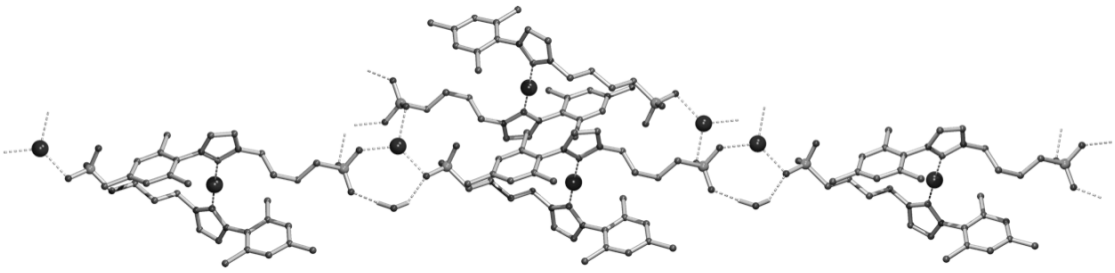

Figure 2. Polymeric structure of compound **2** in the solid state. H-atoms (except for those attached to O_{water}) are omitted for clarity.

Following the pioneering work of Lin et al.,[35] we focused our attention on the synthesis of sulfonate tethered mono-carbene metal complexes, in which the metal centre bears no formal charge, via transmetallation from **2** used as carbene transfer agent. Starting from the halide free Ag-carbene complex **2**, this strategy requires two equivalents of an overall neutral metal precursor to form two neutral metal carbene moieties. In addition, two equivalents of an organic halide salt are necessary to provide each of the two sulfonate groups with a counter ion and to allow the formation of the two equivalents of silver halide.

This principle was first tested using AuCl(tht) as the metal precursor and NBu_4Cl or PPh_4Cl as the halide source, strictly following the stoichiometry of one equivalent of silver for one equivalent of NBu_4Cl or PPh_4Cl and AuCl(tht) (Scheme 2).

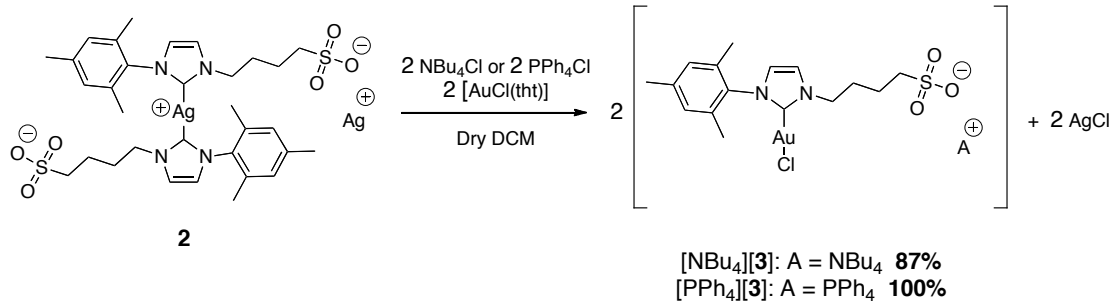

Scheme 2. Transmetallation of **2** with AuCl(tht) in the presence of an external halide source.

The resulting sulfonate-tethered Au^I carbene complexes [NBu_4][**3**] and [PPh_4][**3**] were fully characterised by classical spectroscopic methods (see Experimental Section). The formation of a monomeric, molecular (NHC)-Au^I complex as opposed to the polymeric Ag^I complex **2** was confirmed by the X-ray crystal structure of [PPh_4][**3**] (Figure 3). The molecular structure proved the presence of a non-interacting tetraphenylphosphonium cation as counterion for the sulfonate group. The Au-C distance of 1.976(2) Å and the nearly linear C-Au-Cl angle (178.17(6)°) in [PPh_4][**3**] are consistent with the features of similar (NHC)-Au^I complexes reported in literature (range between 1.942 and 1.998 Å).[36, 37]

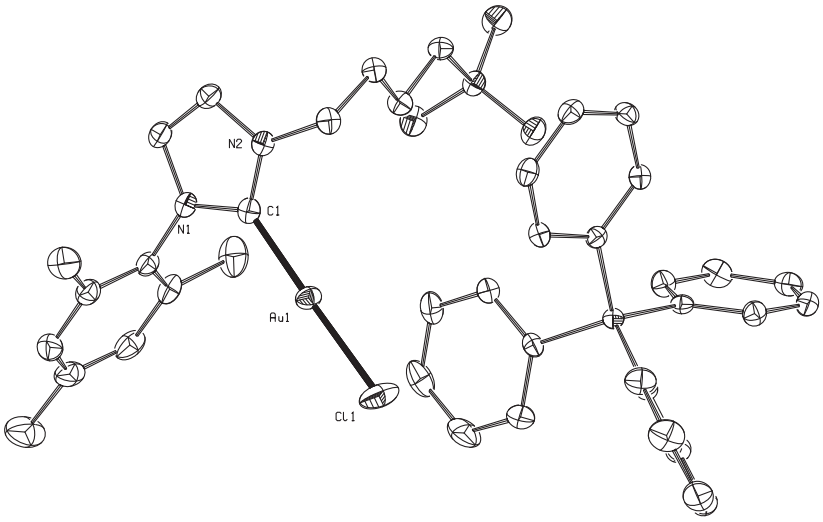

Figure 3. Displacement ellipsoid plot (50% probability level) of the asymmetric unit of [PPh_4][**3**] at 150(2) K. H atoms are omitted for clarity. Selected bond length (Å) and angles (º): C1-Au1 1.976(2), Au1-Cl1 2.2699(6), C1-Au1-Cl1 178.17(6), N1-C1-N2 110.71(18).

To show the wider applicability of our strategy, we applied this synthetic pathway to the synthesis of sulfonate (NHC)-Rh complexes by transmetallation reaction of a silver complex and a suitable Rh precursor, as previously described by Crabtree *et al.*[38] It appeared that the sulfonate Rh^{I} carbene complexes could be readily obtained under similar conditions as described for [NBu_4][**3**] and [PPh_4][**3**] (see Scheme 3) from compound **2** using $[RhCl(cod)]_2$ and an additional halide source in the appropriate stoichiometry.

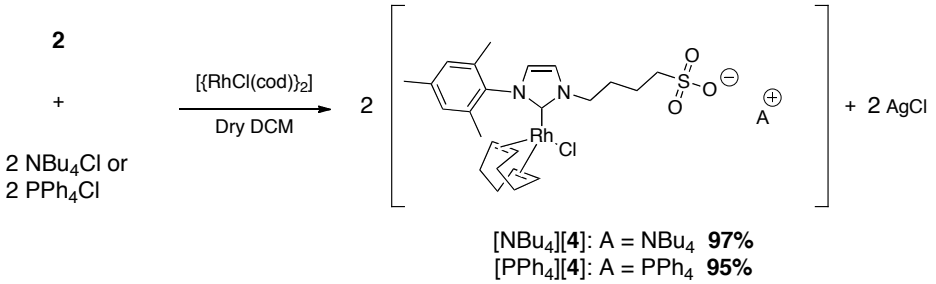

[NBu_4][**4**]: A = NBu_4 **97%**
[PPh_4][**4**]: A = PPh_4 **95%**

Scheme 3. Transmetallation of **2** with $[RhCl(cod)]_2$ and an external halide source.

Characterisation of [NBu_4][**4**] by $^{13}C\{^1H\}$ NMR spectroscopy in CD_2Cl_2 showed that the singlet corresponding to C^2 of **2** had disappeared and had been replaced by a sharp doublet at 181.3 ppm with a coupling constant $^1J_{Rh-C}$ = 51.5 Hz, indicating coordination

of the carbene ligand to Rh. The ^{1}H NMR spectrum measured at 298 K showed splitting of the proton signals corresponding to the ligand. This diastereotopicity of the protons of the NHC ligand can be explained by a hindered rotation around the metal-NHC bond, inducing differentiation of the protons.[38] [PPh_4][**4**] showed very similar spectroscopic characteristics as [NBu_4][**4**], indicating that there is no influence of the counter cation on the formation of the (NHC)-Rh^I complex. It is worth mentioning that in the case of [PPh_4][**3**] no splitting of the aliphatic signals of the carbene ligand was observed, which is consistent with its higher molecular symmetry as compared to [NBu_4][**4**].

Synthesis and characterisation of the supramolecular dendritic assemblies

The immobilisation of transition metal complexes on polycationic dendrimers by means of ionic interactions was previously investigated in our group.[18, 21] The anchoring of anionic guests was typically achieved by means of a biphasic ion exchange protocol that proved to be efficient in many cases. Yet, this protocol implies a two-phase aqueous solvent system that might not be applicable to systems that are sensitive to hydrolysis.

The strategy for the synthesis of the sulfonate mono-carbene complexes [**3**]$^-$ and [**4**]$^-$ uses dry conditions, avoiding any possible hydrolysis. This strategy can be seen as the sum of two separate reactions occurring simultaneously: a transmetallation, which is the transfer of the carbene ligand from silver to gold or rhodium, and an ion exchange in which Ag^+ is replaced by an organic cation. This strategy has proven to be versatile in allowing ionic exchange with different organic chloride salts as the source of chloride ions.

Dendrimer [**5**]Cl_8 has been previously used for non-covalent immobilisation and is an octacationic dendrimer bearing eight ammonium groups with halides as counterions (Scheme 4).[39] Therefore, this dendrimer could in principle combine the functions of dendritic support, as well as of organic halide salt. By taking advantage of these features, we synthesised and immobilised sulfonate-tethered metal carbene complexes in a one pot procedure. Indeed, overnight stirring of 4 equivalents of compound **2** in the presence of 8 equivalents of AuCl(tht) and 1 equivalent of the octacationic dendrimer [**5**]Cl_8 in dichloromethane resulted in the formation of the corresponding metallodendritic assembly [**5**][**3**]$_8$ in good yield (Scheme 4). The use of [RhCl(cod)]$_2$ as metal source in

this one pot transmetalation-immobilisation protocol gave the corresponding dendritic assembly [**5**][**4**]$_8$ in good yield. The metallodendritic assemblies were purified by filtration over Celite, followed by passive dialysis.

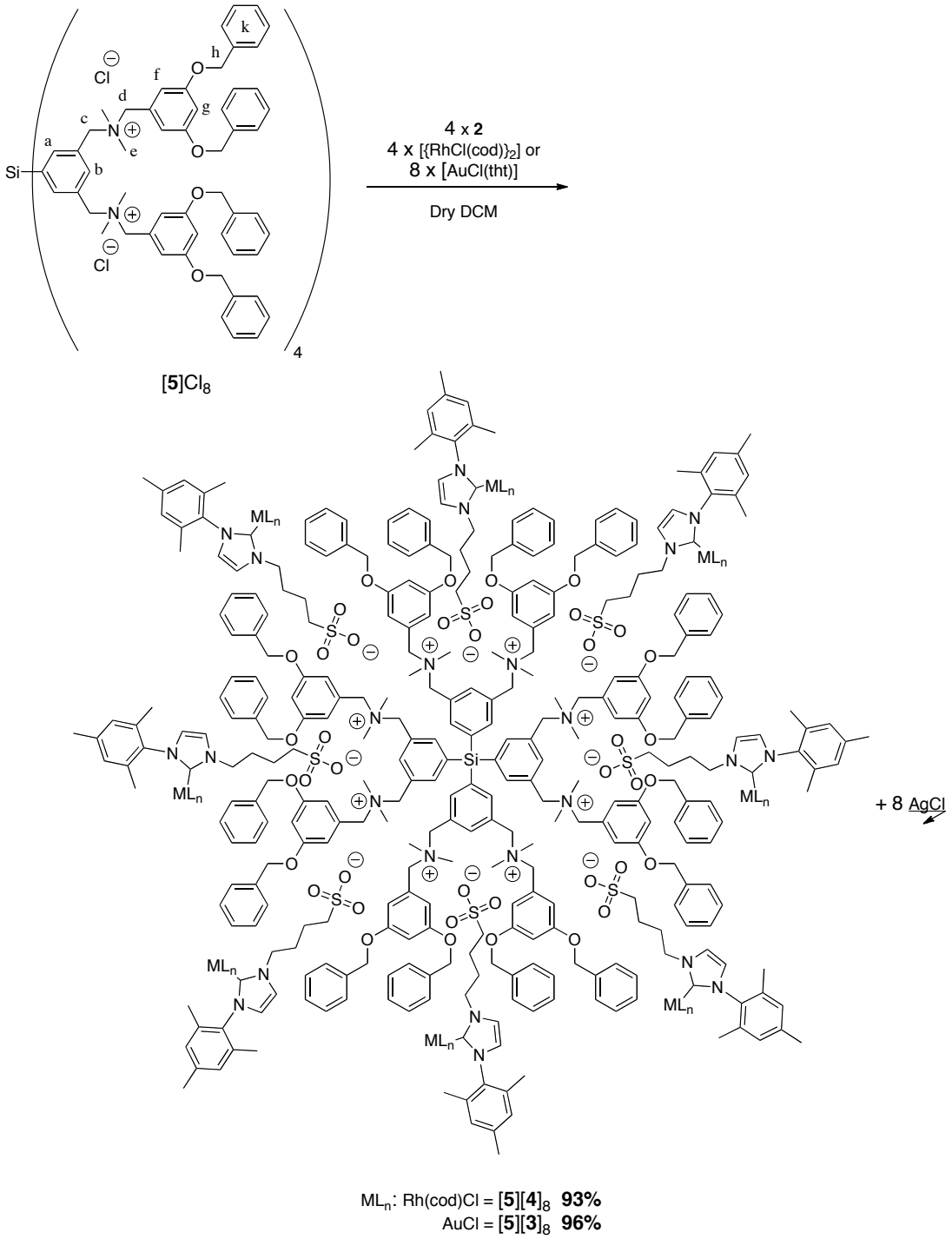

Scheme 4. Transmetallation of **2** with Au and Rh and immobilisation of the resulting NHC-complexes via the formation of metallo-dendritic assemblies [**5**][**4**]$_8$ and [**5**][**3**]$_8$.

As described for [NBu_4][**4**] and [PPh_4][**4**], the $^{13}C\{^1H\}$ NMR spectrum of [**5**][**4**]$_8$ showed a characteristic doublet for C^2 at 181.3 ppm with a coupling constant of $^1J_{Rh-C}$ = 51.5 Hz consistent with the presence of a C-Rh bond. Similarly, the $^{13}C\{^1H\}$ NMR spectrum of [**5**][**3**]$_8$ exhibits a signal at 170.9 ppm coherent with the presence of a C-Au bond as observed with [PPh_4][**3**]. The ^1H NMR spectra of [**5**][**3**]$_8$ (see Figure 4) and [**5**][**4**]$_8$ showed the presence of the typical signals corresponding to both the metal complexes and the dendrimer, though with significant shifts and sharpening of peaks compared to [**5**]Cl_8 which highlights a strong interaction between dendritic host and NHC-guest.[40] Integration of the peaks corresponding to the supported metal complexes and those of the dendrimer indicated that 8 (NHC)-metal complexes are present within a single dendritic assembly.

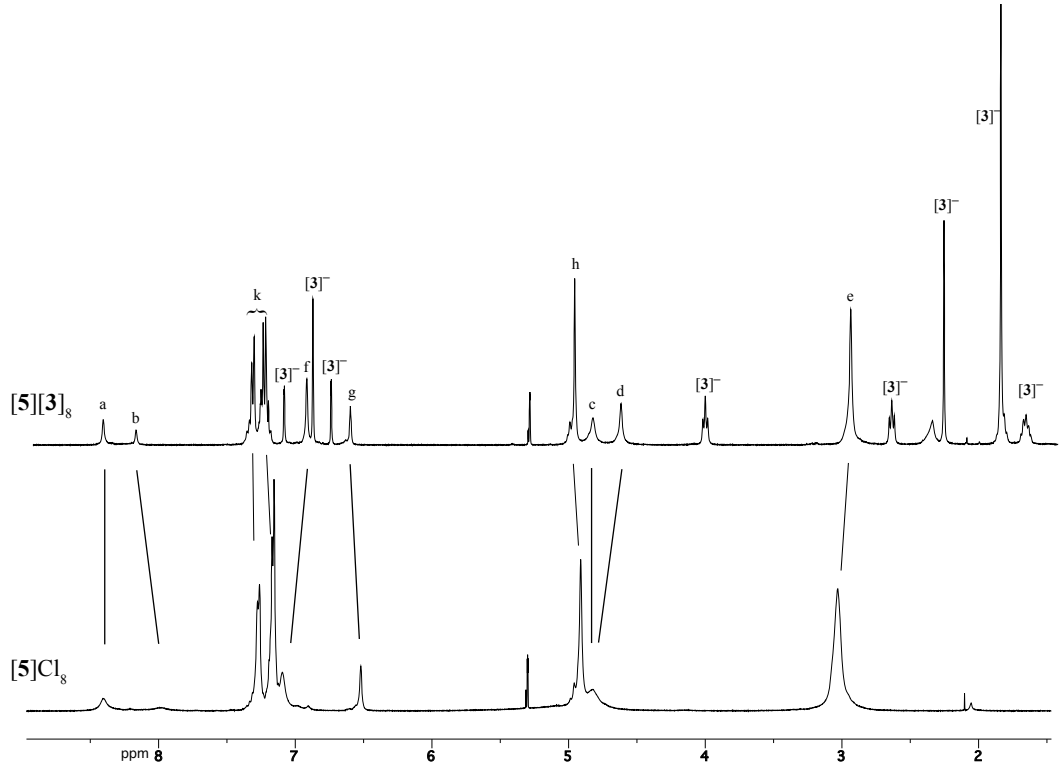

Figure 4. ^1H NMR spectra of [**5**][**3**]$_8$ and [**5**]Cl_8 measured in CD_2Cl_2 at 298 K. (For the labelling of the dendrimer signals, see Scheme 4).

The Rh complex [NBu_4][**4**] shows a pronounced feature in its UV-Vis spectrum at λ = 397 nm (ε = 1.64 $L.mol^{-1}.cm^{-1}$). Based on this feature, the stoichiometry of the Rh complex and dendritic support in [**5**][**4**]$_8$ is 8.2. Metallodendritic assemblies [**5**][**3**]$_8$ and [**5**][**4**]$_8$ were further characterized by electrospray mass spectroscopy (ESI-MS) operating

in positive ion mode (see Figure 5). Cations were generated by dissociation of anionic (NHC)-metal complexes from the assembly to give rise to multiply charged ions. Molecular ion peaks at m/z = 3313.7 and 2019.5 were attributed to the cations [**5**][**4**]$_6^{2+}$ and [**5**][**4**]$_5^{3+}$, which have calculated m/z values of 3314.0 and 2020.0, respectively. In the case of [**5**][**3**]$_8$, molecular peaks at m/z = 3272.3 and 1996.4 were assigned to [**5**][**3**]$_6^{2+}$ and [**5**][**3**]$_5^{3+}$ that have calculated m/z values of 3271.7 and 1996.5.

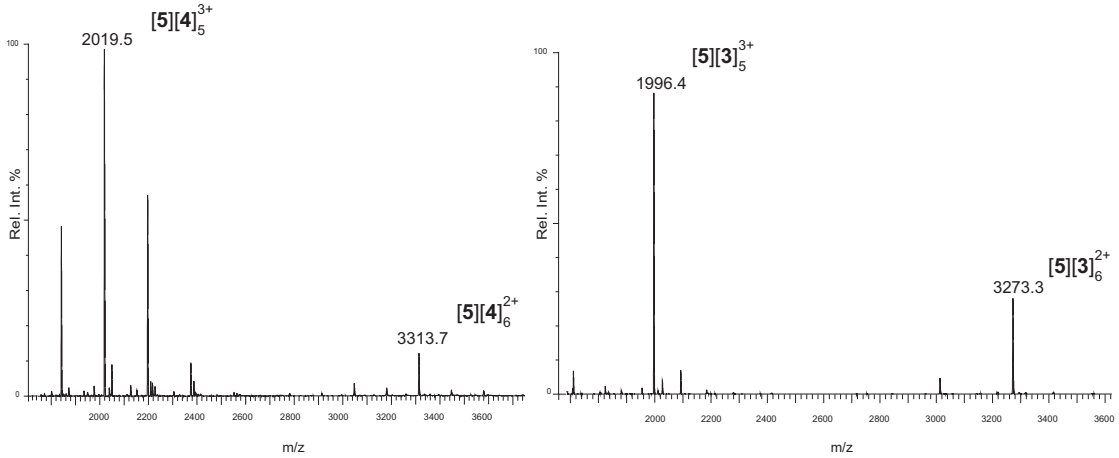

Figure 5. ESI-MS spectra of [**5**][**4**]$_8$ (left) and [**5**][**3**]$_8$ (right).

These combined analytic data unequivocally showed the successful formation of metallodendritic assemblies [**5**][**3**]$_8$ and [**5**][**4**]$_8$ in a single step procedure that involves both the transmetallation of 8 carbene ligands, the formation of 8 equivalents of AgCl and the assembly of 8 anions with an octacationic support.

Catalysis

The hydration of alkynes is an important organic transformation that is able to produce carbonyl compounds from alkynyl substrates in an atom efficient manner. This transformation is a very well known process that can be catalysed by different transition metal salts and complexes.[29] Among those, the use of gold-based catalytic systems to perform this reaction has proven to be successful[41] and more and more popular since the development of ligands that can enhance the electron density on the metal ion such as NHCs.[28]

The catalytic performances of the alkyl sulfonated (NHC)Au(I) [NBu_4][**3**] and its immobilised counterpart [**5**][**3**]$_8$ were tested in the catalytic hydration of alkynes. This reaction implies the use of an "activator" to allow for the formation of the corresponding cationic gold species, which is supposed to be the active catalyst for this transformation (Scheme 5).

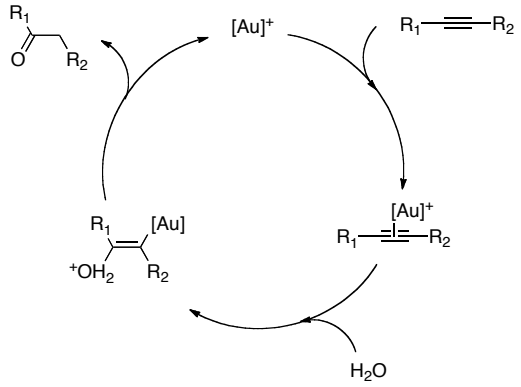

Scheme 5. Mecanisme of the Au catalysed nucleophilic addition of water to alkyne.

Typically in this reaction the cationic gold complex reacts with the alkyne enabling further nucleophilic attack of a molecule of water in a Markovnikov fashion yielding the corresponding ketone.

Table 1. Hydration of terminal alkynes.

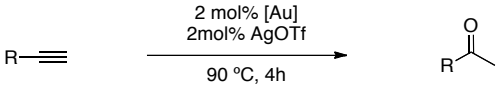

Entry	Substrate	Catalyst[a]	Yields (%)[b]
1	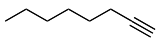	[NBu_4][**3**]	89
2		[**5**][**3**]$_8$	81
3	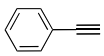	[NBu_4][**3**]	61
4		[**5**][**3**]$_8$	58
5	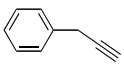	[NBu_4][**3**]	86
6		[**5**][**3**]$_8$	88

[a] Reaction conditions: alkyne (0.5 mmol), H_2O (1 mL), MeOH (3.5 mL), $CHCl_3$ (0.5 mL), (NHC)Au(I) complexes (2 mol %), reflux temperature. [b] Yields determined by GC after 4 h of reaction time, average of 2 independent runs.

The activation of the precatalyst to form the cationic gold species is traditionally performed with silver salts that abstract the halide from the metal centre. As the activity of the catalyst depends on its electrophilicity, the influence of the counter anion can be detrimental.[42] AgOTf was used as a co-catalyst in the hydration of terminal alkynes, the triflate anion possessing the required weakly coordinating properties and is furthermore commonly used as co-catalyst in gold catalysis. The two catalytic systems, [NBu_4][**3**] and [**5**][**3**]$_8$, show a very good and very similar activity. Indeed, the yields obtained with [NBu_4][**3**] and [**5**][**3**]$_8$ are almost identical suggesting that the catalytic performance of the transition metal complex used as the precatalyst is not, or in a very limited fashion, altered by the presence of the support. This finding prompted us to investigate further the influence of the support and more precisely the behaviour in solution of the precatalyst [**5**][**3**]$_8$.

DOSY NMR experiments of compound [**5**][**3**]$_8$ measured in CD_2Cl_2 at 300 K showed that the diffusion coefficient measured for different sets of proton signals corresponding to the cationic dendritic support and to the anionic Au complex is extremely similar. In Figure 6 we indeed observe a clear line corresponding to one diffusion coefficient, which unambiguously proves the presence of only one species in solution. This finding is in complete agreement with a previous study by Van de Coevering *et al.* where a similar metallodendritic assembly, consisting of the same cationic dendrimer as in [**5**][**3**]$_8$ in combination with 8 sulfato-tethered NCN-pincer PdCl moieties, showed a comparable behaviour in dichloromethane.[21] This is indicative of a very strong ion-pairing between the anionic guests and the polycationic host in this specific solvent, which is according to Van de Coevering *et al.* not only imputable to the electrostatic interactions between the host and the guest but also partially to the embedment of the transition metal complexes into the structure of the dendrimer.

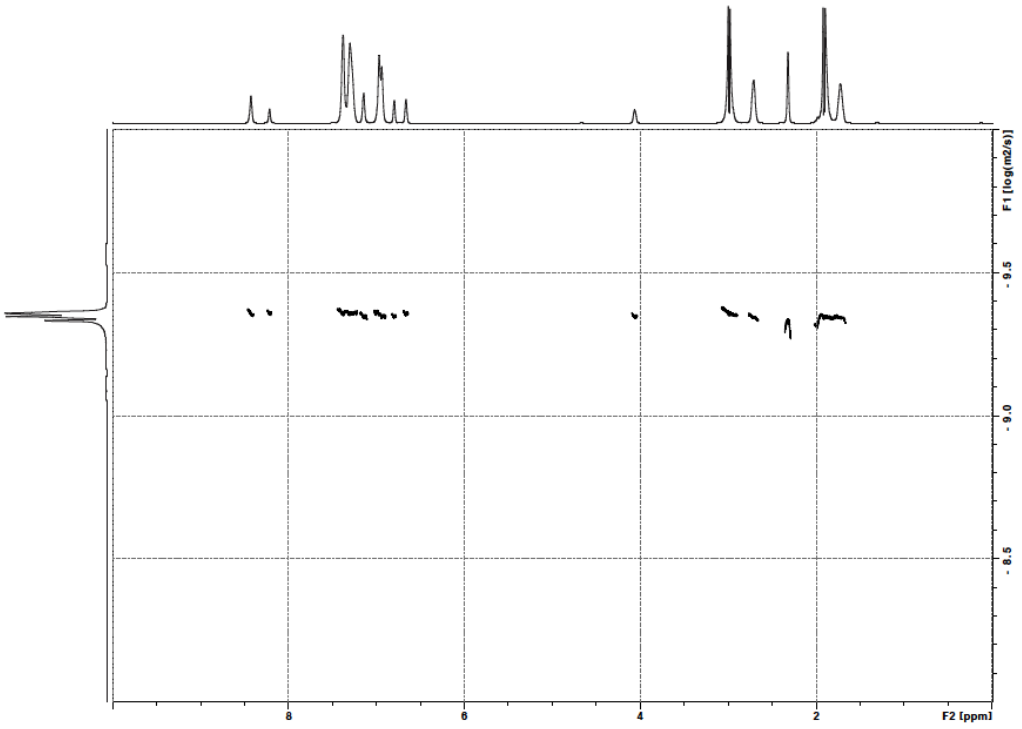

Figure 6. DOSY NMR of [**5**][**3**]$_8$ in CD_2Cl_2 at 300 K.

In order to evaluate the integrity of compound [**5**][**3**]$_8$ under the catalytic conditons, we performed DOSY experiments in the solvent used for the catalysis ($MeOH/H_2O/CHCl_3$ 2:7:1 v/v, the latter solvent was used for solubility reasons, see Experimental Section) in the presence of the co-catalyst (AgOTf). The ^{1}H NMR displayed obvious alterations in comparison with the ^{1}H NMR of [**5**][**3**]$_8$ in CH_2Cl_2, besides the normal differences observed due to the change of solvent. The formation of a cationic gold species is indeed expected to have a major consequence on the ^{1}H NMR chemical shifts. The presence of one or more species can be easily detected by DOSY NMR spectrometry, thus giving a qualitative idea of the ion-pairing strength between the sulfonate moiety of the guest and the ammonium group of the host. The ion-pairing strength is highly influenced by the solvent and is consequently very different depending on the solvent used.

The DOSY NMR experiment as previously shown is able to qualitatively estimate the presence of one or more species in solution depending on their diffusion coefficient. The spectrum displayed in Figure 7 indicates the presence of different species in $MeOH/H_2O/CDCl_3$ as indicated by the different diffusion coefficients obtained.

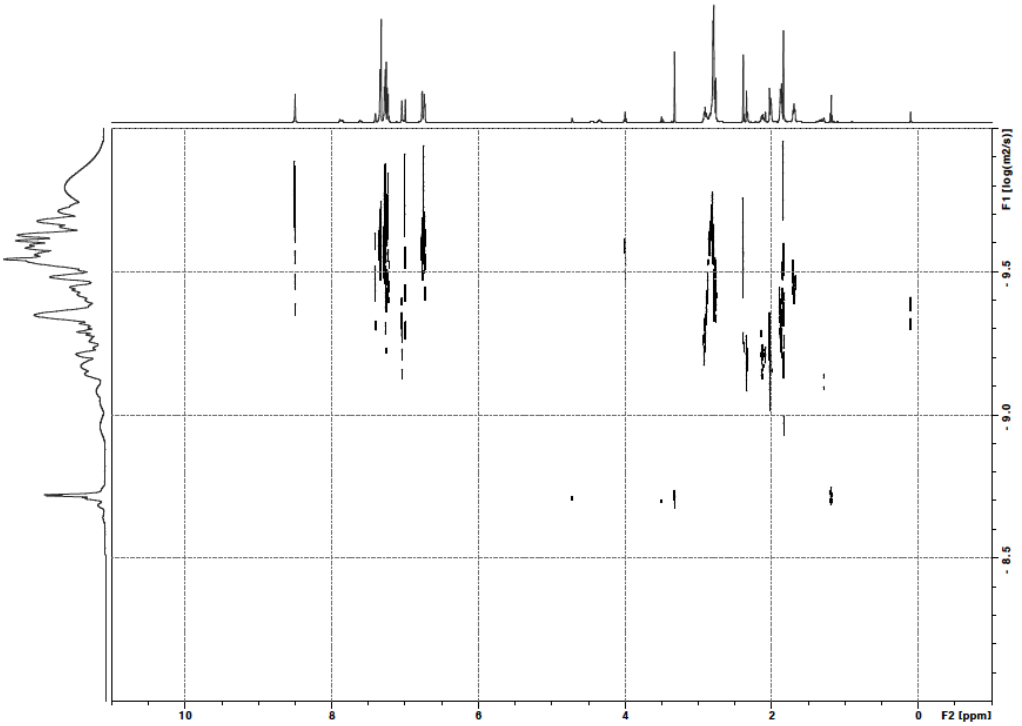

Figure 7. DOSY NMR of [**5**][**3**]$_8$ in a MeOH-d_4/D_2O/$CDCl_3$ mixture at 300 K in presence of AgOTf.

We can legitimately assume that the interaction between the polycationic guest and the Au(I) complex host in the MeOH-d_4/D_2O/$CDCl_3$ mixture is not as strong as in dichloromethane; the formation of zwitterionic NHC-Au(I) species in the solvent MeOH-d_4/D_2O/$CDCl_3$ lead to the formation of different species and/or aggregates. These findings coincide with the fact that the catalytic activity of [NBu_4][**3**] and [**5**][**3**]$_8$ are very similar, suggesting that the reaction is occurring with the zwitterionic species released from the dendritic support.

Next, we turned our attention to a catalytic reaction that does not require polar and/or protic solvent and that is not carried out by a formally cationic metal species. For this reason we investigated the Rh-mediated hydrosilylation of cyclohexanone. This reaction is known to be catalysed by NHC-Rh complexes, fulfils the requirements and does not necessitate to use a halogen scavenger to induce activity.[43] The activity of the (NHC)-Rh(I) complexes [NBu_4][**4**] and [**5**][**4**]$_8$ was evaluated in the catalysed hydrosilylation of cyclohexanone. Initial tests on the catalytic performances are shown in Table 2.

Table 2. Rhodium-catalysed hydrosilylation of cyclohexanone:

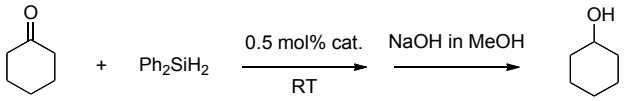

Catalyst	Solvent	Time (h)	Yield (%)[a]
$[NBu_4][\mathbf{4}]$	DCM	3	72
	THF	20	63
$[\mathbf{5}][\mathbf{4}]_8$	DCM	3	43
	THF	20	34

[a] Yields were determined by GC analysis.

Both catalysts were able to convert cyclohexanone into cyclohexanol but with a lower yield in the case of the metallodendritic catalyst. The activity of the Rh-carbene catalyst is influenced both by the type of solvent in which the reaction was carried out, as well as by the immobilisation on the dendrimer. This lack of reactivity of $[\mathbf{5}][\mathbf{4}]_8$ compared to the non-immobilised catalyst can be interpreted as the result of an important steric hindrance around the metal centre causing a difficult diffusion of the substrate to the active catalytic centre and thus a decrease in activity.

3.3 Conclusion

In summary, we have shown that sulfonate-functionalised metal mono-carbene complexes can be very easily and efficiently immobilised on a dendritic support by means of ionic interactions in a one pot transmetallation-immobilisation procedure. Quite remarkably, this procedure involves both transmetallation and ion exchange, which constitutes selective metal complex synthesis and metal complex immobilisation in one single synthetic operation. The application of (NHC)-Au(I) complex in the hydration of alkynes proved to be successful but suffer from the necessity to use a precatalyst to form a zwitterionic precatalyst, rendering the use of a gold metallodendritic assembly incompatible with our first aim of catalyst recycling. The hydrosilylation of ketone by an (NHC)-Rh(I) complex seems more promising as the reaction does not involve conditions susceptible to form complex dynamic systems.

3.4 Experimental section

General information: All reactions (unless otherwise mentioned) were performed under a N_2 atmosphere using standard Schlenk techniques. All reagents were purchased from Aldrich or Acros and were used as received. [**5**]Cl_8,[39] mesitylimidazole,[44] AuCl(tht)[45] and $[RhCl(cod)]_2$[46] were synthesised according to literature procedures. Passive dialysis was performed with commercially available dialysis tubing consisting of benzoylated cellulose membrane with a molecular weight cut-off of 1200 g/mol. The membrane tubing was stored in methanol and pre-treated with the solvent used in the subsequent dialysis. ^1H and $^{13}C\{^1H\}$ NMR spectroscopic measurements were conducted on a Varian Inova 300 or a Varian Oxford AS400 spectrometer at 25 °C and chemical shifts (δ) are given in ppm referenced to the residual solvent peak. Coupling constants are given in Hertz (Hz). Time-of-flight electrospray ionisation mass spectra were recorded on a Micromass LC-T mass spectrometer (Manchester, UK) operating in the positive or negative ion mode. In all experiments dendrimer samples at a concentration of 10-20 µM were introduced into the electrospray needles. The nanospray needle potential was typically set to 1300 V and the cone voltage to 60 V. The source block temperature was set to 80 °C. Maldi-TOF MS measurements were carried out on an Applied Biosystems Voyager DE-STR MALDI-TOF MS. The Elemental Analyses were performed by Dornis and Kolbe, Mikroanalytische Laboratorium, Mülheim a/d Ruhr, Germany. GC samples were analyzed using a Perkin Elmer Clarus 500 GC equipped with an Alltech Econo-Cap EC-5 column.

1-Mesityl-3-(4-sulfonatobutyl)imidazolium (1): Mesitylimidazole (2.044 g, 11 mmol) was added to a solution of 1,4-butane sultone (2.35 mL, 22 mmol) in 40 mL of dry toluene. After 48 h of reflux a white suspension was obtained. The solids were filtered off and washed successively with toluene and acetone and dried in vacuum yielding **1** as a white solid (3.54 g, 100 %).

^1H NMR (300 MHz, DMSO-d_6) δ = 9.46 (s, 1H; NC*H*N), 8.11 (s, 1H; NCH_{IMes}), 7.94 (s, 1H; CHN_{IMes}), 7.14 (s, 2H; Ar*H* Mes), 4.32 (m, 2H; NC$H_2(CH_2)_3SO_3$), 2.48 (m, 2H; $N(CH_2)_3CH_2SO_3$), 2.33 (s, 3H; CH_3 Mes), 2.02 (s, 6H; CH_3 Mes), 2.02-1.96 (m, 2H; $NCH_2CH_2(CH_2)_2SO_3$), 1.60-1.54 (m, 2H; $N(CH_2)_2CH_2CH_2SO_3$) **^{13}C {^1H} NMR (75 MHz, DMSO-d_6)** δ = 140.1, 137.4, 134.3, 131.1, 129.2, 123.9, 123.2, 50.3, 48.9, 28.4, 21.6, 20.6, 16.9 **Elemental Analysis** Calculated for $C_{16}H_{22}N_2O_3S$: C, 59.60; H, 6.88; N, 8.69; O, 14.89; S, 9.95 Found: C, 59.53; H, 6.80; N, 8.56; O, 15.06; S, 9.91.

Bis(1-mesityl-3-(4-sulfonatobutyl)imidazol-2-ylidene)silver silver salt (2): To a supension of **1** (0.607 g, 1.88 mmol) in 20 mL of dry acetonitrile was added silver oxide (0.389 g, 1.68 mmol). The mixture was heated at reflux temperature for overnight under the exclusion of light. The mixture was cooled to ambient temperature, filtered over Celite and the Celite washed with dichloromethane. The resulting solution was concentrated in vacuo to yield **2** as an off-white powder (0.700 g, 87 %).

^{1}H NMR (400 MHz, CD_2Cl_2) δ = 7.37 (d, 1H, $^3J_{HH}$ = 2 Hz; NCH_{IMes}), 6.96 (s, 2H, ArH Mes), 6.95 (d, 1H; CHN$_{IMes}$ overlap with aromatic protons), 4.23 (t, 2H, $^3J_{HH}$ = 7.2 Hz; NCH_2(CH$_2$)$_3$SO$_3$), 2.94 (t, 2H, $^3J_{HH}$ = 7.6 Hz; N(CH$_2$)$_3$CH_2SO$_3$), 2.38 (s, 3H, CH_3 Mes), 2.08-2.01 (m, 2H, NCH$_2$CH_2(CH$_2$)$_2$SO$_3$), 1.87 (s, 6H, CH_3 Mes), 1.87-1.81 (m, 2H; N(CH$_2$)$_2$CH_2CH$_2$SO$_3$ overlap with benzylic protons) **^{13}C {^{1}H} NMR (100 MHz, CD_2Cl_2)** δ = 180.2, 139.4, 135.8, 135.2, 129.3, 123.0, 122.0, 51.7, 50.5, 30.6, 22.4, 21.1, 17.6 **Maldi-TOF** m/z = 429.22 [M/2 + H]$^+$ **Elemental Analysis** Calculated for $C_{32}H_{42}Ag_2N_4O_6S_2$: C, 44.66; H, 5.15; N, 6.51; Ag, 25.07 Found: C, 44.21; H, 5.04; N, 6.48; Ag, 25.08

- **General procedure for the synthesis of compounds [NBu$_4$][3] and [PPh$_4$][3]:**

Compound **2** and PPh$_4$Cl or NBu$_4$Cl were dissolved in 10 mL of dry and degassed dichloromethane followed by addition of AuCl(tht). A white precipitate formed immediately and the reaction mixture was stirred for one extra hour. After this time the reaction mixture was filtered over Celite and the solvent evaporated in vacuum to yield the desired compound as a white powder.

[NBu$_4$][3]: Starting from **2** (0.227 g, 0.264 mmol), NBu$_4$Cl (0.147 g, 0.529 mmol), AuCl(THT) (0.170 g, 0.529 mmol). Yield: 0.368 g (87 %).

^{1}H NMR (400 MHz, CD_2Cl_2) δ = 7.38 (d, 1H, $^3J_{HH}$ = 1.6 Hz; NCH_{IMes}), 7.02 (s, 2H; ArH Mes), 6.91 (d, 1H, $^3J_{HH}$ = 1.6Hz; CHN$_{IMes}$), 4.31 (t, 2H, $^3J_{HH}$ = 7.2 Hz; NCH_2(CH$_2$)$_3$SO$_3$), 3.23 (t, 8H; NBu$_4$), 2.73 (t, 2H, $^3J_{HH}$ = 7.2Hz; N(CH$_2$)$_3$CH_2SO$_3$), 2.35 (s, 3H; CH_3), 2.11 (m, 2H; NCH$_2$CH_2(CH$_2$)$_2$SO$_3$), 2.02 (s, 6H; CH_3), 1.84 (m, 2H; N(CH$_2$)$_2$CH_2CH$_2$SO$_3$), 1.69-1.61 (m, 8H; NBu$_4$), 1.48-1.38 (m, 8H; NBu$_4$), 1.01 (m, 12H; NBu$_4$)

^{13}C{^{1}H} NMR (100 MHz, CD_2Cl_2) δ = 171.0, 139.6, 135.1, 135.0, 129.1, 122.0, 121.4, 58.9 (NBu$_4$), 51.2, 50.8, 30.3, 24.0 (NBu$_4$), 22.5, 20.9, 19.8 (NBu$_4$), 17.6, 13.5 (NBu$_4$) **Elemental Analysis** Calculated for $C_{32}H_{57}AuClN_3O_3S$: C, 48.27; H, 7.21; N, 5.28 Found: C, 48.69; H, 7.09; N, 4.72

[PPh_4][3]: Staring from **2** (0.489 g, 0.57 mmol), PPh_4Cl (0.428 g, 1.14 mmol), AuCl(tht) (0.366 g, 1.14 mmol). Yield: 1.05 g (100 %).

^{1}H NMR (400 MHz, CD_2Cl_2) δ = 8.01-7.94 (m, 4H; Ar*H* PPh_4), 7.85-7.79 (m, 8H; Ar*H* PPh_4), 7.73-7.65 (m, 8H; Ar*H* PPh_4), 7.49 (d, 1H, $^3J_{HH}$ = 2.4 Hz; NC*H*$_{IMes}$), 7.03 (s, 2H; Ar*H* Mes), 6.94 (d, 1H, $^3J_{HH}$ = 2.4 Hz; C*H*N_{IMes}), 4.32 (t, 2H, $^3J_{HH}$ = 9.6 Hz; NC*H*$_2(CH_2)_3SO_3$), 2.75 (t, 2H, $^3J_{HH}$ = 9.6 Hz; $N(CH_2)_3CH_2SO_3$), 2.37 (s, 3H; C*H*$_3$ Mes), 2.18-2.08 (m, 2H; $NCH_2CH_2(CH_2)_2SO_3$), 2.05 (s, 6H; C*H*$_3$ Mes), 1.90-1.80 (m, 2H; $N(CH_2)_2CH_2CH_2SO_3$) **^{13}C{^{1}H} NMR (100 MHz, CD_2Cl_2)** δ = 170.9 (N*C*N), 139.5, 135.7 (d, J_{P-C} = 2.9Hz; PPh_4), 135.2, 135.1, 134.5 (d, J_{P-C} = 10.3 Hz; PPh_4), 130.6 (d, J_{P-C} = 12.7 Hz; PPh_4), 129.1, 121.8, 121.6, 117.5 (d, J_{P-C} = 89.1 Hz; PPh_4), 51.1, 50.5, 30.2, 22.4, 20.9, 17.6 **Elemental Analysis** Calculated for $C_{40}H_{41}AuClN_2O_3PS$: C, 53.79; H, 4.63; N, 3.14 Found: C, 53.64; H, 4.57; N, 3.08

- **General procedure for the synthesis of compounds [NBu_4][4] and [PPh_4][4]:**

Compound **2** and NBu_4Cl or PPh_4Cl were dissolved in dry and degassed dichloromethane followed by addition of $[RhCl(cod)]_2$. A white precipitate formed immediately and the reaction mixture was stirred for one extra hour. After this time the reaction mixture was filtered over Celite and the solvent evaporated in vacuum. The resulting crude product was purified by column chromatography using a gradient from DCM/acetone from (1:1, v/v) to DCM/acetone/MeOH (32:64:4, v/v/v).

[NBu_4][4]: Starting from **2** (0.400 g, 0.466 mmol), NBu_4Cl (0.258 g, 0.932 mmol), $[RhCl(cod)]_2$ (0.229 g, 0.466 mmol). Yield: 0.757 g (97 %).

^{1}H NMR (400 MHz, CD_2Cl_2) δ = 7.14 (d, 1H, $^3J_{HH}$ = 1.6 Hz; NC*H*$_{IMes}$), 7.02 (s, 1H; Ar*H* Mes), 6.88 (s, 1H; Ar*H* Mes), 6.72 (d, 1H, $^3J_{HH}$ = 1.6 Hz; C*H*N_{IMes}), 5.05 (m, 1H; C*H* cod), 4.72 (m, 1H; C*H* cod), 4.57 (m, 1H; C*H* cod), 4.31 (m, 1H; C*H* cod), 3.38 (m, 1H; NC*H*$H(CH_2)_3SO_3$), 3.19 (t, 8H, $^3J_{HH}$ = 8.6 Hz; $N(CH_2(CH_2)_3)_4$), 2.95 (m, 1H; $NCHH(CH_2)_3SO_3$), 2.79 (m, 2H; $N(CH_2)_3CH_2SO_3$), 2.41-2.33 (m, 2H; C*H*$_2$ cod) 2.35 (d, 6H, $^3J_{HH}$ = 2.8 Hz; C*H*$_3$ Mes), 2.25-2.10 (m, 2H; C*H*$_2$ cod), 1.98-1.90 (m, 2H; C*H*$_2$ cod), 1.88-1.81 (m, 2H; NCH_2CH_2 overlapping with NBu_4), 1.81 (s, 3H; C*H*$_3$ Mes), 1.75-1.67 (m, 2H; C*H*$_2$ cod overlapping with NBu_4), 1.64 (m, 8H; NBu_4), 1.53-1.45 (m, 2H; $CH_2CH_2SO_3$ overlapping with NBu_4), 1.43 (m, 8H; NBu_4), 1.00 (t, 12H; NBu_4) **^{13}C{^{1}H} NMR (100 MHz, CD_2Cl_2)** δ = 181.2 (d, $^1J_{Rh-C}$ = 51.2 Hz), 138.4, 136.6, 136.3, 134.6, 129.1, 128.1, 122.9, 121.1, 96.3 (d, $^1J_{Rh-C}$ = 7.3 Hz), 95.9 (d, $^1J_{Rh-C}$ = 7.0 Hz), 68.3 (d, $^1J_{Rh-C}$ = 14.2 Hz), 67.5 (d, $^1J_{Rh-C}$ = 14.5 Hz), 58.7 (NBu_4), 51.3, 51.2, 33.8, 31.6, 30.2,

28.9, 28.0, 23.9 (NBu_4), 22.9, 20.7, 19.6 (NBu_4), 19.3, 17.5, 13.5 (NBu_4) **HRMS (ES⁻)** calculated for $C_{24}H_{33}ClN_2O_3RhS$: m/z = 567.0955 found: 567.0959 $[M\text{-}NBu_4]^-$.

[**PPh_4**][**4**]: Starting from **2** (0.052 g, 0.061 mmol), PPh_4Cl (0.045 g, 0.121 mmol), $[RhCl(cod)]_2$ (0.030 g, 0.061 mmol). Yield: 0.104 g (95 %).

^{1}H NMR (400 MHz, CD_2Cl_2) δ = 7.90 (m, 4H; Ar*H* PPh_4), 7.75 (m, 8H; Ar*H* PPh_4), 7.61 (m, 8H; Ar*H* PPh_4), 7.11 (d, 1H, $^3J_{HH}$ = 1.6 Hz; NC*H*$_{IMes}$), 7.02 (s, 1H; Ar*H* Mes), 6.89 (s, 1H; Ar*H* Mes), 6.71 (d, 1H, $^3J_{HH}$ = 1.6 Hz; C*H*N_{IMes}), 5.15-5.08 (m, 1H; C*H* cod), 4.75-4.70 (m, 1H; C*H* cod), 4.58-4.53 (m, 1H; C*H* cod), 4.26-4.18 (m, 1H; C*H* cod), 3.39 (m, 1H; NC*H*H$(CH_2)_3SO_3$), 2.96 (m, 1H; NCH*H*$(CH_2)_3SO_3$), 2.77-2.70 (m, 2H; N$(CH_2)_3CH_2SO_3$), 2.32 (s, 3H, CH_3 Mes), 2.31 (s, 3H, CH_3 Mes), 2.39-2.27 (m, 2H; CH_2 cod), 2.24-2.17 (m, 2H; CH_2 cod), 2.15-2.05 (m, 2H; CH_2 cod), 1.95-1.85 (m, 2H; $NCH_2CH_2(CH_2)_2SO_3$), 1.78 (s, 3H; CH_3 Mes), 1.70-1.56 (m, 2H; CH_2 cod) 1.53-1.39 (m, 2H; $N(CH_2)_2SO_3CH_2CH_2SO_3$) **^{13}C{^{1}H} NMR (100 MHz, CD_2Cl_2)** δ = 181.4 (d, $^1J_{Rh\text{-}C}$ = 51.2 Hz; N*C*N), 138.5, 136.7, 136.4, 135.8 (d, $J_{P\text{-}C}$ = 3 Hz; PPh_4), 134.8, 134.5 (d, $J_{P\text{-}C}$ = 10.2 Hz; PPh_4), 130.7 (d, $J_{P\text{-}C}$ = 12.9 Hz; PPh_4), 129.2, 128.2, 122.9, 121.2. 117.6 (d, $J_{P\text{-}C}$ = 89 Hz; PPh_4), 96.4 (d, $^1J_{Rh\text{-}C}$ = 7.3 Hz), 95.8 (d, $^1J_{Rh\text{-}C}$ = 7 Hz), 68.4 (d, $^1J_{Rh\text{-}C}$ = 14.1 Hz), 67.6 (d, $^1J_{Rh\text{-}C}$ = 14.4 Hz), 51.5, 51.3, 33.8, 31.7, 30.3, 28.9, 28.2, 23.1, 20.8, 19.4, 17.6 **HRMS (ES⁻)** calculated for $C_{24}H_{33}ClN_2O_3RhS$: 567.0955 found: 567.0978 $[M\text{-}PPh_4]^-$

- **General procedure for the synthesis of compounds [5][3]$_8$ and [5][4]$_8$:**

Compound **2** and [**5**]Cl_8 were dissolved in dry and degassed DCM and AuCl(tht) or $[RhCl(cod)]_2$ was subsequently added. The reaction mixture was stirred at ambient temperature for overnight. After this time the reaction mixture was filtered over Celite to remove AgCl and the filtrate was concentrated in vacuum. The compounds were dissolved in a small amount of DCM and the solution was purified by passive dialysis using DCM/acetone (1:1, v/v) as solvent. The compound was then precipitated with Et_2O from the DCM solution.

[5][3]$_8$: Starting from **2** (0.134 g, 0.156 mmol), [**5**]Cl_8 (0.137 g, 0.039 mmol), AuCl(tht) (0.100 g, 0.312 mmol). Yield: 0.231 g (96 %).

^{1}H NMR (400 MHz, CD_2Cl_2) δ = 8.42 (s, 8H; Ar*H* core Dendr.), 8.18 (s, 4H; Ar*H* core Dendr.), 7.37-7.32 (m, 32H; Ar*H* Dendr. wedge), 7.28-7.21 (m, 48H, Ar*H* Dendr. wedge), 7.09 (d, 8H, $^3J_{HH}$ = 1.6 Hz; NC*H*$_{IMes}$), 6,93 (bs, 16H; Ar*H* Dendr. wedge), 6.88 (s, 16H; Ar*H* Mes), 6.75 (d, 8H, $^3J_{HH}$ = 1.6 Hz; C*H*N_{IMes}), 6.61 (m, 8H; Ar*H* Dendr. wedge), 4.97

(s, 32H; OCH_2 Dendr. wedge), 4.84 (bs, 16H; NCH_2 Dendr. wedge), 4.63 (bs, 16H; NCH_2 core Dendr.), 4.01 (t, 16H, $^3J_{HH}$ = 7.2 Hz; NCH_2(CH$_2$)$_3$SO$_3$), 2.95 (bs, 48H; N(CH_3)$_2$ core Dendr.), 2.65 (t, 16H, $^3J_{HH}$ = 7.2 Hz; N(CH$_2$)$_3$CH_2SO$_3$), 2.27 (s, 24H; CH_3 Mes), 1.88-1.81 (m, 16H; NCH$_2$CH_2(CH$_2$)$_3$SO$_3$ overlap with CH_3 Mes), 1.85 (s, 48H, CH_3 Mes), 1.70-1.63 (m, 16H; N(CH$_2$)$_2$CH_2CH$_2$SO$_3$) **^{13}C{^{1}H} NMR (100 MHz, CD$_2$Cl$_2$)** δ = 170.8, 160.1 (Dendr.), 143.1 (Dendr.), 140.1 (Dendr.), 139.7, 136.7 (Dendr.), 135.9 (Dendr.), 135.0, 134.9, 129.9 (Dendr.), 129.2, 129.1 (Dendr.), 128.6 (Dendr.), 128.1 (Dendr.), 127.9 (Dendr.), 122.3, 121.1, 112.7 (Dendr.), 103.9 (Dendr.), 70.3 (Dendr.), 68.4 (Dendr.), 67.0 (Dendr.), 51.2, 50.9, 48.9 (Dendr.), 30.1, 22.5, 21.0, 17.6 **Elemental Analysis** Calculated for $C_{344}H_{396}Au_8Cl_8N_{24}O_{40}S_8Si$: C, 54.00; H, 5.22; N, 4.39 Found: C, 53.52; H, 5.23; N, 4.09 **ESI-MS** (positive ion mode) m/z = 3272.3 [M-2x**3**]$^{2+}$, 1996.4 [M-3x**3**]$^{3+}$.

[5][4]$_8$: Starting from **2** (0.070 g, 0.082 mmol), [**5**]Cl$_8$ (0.072 g, 0.020 mmol), [RhCl(cod)]$_2$ (0.040 g, 0.82 mmol). Yield: 0.123 g (93 %).

^{1}H NMR (400 MHz, CD$_2$Cl$_2$) δ = 8.45 (s, 8H; ArH core Dendr.), 8.17 (s, 4H; ArH core Dendr.), 7.38-7.32 (m, 32H; ArH Dendr. wedge), 7.26-7.18 (m, 48H, ArH Dendr. wedge), 6.98 (bs, 16H + 8H; ArH Dendr. wedge overlap with NCH_{IMes}), 6.93 (s, 8H; ArH Mes), 6.88 (s, 8H; ArH Mes), 6.61 (d, 8H, $^3J_{HH}$ = 1.6 Hz; CHN$_{IMes}$), 6.60 (m, 8H; ArH Dendr. wedge), 4.98 (bs, 32H + 8H; OCH_2 Dendr. wedge + CH cod), 4.87 (bs, 16H; NCH_2 Dendr. wedge), 4.73-4.62 (m, 8H; CH cod), 4.68 (bs, 16H; NCH_2 core Dendr.), 4.60-4.56 (m, 8H; CH cod), 4.44-4.37 (m, 8H; CH cod), 3.31-3.28 (m, 8H; NCHH(CH$_2$)$_3$SO$_3$), 2,99 (bs, 48H; N(CH_3)$_2$ core Dendr.), 2.93-2.89 (m, 8H; NCHH(CH$_2$)$_3$SO$_3$), 2.75-2.71 (m, 16H; N(CH$_2$)$_3$CH_2SO$_3$), 2.32 (s, 24H; CH_3 Mes), 2.27 (s, 24H; CH_3 Mes), 2.27-2.18 (m, 16H; CH_2 cod), 2.08-1.92 (m, 16H; CH_2 cod), 1.88-1.81 (m, 16H; CH_2 cod), 1.73 (bs, 24H; CH_3 Mes), 1.65-1.59 (m, 16H; NCH$_2$CH_2(CH$_2$)$_2$SO$_3$), 1.54-1.35 (m, 16H + 16H; CH_2 cod overlap with N(CH$_2$)$_2$CH_2CH$_2$SO$_3$) **^{13}C{^{1}H} NMR (100 MHz, CD$_2$Cl$_2$)** δ = 181.2 (d, $^1J_{Rh\text{-}C}$ = 51.5 Hz), 160.0 (Dendr.), 143.1 (Dendr.), 139.9 (Dendr.), 138.5, 136.7 (Dendr.), 136.6, 136.2, 135.9 (Dendr.), 134.4, 130.0 (Dendr.), 129.3 (Dendr.), 129.1, 128.5 (Dendr.), 128.2, 128.0 (Dendr.), 127.8 (Dendr.), 123.1, 120.9, 112.6 (Dendr.), 103.9 (Dendr.), 96.4 (d, $^1J_{Rh\text{-}C}$ = 7 Hz), 96.3 (d, $^1J_{Rh\text{-}C}$ = 7.5 Hz), 70.2 (Dendr.), 68.4 (d, $^1J_{Rh\text{-}C}$ = 13.7 Hz), 68.2 (Dendr.), 67.5 (d, $^1J_{Rh\text{-}C}$ = 13.3 Hz), 67.0 (Dendr.), 51.7, 51.1, 48.8 (Dendr.), 33.9, 31.5, 30.1, 29.0, 28.0, 23.0, 20.8, 19.5, 17.6 **ESI-MS** (positive ion mode) m/z = 3313.7 [M-2x**4**]$^{2+}$, 2019.5 [M-3x**4**]$^{3+}$.

- **General procedure for the catalysed hydrosilylation of ketones:**

The rhodium catalyst (0.005 mmol) was introduced in a Schlenk tube then evacuated and backfilled with N_2 three times. 2 mL of dry and degassed solvent were added followed by addition of the substrate (1 mmol) and pentadecane as internal standard (0.125 mmol). The mixture was stirred for 5 min and diphenylsilane (1.2 mmol) was subsequently added via syringe.
Samples (0.2 mL) were taken from the reaction mixture at regular time intervals, treated with 0.1 mL of a solution of 50 % aqueous NaOH in MeOH (1:30, v/v), taken up in 2 mL DCM and filtered over a short plug of silica.

- **General procedure for the hydration of alkynes:**

In a Schlenk tube were introduced 1 mL of H_2O, 3.25 mL of MeOH, 0.5 mmol of the substrate, 0.25 mL of a stock solution of AgOTf in MeOH (0.04 M) and pentadecane as internal standard (0.25 mmol). The mixture was heated up at reflux temperature followed by addition of 0.5 mL of a stock solution of the catalyst in $CHCl_3$ (0.02 M for **1** and 2.5 mM for **2**). After an appropriate period of time, sample of 0.1 mL were taken from each reaction mixture, diluted with 2 mL of DCM and filtered through a short plug of silica.

- **NMR diffusion experiments:**

DOSY NMR experiments were performed on a Bruker Avance III 600 MHz spectrometer at 300 K. Pseudo-2D stimulated echo DOSY experiments with bipolar gradient pulse pairs and a single spoil gradient were carried out with 64 steps of different gradient strength. 16 scans were accumulated for each FID of 4096 points; the carrier frequency was set at 5ppm and the spectral width was 12 ppm. Processing was done with the standard DOSY-software available in Topspin 2.1.
The NMR samples were prepared by dissolution of 5 mg of compound **2** in 1 mL of the appropriate deuteriated solvent or mixture of solvents.

The translational self-diffusion coefficient of molecules is determine with the Stejskal–Tanner equation:

$$\ln\left(\frac{I}{I_0}\right) = -(\gamma\delta)^2 G^2 \left(\Delta - \frac{\delta}{3}\right) D$$

The diffusion coefficient, D, which is proportional to the slope of the regression line, is obtained by plotting $\ln(I/I_0)$ (I/I_0 = observed spin–echo intensity/intensity without gradients) vs. either Δ, δ^2, $(\Delta-\delta/3)$ or G^2. The Stokes-Einstein equation relates this translational self-diffusion coefficient D_t to the hydrodynamic radius of the molecule- assuming a spherical shape of the molecule- in the following equation:

$$D_t = \frac{kT}{6\pi\eta r_H}$$

- **X-ray crystal structure determination**

All reflection intensities were measured at 150(2) K using a Nonius KappaCCD diffractometer (rotating anode) with graphite-monochromated Mo *K*α radiation (λ = 0.71073 Å) under the program COLLECT.[47] The programs PEAKREF[48] or HKL2000[49] were used to refine cell dimensions. Data were reduced using the integration programs EvalCCD[50] or HKL2000.[49] The structures were solved with DIRDIF99[51] and were refined on F^2 with SHELXL-97.[52] Multi-scan semi-empirical absorption corrections based on symmetry-related measurements were applied to all data using SADABS (Version 2006/1).[53] The data collection temperature was controlled using the system Oxford Cryostream 600 (manufactured by Oxford Cryosystems). The H-atoms (except when specified) were placed at calculated positions (instructions AFIX 23, 43 or 137) with isotropic displacement parameters having values 1.2 or 1.5 times Ueq of the attached C atoms, and were refined with a riding model. For 2, the H-atoms of the non-coordinated water molecule were found from difference Fourier maps were subsequently fixed at their located positions. Geometry calculations, structure validations and illustrations were made with the PLATON program.[54]

2: $C_{32}H_{42}Ag_2N_4O_6S_2 \cdot ½(H_2O)$, Fw = 867.56, colorless needle, 0.27 × 0.09 × 0.06 mm^3, triclinic, $P\bar{1}$ (no. 2), a = 13.1193(3), b = 14.3639(4), c = 20.4339(6) Å, α = 91.3369(19), β = 93.682(2), γ = 110.8574(8)°, V = 3586.48(17) Å^3, Z = 4, D_x = 1.61 g cm^{-3}, μ = 1.26 mm^{-1}, abs. corr. range: 0.56–0.74. 45532 Reflections were measured up to a resolution of $(\sin\theta/\lambda)_{max}$ = 0.61 Å^{-1}. 13459 Reflections were unique (R_{int} = 0.047), of which 10399 were observed [$I > 2\sigma(I)$]. 850 Parameters were refined. $R1/wR2$ [$I > 2\sigma(I)$]: 0.0387/0.0790. $R1/wR2$ [all refl.]: 0.0607/0.0871. S = 1.031. Residual electron density found between −0.88 and 0.88 eÅ^{-3}.

[PPh$_4$][3]: $C_{16}H_{21}AuClN_2O_3PS$, Fw = 893.19, colorless plate, 0.34 × 0.24 × 0.10 mm^3, monoclinic, $P2_1/c$ (no. 14), a = 18.7895(6), b = 7.6882(2), c = 30.8460(10) Å, β = 124.757(2)°, V = 3660.9(2) Å^3, Z = 4, D_x = 1.62 g cm^{-3}, μ = 4.23 mm^{-1}, abs. corr. range:

0.21–0.66. 54414 Reflections were measured up to a resolution of $(\sin \theta/\lambda)_{max}$ = 0.63 Å^{-1}. 7592 Reflections were unique (R_{int} = 0.020), of which 6713 were observed [$I > 2\sigma(I)$]. 445 Parameters were refined. $R1/wR2$ [$I > 2\sigma(I)$]: 0.0165/0.0351. $R1/wR2$ [all refl.]: 0.0235/0.0380. S = 1.098. Residual electron density found between −0.79 and 0.73 eÅ^{-3}.

3.5 References

[1] A. J. Arduengo, *Acc. Chem. Res.* **1999**, *32*, 913-921.

[2] W. A. Herrmann, *Angew. Chem. Int. Ed.* **2002**, *41*, 1290-1309.

[3] S. P. Nolan, *N-Heterocyclic Carbenes in Synthesis*, Wiley-VCH, Weinheim, **2006**.

[4] F. Glorius, *Top. Organomet. Chem.* **2007**, *21*, 1–20.

[5] F. E. Hahn, M. C. Jahnke, *Angew. Chem. Int. Ed.* **2008**, *47*, 3122-3172.

[6] O. Kühl, *Chem. Soc. Rev.* **2007**, *36*, 592-607.

[7] H. M. Lee, C.-C. Lee, P.-Y. Cheng, *Curr. Org. Chem.* **2007**, *11*, 1491-1524.

[8] J. W. J. Knapen, A. W. van der Made, J. C. de Wilde, P. W. N. M. van Leeuwen, P. Wijkens, D. M. Grove, G. van Koten, *Nature* **1994**, *372*, 659-663.

[9] R. A. Gossage, L. A. van de Kuil, G. van Koten, *Acc. Chem. Res.* **1998**, *31*, 423-431.

[10] G. van Koten, J. T. B. H. Jastrzebski, *J. Mol. Catal. A: Chem.* **1999**, *146*, 317-323.

[11] A. W. Kleij, R. A. Gossage, R. J. M. Klein Gebbink, N. Brinkmann, E. J. Reijerse, U. Kragl, M. Lutz, A. L. Spek, G. van Koten, *J. Am. Chem. Soc.* **2000**, *122*, 12112-12124.

[12] P. Wijkens, J. T. B. H. Jastrzebski, P. A. van der Schaaf, R. Kolly, A. Hafner, G. van Koten, *Org. Lett.* **2000**, *2*, 1621-1624.

[13] A. W. Kleij, R. J. M. Klein Gebbink, M. Lutz, A. L. Spek, G. van Koten, *J. Organomet. Chem.* **2001**, *621*, 190-196.

[14] A. W. Kleij, R. J. M. Klein Gebbink, P. A. J. van den Nieuwenhuijzen, H. Kooijman, M. Lutz, A. L. Spek, G. van Koten, *Organometallics* **2001**, *20*, 634-647.

[15] R. van de Coevering, R. J. M. Klein Gebbink, G. van Koten, *Prog. Polym. Sci.* **2005**, *30*, 474-490.

[16] D. E. Bergbreiter, B. L. Case, Y. S. Liu, J. W. Caraway, *Macromolecules* **1998**, *31*, 6053-6062.

[17] E. Schwab, S. Mecking, *Organometallics* **2001**, *20*, 5504-5506.

[18] R. van de Coevering, M. Kuil, R. J. M. Klein Gebbink, G. van Koten, *Chem. Commun.* **2002**, 1636-1637.

[19] M. Ooe, M. Murata, A. Takahama, T. Mizugaki, K. Ebitani, K. Kaneda, *Chem. Lett.* **2003**, *32*, 692-693.

[20] L. Plault, A. Hauseler, S. Nlate, D. Astruc, J. Ruiz, S. Gatard, R. Neumann, *Angew. Chem. Int. Ed.* **2004**, *43*, 2924-2928.

[21] R. van de Coevering, A. P. Alfers, J. D. Meeldijk, E. Martinez-Viviente, P. S. Pregosin, R. J. M. Klein Gebbink, G. van Koten, *J. Am. Chem. Soc.* **2006**, *128*, 12700-12713.

[22] A. R. McDonald, D. Mores, C. D. Donega, C. A. van Walree, R. J. M. Klein Gebbink, M. Lutz, A. L. Spek, A. Meijerink, G. P. M. van Klink, G. van Koten, *Organometallics* **2009**, *28*, 1082-1092.

[23] A. S. K. Hashmi, G. J. Hutchings, *Angew. Chem. Int. Ed.* **2006**, *45*, 7896-7936.

[24] A. Arcadi, *Chem. Rev.* **2008**, *108*, 3266-3325.

[25] G. Dyker, *Angew. Chem. Int. Ed.* **2000**, *39*, 4237-+.

[26] A. S. K. Hashmi, *Chem. Rev.* **2007**, *107*, 3180-3211.

[27] D. J. Gorin, B. D. Sherry, F. D. Toste, *Chem. Rev.* **2008**, *108*, 3351-3378.

[28] N. Marion, S. P. Nolan, *Chem. Soc. Rev.* **2008**, *37*, 1776-1782.

[29] L. Hintermann, A. Labonne, *Synthesis* **2007**, 1121-1150.

[30] L. R. Moore, S. M. Cooks, M. S. Anderson, H.-J. Schanz, S. T. Griffin, R. D. Rogers, M. C. Kirk, K. H. Shaughnessy, *Organometallics* **2006**, *25*, 5151-5158.

[31] M. K. Brown, T. L. May, C. A. Baxter, A. H. Hoveyda, *Angew. Chem. Int. Ed.* **2007**, *46*, 1097 –1100.

[32] C. Fleckenstein, S. Roy, S. Leuthaüßer, H. Plenio, *Chem. Commun.* **2007**, 2870–2872.

[33] Y. Nagai, T. Kochi, K. Nozaki, *Organometallics* **2009**, *28*, 6131-6134.

[34] J. C. Garrison, W. J. Youngs, *Chem. Rev.* **2005**, *105*, 3978-4008.

[35] H. M. J. Wang, I. J. B. Lin, *Organometallics* **1998**, *17*, 972-975.

[36] H. M. J. Wang, C. Y. L. Chen, I. J. B. Lin, *Organometallics* **1999**, *18*, 1216-1223.

[37] P. d. Frémont, N. M. Scott, E. D. Stevens, S. P. Nolan, *Organometallics* **2005**, *24*, 2411-2418.

[38] A. R. Chianese, X. Li, M. C. Janzen, J. W. Faller, R. H. Crabtree, *Organometallics* **2003**, *22*, 1663-1667.

[39] A. W. Kleij, R. van de Coevering, R. J. M. Klein Gebbink, A.-M. Noordman, A. L. Spek, G. van Koten, *Chem. Eur. J.* **2001**, *7*, 181-192.

[40] The chemical shifts and sharpening of peaks are consistent with the findings of R. v. d. Covering et al.: see reference [13] and [16].

[41] Z. G. Li, C. Brouwer, C. He, *Chem. Rev.* **2008**, *108*, 3239-3265.

[42] D. Zuccaccia, L. Belpassi, F. Tarantelli, A. Macchioni, *J. Am. Chem. Soc.* **2009**, *131*, 3170-+.

[43] J. F. Carpentier, V. Bette, *Curr. Org. Chem.* **2002**, *6*, 913-936.

[44] J. Liu, J. Chen, J. Zhao, Y. Zhao, L. Li, H. Zhang, *Synthesis* **2003**, *17*, 2661–2666.

[45] R. Uson, A. Laguna, M. Laguna, *Inorg. Synth.* **1989**, *26*, 85-91.

[46] G. Giordano, R. H. Crabtree, *Inorg. Synth.* **1979**, *19*, 218-220.

[47] B. V. Nonius, *COLLECT*, University of Delft, Delft (The Netherlands), **1999**.

[48] A. M. M. Schreurs, *PEAKREF*, Utrecht University, Utrecht (The Netherlands), **2005**.

[49] Z. Otwinowski, W. Minor, *Processing of X-ray Diffraction Data Collected in Oscillation Mode Methods in Enzymology, Vol. 276* (Eds.: J. C.W. Carter, R. M. Sweet), Macromolecular Crystallography, part A, **1997**, pp. 307-326.

[50] A. J. M. Duisenberg, L. M. J. Kroon-Batenburg, A. M. M. Schreurs, *J. Appl. Cryst.* **2003**, *36*, 220-229.

[51] P. T. Beurskens, G. Beurskens, R. d. Gelder, S. Garcia-Granda, R. Israel, R. O. Gould, J. M. M. Smits, *The DIRDIFF99 Program System*, Technical Report of the Crystallography Laboratory, University of Nijmegen, Nijmegen (The Netherlands), **1999**.

[52] G. M. Sheldrick, *Acta Cryst.* **2008**, *A64*, 112-122.

[53] G. M. Sheldrick, *SADABS, Version 2006/1*, University of Göttingen, Göttingen (Germany), **2006**.

[54] A. L. Spek, *J. Appl. Cryst.* **2003**, *36*, 7-13.

CHAPTER FOUR

Synthesis of Multimetallic Dendrimers through Non-Covalent Interactions

ABSTRACT

Hexa-ammonium functionalised Dendriphos ligands and mono-sulfonate functionalised transition metal complexes have been used as building blocks for the preparation of multimetallic dendritic assemblies containing discrete metal-ligand fragments, which have been assembled through non-covalent interactions. One homo-(Au/Au) and two hetero-(Pt/Au) multimetallic assemblies were synthesised and characterised by NMR and ESI-MS spectroscopy. These metallodendrimers consist of a single metal centre surrounded by an oligocationic dendritic shell formed by the coordinated Dendriphos ligands and multiple (6-12) associated anionic organometallic guest complexes.

4.1 Introduction

Metallodendrimers are usually classified as structures that either contain metal complexes at the periphery, at the core, or throughout the dendritic structure.[1-11] Dendritic structures that contain more than one type of organometallic fragment, especially when either the ligand moieties or the metal ions are different, are less common.[12-18] This is perhaps due to synthetic difficulties and the limited stability associated with this kind of structures. Such heterometallic dendrimers are nevertheless highly interesting, for example in the field of homogeneous catalysis. When both types of metal-ligand fragments are catalytically active, applications such as one-pot sequential or tandem catalysis[19, 20] become possible.

A very powerful method to synthesize metallodendritic structures is the use of building blocks which self-assemble through non-covalent interactions.[21-24] In this respect, the use of ionic interactions has emerged as one of the most effective ways to immobilize organometallic catalysts onto soluble or insoluble supports.[25-27] We have recently reported on octacationic dendrimers containing Fréchet-type dendrons[28] and have applied these as noncovalent supports for homogeneous catalysts.[29] In analogy to these structures, hexacationic *Dendriphos* ligands[30] ([**1**]Cl_6 and [**2**]Cl_6, Scheme 1) were designed. In addition to six permanent cationic charges, these structures contain a single phosphine functionality located at the core of the dendrimer. The use of phosphines as building blocks in coordination-based self-assembly has recently been reviewed.[31] In view of the bifunctional character of *Dendriphos* ligands, we envisaged the use of $[\mathbf{1}]^{6+}$ and $[\mathbf{2}]^{6+}$ as building blocks to construct metallodendritic assemblies. Multiple anionic organometallic guest complexes can be associated to *Dendriphos* ligands through electrostatic interactions with the cationic ammonium groups, while the remaining phosphine functionality allows the formation of a discrete metal-ligand fragment at the core of the dendrimer.

4.2 Results and discussion

The synthesis of multimetallic dendritic assemblies was performed according to a stepwise procedure. First, [**1**]Cl_6 and [**2**]Cl_6 were reacted with either one equivalent of AuCl(tht) or 0.5 equivalent of $PtCl_2$(cod) in CH_2Cl_2 and stirred for 1 h at reflux

temperature (Scheme 1). After evaporation of the solvent and removal of residual tht or cod, respectively, the products were isolated and fully characterized. Analysis of the products by ^{31}P-NMR showed one singlet resonance in all cases, indicating quantitative formation of the corresponding phosphine coordination complexes AuCl(L) (**3** and **4**) and $PtCl_2(L)_2$ (**5** and **6**; L = [**1**]Cl_6, [**2**]Cl_6). In the latter case, $^1J_{P,Pt}$ coupling constants of 2655 and 2661 Hz, respectively, were observed by ^{31}P-NMR. The magnitudes of these coupling constants are consistent with the simultaneous coordination of two equivalents of $[\mathbf{1}]^{6+}$ and $[\mathbf{2}]^{6+}$, respectively, to the Pt(II) centre, with a *trans* configuration.[32] Analysis by ESI-MS of the complexes **3** and **5** showed signals corresponding to the ions $[Au(\mathbf{1})]Cl_{(7-n)}^{n+}$ (n = 2, 3) and $[Pt(\mathbf{1})_2]Cl_{(14-n)}^{n+}$ (n = 3-6) (Table 1, entries 1 and 2, *vide infra*, and Figure 1 for **5**) and confirm the assigned structures. These compounds can be classified as metallodendrimers consisting of a single metal centre surrounded by a dendritic shell formed by the coordinated *Dendriphos* ligands.

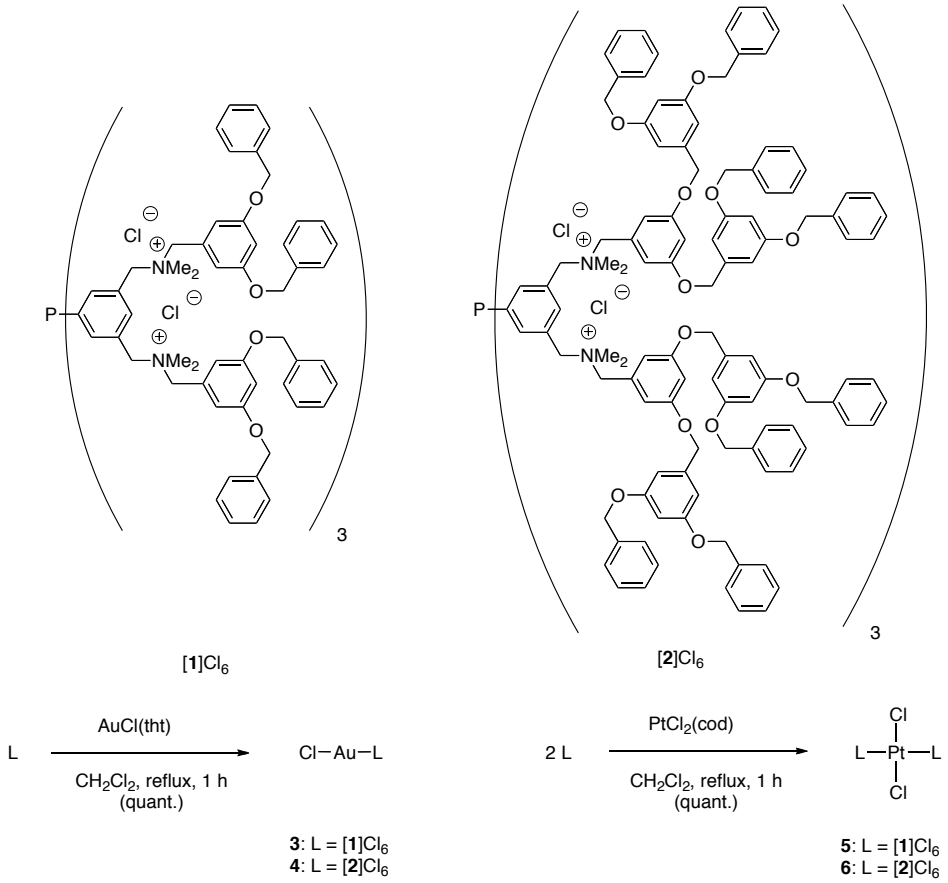

Scheme 1. *Dendriphos* ligands [**1**]Cl_6 and [**2**]Cl_6 and their use in synthesis of Au- and Pt-based metallodendrimers complexes **3**-**6**.

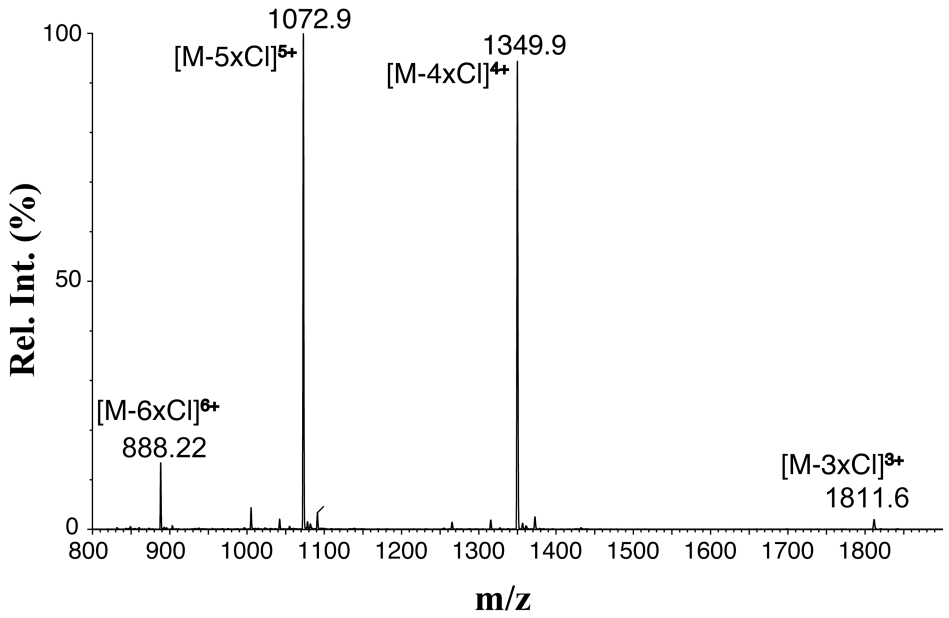

Figure 1. ESI-MS spectrum of **5**.

In a second step, the metallodendrimers [AuCl(**1**)]Cl_6 (**3**) and [$PtCl_2$(**1**)$_2$]Cl_{12} (**5**) were used as hosts for respectively six or twelve equivalents of an organometallic guest molecule containing a single sulfonate functionality. Homo-multimetallic assembly [AuCl(**1**)][**8**]$_6$ (**10**, Scheme 2) was synthesized according to a one-pot transmetalation/immobilisation procedure which has previously been developed in our group.[33] In this one-pot procedure, the ionic dendrimer serves both as supporting agent and as halide source for carbene metal halide complexes. Starting from the Ag-carbene zwitterion **7**, reaction with both a stoichiometric amount of AuCl(tht) as well as one sixth of an equivalent of **3** in CH_2Cl_2, led to the quantitative formation of the anionic carbene-Au complex [**8**]$^-$ and its concomitant immobilization on [AuCl(**1**)]$^{6+}$, along with precipitation of AgCl. After filtration, the resulting clear solution contained [AuCl(**1**)][**8**]$_6$ (**10**) in quantitative yield.

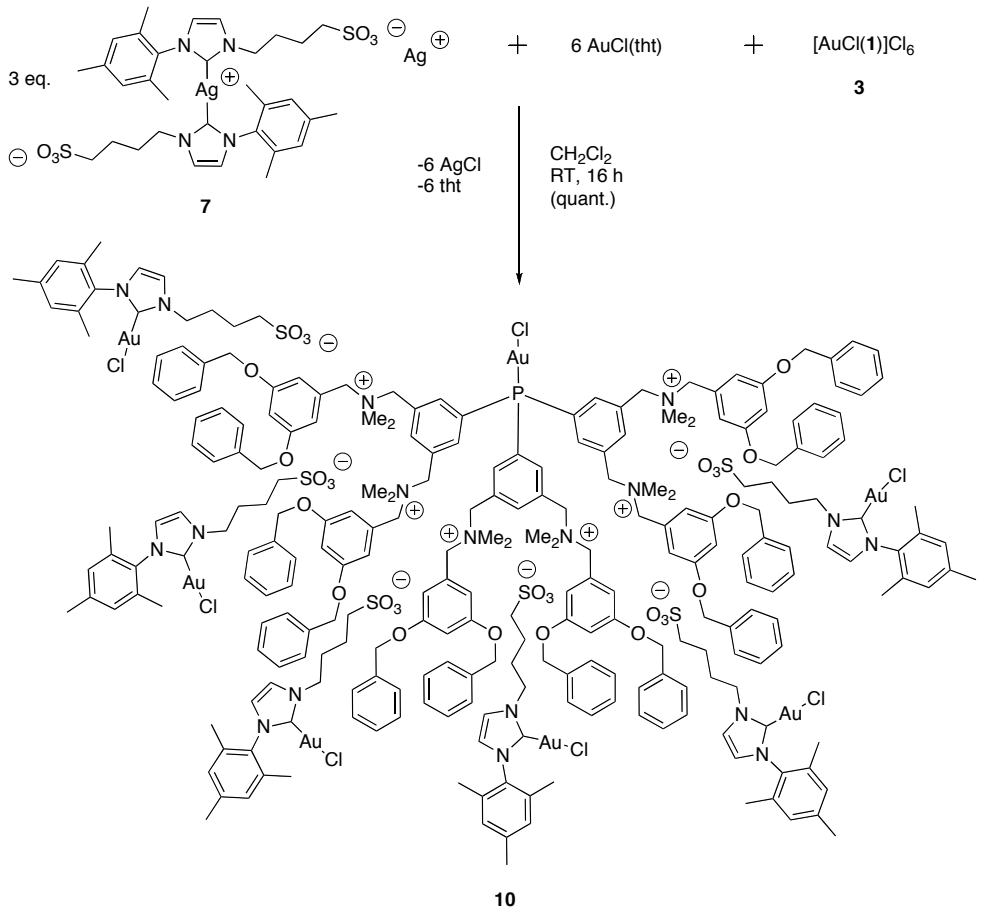

Scheme 2. One pot transmetalation/immobilization procedure leading to homo-multimetallic assembly [AuCl(**1**)][**8**]$_6$ (**10**).

Analysis by ESI-MS led to the detection of ions corresponding to **10** minus two or three equivalents of **8**, *i.e.* [AuCl(**1**)][**8**]$_{6\text{-}n}^{n+}$ (n = 2, 3) (Table 1, entry 3) and confirms the association of multiple guest molecules to the dendritic framework. The dissociation of *n* equivalents of the guest is assumed to occur during the ESI-MS measurement, which is generally observed for this type of non-covalent assemblies.[28, 29, 33-35]

Table 1. Major ions observed by ESI-MS analysis of *Dendriphos* metal complexes and multimetallic assemblies.

Entry	Structure	Major ions observed	Calcd. (m/z)	Found (m/z)
1	[AuCl(**1**)]Cl_6 (**3**)	[Au(**1**)]Cl_5^{2+}	1399.5	1399.5
		[Au(**1**)]Cl_4^{3+}	921.04	921.01
2	[$PtCl_2$(1)$_2$]Cl_{12} (**5**)	[Pt(**1**)$_2$]Cl_{11}^{3+}	1811.8	1811.6
		[Pt(**1**)$_2$]Cl_{10}^{4+}	1350.0	1349.9
		[Pt(**1**)$_2$]Cl_9^{5+}	1072.9	1072.9
		[Pt(**1**)$_2$]Cl_8^{6+}	888.17	888.22
3	[AuCl(**1**)][**8**]$_6$ (**10**)	[AuCl(**1**)][**8**]$_4^{2+}$	2436.5	2436.7
		[AuCl(**1**)][**8**]$_3^{3+}$	1439.7	1439.8
4	[$PtCl_2$(**1**)$_2$][**8**]$_{12}$ (**11**)	[$PtCl_2$(**1**)$_2$][**8**]$_9^{3+}$	3366.9	3367.5
		[$PtCl_2$(**1**)$_2$][**8**]$_8^{4+}$	2386.7	2387.2
5	[$PtCl_2$(**1**)$_2$][**9**]$_{12}$ (**12**)	[$PtCl_2$(**1**)$_2$][**9**]$_9^{3+}$	3426.7	3427.2
		[$PtCl_2$(**1**)$_2$][**9**]$_8^{4+}$	2426.6	2427.1

The ^{1}H-NMR spectrum of **10**, measured in CD_2Cl_2, shows signals of both the hexacationic dendritic phosphine gold halide and the assembled gold-carbene sulfonate anions (Figure 2). A calculation of the number of [**8**]$^-$ molecules per dendritic host, using peak integration values for the ammonium methyl (e) and guest methylene (o, m, l) signals, yields a ratio of 6.1 guest molecules per host. The spectrum furthermore shows a considerable sharpening of the signals attributed to the dendritic framework of the assembly [AuCl(**1**)][**8**]$_6$ (**10**) in comparison with [AuCl(**1**)]Cl_6 (**3**) (Figure 2). Significant changes in the chemical shifts were observed for several of the protons of the dendritic backbone (e, f, g, Figure 2). The signals for the benzylic protons, which coalesce into one broad peak for **3**, were observed as three discrete sharp singlets (c, d, h) for **10**. The signals attributed to the anionic guest also shifted slightly compared to [NBu_4][**8**],[33]

with *e.g.* -0.23 ppm and -0.11 ppm for the two N-heterocyclic ring protons. In the ^{13}C-NMR spectrum, the signals attributed to the [AuCl(**1**)]$^{6+}$ framework slightly shifted in **10** in comparison with **3**; the largest shifts amounting to +0.26 ppm for the *meta* carbon and -0.23 ppm for the *para* carbon of the ammoniomethyl-substituted aromatic ring. The largest shifts of signals attributed to the guest were observed for the two carbon nuclei in the backbone of the N-heterocyclic ring, amounting to +0.20 ppm and -0.32 ppm, compared to [NBu$_4$][**8**]. A characteristic signal at 170.9 ppm was observed, which is attributed to the carbenic carbon coordinated to Au.[33] The signal of the carbenic carbon in **7** had disapppeared, indicating that complete transmetallation from Ag to Au had occurred. The ^{31}P-NMR spectrum of **10** showed a single peak at 36.8 ppm and confirms the integrity of the *Dendriphos*-Au-Cl moiety. These observations indicate that six equivalents of the anionic guest have been incorporated into the voids of the cationic dendrimer and that the guest molecules stay associated with the host in dichloromethane solution.

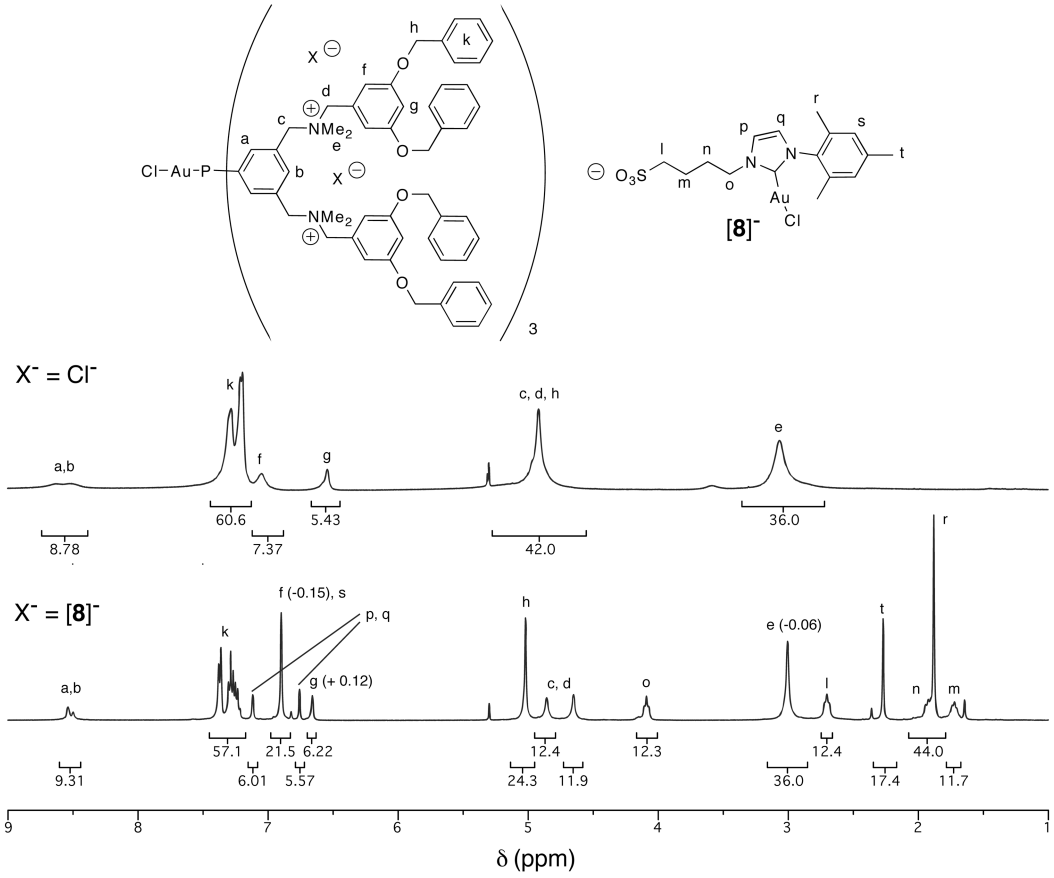

Figure 2. ^{1}H-NMR spectra of [AuCl(**1**)]X$_6$ (X = Cl, [**8**]) in CD_2Cl_2 with peak assignments and integration values.

In a first attempt to prepare a hetero-multimetallic assembly, the procedure outlined in Scheme 2 was carried out using $[RhCl(cod)]_2$ instead of AuCl(tht) as the metal precursor for reaction with transmetallation agent **7**. Unfortunately, ^{31}P-NMR of the product indicated that the *Dendriphos*-Au-Cl moiety had not stayed intact during this procedure and instead had completely transformed into a *Dendriphos*-Rh complex. When the dendritic host was changed from [AuCl(**1**)]Cl_6 (**3**) to $[PtCl_2(\mathbf{1})_2]Cl_{12}$ (**5**) while keeping AuCl(tht) as the metal precursor, ^{13}C-NMR indicated that transmetallation from Ag to Au was not complete, possibly due to an interfering reaction with the Pt centre. A different strategy was thus required for the synthesis of hetero-multimetallic assemblies. Therefore, twelve equivalents of pre-synthesized Au-carbene complex $[NBu_4][\mathbf{8}]$[33] were combined with one equivalent of **5** (Scheme 3). Removal of $[NBu_4]Cl$ was achieved by passive dialysis (see Experimental Section), leading to hetero-multimetallic assembly $[PtCl_2(\mathbf{1})_2][\mathbf{8}]_{12}$ (**11**) in 80 % isolated yield. In addition, employing a slightly different immobilisation strategy, twelve equivalents of TPPMS-Au complex Na[**9**] (TPPMS = monosulfonated triphenylphosphine) were combined with host **5** in dry CH_2Cl_2, which led to precipitation of NaCl, affording the assembly $[PtCl_2(\mathbf{1})_2][\mathbf{9}]_{12}$ (**12**) in quantitative yield, without the need for dialysis (Scheme 3). For both these hetero-multimetallic assemblies, ^{31}P-NMR exclusively showed *Dendriphos*-Pt(II) coordination (see Experimental Section). The observed chemical shifts as well as the $^1J_{P,Pt}$ coupling constants were very similar and did not change significantly compared to $[PtCl_2(\mathbf{1})_2]Cl_{12}$ (**5**). The *Dendriphos*-platinum cores had thus in each case remained intact during the synthesis procedure, despite the presence of a twelve-fold excess of respectively Au-carbene or Au-phosphine complexes. For **12**, the ^{31}P-NMR spectrum shows a second signal, corresponding to the TPPMS phosphine functionality coordinated to gold. No additional signals were observed. The *Dendriphos* phosphorus signal appears as a broad singlet, while the TPPMS phosphorus signal appears as a sharp, very intense singlet. Therefore the two different phosphorus nuclei can be easily distinguished, confirming discrete *Dendriphos*-Pt and TPPMS-Au coordination after the synthetic procedure. Analysis by ESI-MS led to the detection of signals corresponding to the ions $[PtCl_2(\mathbf{1})_2]X_{12-n}^{n+}$ (X = **8**, **9**; n = 3, 4, see Table 1, entries 4 and 5 and Figure 3 for X = **8**) and is consistent with the association of the guests $[\mathbf{8}]^-$ and $[\mathbf{9}]^-$, respectively, to the dendritic host $[PtCl_2(\mathbf{1})_2]^{12+}$.

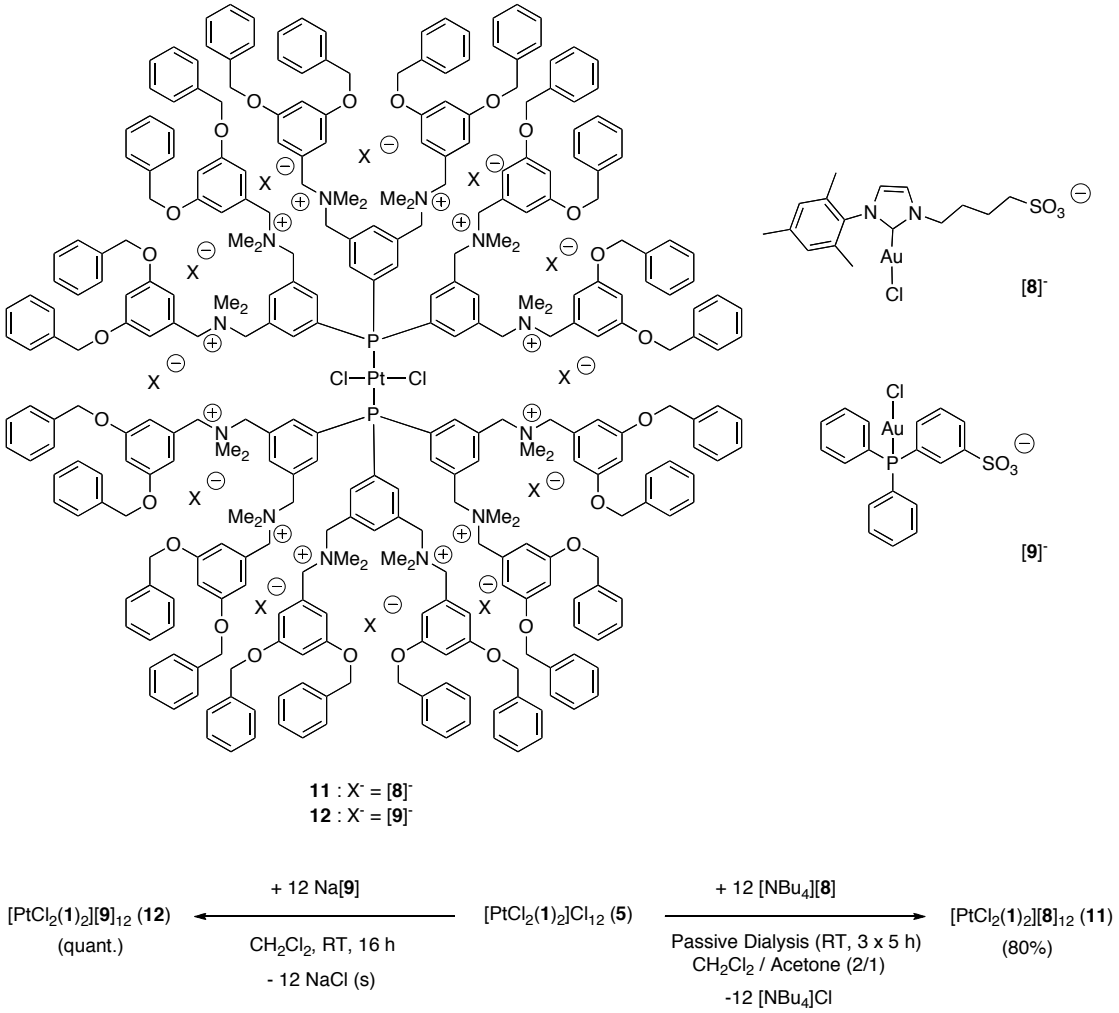

Scheme 3. Synthesis of Pt/Au heterometallic assemblies.

In the ^{1}H-NMR spectra, a sharpening of the signals, similar to that observed for **10** (Figure 2), was observed for **11**. This effect was less pronounced for **12**. A calculation of the guest/host ratios by specific peak integration in ^{1}H-NMR yielded a ratio of 10.6 for **11**. The deviation from the expected ratio of 12 suggests that a slightly lower number of guests have been incorporated into the dendritic host. Most likely this is a consequence of the employed passive dialysis step, in which a small quantity of [NBu$_4$][**8**] might pass through the membrane, resulting in a lower guest/host ratio in **11**.

For **12**, a reliable calculation of the guest/host ratio based upon integration of signals in ^{1}H-NMR was made impossible due to overlap of signals. However, elemental analysis was consistent with quantitative functionalisation for **12**, *i.e.* a guest/host ratio of 12 (see Experimental Section). The ^{13}C-NMR spectrum of **11** showed no [NBu$_4$]Cl after dialysis. Furthermore, the integrity of the carbene-Au fragments in **11** was confirmed by

the presence of a single peak in the carbenic carbon region of the ^{13}C-NMR spectrum, at 170.8 ppm. Similar shifts as those observed for **10** (*vide supra*) were observed for the carbon nuclei of the dendritic framework for **11** compared to **5**. In contrast, smaller shifts were observed for **12** (typically less than 0.10 ppm), suggesting that the guests are located less deeply inside the dendritic structure for **12** compared to **11**. This could be due to the absence of an aliphatic -$(CH_2)_4$- tether in [**9**]$^-$. After the hetero-multimetallic assemblies had been allowed to stand in solution in CD_2Cl_2 for one week at room temperature, ^{31}P-NMR showed that considerable metal-ligand exchange had occurred during this period. In both cases, approximately 20 % of *Dendriphos*-Au coordination was observed (indicated by a singlet at 37 ppm). This indicates the limited kinetic stability of these assemblies, which most likely are dynamic systems in solution. A metal-ligand exchange equilibrium, in which *Dendriphos*-Pt species undergo transmetallation to *Dendriphos*-Au species, most likely exists and may slowly shift to the thermodynamically most stable state. The kinetics of this exchange are expected to depend on the nature of the metal ions, the ligand fragments and the solvent.

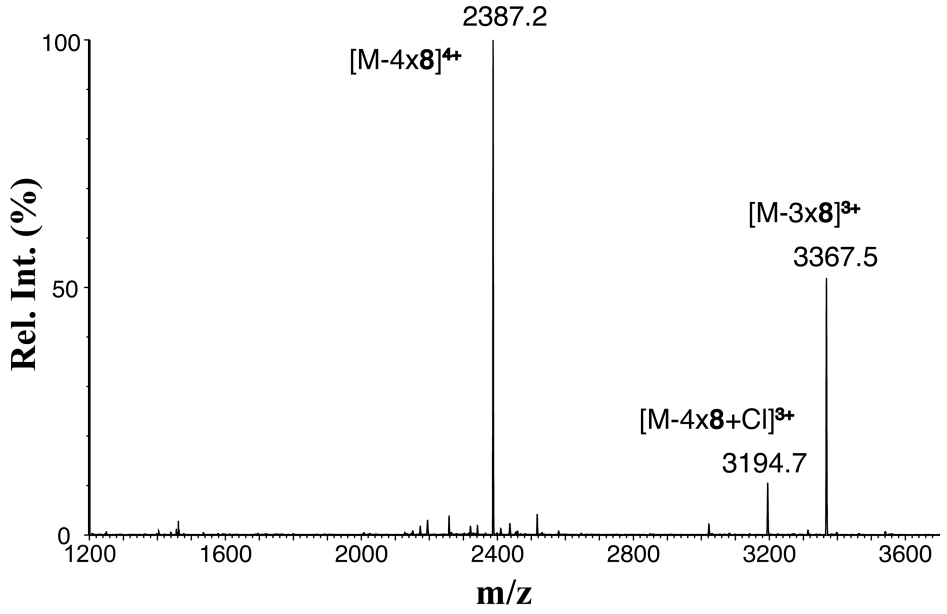

Figure 3. ESI-MS spectrum of **11**.

4.3 Conclusions

Hexa-ammonium functionalised *Dendriphos* ligands $[\mathbf{1}]^{6+}$ and $[\mathbf{2}]^{6+}$ and mono-sulfonate functionalised carbene and phosphine-Au complexes $[\mathbf{8}]^{-}$ and $[\mathbf{9}]^{-}$ have been used as building blocks to construct multimetallic dendritic assemblies through non-covalent interactions. One homo-(Au/Au) and two hetero-(Pt/Au) multimetallic assemblies were synthesized and fully characterised. The employed stepwise synthetic strategy allows facile preparation of metallodendrimers containing discrete metal-ligand fragments, in very high yields. This strategy may be extended towards a range of combinations of transition metal complexes. Of particular interest is the incorporation of two discrete catalytically active transition metal complexes within the same metallodendrimer. Such assemblies could potentially find applications in tandem or sequential catalysis and given their very large molecular weight, may furthermore be easily recycled through nanofiltration. Furthermore, metallodendritic assemblies of the type described in this report represent systems consisting of a number of different components, the combination of which can lead to self-assembled structures of different composition with discretely different kinetic and thermodynamic properties. As such these metallo-dendritic asemblies may also be of interest to the field of systems chemistry.

4.4 Experimental section

General Remarks. Experiments involving sensitive reagents were performed under an atmosphere of dry, oxygen-free N_2 using standard Schlenk techniques. Manipulations involving free phosphines were carried out in deoxygenated solvents. CH_2Cl_2 was dried over CaH_2 and distilled before use. Passive dialysis was performed using a benzoylated cellulose membrane tubing which separates compounds with a molecular weight of ≤1200 from compounds with a molecular weight of >2000, which was obtained from Aldrich. $[\mathbf{1}]Br_6$,[30] $[\mathbf{2}]Br_6$,[30] **7**,[33] $[NBu_4][\mathbf{8}]$[33] and $Na[\mathbf{9}]$[36] were synthesized according to previously reported procedures. NMR spectra were recorded on a Varian Inova 300 or a Varian AS 400 spectrometer at 25 °C. Chemical shifts (δ) are given in ppm referenced to the residual solvent peak or internal standard and coupling constants are given in Hertz (Hz). Elemental analyses were carried out by Dornis & Kolbe, Mikroanalytisches Laboratorium, Müllheim a/d Ruhr, Germany. Time-of-flight electrospray ionization mass spectra were measured on a Micromass LC-T mass spectrometer (Waters, Manchester, UK), operating in positive ion mode. Samples were introduced at

concentrations of 20-50 μM. The nanospray needle potential was typically set to 1300 V and the cone voltage to 20-60 V. The source block temperature was set to 80 °C.

- **Synthesis of *Dendriphos* ligands [1]Cl_6 and [2]Cl_6.**

Exchange of the bromide counterions of [**1**]Br_6 and [**2**]Br_6 to chloride was performed using a biphasic mixture of CH_2Cl_2 (300 mL) and a solution of LiCl in demineralised water (1 M, 3 x 150 mL), under a N2 atmosphere. After separation of the layers, the organic phase was washed twice with demineralised water (150 mL) and evaporated to dryness, affording the products in 80-85 % yield on a two-gram scale.

[1]Cl_6: ^{1}H NMR (400 MHz, $CDCl_3$ / CD_3OD (9/1)) δ = 8.17 (d, $^3J_{P,H}$ = 6.8 Hz, 6H, *o*-Ar), 8.00 (s, 3H, *p*-Ar), 7.24-7.10 (m, 60H, Ph), 6.84 (s, 12H, *o*-Ar'), 6.57 (s, 6H, *p*-Ar'), 4.88 (s, 24H, OCH_2), 4.61 (s, 12H, NCH_2), 4.47 (s, 12H, NCH_2), 2.85 (s, 36H, $N(CH_3)_2$). **^{13}C{^{1}H} NMR (100 MHz, $CDCl_3$ / CD_3OD (9/1))** δ = 159.9 (s, *m*-Ar'), 140.9 (s, Ar), 140.7 (d, $^2J_{P,C}$ = 12.8 Hz, *o*-Ar), 139.0 (s, Ar), 136.1 (s, *o*-Ar'), 129.2 (d, $^3J_{P,C}$ = 7.0 Hz, *m*-Ar), 129.0 (s, Ph), 128.3 (s, Ph), 127.9 (s, Ph), 127.5 (s, Ph), 112.2 (s, *p*-Ar'), 104.0 (s, *i*-Ar'), 70.0 (s, OCH_2), 67.5 (s, NCH_2), 67.0 (s, NCH_2), 48.4 (s, $N(CH_3)_2$). **^{31}P{^{1}H}-NMR (162 MHz, $CDCl_3$)** δ = -3.2. **HRMS (ES$^+$)** calculated for $C_{162}H_{171}Cl_2N_6O_{12}P$: m/z = 623.302 found: 623.307 $[M-4Cl]^{4+}$. **Elemental Analysis** calculated for $C_{162}H_{171}Cl_6N_6O_{12}P$: C, 73.76; H, 6.53; Cl, 8.06; N, 3.19; P, 1.17. Found C, 69.90; H, 6.24; Cl, 8.32; N, 3.25; P, 1.22.

[2]Cl_6: ^{1}H NMR (200 MHz, $CDCl_3$) δ = 8.25 (br. s, 6H, *o*-Ar), 7.8-7.0 (m, 123H, Ph and *p*-Ar), 6.91, 6.58, 6.41 (br. m, 54H, overlapping Ar') 5.0-4.5 (br. m, 96H, overlapping CH_2), 2.97 (br. s, 36H, $N(CH_3)_2$). **^{13}C{^{1}H} NMR (50 MHz, $CDCl_3$)** δ = 160.2, 160.0, 138.9, 136.8, 128.7, 128.1, 127.8, 112.5, 106.8, 101.8, 70.2, 67.7, 49.2. **^{31}P{^{1}H} NMR (81 MHz, $CDCl_3$)** δ = -3.5. **MS (ES$^+$)** m/z = 1699.4 {$[M+O-3Cl]^{3+}$, calc. 1698.2}, 1265.3 {$[M+O-4Cl]^{4+}$, calc. 1264.8}. **Elemental Analysis** calculated for $C_{330}H_{315}Cl_6N_6O_{36}P$: C, 76.45; H, 6.12; Cl, 4.10; N, 1.62; P, 0.60. Found: C, 76.37; H, 6.18; Cl, 3.96; N, 1.57; P, 0.58.

[AuCl(1)]Cl_6 (3): To a solution of [**1**]Cl_6 (246 mg, 0.930 mmol) in CH_2Cl_2 (5 mL) was added AuCl(tht) (30 mg, 0.94 mmol). The solution was heated at reflux temperature for 1 h, and subsequently dried *in vacuo*. The product was precipitated twice from CH_2Cl_2 by addition

of Et_2O, yielding the product as a white powder in quantitative yield. **^{1}H NMR (300 MHz, $CDCl_3$ / CD_3OD (3/1))** δ = 8.62 (d, $^3J_{P,H}$ = 12.0 Hz, 6H, *o*-Ar), 8.44 (s, 3H, *p*-Ar), 7.4-7.1 (m, 60H, Ph), 6.87 (s, 12H, *o*-Ar'), 6.65 (s, 6H, *p*-Ar'), 4.98 (s, 24H, OCH_2), 4.83 (s, 12H, NCH_2), 4.64 (s, 12H, NCH_2), 2.99 (br. s, 36H, $N(CH_3)_2$). **^{13}C{^{1}H} NMR (100 MHz, CD_2Cl_2)** δ = 159.9 (s, *m*-Ar'), 142.9 (br. s, Ar), 141.2 (br. s, Ar), 136.6 (s, *o*-Ar'), 131.3 (br. s, Ar), 129.8 (s, Ph), 128.5 (s, Ph), 128.1 (s, Ph), 127.9 (s, Ph), 112.8 (s, *p*-Ar'), 104.0 (s, *i*-Ar'), 70.2 (s, OCH_2), 67.0 (br. s, NCH_2), 66.0 (br. s, NCH_2), 48.9 (s, $N(CH_3)_2$). **^{31}P{^{1}H} NMR (121 MHz, $CDCl_3$ / CD_3OD (3/1))** δ = 37.6. **MS (ES^+)**: m/z = 1399.5 {$[M-2Cl]^{2+}$, calc. 1399.5}, 921.01 {$[M-3Cl]^{3+}$, calc. 921.04}. **Elemental Analysis** calculated for $C_{162}H_{171}AuCl_7N_6O_{12}P$: C, 67.69; H, 6.01; Cl, 8.65; N, 2.93; P, 1.08. Found C, 67.65; H, 5.94; Cl, 8.43; N, 2.79; P, 1.11.

[AuCl(2)]Cl_6 (4): Starting from [**2**]Cl_6 and AuCl(tht), an analogous procedure as described for [AuCl**1**]Cl_6 was followed, affording the product in quantitative yield. **^{1}H NMR (200 MHz, $CDCl_3$)** δ = 8.86 (br. s, 6H, *o*-Ar), 7.8-7.0 (m, 123H, Ph and *p*-Ar), 6.86, 6.59, (br. m, 54H, overlapping Ar') 5.2-4.4 (br. m, 96H, overlapping CH_2), 2.96 (br. s, 36H, $N(CH_3)_2$). **^{13}C{^{1}H} NMR (50 MHz, $CDCl_3$)** δ = 160.2, 138.8, 136.9, 128.8, 128.2, 127.8, 112.5, 106.7, 104.4, 101.8, 70.2, 49.3. **^{31}P{^{1}H}-NMR (81 MHz, $CDCl_3$)** δ = 36.7. **Elemental Analysis** calculated for $C_{330}H_{315}AuCl_7N_6O_{36}P$: C, 73.17; H, 5.86; Cl, 4.58; N, 1.55; P, 0.57. Found: C, 73.05; H, 5.92; Cl, 4.47; N, 1.53; P, 0.59.

[$PtCl_2$(1)$_2$]Cl_{12} (5): To a solution of [**1**]Cl_6 (530 mg, 0.201 mmol) in CH_2Cl_2 (5 mL) was added $PtCl_2$(cod) (37 mg, 0.99 mmol). The solution was heated at reflux temperature for 1 h, and subsequently dried *in vacuo*. The product was precipitated twice from CH_2Cl_2 by addition of Et_2O, yielding the product as a light yellow powder in quantitative yield. **^{1}H NMR (400 MHz, $CDCl_3$ / CD_3OD (3/1))** δ = 8.1 (br. s, 9H, Ar), 7.4-7.1 (m, 120H, Ph), 6.77 (br. s, 24H, *o*-Ar'), 6.59 (br. s, 12H, *p*-Ar'), 4.89 (s, 48H, OCH_2), 4.62 (br. s, 48H, NCH_2), 2.78 (br. s, 72H, $N(CH_3)_2$). **^{13}C{^{1}H} NMR (100 MHz, $CDCl_3$ / CD_3OD (3/1))** δ = 159.8 (s, *m*-Ar'), 140.8 (br. s, Ar), 136.0 (s, *o*-Ar'), 128.8 (br. s, Ar), 128.2 (s, Ph), 127.9 (s, Ph), 127.8 (s, Ph), 127.4 (s, Ph), 112.3 (s, *p*-Ar'), 103.2 (s, *i*-Ar'), 69.9 (s, OCH_2), 66.9 (br. s, NCH_2), 49.1 (s, $N(CH_3)_2$). **^{31}P{^{1}H} NMR (162 MHz, $CDCl_3$ / CD_3OD (3/1))** δ = 25.4 (br. s, $^1J_{P,Pt}$ = 2655 Hz). **MS (ES^+)** m/z = 1811.6 {$[M-3Cl]^{3+}$, calc. 1811.8}, 1349.9 {$[M-4Cl]^{4+}$, calc. 1350.0}, 1072.9 {$[M-5Cl]^{5+}$, calc. 1072.9}, 888.22 {$[M-6Cl]^{6+}$, calc. 888.17}. **Elemental Analysis** calculated for $C_{324}H_{342}Cl_{14}N_{12}O_{24}P_2Pt$: C, 70.22; H, 6.22; Cl, 8.96; N, 3.03; P, 1.12. Found: C, 69.85; H, 6.20; Cl, 8.87; N, 2.94; P, 1.15.

[$PtCl_2$(2)$_2$]Cl_{12} (6): Starting from [**2**]Cl_6 and $PtCl_2$(cod), an analogous procedure as described for [$PtCl_2$**1**$_2$]Cl_{12} was followed, affording the product in quantitative yield. **^{1}H NMR (400 MHz, $CDCl_3$ / CD_3OD (3/1))** δ = 8.1 (br. s, Ar), 7.4-7.1 (br. m, 240H, Ph), 7.0-6.6 (br. m, 108H, Ar') 4.8-5.2 (br. s, 192H, CH_2), 3.2-2.6 (br. s, 72H, $N(CH_3)_2$). **^{13}C{^{1}H} NMR (100 MHz, $CDCl_3$ / CD_3OD (3/1))** δ = 159.8, 142-138 (br. overlapping signals), 136.1, 136.0, 128.3, 127.9, 127.4, 112.3, 104.2, 104-102 (br. overlapping signals), 70.0, 66.9, 49.4. **^{31}P{^{1}H} NMR (162 MHz, $CDCl_3$ / CD_3OD (3/1))** δ = 27.0 (br. s, $^1J_{P,Pt}$ = 2661 Hz). **Elemental Analysis** calculated for $C_{660}H_{630}Cl_{14}N_{12}O_{72}P_2Pt$: C, 74.53; H, 5.97; Cl, 4.67; N, 1.58; P, 0.58. Found: C, 74.44; H, 6.05; Cl, 4.73; N, 1.54; P, 0.55.

[AuCl(1)][8]$_6$ (10): To a solution of **7** (77.0 mg, 0.0895 mmol, *i. e.* 0.179 mmol Ag) in CH_2Cl_2 (5 mL) were added subsequently AuCl(tht) (58.3 mg, 0.182 mmol) and **3** (85.7 mg, 0.0299 mol), both as solids and in one portion. The mixture was stirred at room temperature for 16 h under an inert atmosphere, filtered over Celite and subsequently dried *in vacuo*, yielding the product as a white powder (0.188 g, quant.) The product was precipitated twice from CH_2Cl_2 by addition of Et_2O, in order to remove residual tetrahydrothiophene. Yield: 0.156 g (87 %). **^{1}H NMR (400 MHz, CD_2Cl_2)** δ = 8.54 (s, 6H, *o*-Ar), 8.50 (s, 3H, *p*-Ar), 7.4-7.2 (m, 60H, Ph), 7.12 (s, 6H, NHC), 6.90 (br. s, 24H, overlapping *o*-Ar' and Mes-ArH), 6.76 (s, 6H, NHC), 6.66 (s, 6H, *p*-Ar'), 5.02 (s, 24H, OCH_2), 4.86 (s, 12H, NCH_2), 4.65 (s, 12H, NCH_2), 4.09 (t, $^3J_{H,H}$ = 6.2 Hz, 12H, NCH_2CH_2), 3.01 (s, 36H, $N(CH_3)_2$), 2.70 (br. s, 12H, $CH_2CH_2SO_3$), 2.27 (s, 18H, Mes-*p*-CH_3), 1.88 (br. s, 48H, overlapping Mes-*o*-CH_3 and NCH_2CH_2), 1.72 (m, 12H, $CH_2CH_2SO_3$). **^{13}C{^{1}H} NMR (100 MHz, CD_2Cl_2)** δ = 170.9 (s, NHC-Au), 160.2 (s, *m*-Ar'), 142.4 (s, Ar), 140.7 (br. s, Ar), 139.7 (s, *p*-Mes), 136.7 (s, *o*-Ar'), 135.0 (s, *o*-Mes), 130.6 (d, $^3J_{C,P}$ = 12.1 Hz, *m*-Ar), 129.6 (s, Ph), 129.2 (s, *m*-Mes), 128.6 (s, Ph), 128.1 (s, Ph), 127.9 (s, Ph), 122.3 (s, NHC), 121.0 (s, NHC), 112.5 (s, *p*-Ar'), 104.2 (s, *i*-Ar'), 70.3 (s, OCH_2), 67.5 (s, NCH_2), 51.2 and 50.9 (s, NCH_2CH_3 and $CH_2CH_3SO_3$), 49.0 (s, $N(CH_3)_2$), 30.1 (s, NCH_2CH_3), 22.5 (s, $CH_2CH_3SO_3$), 20.9 (s, Mes-*p*-CH_3), 17.2 (s, Mes-*o*-CH_3). **^{31}P{^{1}H} NMR (121 MHz, CD_2Cl_2)** δ = 36.8. **MS (ES$^+$)** m/z = 2436.7 {[M-2[**4**]]$^{2+}$, calc. 2436.5}, 1439.8 {[M-3[**4**]]$^{3+}$, calc. 1439.7}. **Elemental Analysis** calculated for $C_{258}H_{297}Au_7Cl_7N_{18}O_{30}PS_6$: C, 51.81; H, 5.01; N, 4.22. Found: C, 49.72; H, 5.19; N, 3.99.

[$PtCl_2$(1)$_2$][8]$_{12}$ (11): To a solution of [NBu_4][**8**] (84 mg, 0.11 mmol) and **5** (48 mg, 8.7 µmol) in CH_2Cl_2 (30 mL) was added demineralised water (20 mL). The mixture was

stirred at room temperature for 16 h, the organic layer was separated, concentrated and purified by passive dialysis using CH_2Cl_2/acetone (2:1, v/v) as solvent at room temperature (3 x 5 h). The product was precipitated twice from CH_2Cl_2 by addition of Et_2O. Yield: 65 mg (80 %). **^{1}H NMR (400 MHz, CD_2Cl_2)** δ = 8.4 (br. s, 18H, Ar), 7.4-7.2 (m, 120H, Ph), 7.07 (s, 12H, NHC), 6.87 (s, 24H, Mes-ArH), 6.9 (br. m, 24H, *o*-Ar') 6.69 (s, 12H, NHC), 6.7 (br. m, 12H, *p*-Ar') 5.1-4.6 (br. m, 96H, OCH_2 and NCH_2), 3.97 (br. s, 24H, NCH_2CH_2), 2.95 (br. s, 72H, $N(CH_3)_2$), 2.68 (br. s, 12H, $CH_2CH_2SO_3$), 2.25 (s, 36H, Mes-*p*-CH_3), 1.84 (s, 96H, overlapping Mes-*o*-CH_3 and NCH_2CH_2), 1.67 (m, 12H, $CH_2CH_2SO_3$). **^{13}C{^{1}H} NMR (100 MHz, CD_2Cl_2)** δ = 170.8 (s, NHC-Au), 160.2 (s, *m*-Ar'), 139.7 (s, *p*-Mes), 136.7 (s, *o*-Ar'), 135.0 and 134.9 (s, *o*-Mes), 129.8 (s, Ph), 129.2 (s, *m*-Mes), 128.6 (s, Ph), 127.9 (s, Ph), 127.8 (s, Ph), 122.1 (s, NHC), 121.2 (s, NHC), 112.5 (s, *p*-Ar'), 103.6 (br. s, *i*-Ar'), 70.3 (s, OCH_2), 67.6 (br. s, NCH_2), 51.2 and 50.9 (s, NCH_2CH_3 and $CH_2CH_3SO_3$), 49.1 (s, $N(CH_3)_2$), 30.2 (s, NCH_2CH_3), 22.5 (s, $CH_2CH_3SO_3$), 20.9 (s, Mes-*p*-CH_3), 17.6 (s, Mes-*o*-CH_3). **^{31}P{^{1}H} NMR (121 MHz, CD_2Cl_2)** δ = 25.1 ($^1J_{P,Pt}$ = 2680 Hz). **MS (ES$^+$)** m/z = 3367.5 {[M-3[**4**]]$^{3+}$, calc. 3366.9}, 2387.2 {[M-4[**4**]]$^{4+}$, calc. 2386.7}. **Elemental Analysis** calculated for $C_{516}H_{594}Au_{12}Cl_{14}N_{36}O_{60}P_2PtS_{12}$: C, 52.69; H, 5.09; N, 4.29. Found: C, 50.76; H, 5.01; N, 4.01.

[$PtCl_2$(1)$_2$][9]$_{12}$ (12): To a solution of **5** (43.2 mg, 0.00780 mmol), in dry CH_2Cl_2 (5 mL) was added Na[**9**] (56.0 mg, 0.0938 mmol) as a solid, in one portion. The mixture was stirred at room temperature for 16 h, filtered over Celite and subsequently dried *in vacuo*, yielding the product as a white powder (92 mg, quant.). **^{1}H NMR (300 MHz, CD_2Cl_2)** δ = 9.3 (br. s, Ar), 8.3 (br. s, Ar), 8.01 (d, $J_{H,P}$ = 13.5 Hz, 12H, tppms-AuCl), 7.93 (br. s, 12H, tppms-AuCl) 7.4-6.9 (br. m, 264H, overlapping Ph and tppms-AuCl), 6.8-6.4 (br. m, 36H, Ar'), 4.9-4.3 (br. m, 96H, OCH_2 and NCH_2), 3.0-2.4 (br. s, 72H, $N(CH_3)_2$). **^{13}C{^{1}H} NMR (100 MHz, CD_2Cl_2)** δ = 160.0 (s, *m*-Ar'), 148.2 (d, $J_{C,P}$ = 12.1 Hz, tppmsAuCl), 136.6 (s, *o*-Ar'), 134.4 (d, $J_{C,P}$ = 11.1 Hz, tppmsAuCl), 134.0 (d, $J_{C,P}$ = 13.7 Hz, tppmsAuCl), 132.1 (s, tppmsAuCl), 131.6 (d, $J_{C,P}$ = 16.6 Hz, tppmsAuCl), 129.7 (s, tppmsAuCl), 129.3 (d, $J_{C,P}$ = 12.1 Hz, tppmsAuCl), 128.5 (s, Ph) 127.9 (s, Ph), 127.8 (s, Ph), 112.4 (br. s, *p*-Ar'), 104.2 (br. s, *i*-Ar'), 70.1 (s, OCH_2), 67.6 (br. s, NCH_2), 49.1 (s, $N(CH_3)_2$). **^{31}P{^{1}H} NMR (121 MHz, CD_2Cl_2)** δ = 34.4 (tppmsAuCl), 25.1 (*Dendriphos*, $^1J_{P,Pt}$ = 2700 Hz). **MS (ES$^+$)** m/z = 3427.2 {[M-3[**5**]]$^{3+}$, calc. 3426.7}, 2427.1 {[M-4[**5**]]$^{4+}$, calc. 2426.6}. **Elemental Analysis** calculated for $C_{540}H_{510}Au_{12}Cl_{14}N_{12}O_{60}P_{14}PtS_{12}$: C, 54.04; H, 4.28; N, 1.40; P, 3.61. Found: C, 54.00; H, 4.34; N, 1.37; P, 3.52.

4.5 References

[1] D. Astruc, F. Chardac, *Chem. Rev.* **2001**, *101*, 2991-3023.

[2] G. E. Oosterom, J. N. H. Reek, P. C. J. Kamer, P. W. N. M. van Leeuwen, *Angew Chem Int Edit* **2001**, *40*, 1828-1849.

[3] R. Kreiter, A. W. Kleij, R. J. M. Klein Gebbink, G. Van Koten, *Top. Curr. Chem.* **2001**, *217*, 163-199.

[4] J. N. H. Reek, D. De Groot, G. E. Oosterom, P. C. J. Kamer, P. W. N. M. Van Leeuwen, *Rev. Mol. Biotechnol.* **2002**, *90*, 159-181.

[5] R. van Heerbeek, P. C. J. Kamer, P. W. N. M. van Leeuwen, J. N. H. Reek, *Chem. Rev.* **2002**, *102*, 3717-3756.

[6] L. J. Twyman, A. S. H. King, I. K. Martin, *Chem. Soc. Rev.* **2002**, *31*, 69-82.

[7] P. A. Chase, R. J. M. Klein Gebbink, G. van Koten, *J. Organomet. Chem.* **2004**, *689*, 4016-4054.

[8] B. Helms, J. M. J. Frechet, *Adv. Synth. Catal.* **2006**, *348*, 1125-1148.

[9] A. Berger, R. J. M. Klein Gebbink, G. Van Koten, *Top. Organomet. Chem.* **2006**, *20*, 1-38.

[10] D. Mery, D. Astruc, *Coord. Chem. Rev.* **2006**, *250*, 1965-1979.

[11] N. J. M. Pijnenburg, T. J. Korstanje, G. Van Koten, R. J. M. Klein Gebbink, *Palladacycles*, Wiley-VCH, Weinheim, **2008**, pp. 361-399.

[12] S. Achar, C. E. Immoos, M. G. Hill, V. J. Catalano, *Inorg. Chem.* **1997**, *36*, 2314-2320.

[13] M. Sommovigo, G. Denti, S. Serroni, S. Campagna, C. Mingazzini, C. Mariotti, A. Juris, *Inorg. Chem.* **2001**, *40*, 3318-3323.

[14] I. Angurell, G. Muller, M. Rocamora, O. Rossell, M. Seco, *Dalton Trans.* **2004**, 2450-2457.

[15] S. H. F. Chong, S. C. F. Lam, V. W. W. Yam, N. Y. Zhu, K. K. Cheung, S. Fathallah, K. Costuas, J. F. Halet, *Organometallics* **2004**, *23*, 4924-4933.

[16] I. Angurell, J. C. Lima, L. I. Rodriguez, L. Rodriguez, O. Rossell, M. Seco, *New J. Chem.* **2006**, *30*, 1004-1008.

[17] M. Zamora, B. Alonso, C. Pastor, I. Cuadrado, *Organometallics* **2007**, *26*, 5153-5164.

[18] I. Angurell, O. Rossell, M. Seco, *Chem. Eur. J.* **2009**, *15*, 2932-2940.

[19] D. E. Fogg, E. N. dos Santos, *Coord. Chem. Rev.* **2004**, *248*, 2365-2379.

[20] J. C. Wasilke, S. J. Obrey, R. T. Baker, G. C. Bazan, *Chem. Rev.* **2005**, *105*, 1001-1020.

[21] G. F. Swiegers, T. J. Malefetse, *Chem. Rev.* **2000**, *100*, 3483-3537.

[22] H. B. Yang, A. M. Hawkridge, S. P. D. Huang, N. Das, S. D. Bunge, D. C. Muddiman, P. J. Stang, *J. Am. Chem. Soc.* **2007**, *129*, 2120-2129.

[23] H. T. Baytekin, M. Sahre, A. Rang, M. Engeser, A. Schulz, C. A. Schalley, *Small* **2008**, *4*, 1823-1834.

[24] F. Grimm, K. Hartnagel, F. Wessendorf, A. Hirsch, *Chem. Commun.* **2009**, 1331-1333.

[25] R. van de Coevering, R. J. M. Klein Gebbink, G. van Koten, *Prog. Polym. Sci.* **2005**, *30*, 474-490.

[26] J. M. Fraile, J. I. Garcia, J. A. Mayoral, *Chem. Rev.* **2009**, *109*, 360-417.

[27] P. Barbaro, F. Liguori, *Chem. Rev.* **2009**, *109*, 515-529.

[28] A. W. Kleij, R. van de Coevering, R. J. M. Klein Gebbink, A.-M. Noordman, A. L. Spek, G. van Koten, *Chem. Eur. J.* **2001**, *7*, 181-192.

[29] R. van de Coevering, A. P. Alfers, J. D. Meeldijk, E. Martinez-Viviente, P. S. Pregosin, R. J. M. Klein Gebbink, G. van Koten, *J. Am. Chem. Soc.* **2006**, *128*, 12700-12713.

[30] R. Kreiter, R. J. M. Klein Gebbink, G. van Koten, *Tetrahedron* **2003**, *59*, 3989-3997.

[31] S. L. James, *Chem. Soc. Rev.* **2009**, *38*, 1744-1758.

[32] I. M. Al-Najjar, *Inorg. Chim. Acta* **1987**, *128*, 93-104.

[33] M. A. N. Virboul, M. Lutz, M. A. Siegler, A. L. Spek, G. van Koten, R. J. M. Klein Gebbink, *Chem. Eur. J.* **2009**, *15*, 9981-9986.

[34] R. van de Coevering, P. C. A. Bruijnincx, M. Lutz, A. L. Spek, G. van Koten, R. J. M. Klein Gebbink, *New J. Chem.* **2007**, *31*, 1337-1348.

[35] R. van de Coevering, P. C. A. Bruijnincx, C. A. van Walree, R. J. M. Klein Gebbink, G. van Koten, *Eur. J. Org. Chem.* **2007**, 2931-2939.

[36] S. Sanz, L. A. Jones, F. Mohr, M. Laguna, *Organometallics* **2007**, *26*, 952-957.

CHAPTER FIVE

Sulfonate-tethered (η^6-arene) Ru(II) Complexes for Application in Asymmetric Transfer Hydrogenation in Water

ABSTRACT

A new water-soluble arene ruthenium(II) dimer appended with a butyl sulfonate group has been synthesised. Its coordination with the chiral diamine ligand (S, S)TsDPEN led to the formation of the corresponding hydrophilic half-sandwich complex. The activity of this chiral transition metal complex was tested in the asymmetric transfer hydrogenation (ATH) of ketones in neat water and showed good activity and enantioselectivity. The catalyst was easily recycled and reused at the end of the reaction.

5.1 Introduction

The development of greener approaches to known and effective industrial processes is an important field of research in homogeneous catalysis. From an economical point of view and because of environmental considerations, the use of water as reaction medium is a very interesting strategy within this field. As a result, a great number of important catalytic organic transformations have already been studied in aqueous environments.[1-3] Because of the poor solubility in water of most of the well-known homogeneous catalysts, derivatisation of the transition metal complex is often required to allow their use as water-soluble catalysts. One way to induce water-solubility properties to a metal complex is by coordination of a hydrophilic ligand to the metal centre.[4, 5]

During the last 30 years the chemistry of arene-ruthenium complexes has been extensively studied.[6-8] Because these compounds are valuable precursors for a wide variety of catalysts, the last years have seen the development of functionalised η^6-arene ruthenium complexes.[9] The increasing interest in these molecules can be explained by the development of straightforward methods for their preparation, making them easily accessible precatalysts for a lot of catalytic applications, e. g. hydrogenation,[10-12] polymerisation,[13] and metathesis.[14] Synthesis of a ruthenium-arene precursor of the type [{$RuX_2(\eta^6$-arene)}$_2$] bearing a hydrophilic functionalised arene ligand is of interest for the preparation of water-soluble half-sandwich arene-ruthenium (II) complexes. Functionalisation of the metal precursor at this stage would indeed allow for the formation of many different catalyst precursors by simple coordination of such "task specific" ligands, permitting an easy access to water-soluble transition metal complexes that would have otherwise required tedious synthetic work. Despite the numerous examples of functionalised arene-ruthenium complexes, their hydrophilic counterparts have attracted little attention. In 2009 Crochet *et al.* reported on the hydrophilic properties of a ruthenium arene complex functionalised with a hydroxyethoxy tail on its arene ligand (previously synthesised by the group of White *et al.*) and its application in catalysis in water.[15, 16] To the best of our knowledge, this is the only example of this type of transition metal complex demonstrating water-soluble properties reported up to date.

Among the organic reactions that require the use of arene-ruthenium complexes as metal precursors, our attention focused on the asymmetric transfer hydrogenation (ATH).[17-19] This transformation is an interesting alternative to classical asymmetric hydrogenation as it does not necessitate the use of (pressurised) hydrogen gas.[20, 21] Since the development by Noyori *et al.* of the very active and selective [(TsDPEN)Ru(*p*-cymene)Cl] ruthenium catalyst for this transformation,[22-24] efforts have been pursued since the first reports in this field by Williams *et al.* and Chung *et al.* towards the use of water as solvent for this reaction.[25-29] Several examples of ligand modification have appeared recently in the literature in which most of the functionalisation is occurring on the chiral ligand (Figure 1). It has been shown that hydrophilicity of the ruthenium precatalyst is not a prerequisite for the catalytic reaction to proceed in water, however in this case no recyclability of the catalyst can be envisaged.[29, 30]

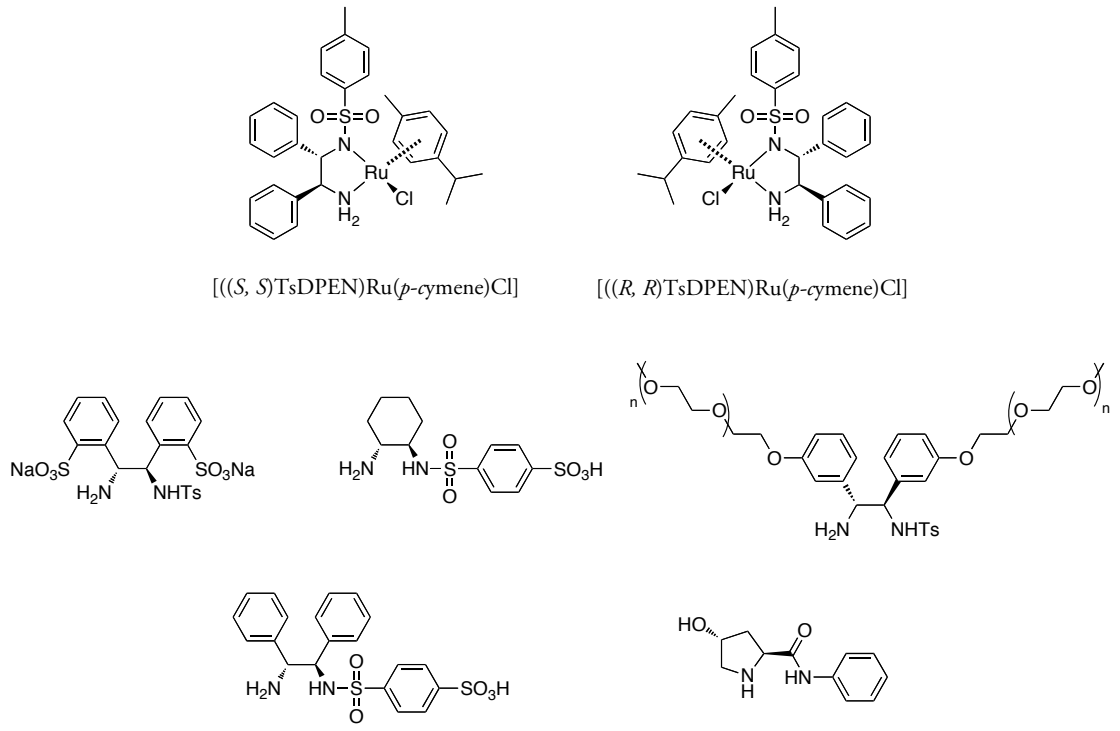

Figure 1. Noyori's Ruthenium complexes for ATH and examples of modified chiral diamine ligands for ATH in water.

Several examples of ligand modification have appeared recently in the literature in which most of the functionalisation is occurring on the chiral ligand (Scheme 1). Introduction of ionic tags such as $-SO_3^-$ or $-NR_3^+$ groups is a very common approach to alter the solubility of a ligand.[31, 32] We recently reported on a new methodology to introduce an

n-butyl sulfonate functionality and on the use of this sulfonate moiety as a versatile tool for catalyst immobilisation (see Chapter Two and Three).[33] Here we would like to demonstrate the effectiveness of such a functional group to fine-tune the solubility of the molecular scaffold it is connected to. The approach developed here allowed us to straightforwardly synthesise a chiral sulfonate-functionalised arene-ruthenium compound. The activity of this precatalyst was tested in the ATH of acetophenone in water and the preliminary results indicated a good catalytic activity in non-optimised conditions.

5.2 Results

Synthesis

The most common preparation method to access arene-ruthenium complexes is by reaction of $RuCl_3.xH_2O$ with a cyclohexadiene derivative in an EtOH/water mixture.[34, 35] During the course of such a reaction, the cyclohexadiene is dehydrogenated to yield the arene ligand with concomittent reduction of $Ru^{III}Cl_3$ to yield a dimeric chloro-bridged arene-ruthenium(II) compound. The first step towards the synthesis of a functionalised arene-ruthenium complex is therefore the synthesis of the desired cyclohexadiene derivative.

Starting from 3-(cyclohexa-1,4-dien-1-yl)propan-1-ol, which is readily available from 3-phenylpropan-1-ol via a Birch reduction,[36] alkyl bromide compound **1** was obtained in 60 % by bromination using PBr_3 in ether (Scheme 1). Reaction of isobutyl methylsulfonate with *n*BuLi generated the corresponding lithiated species,[37] which was subsequently reacted with **1** to afford the isobutyl protected sulfonate **2** in reasonable yields. Compound **2** was deprotected with NaI in refluxing acetone to give the alkyl sulfonate tethered cyclohexadiene **3** as the sodium salt in excellent yields.

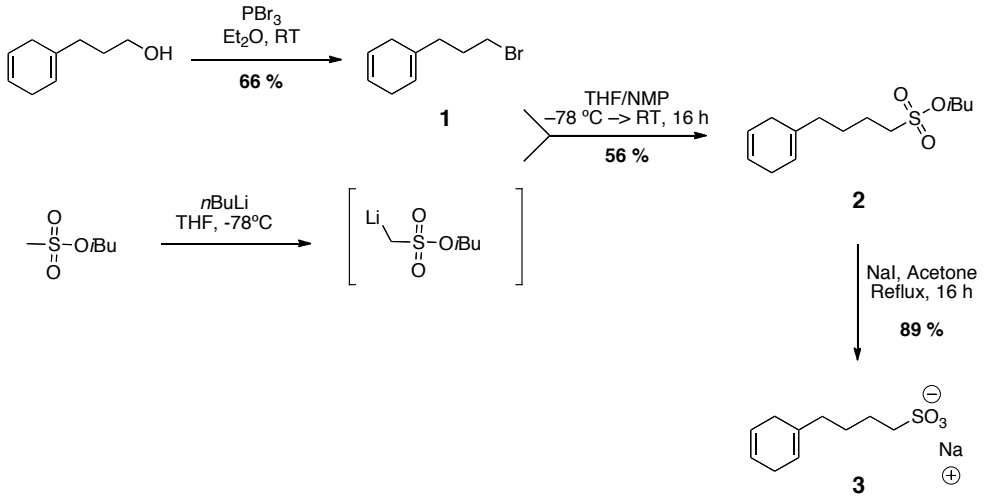

Scheme 1. Synthesis of the cyclohexadiene derivatives.

The coordination of **3** to ruthenium was first attempted in refluxing aqueous ethanol in the presence of $RuCl_3.xH_2O$ for 6 h. After cooling and concentration of the reaction mixture an orange solid was obtained. The ^1H NMR spectrum of the crude product clearly indicated the presence of at least two different species (Scheme 2, conditions 1). The products present were found to have different chemical shifts than the starting material **3** and attempts to separate the different species were unsuccessful. A possible reaction product was thought to be the isomerised ligand **3**, as isomerisation is a preliminary step involved in the coordination of the Ru metal centre.[35] In order to improve the synthesis of the ruthenium dimer, the reaction was performed in a mixture of MeOH / water (conditions 2) instead of aqueous EtOH. In these conditions another side product formed which is believed to be the oxidised form of the ligand **3**, as evidenced by the presence of signals in the aromatic region (see Scheme 2, conditions 2).

Conditions 1:

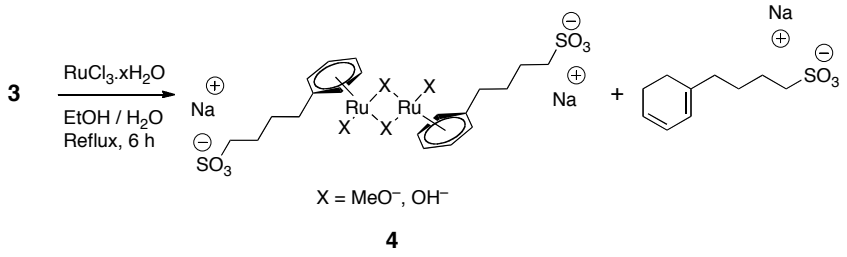

Conditions 2:

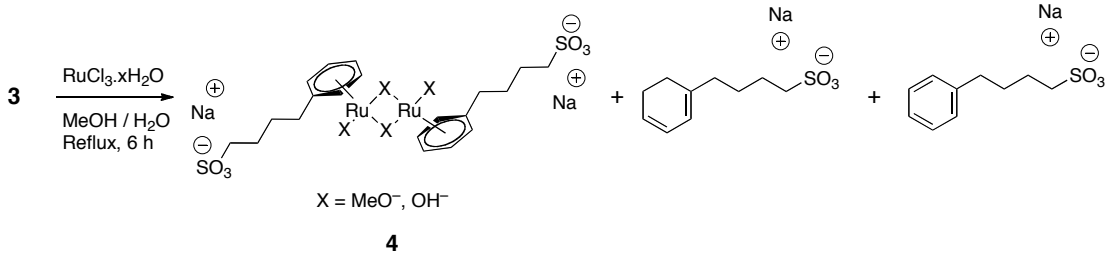

Scheme 2. Synthesis of arene ruthenium dimer in EtOH/water (conditions 1) and MeOH / water (conditions 2).

The crude product mixture obtained in both sets of conditions was further analysed by ESI-MS measurements, confirming the presence of arene-ruthenium dimers. These compounds do not bear chloride bridging ligands but hydroxy and methoxy ligands as evidenced by ESI-MS (see Figure 2). The dimers observed in ESI-MS correspond to the species with the general formula $[Ru_2(arene)_2(OH)_n(MeO)_{3-n}]^-$, where arene stands for the negatively charged η^6-coordinated ligand 4-phenylbutanesulfonate.

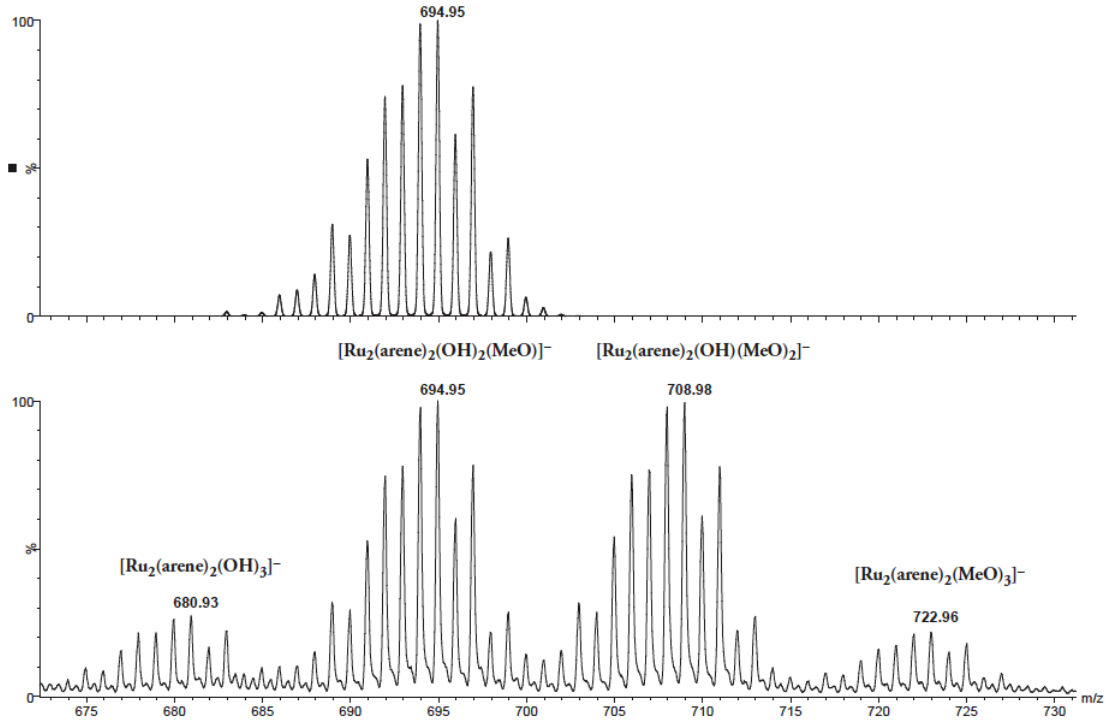

Figure 2. ESI-MS spectrum of **4** (conditions 2) measured in negative ion mode in MeOH. The top spectrum represents the theoretical isotopic pattern of $[Ru_2(arene)_2(OH)_2(MeO)]^-$.

Despite the successful formation of sulfonate functionalised arene-ruthenium dimers, the synthetic method used did not allow for the isolation of one of thesedimeric products in a pure form. Due to theses difficulties, another approach was envisaged for the synthesis of a water-soluble arene-ruthenium complex. The alternative synthetic route that was investigated involves the deprotection of the sulfonate moiety at a later stage (Scheme 3). Ruthenium dimer **5** was synthesised very straightforwardly by refluxing the sulfonate-functionalised cyclohexadiene **2** with $RuCl_3.xH_2O$ in aqueous ethanol for 6 h. The resulting chloro-bridged dimer **5** was then suspended with KI in refluxing aqueous ethanol for 2 h to yield the neutral iodo-bridged dimer **6**. This halide exchange was necessary to avoid any possible halide scrambling that could occur during the deprotection of the sulfonate as this step requires the use of NaI.

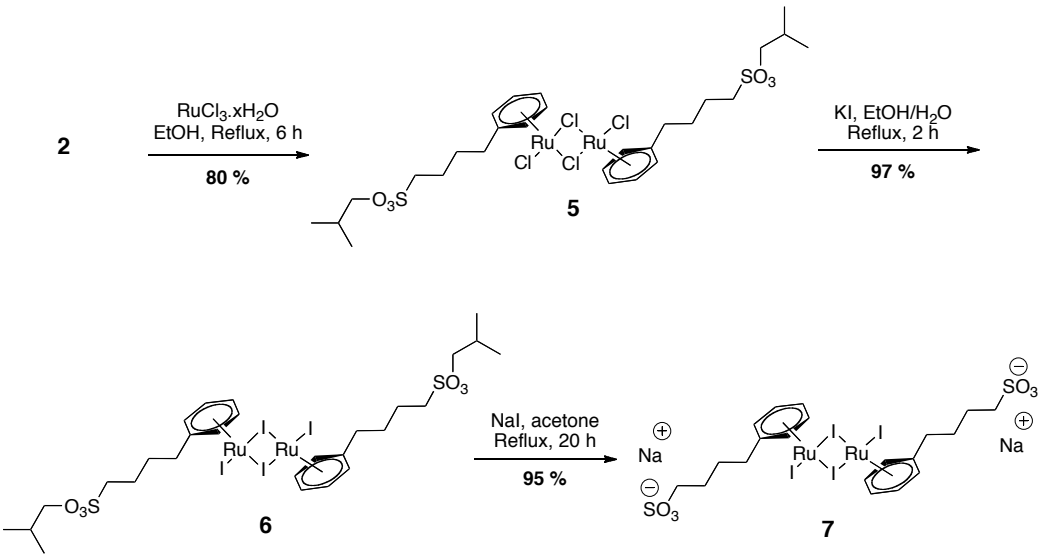

Scheme 3. Synthesis of a water soluble arene-ruthenium dimer.

Compound **6** was deprotected in the presence of NaI in refluxing acetone affording the Ru(II) dimer **7** as a purple solid in excellent 95 % yield. Compound **7** was alternatively synthesised by refluxing **5** in acetone with NaI for 48 h, yielding the expected product. **7** was analysed by ^{1}H and ^{13}C NMR in D_2O, with both spectra confirming the absence of the peaks corresponding to the isobutyl protecting group, thus confirming the successful deprotection of **5** or **6**. High resolution mass spectrometry of **7** displayed a typical isotopic pattern at m/z = 1160.6030 corresponding to the monoanion $[7 - Na]^-$.

The formation of a monomeric precatalyst with a task-specific ligand was evaluated by coordination of the chiral diamino ligand (1S, 2S)-*N*-*p*-toluenesulfonyl-1,2-diphenylethylenediamine ((*S, S*)TsDPEN), well known for its ability of chiral induction. Because of the low solubility of dimer **7** in organic solvents, the coordination was attempted in water. Unfortunately the poor solubility of the (*S, S*)TsDPEN ligand in water did not allow coordination in water. The coordination was then performed using neutral compound **6** in 2-propanol in the presence of NEt_3 to allow for deprotonation of the amine group (Scheme 4). Deprotection of the sulfonate group was then carried out in a separate step by treating the reaction product with NaI in refluxing acetone to yield sulfonato complex **8** as a purple solid in 52 % yield starting from **6**. The solubility profile of **8** was dramatically changed by the deprotection of the sulfonate moiety: the so formed ruthenium complex is highly soluble in water, not soluble in organic solvent and poorly soluble in ethanol and methanol.

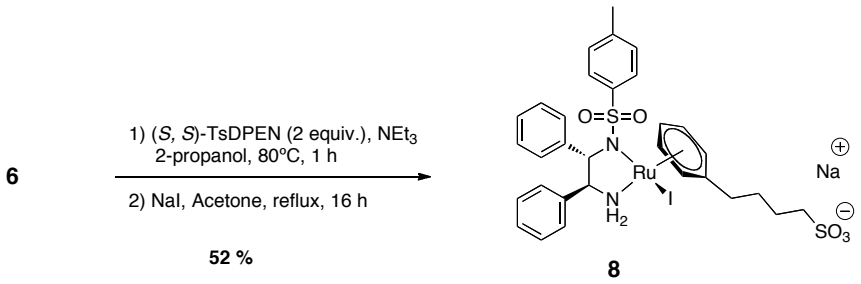

Scheme 4. Synthesis of a chiral half sandwich Ru(II).

The compound **8** was characterised by ^{1}H and ^{13}C NMR spectroscopy and ESI-MS spectroscopy, showing the successful coordination of the chiral ligand (*S, S*)TsDPEN on the ruthenium metal center. The high resolution mass spectrum of **8** displayed a characteristic isotopic pattern at m/z = 806.9997 coinciding with the calculated isotopic pattern of the monoanion [**8** - Na]$^{-}$. The coordination of the chiral diamine ligand to the ruthenium metal center was also demonstrated by the presence in ^{1}H and ^{13}C NMR of the typical peaks corresponding to the TsDPEN ligand.

Catalysis

The water-soluble ruthenium complex 8 was tested in the catalytic asymmetric transfer hydrogenation (ATH) of ketones. The benchmark substrate acetophenone was used as substrate in this study and the reaction was performed in neat water using sodium formate as the hydrogen source (Scheme 5).

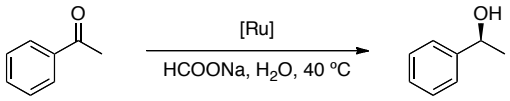

Scheme 5. Asymmetric reduction of acetophenone.

First, the precatalyst was generated *in situ* by mixing the arene-ruthenium (II) dimer **7** in the presence of two equivalents of the chiral ligand (*S, S*)TsDPEN in water at 40 °C for 1 h, following catalytic conditions developed by several groups for the same reaction in water.[38, 39] The catalytic run was then started by the introduction of sodium formate followed by acetophenone. Different catalyst loadings were tested and the use of 2 mol % of the precatalyst was found to be the most efficient concentration (see

Table 1). It is noteworthy that for a catalyst loading of 3 mol % the reaction mixture turned black, which can explain the low conversion observed in this case (entry 2).

The activity of the *in situ* formed catalyst was compared to that of the preformed complex 8 and the results are displayed in Table 1. From these preliminary catalytic studies, it is clear that the preformed complex **8** has a higher activity than its in situ congener (entries 3 and 6). The completion of the reaction was achieved in 4 h with preformed catalyst 8 and required 20 h in case of the *in situ* formed catalyst.

Table 1. Catalytic activity of preformed catalyst **8** and its *in situ* form (*S, S*)TsDPEN/**7**.

Entry	Run	Catalyst	Loading	Time (h)	Yield (%)[a]	ee (%)[b]
1	1	(S, S)TsDPEN/**7**	1 mol %	24	26	91
2	1	(S, S)TsDPEN/**7**	3 mol %	20	27	92
3	1	(S, S)TsDPEN/**7**	2 mol %	24	100	94
4	2	(S, S)TsDPEN/**7**	2 mol %	20	99	94
5	3	(S, S)TsDPEN/**7**	2 mol %	nd	nd	nd
6	1	**8**	2 mol %	4	>99	94
7	2	**8**	2 mol %	20	97	93
8	3	**8**	2 mol %	13	21	93

[a] Yields were determined by chiral GC analysis. [b] ee were determined by Chiral GC analysis and the *S* configuration of the product was confirmed by comparison with an authentic enantiopure sample.

In order to test the recyclability of the catalysts, they were used in three consecutive runs. To this end, the reaction mixture at the end of a catalytic run was extracted three times with a 2 mL portion of degassed ether to remove all organic products formed and the new catalytic run (run 2) started after addition of sodium formate and acteophenone. As can be seen in Table 1 (entries 4 and 7) (S, S)TsDPEN/**7** and complex **8** were able to reduce acetophenone in phenylethanol with high yields and high enantioselectivities in the second run. A second recycling run (run 3) with compound **8** shows a decrease in activity however without loss of selectivity. For practical reasons, a third run with (S, S)TsDPEN/**7** could not be performed because of the poor homogeneity of the

reaction mixture, likely induced by considerable amounts of salts generated during the previous catalytic runs.

5.3 Discussion

η^6-Arene ruthenium(II) complexes are commonly synthesised by reduction of $RuCl_3.xH_2O$ in presence of an excess of 1, 4-cyclohexadiene in refluxing aqueous ethanol. Under these conditions, the $[RuCl_2(\eta^6\text{-arene})]_2$ dimer precipitates from the reaction medium and can be easily isolated by simple filtration. Our attempts to synthesise a $[RuCl_2(\eta^6\text{-arene})]_2$ with this method in the presence of the sulfonate-modified 1, 4-cyclohexadiene compound **3** were unsuccessful. Instead of the expected chloro-bridged arene-ruthenium dimer, methoxy- and/or hydroxy-bridged ligand ruthenium dimers were formed, as evidenced by ESI-MS analysis. This result is noteworthy considering that this type of alkoxy-bridged dimers are usually prepared by ligand exchange from the halide bridged counterpart, usually in the presence of a strong base.[40] The formation of $[RuX_2(\eta^6\text{-arene})]_2$ can be explained by the high solubility of both reagent and product in the reaction medium; when the reaction is performed with a less polar ligand, the product precipitates immediately from the reaction mixture and can not be engaged in further reactions like ligand exchange. We can postulate that the reaction medium is basic enough to promote this ligand exchange from Cl^- to OH^-, EtO^- or MeO^-, leading to the formation of the unexpected dimers. In the case of the ruthenium dimer formed in aqueous ethanol, it is thought that another ligand exchange occur during the ESI-MS measurement which is performed in methanol, yielding the formation of methoxy-bridged ruthenium dimer and not ethoxy-bridged dimers.

During the formation of the ruthenium dimer, several reactions occur at the same time: the reduction of the metal precursor from Ru(III) to Ru(II), the isomerisation and dehydrogenation of the ligand, and the oxidation of the solvent.[35] These processes consequently lead to the formation of the desired compound but also of side products like the dehydrogenated ligand (the 4-phenylbutane sulfonate) or the isomerised ligand (1-(4-sulfonatobutyl)-1, 3-cyclohexadiene sodium salt) as an excess of the ligand is necessary for the reaction to go to completion (see Scheme 2). Remarkably, the formation of the 4-phenylbutane sulfonate was only observed when an aqueous solution of methanol was used, suggesting that the oxidation of the solvent is less favorable in

these conditions than the oxidation of the ligand. In general the formation of the side products is not an issue as the ruthenium complex precipitates, leaving the side products in the reaction medium and enabling an easy purification. Due to the polar nature of the ligand used here for the reaction, the alkoxy-bridged ruthenium dimer could not be separated from the side products formed during the course of the reaction in spite of all the efforts to selectively crystallise or precipitate it.

The *in situ* prepared and the preformed catalysts were tested in the catalytic asymmetric transfer hydrogenation in water. As a benchmark substrate, acetophenone was used to study this reaction with our catalytic systems, enabling a fair comparison with previous studies. The choice of the hydrogen source for the reduction of acetophenone, *i. e.* the sodium formate, is crucial for the achievement of good enantioselectivity and conversion as the use of this reductant avoids the possibility of the reversible reaction (oxidation of phenylethanol) to occur.[17] The other advantages of using HCO_2Na are the easy handling of this reagent and its high solubility in water. The preliminary catalytic studies presented in Table 1 show that both *in situ* prepared and preformed complexes are able to perform this reaction with comparable enantioselectivities but an activity somewhat lower, than for comparable systems reported up to now.[29]

The optimised catalytic concentration for (*S, S*)TsDPEN-**7** appeared to be 2 mol % which is twice as much as what is generally reported for similar systems in water.[27, 41] This difference can be attributed to the sluggish formation of the precatalyst *in situ* which could suffer from the different solubility properties of the two reaction partners, although it is worth mentioning that a very good activity with the (*S, S*)TsDPEN ligand and [{$RuCl_2$(*p*-cymene)}$_2$] was observed despite their very poor solubility in water.[28, 30]

The catalytic activity of the preformed catalyst **8**, with a catalyst loading of 2 mol %, showed an increased activity compared to the (*S, S*)TsDPEN/**7** system. This difference between the two catalytic systems can stem from the relative solubility of the active species in water. Indeed in the ATH of acetophenone in water the substrate is not soluble in the reaction medium and consequently a biphasic mixture is obtained. When the reaction is performed with (*S, S*)TsDPEN/[{$RuCl_2$(*p*-cymene)}$_2$], the catalyst resides in the organic phase which implies a higher catalyst concentration.[42] We can assume that for a catalyst soluble in water the reaction is occuring at the interface and that the activity of the catalyst is controlled by the diffusion of the reactants in the medium. In

view of our results, it seems that the diffusion is more efficient when the precatalyst is formed prior to the reaction.

Recycling experiments were also performed with both systems and showed that the recycled catalysts are active at least to some extend, without compromising the enantioselectivity of the reaction. The conditions used for the recycling experiments were exactly identical as that of the first run, implying the use of HCO_2Na as the reductant. These conditions seem not to be ideal as the activity of the catalyst rapidly decreased after the first run. This finding can be attributed to the fact that ATH in water is dependent on the pH and that repeated addition of HCO_2Na can induce a dramatic pH change,[42, 43] resulting in lower activity of the catalyst. It is also likely that a high concentration of salt can have consequences on the diffusion of the reactants in the medium, thus contributing to the observed lower activity.

5.4 Conclusion

In summary, we have shown that the introduction of an alkyl sulfonate chain to the arene ligand of the prototypical $[Ru(arene)Cl_2]_2$ complex renders it hydrophilic. This hydrophilic precursor enabled the synthesis of versatile water-soluble chiral TsDPEN-ruthenium arene complexes of interest for the asymmetric transfer hydrogenation in water. Indeed, the new sulfonate appended η^6-arene ruthenium(II) complexes have proven to be efficient for this reaction, keeping their activity and stereoselectivity after recycling even in non-optimised conditions. We believe the applicability of sulfonated ruthenium precursor **7** is not limited to ATH and that this compound could be of interest to construct other water soluble complexes and catalysts.

5.5 Experimental section

General information: All reactions (unless otherwise mentioned) were performed under a N_2 atmosphere using standard Schlenk techniques. Toluene, Et_2O and THF were dried through a solvent purification system (SPS) and CH_2Cl_2 was dried over CaH_2, distilled, and degassed before use. Extra dry NMP was purchased from Aldrich and distilled before use. All reagents were purchased from Aldrich or Acros and were used as received. 3-(cyclohexa-1,4-dien-1-yl)propan-1-ol was prepared as reported in the literature.[36] ^1H and $^{13}C\{^1H\}$ NMR spectroscopic measurements were conducted at 25 °C on a Varian Inova 300, a Varian Oxford AS400 spectrometer or a Bruker Avance III 600 MHz. Chemical shifts (δ) are given in ppm referenced to the residual solvent peak and coupling constants are given in Hertz (Hz). Time-of-flight electrospray ionisation mass spectra (ESI-MS) were measured by the Biomolecular Mass Spectrometry and Proteomics Group, Utrecht University, on a Micromass LC-T mass spectrometer (Waters, Manchester, UK), operating in negative ion mode. The nanospray needle potential was typically set to 1300 V and the cone voltage to 60 V. The source block temperature was set to 80 °C. The Elemental analyses were performed by Dornis and Kolbe, Mikroanalytische Laboratorium, Mülheim a/d Ruhr, Germany. GC samples were analyzed using a Perkin Elmer Clarus 500 GC equipped with a Chromapack Chirasil-Dex CB (25 m x 0.25 mm) column.

1-(3-bromopropyl)-1,4-cyclohexadiene (1): To a solution of 3-(cyclohexa-1,4-dien-1-yl)-propan-1-ol (2.77 g, 20 mmol) in dry Et_2O (30 mL) was added PBr_3 (0.7 mL, 7.33 mmol) at 0 °C. The mixture was then stirred for 4 h at room temperature. The reaction was quenched with water (15 mL) and the product extracted with Et_2O (3 x 20 mL). The volatiles were evaporated and the crude product purified by silica gel column chromatography using hexane/Et_2O (95:5, v/v) as the eluent, yielding a colourless oil (2.65 g, 66%).
^1H NMR (400 MHz, $CDCl_3$) δ = 5.74-5.73 (br, 2H; C*H*C*H* diene), 5.47 (br 1H; C*H* diene), 3.40 (t, 2H, $^3J_{HH}$ = 6.9 Hz; $(CH_2)_2CH_2Br$), 2.72-2.65 (m, 2H; CH_2 diene), 2.61-2.55 (m, 2H; CH_2 diene), 2.11 (t, 2H, $^3J_{HH}$ = 6.9 Hz; $CH_2(CH_2)_2Br$), 2.02-1.92 (m, 2H; $CH_2CH_2CH_2Br$) **$^{13}C\{^1H\}$ NMR (100 MHz, $CDCl_3$)** δ = 133.2, 124.4, 124.2, 119.7, 35.8, 33.6, 30.5, 28.9, 26.8 **Elemental Analysis** calculated for $C_9H_{13}Br$: C, 53.75; H, 6.52; Found: C, 54.19; H, 6.41.

Isobutyl 4-(cyclohexa-1,4-dien-1-yl)butane-1-sulfonate (2): In a Schlenk flask was introduced isobutylmethanesulfonate (3.66 g, 24 mmol) with THF (25 mL). The reaction mixture was cooled to –78 °C followed by dropwise addition of a solution of 1.6 M of *n*BuLi in

hexane (11 mL, 17.6 mmol) and the mixture was stirred at this temperature for 2 h. The mixture was then added via canula to a solution of **1** (2.78 g, 13.8 mmol) in a mixture of THF (35 mL) and NMP (15 mL). The reaction mixture was allowed to warm to room temperature and was stirred for another 20 h. The resulting mixture was quenched with water (20 mL) and extracted with diethyl ether (3 x 30 mL). The crude product was concentrated *in vacuo* and purified by silica gel column chromatography using hexane/ether (8:2, v/v) as the eluent, yielding the pure compound as a colorless liquid (2.10 g, 56 %).

^{1}H NMR (400 MHz, $CDCl_3$) δ = 5.68 (br, 2H; C*H*C*H* diene), 5.41 (br, 1H; C*H* diene), 3.95 (d, 2H, $^3J_{HH}$ = 6.4 Hz; CH_2 *i*Bu), 3.08 (t, 2H, $^3J_{HH}$ = 7.6 Hz; $(CH_2)_3CH_2SO_3$), 2.68-2.63 (m, 2H; CH_2 diene), 2.57-2.53 (m, 2H; CH_2 diene), 2.06-1.96 (m, 1H + 2H; overlap C*H* *i*Bu and $CH_2(CH_2)_3SO_3$), 1.87-1.79 (m, 2H; $(CH_2)_2CH_2CH_2SO_3$), 1.59-1.52 (m, 2H; $CH_2CH_2(CH_2)_2SO_3$), 0.96 (d, 6H, $^3J_{HH}$ = 6.8 Hz; $(CH_3)_2$ *i*Bu) **^{13}C{^{1}H} NMR (100 MHz, $CDCl_3$)** δ = 133.8, 124.3, 124.1, 119.3, 75.3, 50.1, 36.7, 28.7, 28.3, 26.7, 25.7, 23.1, 18.7 **Elemental Analysis** calculated for $C_{14}H_{24}O_3S$: C, 61.73; H, 8.88; Found: C, 61.10; H, 8.75.

1-(4-sulfonatobutyl)-1,4-cyclohexadiene sodium salt (3): Compound **2** (0.560 g, 2.06 mmol) and NaI (0.616 g, 4.11 mmol) were stirred at reflux temperature for 48 h in acetone (25 mL). The resulting mixture was cooled down and the solids were filtered and washed with acetone and Et_2O, yielding the desired compound as a white solid (0.436 g, 89 %).

^{1}H NMR (400 MHz, MeOH-d_4) δ = 5.67 (br, 2H; C*H*C*H* diene), 5.44 (br, 1H; C*H* diene), 2.80 (t, 2H, $^3J_{HH}$ = 8 Hz; $(CH_2)_3CH_2SO_3$), 2.65-2.63 (m, 2H; CH_2 diene), 2.60-2.55 (m, 2H; CH_2 diene), 2.01 (t, 2H, $^3J_{HH}$ = 8 Hz; $CH_2(CH_2)_3SO_3$), 1.82-1.74 (m, 2H; $(CH_2)_2CH_2CH_2SO_3$), 1.58-1.51 (m, 2H; $CH_2CH_2(CH_2)_2SO_3$) **^{13}C{^{1}H} NMR (100 MHz, MeOH-d_4)** δ = 135.8, 125.3, 125.2, 119.8, 67.0, 38.3, 29.7, 27.7, 27.6, 25.8 **Elemental Analysis** calculated for $C_{10}H_{15}NaO_3S$: C, 50.41; H, 6.35; Found: C, 50.17; H, 6.32.

[{$RuCl_2(\eta^6$-$C_6H_5(CH_2)_4SO_3$*i*Bu)}$_2$] (5): $RuCl_3.xH_2O$ (0.321 g, 1.27 mmol) and **2** (1.39 g, 5.09 mmol) were dissolved in ethanol (25 mL) and heated at reflux temperature for 5 h. After cooling down of the reaction mixture, the precipitate was filtered, washed with cold ethanol and dried *in vacuo*, yielding the product (0.449 g, 80 %) as an orange solid.

^{1}H NMR (400 MHz, CD_2Cl_2) δ = 5.62-5.58 (m, 4H+2H; *m*-Ar*H* overlap with *p*-Ar*H*), 5.35 (d, 4H, $^3J_{HH}$ = 5.6 Hz ; *o*-Ar*H*), 3.97 (d, 4H, $^3J_{HH}$ = 6.4 Hz; CH_2 *i*Bu), 3.15 (t, 4H, $^3J_{HH}$ = 7.6 Hz; $(CH_2)_3CH_2SO_3$), 2.55 (t, 4H, $^3J_{HH}$ = 8 Hz; $CH_2(CH_2)_3SO_3$), 2.07-1.97 (m, 2H; C*H* *i*Bu), 1.95-1.87 (m, 4H; $(CH_2)_2CH_2CH_2SO_3$), 1.82-1.74 (m, 4H;

$CH_2CH_2(CH_2)_2SO_3$), 0.98 (d, 12H, $^3J_{HH}$ = 6.8 Hz; $(CH_3)_2$ *i*Bu) **$^{13}C\{^1H\}$ NMR (100 MHz, CD_2Cl_2)** δ = 100.4, 84.3, 80.7, 80.6, 76.2, 50.0, 33.1, 28.8, 28.0, 23.7, 18.9 **Elemental Analysis** calculated for $C_{28}H_{44}Cl_4O_6Ru_2S_2$: C, 38.01; H, 5.01 Found: C, 38.41; H, 4.95.

[{$RuI_2(\eta^6$-$C_6H_5(CH_2)_4SO_3$*i*Bu)}$_2$] (6): Compound **5** (0.192 g, 0.217 mmol) was suspended in a mixture of aqueous ethanol (50 % v/v, 10 mL) with KI (0.360 g, 2.17 mmol). After 2 h at reflux temperature, the precipitate was collected by filtration, washed with ethanol and dried *in vacuo* to yield the product as a purple solid (0.264 g, 97 %).

^1H NMR (400 MHz, CD_2Cl_2) δ = 5.71 (t, 2H, $^3J_{HH}$ = 5.6 Hz; *p*-Ar*H*), 5.63 (t, 4H, $^3J_{HH}$ = 5.6 Hz; *m*-Ar*H*), 5.49 (d, 4H, $^3J_{HH}$ = 6 Hz; *o*-Ar*H*), 3.97 (d, 4H, $^3J_{HH}$ = 6.4 Hz; CH_2 *i*Bu), 3.17 (t, 4H, $^3J_{HH}$ = 7.6 Hz; $(CH_2)_3CH_2SO_3$), 2.70 (t, 4H, $^3J_{HH}$ = 7.6 Hz; $CH_2(CH_2)_3SO_3$), 2.07-1.97 (m, 2H; C*H* *i*Bu), 1.96-1.88 (m, 4H; $(CH_2)_2CH_2CH_2SO_3$), 1.83-175 (m, 4H; $CH_2CH_2(CH_2)_2SO_3$), 0.98 (d, 12H, $^3J_{HH}$ = 6.8 Hz; $(CH_3)_2$ *i*Bu) **$^{13}C\{^1H\}$ NMR (100 MHz, CD_2Cl_2)** δ = 101.1, 84.5, 83.5, 83.4, 76.2, 50.1, 34.2, 28.5, 28.4, 23.3, 18.5.

[{$RuI_2(\eta^6$-$C_6H_5(CH_2)_4SO_3)$}$_2$][Na]$_2$ (7): Compound **6** (0.134 g, 0.107 mmol) was suspended in acetone (20 mL) with NaI (0.272 g, 1.82 mmol). After 20 h of stirring at reflux temperature, the precipitate was collected by filtration, washed with ethanol and dried *in vacuo* to yield the product as a purple solid (0.126 g, 100 %).

Compound **7** was alternatively synthesised by refluxing compound **5** with NaI in acetone for 48 h, yielding a compound with the same spectroscopic features as described below.

^1H NMR (400 MHz, D_2O) δ = 5.93-5.84 (m, 10H; Ar*H*), 3.01-2.92 (m, 4H; $(CH_2)_3CH_2SO_3$), 2.73-2.59 (m, 4H; $CH_2(CH_2)_3SO_3$), 1.90-1.73 (m, 4H; $CH_2(CH_2)_2CH_2SO_3$) **$^{13}C\{^1H\}$ NMR (100 MHz, D_2O with MeOH-d_4 as internal standard)** δ = 101.8, 82.4, 81.3, 81.2, 51.3, 34.3, 29.4, 24.4 **HRMS (ES^-)** calculated for $C_{20}H_{26}I_4NaO_6Ru_2S_2$: m/z = 1160.5334 found: 1160.6030 $[M\text{-}Na]^-$.

[RuI(η^6-$C_6H_5(CH_2)_4SO_3$){(*S, S*)TsDPEN}][Na] (8): Compound **6** (73 mg, 0.0584 mmol), (*S, S*)-TsDPEN (41 mg, 0.112 mmol) and NEt_3 (23 mg, 0.224 mmol) were mixed in 2-propanol (10 mL) and heated at 80 °C for 1 h. The orange solution was concentrated and the resulting solid filtered. The solids were washed with a small amount of water and dried *in vacuo*. The resulting material was mixed with NaI (18 mg, 0.12 mmol) in acetone (15 mL) and refluxed for 24 h. The mixture was then cooled to ambient temperature

and the solids were filtered and washed with acetone (10 mL) and Et_2O (10 mL), yielding the desired compound as a purple solid (50 mg, 52 %).

^{1}H NMR (600 MHz, DMSO-d_6) δ = 7.10-6.55 (m, 14H; Ar*H* *p*-Ts and $SO_2NCH(C_6H_5)CH(C_6H_5)NH_2$), 6.03 (m, 1H; NH*H*), 5.83-5.53 (m, 5H; Ar*H* arene), 3.77-3.69 (m, 1H+1H; overlap of PhC*H*NH_2 and PhC*H*NTs), 3.17 (m, 1H; N*H*H), 2.57 (m, 2H; $CH_2(CH_2)_3SO_3^-$), 2.47 (t, $^3J_{HH}$ = 7.8 Hz, 2H; $(CH_2)_3CH_2SO_3^-$), 2.21(s, 3H, CH_3 *p*-Ts), 1.67 (m, 4H; $CH_2(CH_2)_2CH_2SO_3$). **^{13}C{^{1}H} NMR (150 MHz, DMSO-d_6)** δ = 143.8, 139.9, 139.2, 137.9, 128.9, 128.0, 127.6, 127.5, 127.0,126.4, 126.3, 125.8, 99.9, 84.8, 83.1, 82.2, 81.9, 81.0, 71.4, 68.2, 51.2, 32.6, 29.1, 24.8, 20.7. **HRMS (ES$^-$)** calculated for $C_{31}H_{34}IN_2S_2O_5Ru$: m/z = 806.9997 found: 807.0016 [M-Na]$^-$.

- **General procedure for the asymmetric transfer hydrogenation of acetophenone**

The ruthenium dimer **7** (11.8 mg, 0.01 mmol) and (*S, S*)TsDPEN (8.8 mg, 0.024 mmol) were suspended in degassed water (2 mL). After stirring at 40 °C for 1 h, the suspension was used for the reduction reactions. In the case of the preformed precatalyst, **8** (8.3 mg, 0.01 mmol) was dissolved in degassed water (2 mL) and the solution was heated at 40 °C. After preparing the precatalysts, HCO_2Na (340 mg, 5 mmol) and acetophenone (120 mg, 1.0 mmol) were added to the solution and allowed to react for a certain period of time. After cooling to room temperature, the organic phase was extracted with Et_2O (3 x 2 mL) and passed through a short silica gel column before being subjected to chiral GC analysis.

For the recycling tests, the reaction mixture was extracted in the same manner with degassed Et_2O (3 x 2 mL) and the resulting water phase was heated at 40 °C and flushed with N_2 to ensure evaporation of residual Et_2O. HCO_2Na (340 mg, 5 mmol) and acetophenone (120 mg, 1.0 mmol) were subsequently added to the solution and allowed to react for a certain period of time.

The yields and enantiomeric excess were determined with a chiral GC (carrier gas: helium, 80 psi; injection temperature: 250 °C; column temperature: 120 °C; retention time: 7.20 min (*R*) and 7.47 (*S*)). The absolute configuration of the product was confirmed by injection of an authentic enantiopure sample on the chiral GC.

5.6 References

[1] C. J. Li, *Chem. Rev.* **2005**, *105*, 3095-3165.

[2] C. J. Li, L. Chen, *Chem. Soc. Rev.* **2006**, *35*, 68-82.

[3] U. M. Lindstrom, *Chem. Rev.* **2002**, *102*, 2751-2771.

[4] F. Joo, *Aqueous organometallic catalysis*, Kluwer academic publishers, **2001**.

[5] B. Cornils, Herrmann, W. A., *Aqueous-Phase Organometallic Catalysis*, Wiley-VCH, Weinheim, **2004**.

[6] S.-I. Murahashi, *Ruthenium in Organic Synthesis*, Wiley-VCH, Weinheim, **2004**.

[7] M. A. Bennett, *Coord. Chem. Rev.* **1997**, *166*, 225-254.

[8] J. H. Rigby, M. A. Kondratenko, *Top. Organomet. Chem.* **2004**, *7*, 181–204.

[9] B. Therrien, *Coord. Chem. Rev.* **2009**, *253*, 493-519.

[10] J. Canivet, L. Karmazin-Brelot, G. Suss-Fink, *J. Organomet. Chem.* **2005**, *690*, 3202-3211.

[11] T. J. Geldbach, P. J. Dyson, *J. Am. Chem. Soc.* **2004**, *126*, 8114-8115.

[12] A. B. Chaplin, P. J. Dyson, *Organometallics* **2007**, *26*, 4357-4360.

[13] F. Simal, A. Demonceau, A. F. Noels, *Angew. Chem. Int. Ed.* **1999**, *38*, 538-540.

[14] E. L. Dias, R. H. Grubbs, *Organometallics* **1998**, *17*, 2758-2767.

[15] J. Soleimannejad, C. White, *Organometallics* **2005**, *24*, 2538-2541.

[16] B. Lastra-Barreira, J. Diez, P. Crochet, *Green Chem.* **2009**, *11*, 1681-1686.

[17] R. Noyori, S. Hashiguchi, *Acc. Chem. Res.* **1997**, *30*, 97-102.

[18] T. Ikariya, A. J. Blacker, *Acc. Chem. Res.* **2007**, *40*, 1300-1308.

[19] J. S. M. Samec, J. E. Backvall, P. G. Andersson, P. Brandt, *Chem. Soc. Rev.* **2006**, *35*, 237-248.

[20] K. Everaere, A. Mortreux, J. F. Carpentier, *Adv. Synth. Catal.* **2003**, *345*, 67-77.

[21] S. Gladiali, E. Alberico, *Chem. Soc. Rev.* **2006**, *35*, 226-236.

[22] K. J. Haack, S. Hashiguchi, A. Fujii, T. Ikariya, R. Noyori, *Angew. Chem. Int. Ed.* **1997**, *36*, 285-288.

[23] S. Hashiguchi, A. Fujii, K. J. Haack, K. Matsumura, T. Ikariya, R. Noyori, *Angew. Chem. Int. Ed.* **1997**, *36*, 288-290.

[24] A. Fujii, S. Hashiguchi, N. Uematsu, T. Ikariya, R. Noyori, *J. Am. Chem. Soc.* **1996**, *118*, 2521-2522.

[25] C. Bubert, J. Blacker, S. M. Brown, J. Crosby, S. Fitzjohn, J. P. Muxworthy, T. Thorpe, J. M. J. Williams, *Tetrahedron Lett.* **2001**, *42*, 4037-4039.

[26] H. Y. Rhyoo, H. J. Park, Y. K. Chung, *Chem. Commun.* **2001**, 2064-2065.

[27] Y. P. Ma, H. Liu, L. Chen, X. Cui, J. Zhu, J. E. Deng, *Org. Lett.* **2003**, *5*, 2103-2106.

[28] X. F. Wu, X. G. Li, W. Hems, F. King, J. L. Xiao, *Org. Biomol. Chem.* **2004**, *2*, 1818-1821.

[29] X. F. Wu, J. L. Xiao, *Chem. Commun.* **2007**, 2449-2466.

[30] X. F. Wu, X. G. Li, F. King, J. L. Xiao, *Angew. Chem. Int. Ed.* **2005**, *44*, 3407-3411.

[31] K. H. Shaughnessy, *Chem. Rev.* **2009**, *109*, 643-710.

[32] D. J. M. Snelders, G. van Koten, R. J. M. Klein Gebbink, *Chem. Eur. J.* **2010**, Accepted for publication.

[33] M. A. N. Virboul, M. Lutz, M. A. Siegler, A. L. Spek, G. van Koten, R. J. M. Klein Gebbink, *Chem. Eur. J.* **2009**, *15*, 9981-9986.

[34] R. A. Zelonka, M. C. Baird, *Can. J. Chem.* **1972**, *50*, 3063-3072.

[35] M. A. Bennett, A. K. Smith, *J. Chem. Soc., Dalton Trans.* **1974**, 233-241.

[36] T. Ohnishi, Y. Miyaki, H. Asano, H. Kurosawa, *Chem. Lett.* **1999**, 809-810.

[37] M. Q. Xie, T. S. Widlanski, *Tetrahedron Lett.* **1996**, *37*, 4443-4446.

[38] X. G. Li, X. F. Wu, W. P. Chen, F. E. Hancock, F. King, J. L. Xiao, *Org. Lett.* **2004**, *6*, 3321-3324.

[39] Y. Arakawa, A. Chiba, N. Haraguchi, S. Itsuno, *Adv. Synth. Catal.* **2008**, *350*, 2295-2304.

[40] T. Arthur, D. R. Robertson, D. A. Tocher, T. A. Stephenson, *J. Organomet. Chem.* **1981**, *208*, 389-400.

[41] J. T. Liu, Y. G. Zhou, Y. N. Wu, X. S. Li, A. S. C. Chan, *Tetrahedron: Asymmetry* **2008**, *19*, 832-837.

[42] X. F. Wu, J. K. Liu, D. Di Tommaso, J. A. Iggo, C. R. A. Catlow, J. Bacsa, J. L. Xiao, *Chem. Eur. J.* **2008**, *14*, 7699-7715.

[43] C. Wang, C. Q. Li, X. F. Wu, A. Pettman, J. L. Xiao, *Angew. Chem. Int. Ed.* **2009**, *48*, 6524-6528.

Study on the Activity of an Alkylsulfonate [(NHC)-Ag] Complex as Antimicrobial Agent

ABSTRACT

The application of N-Heterocyclic Carbene complexes besides the field of catalysis is still rare. The strong metal-carbene bonds that these ligands form with transition metal centres have a lot of advantages that might be employed in the application of NHC-Ag complexes as antimicrobial agents. Here, we propose to evaluate the activity of an alkyl-sulfonate tethered NHC-Ag complex as antibiotic.

Introduction

Since the isolation by Arduengo in 1991 of a stable free carbene, the field of *N*-Heterocyclic Carbene (NHC) chemistry has constantly attracted interest.[1-4] The properties of these compounds as ligand in organometallic chemistry and catalysis have made them very interesting compounds. The electronic properties of the NHCs in terms of good σ-donating and poor π-accepting ligands have shed light on their potential as ligands as they can form strong metal-carbene bonds. This robustness brought by NHCs finds application in organometallic chemistry and catalysis and beyond.[5]

Silver is known for centuries as being an antiseptic and has been used to treat for example extensive burn wounds and chronic ulcers. Even though the mode of action of silver is not clearly understood, silver cations are known to bind to bacteria cell surfaces and to interact with enzymes necessary to the wall cell synthesis.[6] NHC silver complexes have received a lot of attention because of their interesting properties as transmetallating agent to form transition metal-carbene complexes and as catalysts.[7, 8] Besides these useful applications, recent scientific articles report on the activity of these compounds as antimicrobial agents.[6, 9-12] Here, we propose to investigate the antimicrobial activity of a sulfonate-functionalised bis-carbene silver complex against different strains of bacteria and fungi.

Results and discussion

The synthesis of the butyl-sulfonate-functionalised compound **2** was previously described by our group.[13] The zwiterionic imidazolium salt **1** bearing an alkyl-sulfonate moiety was reacted (overnight) with Ag_2O in acetonitrile at reflux temperature to form the desired bis-carbene complex. Compound **2** was obtained in excellent yield and good purity after filtration over celite.

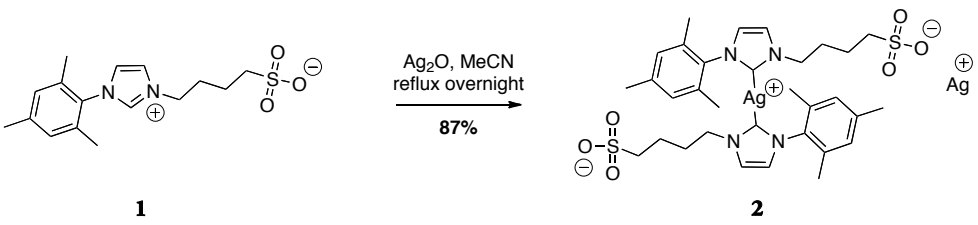

1 **2**

Scheme 1. Synthesis of NHC-Ag complex **2**.

The antimicrobial activity of compound **2** was tested on different bacteria and yeast of biological interest: the gram negative bacteria *Escherichia Coli* (*E. Coli*), the gram positive bacteria *Bacillus Subtilis* (*B. Subtilis*) and the yeast *Saccharomyces cerevisiae* (*S. cervisiae*). This activity was estimated by determining the minimum inhibitory concentration (MIC), which is the standard method to evaluate the interaction between bacteria and antimicrobial agents. The MIC value reflects the minimal concentration of a drug necessary to visibly inhibit the growth of bacteria after overnight incubation.[14]
The activity of complex **2** was compared to that of $AgNO_3$, used as a standard reference and to the imidazolium salt **1**, taken as the control experiment.

Table 1. MIC values of **1**, **2** and **$AgNO_3$** against E. coli, B. subtilis and S. cervisiae expressed in µg/mL and µM (in brackets).

	E. coli	*B.subtilis*	*S. cervisiae*
1	>200 (>620)	>200 (>620)	>200 (>620)
2	2.05 (4.78)	2.74 (6.37)	2.93 (6.83)
$AgNO_3$	0.88 (5.18)	0.88 (5.18)	0.98 (5.75)

The data displayed in Table 1 indicate that complex **2** is active against the three strains studied. As expected, the imidazolium salt has no bactericidal or fungicidal activity, demonstrating that the metal ion is indeed responsible for the antimicrobial activity. The bactericidal effect of **2** against *E. coli* is slightly higher than $AgNO_3$ when the concentration is rationalised to the actual concentration of Ag^+. However, in the case of *B. subtilis* and *S. cervisiae* the activity of **2** does not surpass that of $AgNO_3$. The moderate activity of **2** can be explained by the relative stability of the bis-carbene complex in the medium. Indeed, ^1H NMR spectroscopy indicates that complex **2** is stable in deuterated water for at least two days. The stability in the growth medium was not studied even though a discoloration of the solution was observed during the experiment, suggesting a faster decomposition of the complex in the medium. Still, bis-carbene silver complex **2** possesses two different types of silver ions, one is the counter-ion of the sulfonate moiety and is readily accessible, the other one being coordinated to two carbene ligands. It seems that the metal-carbene bond is not strong enough to withstand the conditions of

the testing medium inducing a quick release of Ag^+. It is noteworthy that the Ag-carbene bonds present a moderate strength compared to other transition metals as they are very often used as metal transfer agent for this very reason.

Conclusion

We have demonstrated that the bis-carbene silver complex **2** shows antimicrobial activity against a variety of microorganism. Its activity remains slightly higher (for *E. coli*) or even lower (for *B. subtilis* or *S. cerisiae*) compared to the benchmark antimicrobial $AgNO_3$. Different studies on the same subjects have shown that the activity of NHC-Ag complexes is comparable to that of $AgNO_3$ unless the silver compound is encapsulated in polymers,[9] inducing a slower release of Ag^+. In order to address the question of activity enhancement, it seems that controlling the release of Ag^+ is an effective way to achieve this goal. There is still some improvement to be done on the stability of the NHC-Ag complexes and more specifically on the carbene-Ag bond strength, which can be fine-tuned by rational design of the carbene ligand.

Experimental section

General information: The zwiterionic salt and the corresponding silver complex **1** were synthesised as previously published.[13] $AgNO_3$ was purchased from Aldrich or Acros and used as received. *E. coli*, *B. subtilis* and yeast *S. cerevisiae* were purchased from Fisher.

Strains and growth conditions. In this study, the gram negative bacteria *Escherichia coli* (*E. coli*; strain DH5α), gram positive bacteria *Bacillus subtilis* (*B. subtilis*) and yeast *Saccharomyces cerevisiae* (*S. cerevisiae;* strain RH448*)* were used. Bacteria were grown at 37 °C in Luria Broth (LB) and yeast was grown at 30 °C in YPD (10 g/L yeast extract, 20 g/L bacto peptone and 20 g/L dextrose). For all experiments, medium was inoculated directly from plates with colonies that were not older than two weeks and the cultures were grown overnight.

MIC value determinations. Stock solutions of $AgNO_3$, silver complex or imidazolium salt were prepared in sterile Milli-Q water to a concentration of 10 mg/mL. Minimum inhibitory concentrations (MICs) were determined by diluting the stock concentrations of these compounds to a concentration of 200, 175, 150 and 125 µg/mL of which 100 µL was added

to the first row of a 96-wells suspension culture plate (U-form, Greiner Bio One). This was followed by a 1:1 dilution series in sterile Milli-Q water. Overnight cultures were diluted back in the appropriate medium to an OD_{600} 0.0001, of which 100 µL was added to the culture plate. The total volume per well was 200 µL. The MIC value was determined to be the lowest concentration of antibiotic, which inhibits the growth of the strains and could be determined by eye on the 96-wells plate after an incubation of 24 h at 37 °C or 30 °C. The experiments were performed in duplicate.

References

[1] A. J. Arduengo, R. L. Harlow, M. Kline, *J. Am. Chem. Soc.* **1991**, *113*, 361-363.

[2] W. A. Herrmann, *Angew. Chem. Int. Ed.* **2002**, *41*, 1290-1309.

[3] D. Bourissou, O. Guerret, F. P. Gabbai, G. Bertrand, *Chem. Rev.* **2000**, *100*, 39-91.

[4] S. P. Nolan, *N-Heterocyclic Carbenes in Synthesis*, Wiley-VCH, Weinheim, **2006**.

[5] L. Mercs, M. Albrecht, *Chem. Soc. Rev.* **2010**, *39*, 1903-1912.

[6] A. Kascatan-Nebioglu, M. J. Panzner, C. A. Tessier, C. L. Cannon, W. J. Youngs, *Coord. Chem. Rev.* **2007**, *251*, 884-895.

[7] J. C. Garrison, W. J. Youngs, *Chem. Rev.* **2005**, *105*, 3978-4008.

[8] I. J. B. Lin, C. S. Vasam, *Coord. Chem. Rev.* **2007**, *251*, 642-670.

[9] A. Melaiye, Z. H. Sun, K. Hindi, A. Milsted, D. Ely, D. H. Reneker, C. A. Tessier, W. J. Youngs, *J. Am. Chem. Soc.* **2005**, *127*, 2285-2291.

[10] S. Ray, R. Mohan, J. K. Singh, M. K. Samantaray, M. M. Shaikh, D. Panda, P. Ghosh, *J. Am. Chem. Soc.* **2007**, *129*, 15042-15053.

[11] A. Melaiye, R. S. Simons, A. Milsted, F. Pingitore, C. Wesdemiotis, C. A. Tessier, W. J. Youngs, *J. Med. Chem.* **2004**, *47*, 973-977.

[12] K. M. Hindi, M. J. Panzner, C. A. Tessier, C. L. Cannon, W. J. Youngs, *Chem. Rev.* **2009**, *109*, 3859-3884.

[13] M. A. N. Virboul, M. Lutz, M. A. Siegler, A. L. Spek, G. van Koten, R. J. M. Klein Gebbink, *Chem. Eur. J.* **2009**, *15*, 9981-9986.

[14] J. M. Andrews, *J. Antimicrob. Chemother.* **2001**, *48*, 5-16.

GRAPHICAL ABSTRACT

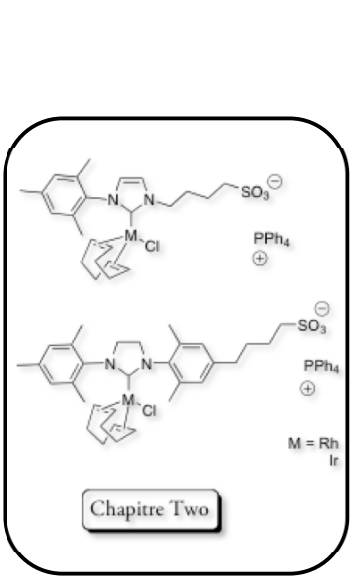

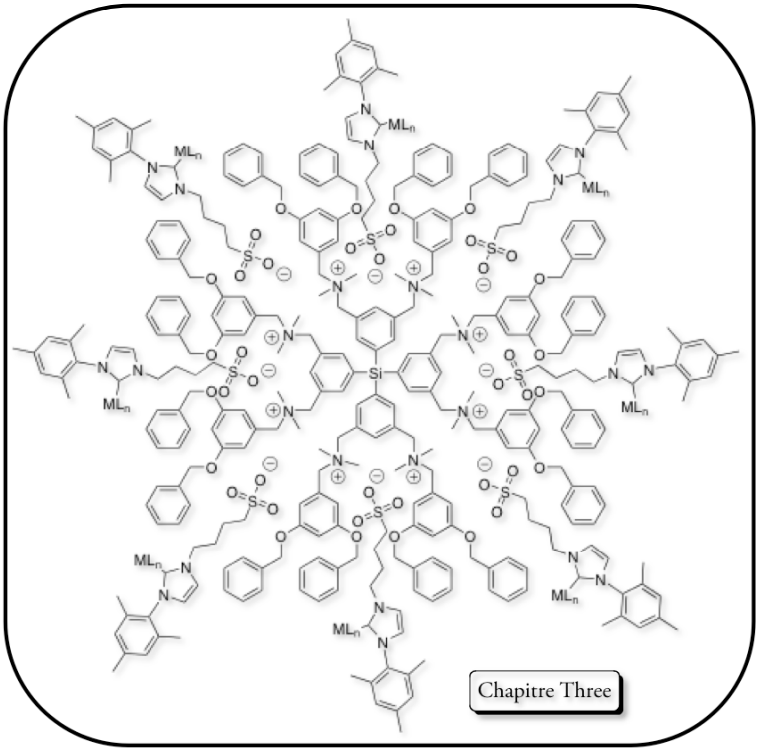

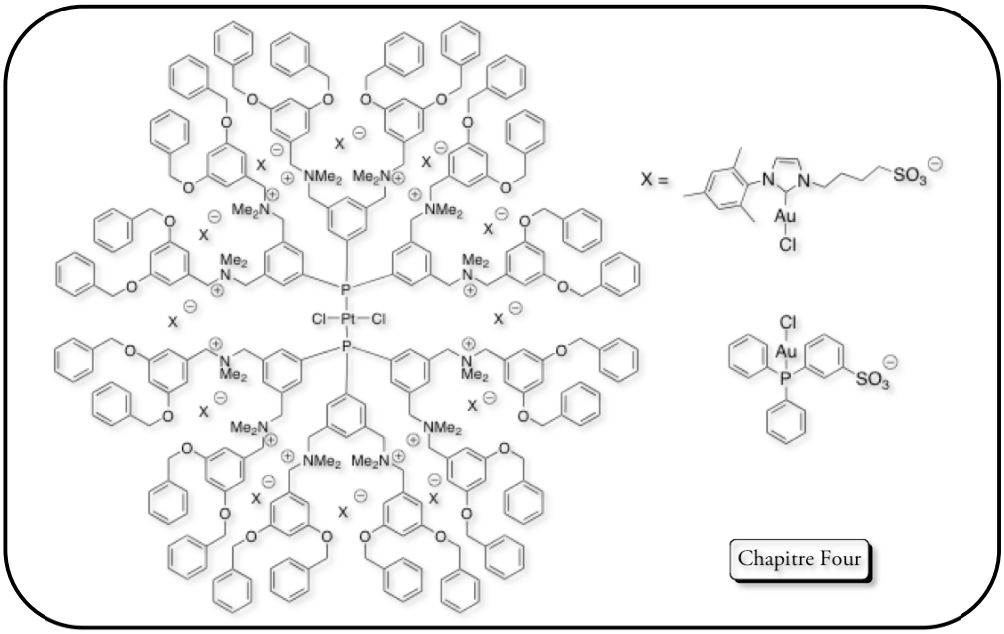

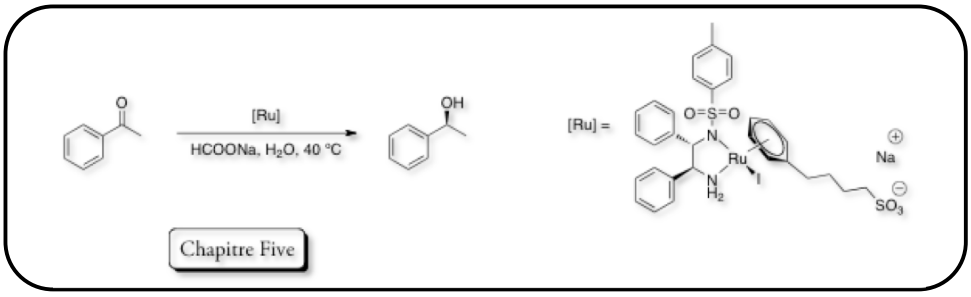

SUMMARY

The development of well-defined catalysts that enable rapid and selective chemical transformations and can be separated completely from the product is still a challenging task. To overcome the problems in homogeneous catalyst recovery, many conceptual strategies have been developed using for example fluorous phase catalysis, ionic liquids, supercritical fluids and supported aqueous phase catalysis. A widely studied approach to facilitate catalyst-product separation is the attachment of homogeneous catalysts to insoluble as well as soluble organic, inorganic, or hybrid supports.

Dendritic catalysts have often been proposed to fill the gap between homogeneous and heterogeneous catalysts. Because of their size, enhanced solubility profile, and well-defined molecular architecture, metallodendritic macromolecules can easily be recovered from reaction mixtures, e.g., by means of precipitation. In principle, dendritic catalysts can show the kinetic behavior and, accordingly, the activity and selectivity of a conventional homogenous catalyst, while they can also be easily recovered from the reaction medium; in this way they combine the advantages of both homogeneous and heterogeneous catalysis. As described in *Chapter 1*, an increasing number of research groups have focused their interest on the use of dendrimers as soluble support for (enantioselective) transition metal catalysts. Indeed, such functionalised dendrimers can also be separated and recovered by simple filtration techniques, that include dialysis and nanofiltration, and which ultimately would also allow for continuous operation modes to be used for homogeneous catalysts.

The present thesis describes the design and synthesis of sulfonate-tagged transition metal complexes and their use in non-covalent catalyst immobilisation on polycationic dendrimers and in aqueous catalysis.

The high basicity of N-Heterocyclic Carbene (NHC) ligands confers specific properties to a metal center in terms of electronic donation, which has recently led to an increased use of NHC-ligands in organometallic chemistry and homogeneous catalysis. *Chapter Two* of this thesis is devoted to the synthesis of structurally different NHC

ligand precursors (compounds **1** and **2** in Figure 1) both functionalised with an alkylsulfonate tether.

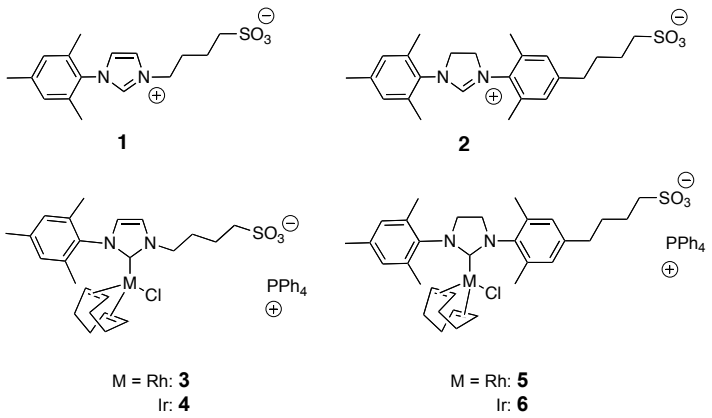

Figure 1. Alkylsulfonate-tethered NHC carbene ligand precursors and their respective metal complexes.

After deprotonation of **1** or pretreatment of **2** with Ag_2O, the coordination of the resulting NHC ligands to Rh(I) and Ir(I) metal centers to form complexes **3**-**6** was investigated. The differences in reactivity in terms of metal coordination between these complexes are attributed to their structural variation. These differences were further studied through the formation of carbonyl complexes, whose carbonyl stretching frequency was measured by IR spectroscopy and compared to similar compounds reported in literature. This technique did not allow for any clear distinction between the two NHC ligands in terms of electron donation, though it demonstrated the higher basicity of these compounds compared to electron rich phosphines.

In *Chapter Three*, the synthesis of Au(I) and Rh(I) complexes derived from **1** was investigated. The synthetic route employed the use of a halide free silver-biscarbene complex $[(NHC)_2Ag]$ which was used as a carbene transfer agent. Thanks to the transmetallation strategy developed for the formation of the corresponding metal complexes, the NHC complexes were directly immobilised on the polycationic dendrimer through interactions between the sulfonate tag of the transition metal complexes and the ammonium groups of the dendrimer (see Figure 2). This one pot transmetallation/immobilisation procedure was successfully applied to the synthesis of metallodendritic assemblies bearing eight gold or rhodium complexes per dendrimer.

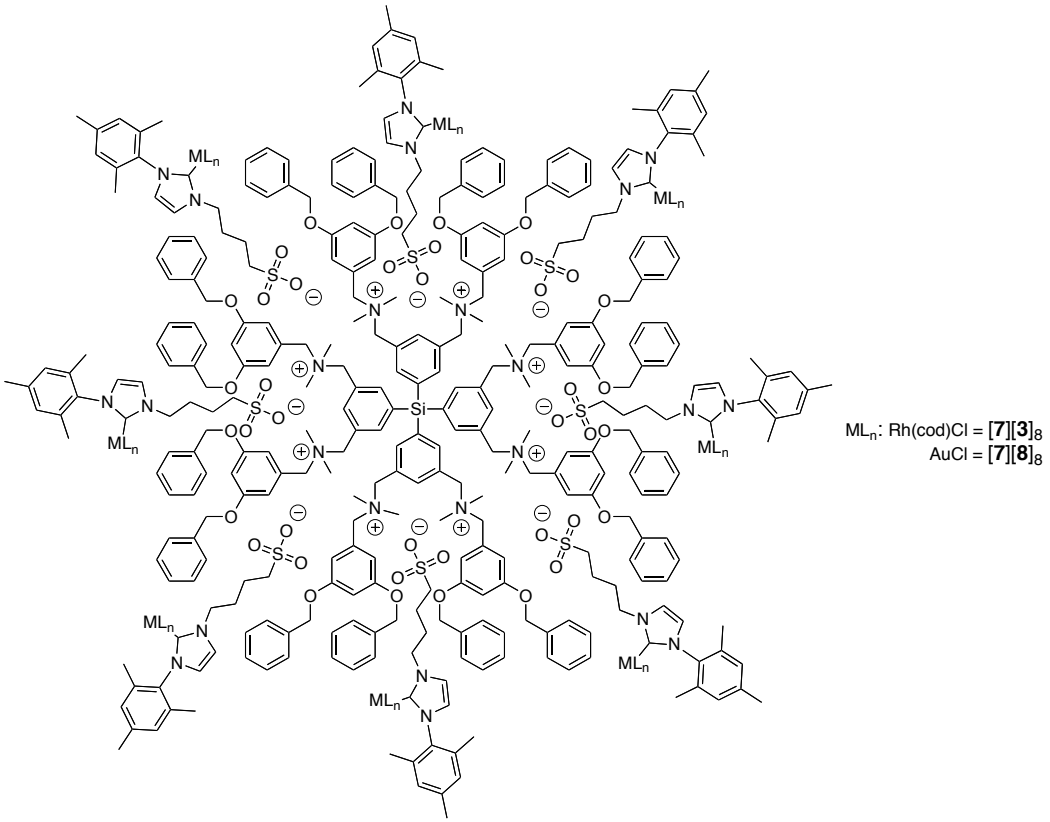

Figure 2. Non-covalent metallodendritic assemblies bearing NHC-metal complexes.

Compounds [7][**3**]$_8$ and [7][**8**]$_8$ as well as their parent compounds [NBu_4][**3**] and [NBu_4][**8**] were tested in the catalytic hydration of alkynes and the hydrosilylation of ketones, respectively. Both immobilised catalysts appeared to be active for the corresponding transformation, however the conditions used for the hydration of alkynes did not allow for a permanent immobilisation of the catalyst as evidenced by DOSY NMR experiments, thus limiting the use of [7][**3**]$_8$ as recoverable catalyst.

Chapter Four describes the synthesis of multimetallic dendritic assemblies constructed via non-covalent interactions between a polycationic transition metal complex and anion-tagged transition metal complexes. The one-pot transmetallation/immobilisation approach was used to synthesise homo-metallic assemblies bearing seven Au-centers. This one-pot method proved not to be suitable for the synthesis of hetero-metallic assemblies, as these were found to be kinetically unstable under these conditions; i.e. metal scrambling was observed. A two-step procedure was developed for the synthesis of hetero-metallic assemblies bearing up to thirteen metal centers (see Figure 3). In this

case, the $PtCl_2$ bis-dendrimer adduct was generated and purified in the first step and, subsequently, treated with a sulfonated Au-NHC complex (**8**) or a sulfonated Au-phosphine complex (**9**). Simple dialysis was sufficient to isolate and purify the resulting hetero-metallic assemblies.

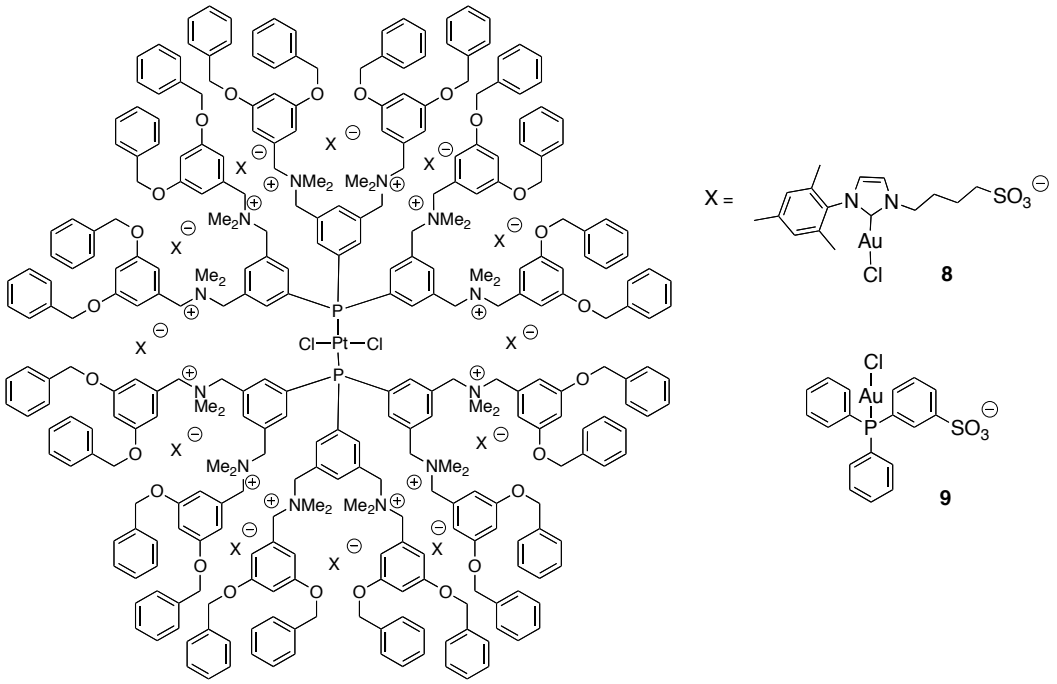

Figure 3. Multimetallic dendritic assemblies.

Chapter Five focuses on the synthesis of alkylsulfonate appended η^6-arene ruthenium complexes **10** and **11** (see Figure 4). The introduction of this functionality on a molecule has the direct consequence that the compound becomes highly hydrophilic, i.e. the Ru-complexes become perfectly soluble in water and aqueous solutions. This property was used to test the catalytic activity of these new compounds in the asymmetric transfer hydrogenation (ATH) of ketones in water giving good yields (>99 %) and good selectivity with up to 94 % ee for the catalytic systems studied. These catalytic data compare well to those of the original, non-hydrophilic system reported by Noyori *et al*.

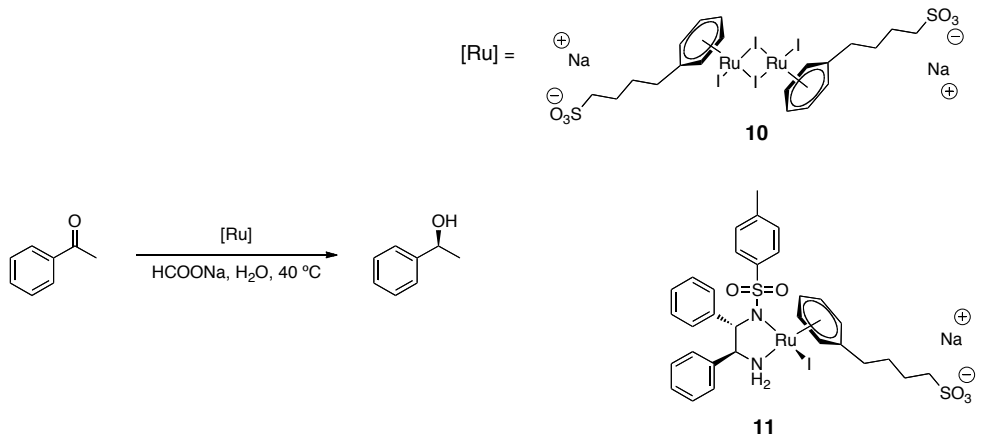

Figure 4. ATH in water with complexes **10** and **11**.

The recyclability of **11** was studied in three consecutive runs using phase separation. The enantiomeric excess of the secondary alcohol product remained constant at 94% in these runs, while a sudden drop in yield was observed from >95% to 20% in the third run. Most likely, the increased concentration of salts in the aqueous phase and concomitant changes in the pH are detrimental in this respect.

The last part of this thesis, the *Addendum*, presents the activity of a sulfonate functionalised $[(NHC)_2Ag]$ complex as antimicrobial agent. The potential bactericidal activity of this compound was investigated on different strains of bacteria and yeast. The study was performed in comparison with $AgNO_3$ and showed that the activity of these two compounds is similar, although $[(NHC)_2Ag]$ in general performs slightly but not significantly better.

SAMENVATTING

Het ontwikkelen van goed gedefinieerde katalysatoren die zowel snelle en selectieve chemische reacties mogelijk maken, als compleet gescheiden kunnen worden van het reactieproduct, is nog altijd geen gemakkelijke zaak. In het geval van homogene katalysatoren zijn er enkele strategieën ontwikkeld om dit probleem aan te pakken, bijvoorbeeld het gebruik van katalysatoren die oplosbaar zijn in fluorbevattende of ionische vloeistoffen, superkritisch koolstofdioxide of water. Een andere belangrijke strategie is het verankeren van homogene katalysatoren aan onoplosbare of anderzijds oplosbare organische, anorganische of hybride dragermaterialen.

Dendritische katalysatoren worden vaak genoemd als kandidaat om de kloof tussen homogene en heterogene katalyse te dichten. Vanwege hun grootte, buitengewoon goede oplosbaarheid en nauwkeurig gedefinieerde moleculaire structuur kunnen metallodendritische macromoleculen makkelijk gescheiden worden van reactiemengsels, bijvoorbeeld door precipitatie. In principe zijn dendritische katalysatoren in staat om zowel de activiteit als selectiviteit van conventionele katalysatoren te evenaren, terwijl ze tevens van het reactiemengsel gescheiden kunnen worden. Zodoende combineren ze de voordelen van zowel homogene als heterogene systemen.

Zoals beschreven in *Hoofdstuk 1*, heeft een groot aantal onderzoeksgroepen dendrimeren gebruikt als oplosbare dragermaterialen voor (enantioselectieve) overgangsmetaal-gebaseerde homogene katalysatoren. Dit soort systemen kan ook worden gescheiden en teruggewonnen uit reactiemengsels door eenvoudige filtratietechnieken zoals dialyse en nanofiltratie. Daarnaast behoort het hergebruik van deze dendritische homogene katalysatoren in continue systemen tot de mogelijkheden.

Dit proefschrift beschrijft het ontwerp en de synthese van overgangsmetaalcomplexen die sulfonaatgroepen bevatten. Zowel het verankeren van deze systemen aan polykationische dendrimeren via noncovalente interacties als hun toepassing als wateroplosbare katalysatoren komen aan bod.

De hoge basiciteit van N-heterocyclische carbeen (NHC) liganden maakt een metaalcentrum relatief rijk aan electrondichtheid, wat om verschillende redenen interessant kan

zijn. Dit heeft recentelijk geleid tot een toename van de toepassingen van NHC-liganden in de organometaalchemie en homogene katalyse. *Hoofdstuk 2* van dit proefschrift behandelt de synthese van twee structureel verschillende voorlopers (verbindingen **1** en **2** in Figuur 1) van NHC liganden die beide een alkylsulfonaatgroep bevatten.

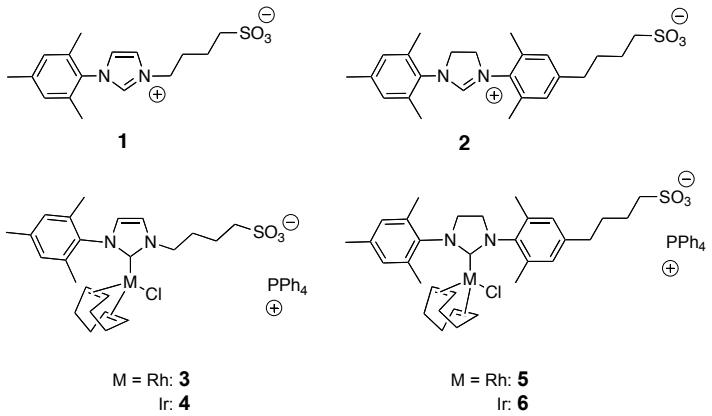

Figuur 1. Voorlopers van NHC liganden die een alkylsulfonaatgroep bevatten en de daarvan afgeleide metaalcomplexen.

Na deprotonering van **1** of voorbehandeling van **2** met Ag_2O werd de coördinatie van deze liganden aan Rh(I) en Ir(I) metaalcentra bestudeerd, wat leidde tot de complexen **3**-**6**. Deze complexen vertonen (add description of differences) Deze verschillen zijn toe te schrijven zijn aan de structurele eigenschappen van de NHC liganden. Uit de IR spectra van CO-bevattende analogen van deze complexen werd de basiciteit van de liganden vastgesteld. Deze techniek gaf geen significant verschil aan tussen de basiciteit van de liganden onderling, maar door een vergelijking met de literatuur kon worden vastgesteld dat de liganden een hogere basiciteit vertonen dan elektronrijke fosfineliganden.

In *Hoofdstuk 3* wordt de synthese van Au(I) en Rh(I) complexen die zijn afgeleid van **1** beschreven. In de syntheseroute werd gebruik gemaakt van een onafhankelijk gesynthetiseerd halidevrij zilver-biscarbeen complex $[(NHC)_2Ag]$, waarin NHC staat voor de carbeen analoog van **1**, als carbeen-overdrachtsreagens en één equivalent van een ammonium of fosfonium chloride zout als additionele bron voor halide ionen. De één-potsreactie van ofwel [AuCl(tht)] of $[\{RhCl(cod)\}_2]$ met $[(NHC)_2Ag]$ in combinatie met $[NBu_4]Cl$ of $[PPh_4]Cl$ in een respectievelijke verhouding van 2:1:1 of van 1:1:1 gaf de overeenkomstige NHC complexen en één equivalent AgCl. Dezelfde één-pot-transmetalleringstrategie maakte het mogelijk om in één stap zowel de

transmetallatiereactie, als de verankering van het verkregen anionische complex aan het polykationisch dendrimeer [**5**]Cl_8 te realiseren. De verankering van de complexen berust op electrostatische interacties tussen de sulfonaatgroepen van de complexen en de ammoniumgroepen van het dendrimeer. In deze procedure vervult het poly-kationische dendrimeer zowel de rol van dragermateriaal als de rol van halide bron. Op deze manier werden twee verschillende metallodendritische assemblages gesynthetiseerd, die respectievelijk acht goud- of rhodiumcomplexen bevatten (zie Figuur 2).

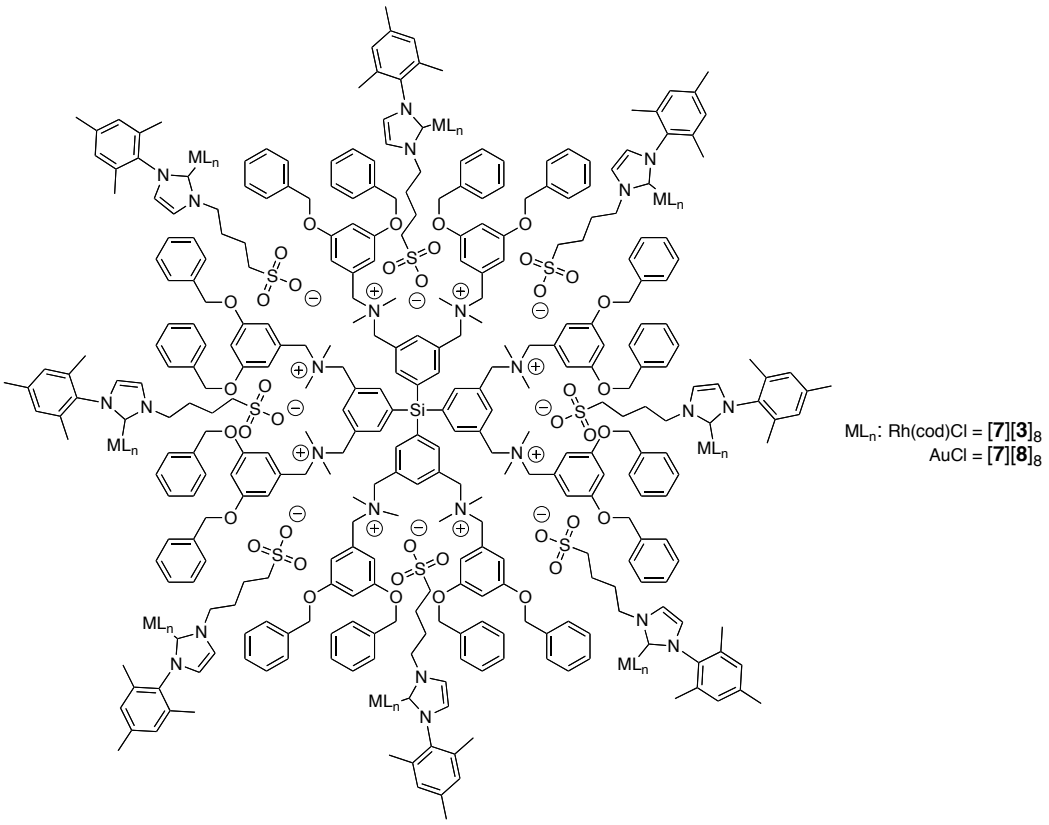

Figuur 2. Noncovalente metallodendritische assemblages die NHC-metaalcomplexen bevatten.

De assemblages [**7**][**3**]$_8$ en [**7**][**8**]$_8$ evenals de monomerische complexen [NBu_4][**3**] en [NBu_4][**8**] werden getest in twee katalytische reacties; respectievelijk de hydratie van alkynen en de hydrosilylering van ketonen. Beide assemblages bleken effectieve katalysatoren voor de bestudeerde reacties. In het geval van [**7**][**3**]$_8$ werd echter via DOSY NMR experimenten vastgesteld dat de complexen niet permanent verankerd bleven. Dit betekent dat hergebruik van [**7**][**3**]$_8$ als katalysator slechts beperkt mogelijk is.

In *Hoofdstuk 4* wordt de synthese beschreven van multimetallische dendritische assemblages die zijn opgebouwd uit polykationische dendrimeren en anionische overgangsmetaalcomplexen.

De verankering van de complexen aan de dendrimeren berust op electrostatische interacties. De syntheseroute van deze assemblages hing af van het type assemblage. In het geval van homo-multimetallische assemblages kon de procedure voor transmetallatie en verankering in één stap, zoals beschreven in *Hoofdstuk 3*, gebruikt worden. In het geval van hetero-multimetallische assemblages werd een syntheseroute in twee stappen ontwikkeld die leidde tot twee verschillende assemblages met elk maximaal dertien metaalcentra (Figuur 3). In deze syntheseroute werd een $PtCl_2$ bis-dendrimeer adduct in de eerste stap gegenereerd en gezuiverd, waarna deze in de tweede stap gecombineerd werd met een gesulfoneerd Au-NHC complex (**8**) of een gesulfoneerd Au-fosfine complex (**9**). Hierna konden de hetero-metallische assemblages simpelweg via dialyse gezuiverd en geïsoleerd worden.

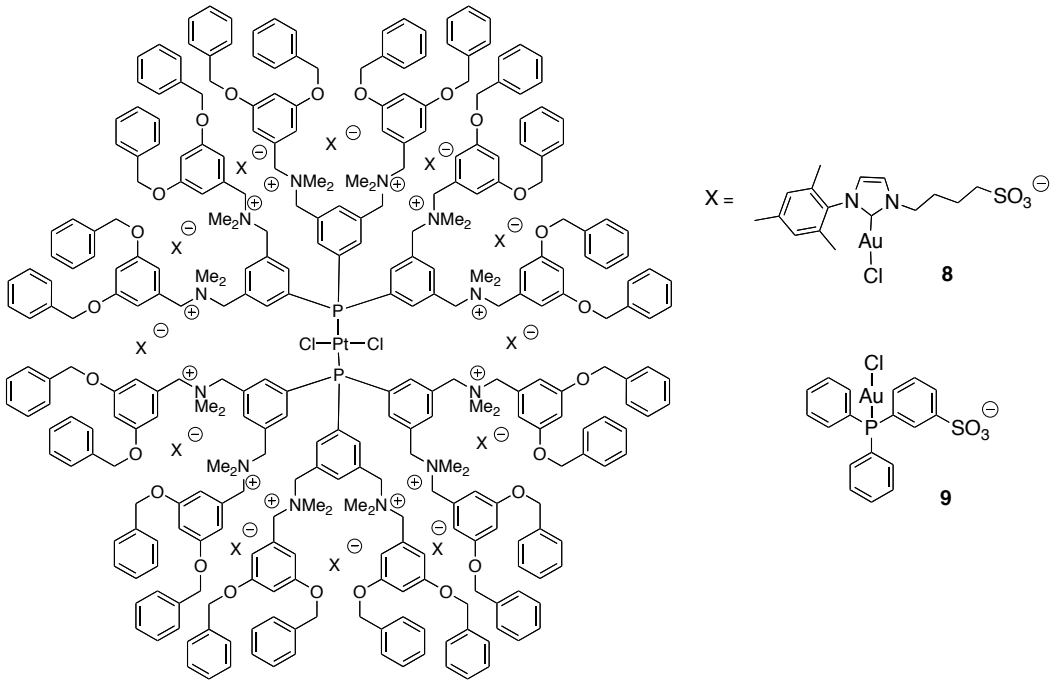

Figuur 3. Multimetallische dendritische assemblages.

Hoofdstuk 5 behandelt de synthese van de η^6-areen ruthenium complexen **10** en **11**, die beide een alkylsulfonaatgroep bevatten (zie Figuur 4). Het introduceren van deze groep heeft als consequentie dat de betreffende complexen een hoge wateroplosbaarheid krijgen. Deze nieuwe complexen werden getest in de asymmetrische waterstofoverdrachtsreactie van ketonen in water. De bestudeerde systemen gaven hoge opbrengsten (>99 %) en enantioselectiviteit (tot 94 %). Deze katalytische data verschillen van die van het oorspronkelijk, niet-wateroplosbare systeem dat eerder door Noyori et al. bestudeerd is. Vervolgens is het hergebruik van de wateroplosbare

katalysatoren via fasescheiding getest in drie opeenvolgende reacties. De enantiomere overmaat van het secundaire alcohol product van deze reacties bleef in de drie reacties constant op zo'n 94 %. De reactieopbrengst daalde dramatisch van >95 % naar 20 % in de derde reactie. De verhoogde concentratie van zouten en de daarmee gepaard gaande verandering van de pH van de oplossing spelen hierin waarschijnlijk een negatieve rol.

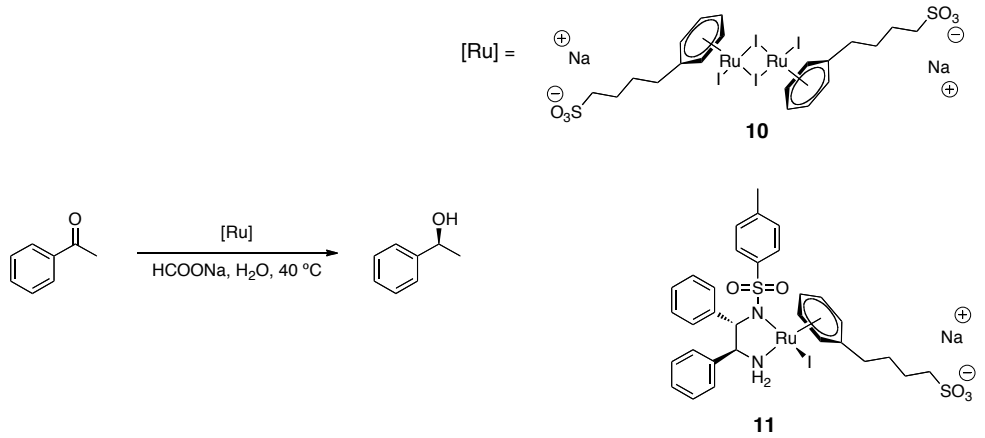

Figuur 4. Katalytische asymmetrische waterstofoverdrachtsreactie met complexen **7** en **8**.

In het laatste deel van dit proefschrift, het *Addendum*, wordt een studie gepresenteerd over de antimicrobiële activiteit van biscarbeen zilvercomplex $[(NHC)_2Ag]$ tegen verschillende lijnen van bacteriën en gist. De studie werd uitgevoerd in vergelijking tot $AgNO_3$ en gaf een klein verschil in activiteit aan ten gunste van $[(NHC)_2Ag]$.

RÉSUMÉ

L'émergence de catalyseurs capables d'effectuer des transformations chimiques rapides et sélectives et pouvant être aisément séparés du milieu réactionnel demeure une gageure dans le domaine de la catalyse. De nombreuses approches ont été développées pour répondre à l'exigence de recyclabilité des catalyseurs homogènes, parmi lesquelles la catalyse en phase fluorée, les liquides ioniques, les fluides supercritiques ou encore la catalyse en phase aqueuse. L'immobilisation de catalyseurs homogènes sur des supports organiques solubles ou insolubles ou encore sur des supports hybrides est une alternative très fréquemment employée pour permettre la séparation du catalyseur.

En raison de leur taille, de leur solubilité et de leur structure architecturale, les métallo-dendrimères sont des macromolécules pouvant être facilement récupérées à la fin de la réaction notamment par simple nanofiltration. A priori, les métallodendrimères présentent les mêmes caractéristiques cinétiques que les catalyseurs homogènes correspondants -et par conséquent la même activité et sélectivité- mais peuvent être également récupérés en fin de réaction ce qui donne à ces molécules à la fois les avantages d'un catalyseur homogène et d'un catalyseur hétérogène.

La recherche bibliographique effectuée sur le thème des dendrimères comme catalyseurs énantiosélectifs présentée dans le *Chapitre 1* a permis de démontrer l'intérêt toujours croissant de nombre de groupes de recherches dans l'utilisation des dendrimères comme support pour l'immobilisation de catalyseurs énantiosélectifs. Leur utilisation permet ainsi le recyclage par des techniques de nanofiltration ou de dialyse, pouvant éventuellement conduire à des procédés de recyclage en continu.

Le travail décrit dans cette thèse traite du "design" et de la synthèse de complexes de métaux de transition fonctionnalisés avec un groupement alkylsulfonate, de leur immobilisation de façon non-covalente sur des dendimères polycationiques ou en phase aqueuse et de leur utilisation comme catalyseur homogène.

Les propriétés spécifiques des ligands carbènes N-Hétérocycliques (NHC), en particulier leur très grande basicité, a nettement contribué à leur usage croissant en

chimie organométallique et en catalyse homogène. Le *Chapitre 2* est consacré à la synthèse de précurseurs de ligands NHC, les composés **1** et **2**, différents structurellement mais tout deux fonctionnalisés avec une chaîne alkyl-sulfonate.

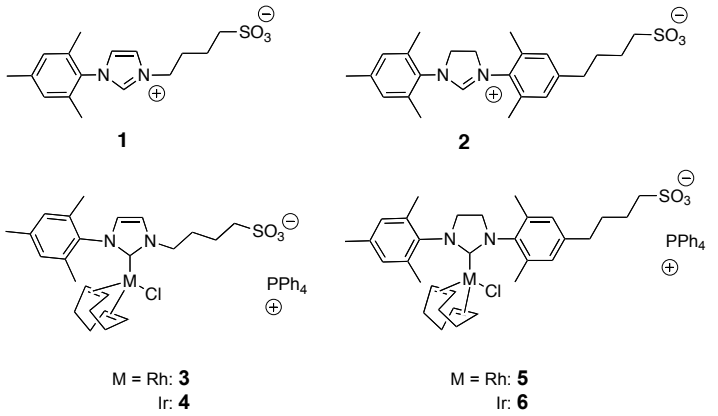

Figure 1. Ligands carbènes de type NHC fonctionnalisés avec un groupement alkyl-sulfonate et leurs complexes de métaux de transition correspondants.

La coordination de ces ligands avec du rhodium et de l'iridium a abouti à la synthèse des complexes de métaux de transition **3**-**6** (voir Figure 1), cependant avec des différences imputables aux variations structurelles des ligands **1** et **2**. La synthèse des complexes carbonyles correspondants a permis l'étude plus avant de ces différences par la mesure des fréquences de vibration des groupes carbonyles en spectroscopie infra-rouge, sans cependant mettre en évidence de variations flagrantes en matière de propriétés électroniques entre les deux types de ligands. Toutefois, la basicité de ces deux ligands a pu être comparée à celle de phosphines électroniquement riches, démontrant ainsi leur basicité supérieure.

Le *Chapitre 3* présente la synthèse de complexes d'or et de rhodium à partir du ligand **1**. La stratégie développée pour la synthèse de ces complexes propose l'utilisation du complexe d'argent $[(NHC)_2Ag]$ en tant qu'agent de transmétallation et d'un sel organique permettant la formation d'AgCl, qui est le moteur de la réaction. Cette stratégie permet également la formation concomitante du complexe et de l'immobilisation sur le support dendritique au moyen d'interactions ioniques entre les groupements sulfonates du complexe et les groupements ammonium du dendrimère, débouchant sur la formation des métallodendrimères [**5**][**4**]$_8$ et [**5**][**3**]$_8$ (voir Figure 2).

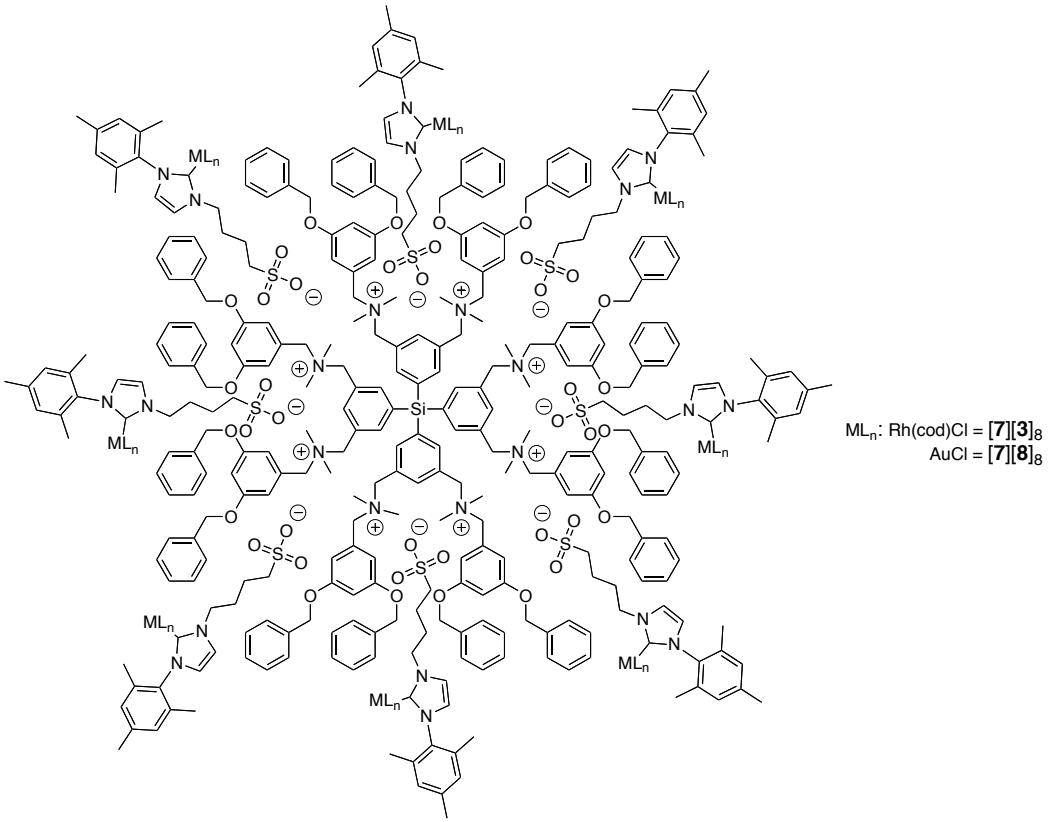

Figure 2. Complexes métaux carbènes immobilisés de façon non-covalente sur des dendrimères polycationiques.

L'activité catalytique des composés [**7**][**3**]$_8$ et [**7**][**8**]$_8$ ainsi que les composés parents [NBu$_4$][**3**]et [NBu$_4$][**8**] a été étudiée respectivement dans l'hydratation des alcynes et l'hydrosilylation des cétones. Les catalyseurs immobilisés et non-immobilisés sont actifs pour les réactions précitées, toutefois les conditions utilisées pour l'hydratation des alcynes ne permettent pas une immobilisation permanente du catalyseur comme il a été demontré par RMN DOSY, et limitent donc l'usage de [**7**][**3**]$_8$.

Le *Chapitre 4* présente la synthèse de plusieurs structures métallodendritiques construites à partir de complexes de métaux de transition portant un groupement sulfonate et d'un complexe de métal de transition polycationique via des interactions non-covalentes. La formation de composés homo- et hétéro-multimétalliques a ainsi pu être réalisée, certains de ces composés pouvant contenir jusqu'à treize fragments métalliques (voir Figure 3).

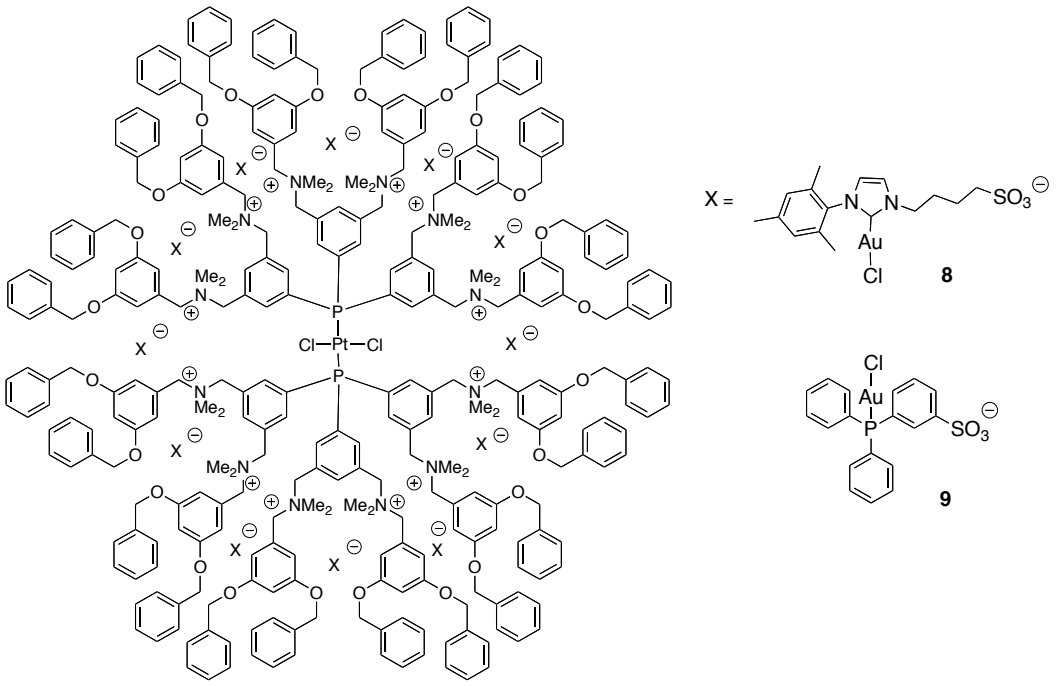

Figure 3. Dendrimères multimétalliques.

Le *Chapitre 5* décrit la synthèse de complexes η^6-arène ruthénium **10** et **11** possédant un groupement alkylsulfonate (voir Figure 4). L'introduction de ce groupement dans la molécule a pour conséquence directe une nette augmentation de l'hydrophilicité de la molécule, i.e. la rendant soluble dans l'eau. Cette propriété remarquable des complexes **10** et **11** a pu être mise à profit dans leur utilisation comme catalyseurs dans le transfert asymétrique d'hydrogène en phase aqueuse. Les rendements obtenus sont très satisfaisants (>99 %), la sélectivité donnant également de très bons résultats avec des excès énantiomériques jusqu'à 94 % selon le système catalytique étudié. La recyclabilité du catalyseur a également été testée et montre la persistance de l'activité catalytique après plusieurs cycles.

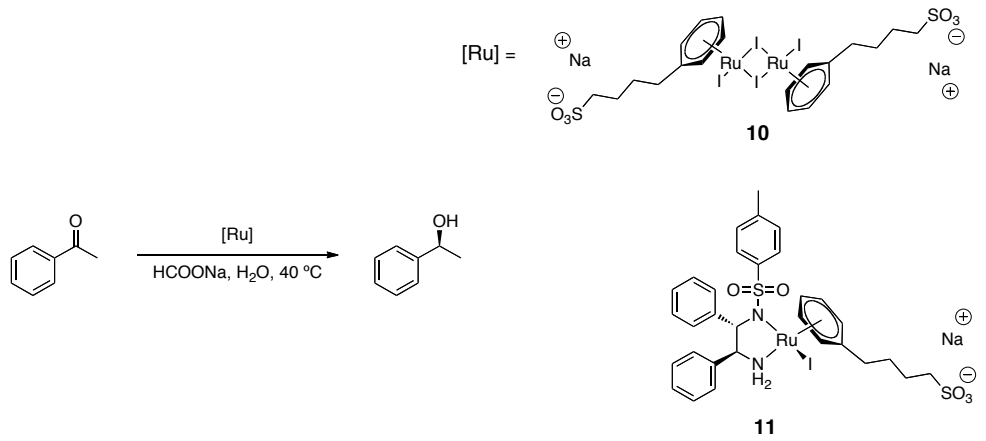

Figure 4. Transfert asymétrique d'hydrogène en phase aqueuse avec les complexes **10** et **11**.

La dernière partie de cette thèse, l'*Addendum*, présente l'activité du complexe d'argent [$(NHC)_2Ag$] fonctionnalisé avec un sulfonate en tant qu'agent antibactérien. L'activité bactéricide de ce composé a été étudiée sur différentes souches bactériennes ainsi que sur des levures et comparée à celle, notoire, d'$AgNO_3$. Il apparaît que les activités de ces deux composés sont similaires, [$(NHC)_2Ag$] donnant toutefois des résultats légèrement meilleurs mais pas de façon significative.

ACKNOWLEDGMENTS

I would like to conclude this thesis by thanking all the people who contributed to this work, directly or indirectly.

First, I wish to thank prof. dr. Gerard van Koten and prof. dr. Bert Klein Gebbink for welcoming me in their group. The decision I made to join your group was one I will never regret.
Dear Bert, I would like to express all my gratitude for the help you provided in making this thesis real. I greatly appreciated the freedom you gave me in allowing me to follow my own path and helping me to develop my self into the chemist that I am. I wish you all the best with your scientific career.
Dear Gerard, even though we had few occasions to discuss about chemistry your experience and encouragements have helped me considerably during the moments of doubt, and they were plenty!
I would like to thank also the rest of the permanent staff members of the group, Milka Westbeek, Henk Klein and Johann Jasztrebski, for their daily contribution.

During this research period I had the privilege to collaborate with several people, who contributed to a great extend to the success of this thesis.
I would like to thank prof. dr. Martin Albrecht who introduced me to the world of NHC carbenes and inspired my work. Thank you for welcoming me in your group and for the stimulating discussions. Good luck with your research in Dublin.
Prof. dr. Cees Elsevier, thank you for allowing me to come to your group and learn your own techniques.
Cees Versluis, many thanks for all the characterisations and the amazing mass spectra you measured.
Maxime Siegler, Martin Lutz and prof. Anthony Spek thank you for the determination of the crystal structures.

Yvonne, it was really nice working with you; I really enjoyed our collaboration (and especially killing bacteria!).

Special thanks to the post-docs of the group Harm Dijkstra, Sylvestre Bonnet and Yves Cabon for their input on my research. Thanks to my students Teresa, Maialen and Bart for their dedication and hard work on this project. I would also like to thank all the former and present members of the Organic Chemistry & Catalysis group who brought a very nice atmosphere to the group and made it a friendly environment to work in during these four years and a half: Nesibe, Elena, Birgit, Sipke, Ties, Aidan, Preston, Maaike, Marcel, Silvia, Bart, Pieter, Marcella, Peter Hausoul, Peter Spannring, Thomas, Jie, Erwin, Iréna, Ilenia, Kees, Kamil, Layo, Vital. I should had as well our neighbours on the eight floor, the "biologists", Lucie, Jacques, Yvonne, Erica and Tania.

Jacco and Niels it was a great pleasure to have become one of your friends. The life of a PhD was much more bearable with your constant support and encouragement. Thanks for all the good vibes from Brabant.
Dennis, les mots me manquent pour évoquer la valeur que je porte à notre amitié. J'espère qu'elle n'aura pas de frontières.

J'aimerais enfin remercier toute ma famille qui a été d'un soutien sans faille durant toutes ces années et leur exprimer ma plus profonde gratitude: merci Papa, Maman, Pascale, Jean-Marc, Maiwenn et Aënaelle. Enfin, Pierre, merci pour ton extrême patience, ton indéfectible support et bien plus encore.

Morgane

CURRICULUM VITAE

Morgane Virboul was born on the 18th of november 1977 in Rennes, France. In 1999, she started her chemistry studies at the University of Rennes I, Rennes, France. During her cursus, she followed an industrial internship at OmniChem-Ajinomoto in Louvain-la-neuve, Belgium, on palladium assisted [3+2] cycloaddition for the synthesis of synthetic intermediates. She carried out an MSc research project in the group of Dr. Michel Vaultier under the supervision of Dr. Gilles Alcaraz at the University of Rennes I, Rennes, France, on the synthesis of dispirofluoreneindenofluorene and their use as blue light emitting OLEDs. She obtained her MSc Chemistry diploma from the same University in 2005.

In October 2005 she started her PhD program in the group of prof. Dr. Gerard van Koten under the supervision of prof. Dr. Bert Klein Gebbink. The research she performed during this time on immobilisation of transition metal complexes through sulfonate functionalisation is described in the present thesis. Part of this work was presented at several national and international congresses, among which the International Dendrimer Symposium (IDS5) in Toulouse, the 23rd International Congress on Organometallic Chemistry (ICOMC) in Rennes, and the 15th IUPAC Symposium on Organometallic Chemistry Directed Towards Organic Synthesis (OMCOS 15) in Glasgow.

She is currently working as a research chemist in the field of organic electronics for Solvay S.A..

LIST OF PUBLICATIONS

Dispirofluorene-indenofluorene (DSFIF): Synthesis, Electrochemical, and Optical Properties of a Promising New Family of Luminescent Materials

David Horhant, Jing-Jing Liang, Morgane Virboul, Cyril Poriel, Gilles Alcaraz and Joëlle Rault-Berthelot, *Org. Lett.* **2006**, 8(2), 257-260.

Dispirofluorene-indenofluorene Derivatives as New Building Blocks for Blue Organic Electroluminescent Devices and Electroactive Polymers

Cyril Poriel, Jing-Jing Liang, Joëlle Rault-Berthelot, Frédéric Barrière, Nicolas Cocherel, Alexandra M. Z. Slawin, David Horhant, Morgane Virboul, Gilles Alcaraz, Nathalie Audebrand, Laurence Vignau, Nolwenn Huby, Guillaume Wantz and Lionel Hirsch, *Chem. Eur. J.* **2007**, 13(36), 10055-10069.

One-pot Synthesis and Immobilisation of Sulfonate-tethered N-heterocyclic Carbene Complexes on Polycationic Dendrimers

Morgane A. N. Virboul, Martin Lutz, Maxime A. Siegler, Anthony L. Spek, Gerard van Koten and Robertus J. M. Klein Gebbink, *Chem. Eur. J.* **2009**, 15(39), 9981-9986.

Enantioselective Catalytic Dendrimers

Morgane A. N. Virboul and Robertus J. M. Klein Gebbink, submitted for publication.

Synthesis of Multimetallic Dendrimers through Non-Covalent Interactions

Dennis J. M. Snelders, Morgane A. N. Virboul, Robert Kreiter, Cees Versluis, Gerard van Koten and Robertus J. M. Klein Gebbink, submitted for publication.

Sulfonate-tethered (η^6-arene) Ru(II) Complexes for Application in Asymmetric Transfer Hydrogenation in Water

Morgane A. N. Virboul and Robertus J. M. Klein Gebbink, submitted for publication.